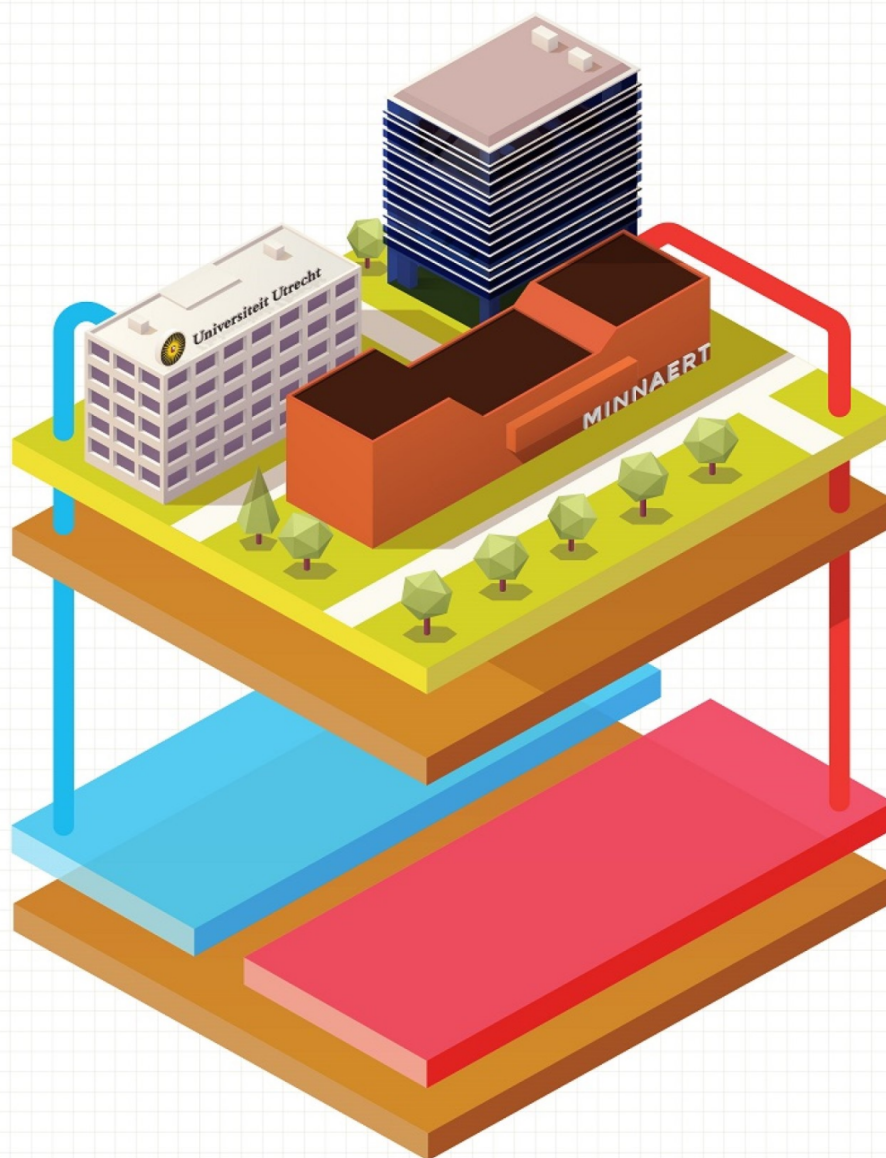


# Short-term operational stability of 5th generation district heating and cooling substations

Performance improving control strategies for prosumer  
substations in an ATEs ring network

F.P.J.H. Janssen

Master of Science Thesis





# **Short-term operational stability of 5th generation district heating and cooling substations**

**Performance improving control strategies for prosumer substations in an ATES ring network**

MASTER OF SCIENCE THESIS

For the degree of Master of Science in Systems and Control and in Mechanical Engineering: Energy, Flow and Process Technology

F.P.J.H. Janssen

5 July, 2022

Faculty of Mechanical, Maritime and Materials Engineering (3mE) · Delft University of Technology



**Universiteit Utrecht**

The work in this thesis was supported by Utrecht University. Their cooperation is hereby gratefully acknowledged.

Cover image by [1].



Copyright © Delft Center for Systems and Control (DCSC)  
All rights reserved.



DELFT UNIVERSITY OF TECHNOLOGY  
DEPARTMENT OF  
DELFT CENTER FOR SYSTEMS AND CONTROL (DCSC) AND PROCESS AND ENERGY

The undersigned hereby certify that they have read and recommend to the Faculty of  
Mechanical, Maritime and Materials Engineering (3mE) for acceptance a thesis  
entitled

SHORT-TERM OPERATIONAL STABILITY OF 5TH GENERATION DISTRICT HEATING  
AND COOLING SUBSTATIONS

by

F.P.J.H. JANSSEN

in partial fulfillment of the requirements for the degree of

MASTER OF SCIENCE SYSTEMS AND CONTROL

AND

MECHANICAL ENGINEERING: ENERGY, FLOW AND PROCESS TECHNOLOGY

Dated: 5 July, 2022

Supervisor(s):

\_\_\_\_\_  
Prof.dr.ir. T. Keviczky      DCSC TU Delft

\_\_\_\_\_  
Dr.ir. I.W.M. Pothof      P&E TU Delft, Deltares

Reader(s):

\_\_\_\_\_  
Prof.dr.ir. W. de Jong      P&E TU Delft

\_\_\_\_\_  
Ir. M.W. Sibeiijn      DCSC TU Delft



---

# Abstract

Energy demand for heating and cooling makes up 73% of total energy use of buildings [2]. This figure is expected to increase over the coming decades, as demand for cooling energy may rise in the Netherlands due to climate change. The heating and cooling of buildings are at relatively low temperature compared to the industry and thus allowing for a 5th Generation District Heating and Cooling (5GDHC) network with thermal energy storage. Several guidelines are available for the design of 5GDHC substations [3], however they do not integrally consider the control design.

Currently, in literature the performance of the substations is generally based on 1-hour measurements yet the control of the short term dynamics have a significant impact on the performance, thus shorter time steps are required to improve the performance.

This study considers the short term dynamics of substations of large utility buildings connected to a 5GDHC grid, allowing for seasonal thermal energy storage and independent bi-directional consumption for all buildings. A hydro- and thermodynamic model including the controllers are compared with a case study of utility buildings at Utrecht University where high frequency operational data is gathered. This provides a view on the causes of the problems and inefficiencies and new insights into improvements on the hydro- and thermodynamics and control of the substation. A new control method for the heat exchanger and for the Heat Pump (HP) group is proposed to maximise the networks capacity.

The use of Model Predictive Control (MPC) controllers is investigated to determine the performance improvements that can be achieved based on a simple physical system model and the energy demand and temperature setpoint predictions. As the short-term dynamics are discussed, the time steps for the MPC optimisation are relatively small while the many on/off switches that are allowed might make it computationally intensive due to large number of binary variables. The flow in some parts might be reversed, which is modelled using binary variables. Finally, as the system is transporting water at different temperatures and different mass flow rates, it is described by bilinear equations. These equations can be linearised by the McCormick relaxations, however they once again increase the computational burden as new binary variables have to be introduced.

The changed proposal for switching conditions could easily be implemented and reduces the temperature limit violations as well as the proposed control method for the warm Heat exchanger (HEX) as it stabilises the substation control. The proposed method for the temperature setpoint and capacity control showed an improved regulation of the temperature and

energy provided by the heat pumps and could even reduce the consumption of conventional heating sources. Finally the MPC controller shows an increased performance both for the constant and variable flow conditions, but cannot yet be implemented as the computational burden is too large.

---

# Contents

<b>Abstract</b>	<b>i</b>
<b>Preface</b>	<b>xi</b>
<b>1 Introduction</b>	<b>1</b>
1-1 General . . . . .	1
1-1-1 ATES and 5GDHC . . . . .	1
1-1-2 Substations . . . . .	3
1-2 Literature review on 5GDHC and related control . . . . .	4
1-3 Problem statement and research objective . . . . .	7
1-4 Methodology and outline . . . . .	9
<b>2 System description</b>	<b>11</b>
2-1 System description . . . . .	12
2-1-1 Control . . . . .	14
2-1-2 Comparison with ISSO39 . . . . .	17
2-2 Data Analysis . . . . .	20
2-2-1 Analysis of year data . . . . .	23
2-2-2 Analysis of high-frequency measurements . . . . .	34
2-3 Observations based on data analysis . . . . .	41
2-4 Summary . . . . .	43
<b>3 Thermo-hydraulic modelling of the system</b>	<b>45</b>
3-1 Modelling - WANDA . . . . .	45
3-2 Simulations . . . . .	53
3-3 Low level control and thermodynamic improvements . . . . .	54
3-3-1 Matching components with building demand . . . . .	54
3-3-2 Peak shaving . . . . .	54

3-3-3	HEX - heat pump instability . . . . .	55
3-3-4	Cold buffer short-cut network . . . . .	56
3-3-5	On/off switching cold heat exchanger . . . . .	56
3-3-6	Capacity and temperature control heat pumps . . . . .	56
3-4	Summary . . . . .	61
<b>4</b>	<b>Model Predictive Control</b>	<b>63</b>
4-1	MPC theory . . . . .	63
4-2	Mathematical system model . . . . .	64
4-2-1	Components . . . . .	67
4-2-2	Nodes . . . . .	71
4-3	MPC strategy . . . . .	72
4-3-1	Constraints . . . . .	72
4-3-2	Move blocking . . . . .	82
4-3-3	Cost function . . . . .	82
4-3-4	MPC variable flow . . . . .	86
4-4	MPC variations . . . . .	88
4-5	Summary . . . . .	88
<b>5</b>	<b>Results</b>	<b>91</b>
5-1	Validation WANDA model . . . . .	91
5-2	Low level control and thermodynamic improvements . . . . .	98
5-2-1	Matching components with building demand . . . . .	98
5-2-2	HEX operation . . . . .	101
5-2-3	Capacity and temperature control heat pumps . . . . .	102
5-3	MPC . . . . .	113
5-3-1	Constant flow . . . . .	113
5-3-2	Variable flow . . . . .	115
<b>6</b>	<b>Discussion</b>	<b>123</b>
6-1	Model . . . . .	123
6-2	Comparison control strategies . . . . .	123
6-2-1	Temperature & capacity control . . . . .	124
6-2-2	MPC - constant flow . . . . .	126
6-2-3	MPC - variable flow . . . . .	129
<b>7</b>	<b>Conclusion and recommendation</b>	<b>133</b>
7-1	Summary of results and discussion . . . . .	133
7-2	Further research . . . . .	136
	<b>Glossary</b>	<b>143</b>
	List of Acronyms . . . . .	143
	List of Symbols . . . . .	143

---

# List of Figures

1-1	The aquifer thermal energy storage in heating and cooling operation. [4] . . . . .	2
2-1	Main components of the substation at the VJK building. (Not hydraulically correct)	12
2-2	State transition diagram of the VJK building derived from the 'Regel Technische Omschrijving'. The abbreviations of the component groups and the variables are defined in respectively, Table 2-2 and 2-3. . . . .	16
2-3	The split range for the PI controller over the valve and pump at the network heat exchangers. . . . .	18
2-4	Relevant basic schemes in ISSO-39 [3] . . . . .	19
2-5	$T_{\text{HEX}_h, \text{prim}, \text{out}}$ correlated with the flow on primary and secondary side of $\text{HEX}_h$ .	24
2-6	Correlation between the evaporator, DC and $\text{HEX}_h$ at the secondary side . . . . .	25
2-7	Correlation between the measured condenser and evaporator energies. . . . .	26
2-8	The flows measured by the energymeter of the condensers correlated with flow measurements of the pumps itself. . . . .	27
2-9	Correlation between the evaporator energies and the condenser energies when calculated according to $Q_{\text{cond}} = Q_{\text{evap}} + W_{\text{comp}}$ . . . . .	27
2-10	Energy heat demand correlated with the building supply temperature. . . . .	28
2-11	Measured condenser energy correlated with the building heat demand. . . . .	29
2-12	Correlation of the cold building distribution network entering and leaving temperatures with the cooling demand. . . . .	30
2-13	Temperature leaving the evaporators correlated with the temperature entering the secondary side of the warm heat exchanger. . . . .	31
2-14	Correlation between the energy provided by the warm heat exchanger and the energy consumed by the evaporators of the heat pump. . . . .	31
2-15	Correlation between the energy provided by the warm heat exchanger and the energy consumed by the evaporators of the heat pump under the condition $T_{\text{HEX}_h, \text{sec}, \text{in}} \leq 7.0^\circ\text{C}$ and $T_{\text{evaps}, \text{out}} \geq 8.0^\circ\text{C}$ . . . . .	32
2-16	Correlation of the outside temperature with the cooling and heating energy extracted from the thermal storage. . . . .	32

2-17	Correlation of the outside temperature with the heating and cooling demand of the building. . . . .	33
2-18	On/off switching of the cold heat exchanger as a result of $T_{c, \text{buffer, bottom}} \leq 9.0^\circ\text{C}$	35
2-19	The effect of the drycooler and the server room on the temperatures to the grid .	36
2-20	Short-cut flow over the cold buffer causing too high $T_{\text{HEX}_h, \text{sec, in}}$ . . . . .	37
2-21	The instability of the complete substation . . . . .	38
2-22	Various building energy demand curves . . . . .	39
2-23	Various building heating demands responses including the HT . . . . .	40
3-1	WANDA model of the substation . . . . .	50
3-2	WANDA model of the substation including the control systems . . . . .	51
3-3	The added 3way valve at the condenser side of the heat pump to improve the temperature control . . . . .	57
3-4	The distribution of the heat pump capacity steps over the PI controller output .	58
4-1	MPC receding horizon policy [5] . . . . .	64
5-1	Case 0: warm building network modelled with the standard control methods . . .	92
5-2	Case 1: warm building network modelled with the standard control methods . . .	93
5-3	Case 2: warm building network modelled with the standard control methods . . .	93
5-4	Case 3: warm building network modelled with the standard control methods . . .	94
5-5	Case 4: warm building network modelled with the standard control methods . . .	94
5-6	Case 5: warm building network modelled with the standard control methods . . .	95
5-7	Case 6: warm building network modelled with the standard control methods . . .	95
5-8	Case 7: warm building network modelled with the standard control methods . . .	96
5-9	Case 8: warm building network modelled with the standard control methods . . .	96
5-10	Case 9: warm building network modelled with the standard control methods . . .	97
5-11	Case 10: warm building network modelled with the standard control methods . . .	97
5-12	Case 11: warm building network modelled with the standard control methods . . .	98
5-13	A simulation of the response of the current heat pumps (LT-HP) to the temperature and energy demand with a significant response of the HT . . . . .	99
5-14	A simulation of the response of heat pumps that can reach higher temperatures (HT-HP), where there is only a short response of the HT due to the slow HP response. . . . .	100
5-15	A simulation of the response of the current heat pumps (LT-HP) to the temperature and energy demand with a significant response of the HT . . . . .	100
5-16	A simulation of the response of heat pumps that can reach higher temperatures (HT-HP), where there is only a short response of the HT due to the slow HP response. . . . .	101
5-17	The effect of the proposed changes on the control of the warm heat exchanger. .	102
5-18	The effect of the proposed changes on the control of the warm heat exchanger at the heat pump group. . . . .	103

5-19	The response on different changes with different pump and three-way operations to control $T_{HP1, cond, out}$ . . . . .	104
5-20	Case 0: warm building network modelled with the temperature and capacity PI control . . . . .	106
5-21	Case 1: warm building network modelled with the temperature and capacity PI control . . . . .	107
5-22	Case 3: warm building network modelled with the temperature and capacity PI control . . . . .	107
5-23	Case 5: warm building network modelled with the temperature and capacity PI control . . . . .	108
5-24	Case 7: warm building network modelled with the temperature and capacity PI control . . . . .	108
5-25	Case 9: warm building network modelled with the temperature and capacity PI control . . . . .	109
5-26	Case 10: warm building network modelled with the temperature and capacity PI control . . . . .	109
5-27	Case 11: warm building network modelled with the temperature and capacity PI control . . . . .	110
5-28	Case 1: warm building network modelled with the temperature and capacity PI control with setpoint adjustment based on the net condenser mass flow . . . . .	111
5-29	Case 11: warm building network modelled with the temperature and capacity PI control with setpoint adjustment based on the net condenser mass flow . . . . .	111
5-30	Case 1: warm building network modelled with the temperature and capacity PI control with setpoint adjustment based on buffer temperatures . . . . .	112
5-31	Case 11: warm building network modelled with the temperature and capacity PI control with setpoint adjustment based on buffer temperatures . . . . .	112
5-32	Case 0 using the MPC controller with a fixed mass flow over the condensers according to the strategy described in Table 5-1 . . . . .	114
5-33	Case 1 using the MPC controller with a fixed mass flow over the condensers according to the strategy described in Table 5-1 . . . . .	115
5-34	Case 11 using the MPC controller with a fixed mass flow over the condensers according to the strategy described in Table 5-1 . . . . .	116
5-35	Case 1 using the MPC controller with a variable mass flow over the condensers. ( $N_{McC}=1$ ) . . . . .	117
5-36	Case 11 using the MPC controller with a variable mass flow over the condensers. ( $N_{McC}=1$ ) . . . . .	118
5-37	Case 11 using the MPC controller with a variable mass flow over the condensers and a maximum computation time of 60 °C. ( $N_{McC}=1$ ) . . . . .	118
5-38	Case 1 using the MPC controller with a variable mass flow over the condensers. ( $N_{McC}=3$ ) . . . . .	119
5-39	Case 1 using the MPC controller with a variable mass flow over the condensers and a maximum computation time of 60 °C. ( $N_{McC}=3$ ) . . . . .	120
5-40	Case 11 using the MPC controller with a variable mass flow over the condensers. ( $N_{McC}=3$ ) . . . . .	120
5-41	Case 11 using the MPC controller with a variable mass flow over the condensers and a maximum computation time of 60 °C. ( $N_{McC}=3$ ) . . . . .	121
6-1	Case 0: Comparison of capacity changes for the current control methods and the capacity control method proposed . . . . .	124

---

6-2	Case 0 using the capacity controller, the temperatures at all locations in the warm substation network. . . . .	125
6-3	Case 0 using the MPC controller with the corresponding optimisation times. . . . .	128
6-4	Case 1 using the MPC controller with the corresponding optimisation times. . . . .	128
6-5	Case 11 using the MPC controller with the corresponding optimisation times. . . . .	129
6-6	Case 1 using the MPC controller with a variable mass flow over the condensers with the optimisation times. ( $N_{McC}=1$ ) . . . . .	130
6-7	Case 11 using the MPC controller with a variable mass flow over the condensers with the optimisation times. ( $N_{McC}=1$ ) . . . . .	131

---

# List of Tables

1-1	Definitions of the primary and secondary sides for heat transfer devices. . . . .	4
2-1	Overview of substation component specifications . . . . .	13
2-2	Substation component abbreviations explained . . . . .	15
2-3	Variable definitions used in the state transition diagram of the case study (Figure 2-2)	15
2-4	Actively controlled components in the substation . . . . .	17
2-5	The ranges and goals of the temperature and energy deliveries. . . . .	18
3-1	Overview of the assumptions . . . . .	52
3-2	The selection of the cases and their warm distribution building network properties	53
3-3	PI-control values, 3-way control valve and capacity . . . . .	61
4-1	Properties of the heat pump. . . . .	69
4-2	Heat exchanger properties . . . . .	70
4-3	Drycooler connection properties. The energy added/removed in a cell is the total energy divided by the number of cells . . . . .	70
4-4	The input variables and the corresponding constraints and conditions, from which the implementable auxiliary variables and constraints can be introduced . . . . .	75
4-5	List of input variables that require multiple methods to determine the input . . . .	78
4-6	Constraints linked to state variables . . . . .	82
5-1	The values that determine the MPC strategy . . . . .	113



---

# Preface

This thesis report forms my final tasks in completing the Master study programs of Systems and Control and of Mechanical engineering: Energy, Flow and Process Technology at the TU Delft. This project has once again confirmed my drive for the combined approach of control and energy. The devil is in the details and a proper understanding of both fields is required to ensure a satisfactory operating system.

I am thankful of the TU Delft for providing me the opportunities to complete my academic career with this interesting project which combined my interest of both fields. It introduced me to the dynamics and the challenges facing energy systems which will become more important over the upcoming decades. A proper tuning of both fields is required to achieve the goals. I am thankful of the University of Utrecht where my case study is hosted and where I got involved in a project to standardise the design of these substations. I want to thank all who have contributed to my thesis project in many different ways. In particular I would like to thank the following people:

Dr. Ivo Potfhof. I remember our first meeting to discuss a possible thesis opportunity regarding control problems faced in the 5GDHC substations. You sparked my interest in district heating heat networks, which allowed me to learn that this is an increasingly active and interesting field. Thank you for your guidance and discussions regarding the approach and the counselling throughout the past months. I particularly want to thank you for encouraging me to hand in an abstract for the International Sustainable Energy Conference 2022 in Austria as I enjoyed the experience of the conference. This and my whole thesis project has also contributed to my believe that I would like to continue to be involved in research.

Prof. dr. ir. Tamas Keviczky. During my first year at Systems and Control, you taught several of the courses I was taking, with great knowledge. Thank you for your trust and confidence to allow me to work on my own towards my own goals. While simultaneously if I was running into a problem your expertise always guided me in the right direction.

Ing. Frans Tak. Thank you for guiding me through the bureaucratic at Utrecht University. Your expertise in the practical field was of great importance to get a proper image of how these systems are set up and what all has to be considered to ensure a proper operation.

My family and friends. Thank you for your support throughout these times. Your input, feedback and encouragements as well as the valuable distractions have helped me tremendously over the past months.

Delft, University of Technology  
5 July, 2022

F.P.J.H. Janssen



---

# Chapter 1

---

## Introduction

### 1-1 General

Heating and cooling energy consumed in buildings make up 73% of the total energy use of buildings and it is therefore relevant to improve the use of renewable sources of heat energy, to reduce the production of greenhouse gasses and to meet the goals of the Paris Climate Agreement [2]. As the heating and cooling demand of residential and utility buildings are at relatively low temperatures compared to the industry, making it sustainable is also easier. Many systems that have been designed and improvements that have been made to reduce the energy consumption and shift to renewable sources, are becoming more widely available. Keeping in mind that the cooling demand will also increase, the use of warm and cold thermal energy storage using ATES will become more relevant.

Networks connecting ATES wells and large utility buildings require a substation that is able to operate within strict limits. Several substations (in Dutch 'Bodemenergie centrale') have already been installed, but they are often not meeting the expected performance and are possibly degrading the quality of the wells. Problems around these substations are generally a result of the interaction of the thermo and hydraulic components and the controllers installed.

In the Netherlands proper guidelines have been developed for the design and demand of such substations. Stated in ISSO-39 [3], however there is no information provided on how to control such a substation in a stable and efficient manner, besides the type of operations that it can run. Also the certification and the guidelines provided by the BRL6000 [6] only consider the types of certification and demand that have to be considered, there are no standards available on how to control such substations.

#### 1-1-1 ATES and 5GDHC

Aquifer Thermal Energy Storage (ATES) is an underground thermal energy storage. Utilising a double well system (doublet) where relatively warm and cold water is stored in aquifers, the subsurface sandy layers storing groundwater. Commonly, ATES is used for seasonal storage of thermal energy, which is extracted to either heat or cool a building. These wells consists

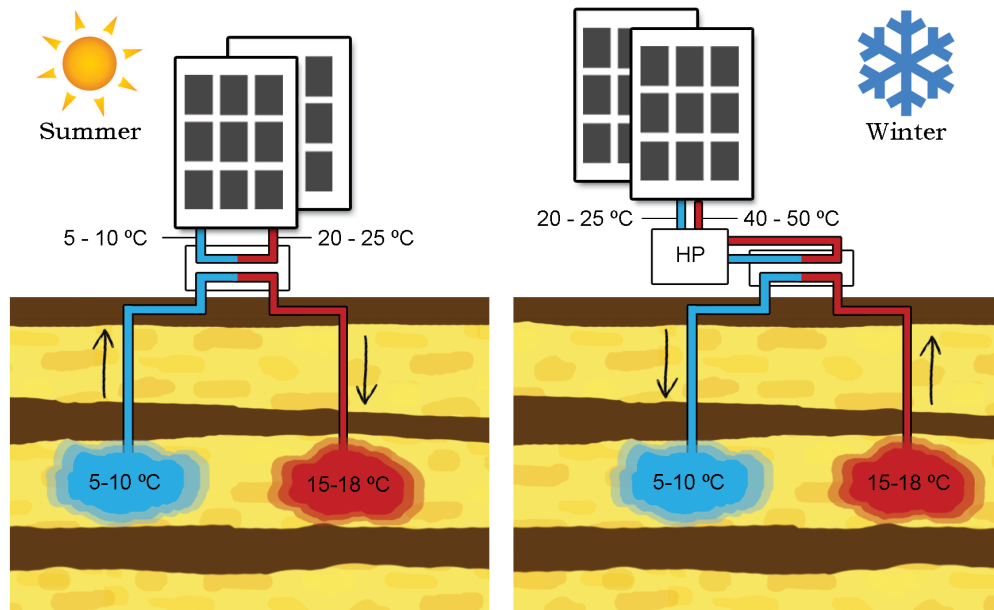


**Figure 1-1:** The aquifer thermal energy storage in heating and cooling operation. [4]

of large quantities of water where the temperature difference of the well compared to the surroundings is relatively small, resulting in a limited heat loss which is generally a huge problem for thermal energy storage [4].

The ATES system shown in Figure 1-1 can be operated in two directions, the case where building heating is required, generally in the winter, will be explained first. Water is extracted from the hot wells using pumps after which it passes a heat exchanger, which cools down the water from the wells to around 5-8°C while the water on the building side is heated. The cooled water is then stored in the cold aquifer. The well side is referred to as the primary side while the building side is called the secondary side. In the heat exchanger the temperature difference between both sides is generally very small to maximize the thermal energy usage, this results in a temperature difference between the entrance and exit of the heat exchanger at the secondary side however the temperature is still too low for the water to be directly used to heat the building.

In the summer the system is reversed, water is extracted from the cold wells and heated in the heat exchanger by heat excess of the building and then stored in the warm wells. The secondary side is cooled down and can be used to extract heat from the buildings, providing a cooler indoor climate in the summer. Fluid from the wells cannot directly be used by buildings as this fluid should remain at a high pressure to prevent degassing of the ground water. Furthermore, there might be dirt or residuals in the groundwater, while the building systems require clean water. A heat exchanger is required between the network (primary) and the building system (secondary).

District Heating (DH) networks have been used since the late 19<sup>th</sup> century, however, several major changes have happened. They accommodate an increase in efficiency of heat consumption and a reduction of the environmental impact compared to boilers and heating

systems at a local/building level. First generation DH used steam as a heat carrier, these had a large heat loss and problems with corrosion due to condensation. While second generation DH network operates with pressurized hot water, using temperatures over 100 °C, the heat losses were still large. Third generation DH networks appeared from the 1970s onwards, it used pressurized water as a heat carrier, however, the temperature has been reduced to below 100 °C. Since most buildings relied on space heating by radiators with a supply temperature of around 80 °C the temperatures in the third generation DH network are always above 70 °C. These high temperatures did not allow for the implementation of renewable resources and still had high heat losses. Fourth generation DH networks, developed from 2015 onwards, utilises temperatures below 70 °C, which was possible because of the lower heat demands and supply temperature demands by buildings since the buildings themselves reduced their heat loss and because of the installation of floor heating.

Lower temperatures allow for the connection of renewable resources to the network. Even though 4GDH was only recently developed, the introduction of the 5th Generation District Heating and Cooling (5GDHC) network was introduced quickly after. The 5GDHC network is provided with multiple names in literature, like cold district heating network and can be compared to a water-loop heat pump system (WLHP). It can be defined as a DH network that allows simultaneously producing hot and cold water at substations by distributing water in the range between 10 °C and 25 °C. [7, 8].

Since the ATES network is based on heat and cold storage, the primary return temperature of the substation has to be within strict limits to stay within the regulations for the energy storage in the groundwater and to maintain operational temperatures for other buildings to cool or warm [9]. These limits and guidelines are not required in other generation heat networks and have therefore not extensively been studied on the building side.

## 1-1-2 Substations

Substations have generally not been used in older generation networks as it is solely a heat exchanger with some valves and pumps. However, buildings not connected to a network are well familiar with a central point of the heating (and cooling) building distribution systems, where the energy is generated. In the 5GDHC substation both these functions are combined and therefore consider multiple components. The design of such substations is discussed in Section 2-1.

### Definitions

As the substation is in between the network and the building delivery units like the distribution system, radiators and other components. It is important to make this demarcation properly as it also determines the goals and the requirements it must meet from other sections. There can be a great deal of confusion about which pipes, connections and sensors are meant. This confusion originates from the general terms return and supply. These terms seem to be rather simple and straight forward, however they depend on from which perspective you are looking, the network side, the substation side or the building side. The heat exchanger between the substation and the network contains two sides, the primary side, connected to the network and the secondary side connected to the substation:

Heat exchanger	Primary	Secondary
Cold delivery 5GDHC	Network	Substation
Heat delivery 5GDHC	Network	Substation
Building delivery hot	Substation	Building
Building delivery cold	Substation	Building
Heat pump	Evaporator	Condenser
Drycooler HEX cold	Drycooler	Substation
Drycooler HEX hot	Drycooler	Substation
High temperature HEX	HT network / conventional heater	Substation

**Table 1-1:** Definitions of the primary and secondary sides for heat transfer devices.

- The primary side contains an in and out flow, which are often respectively referred to as network supply and network return.
- The secondary side also contains an in and out flow, however they are referred to differently depending on observer's perspective, from the component or network or from the building.

If the perspective is from the network or the component (heat exchanger), the in and out flow are respectively referred to the (heat exchanger) supply and the return flow/temperature/pipe. However from the buildings perspective, it is often referred to as the building return and the building supply flow/temperature/pipe, as it contains the water that is returned from the building and supplied to the building. There have even been occasions where the secondary in and out flow are referred to as supply from building and return to building. To avoid confusion in this report the flows of the heat exchangers have been assigned primary/secondary in/out, where in and out are defined by the flow direction and the primary and secondary sides are defined by convention shown in Table 1-1. In general the side providing the heat or the cold is called the primary side and the side requesting the heating/cooling is called the secondary side.

Furthermore, as at the Heat Pump (HP) the same confusions can arise, the sides are generally defined by the location at which they are connected, the evaporator and the condenser, however in some systems these are respectively defined by the primary and secondary side as the main function is heating, when the same device is also used for cooling this definition remains the same. To prevent confusion, in this report it will be referred to as evaporator and condenser side.

## 1-2 Literature review on 5GDHC and related control

As 5GDHC networks operate at low temperatures, the substation design becomes more complicated [10]. Requirements on returning temperatures to the network are strict due to temperatures on the ATEs doublet, while simultaneously the heat/cold demand in large utility buildings might vary a lot. Current research has mainly focussed on individual components of a substation or a complete grid. Connection between network and utility buildings are only roughly covered and (short term) control recommendations are not available [7] [11]. However, these 5GDHC substations are more complex and have a wider variety of demand

and responses, and consist of hybrid control, influencing the short-term stability. Connections from the utility building to the 5GDHC network provide strict restrictions, to allow for seasonal storage and/or the opposite heat/cold consumption in other buildings. At Utrecht University, the 5GDHC network is connected to Aquifer Thermal Energy Storage (ATES) wells, thereby there are strict limitations on the minimum and maximum temperatures that are allowed to be injected in the cold, respectively warm wells by law. Besides the minimum and maximum temperature it is important to not deviate too much from the preferred temperature to maintain the quality of the wells.

Some of the known problems with return temperatures of 4GDH and its causes can also be considered for 5GDHC. Examples are short-circuited flows, low supply temperatures and setpoint errors [9]. Known issues and challenges familiar to 4GDH are related to low return temperatures as a result of setpoint errors and control problems. But, according to [12], the system design itself may also contribute to these issues. where the most issues regarding low return temperatures are a result of setpoint errors and control problems, however system design can also contribute to it. Here the need for better and more intense metering systems is highlighted to understand and undertake action on these problems and improve the systems performance. Additionally, set-point temperature errors and substation control are known problems in DH substations for proper return temperatures [13].

There is extensive literature available on every individual type of component within a 5GDHC substation. Many components influence the hydraulics characteristics of a system, but there are only a few components that affect heating/cooling significantly. Main components related to thermal characteristics of a 5GDHC substation are the HP, the heat exchanger connecting the grid and possibly a conventional heater or dry cooler. As there are many different types, they are specifically selected for the purpose they have to fulfil, very small approach temperature or large temperature jumps. As well as their performance is generally well studied, the effect of control strategies and off-design conditions is often not considered in detail or not in the larger picture.

The control of district heating networks is widely discussed in literature, however control strategies in conventional district heating networks cannot simply be copied to 5GDHC networks or the ATES ring network. Examples of frequently applied control strategies in earlier generation district heating networks are differential pressure control and supply temperature control [10]. Older DH networks only had the function to heat buildings and not to cool, the hot branch was always the supply branch and required a higher pressure to ensure a proper direction of the flow. In 5GDH the pressure in both loops should be equal as the supply can be either the cold or the hot pipe depending on the operation type, cooling or heating, as a result, the pressure in both pipes should be similar. Any pressure difference should be a result of the decentralised pumps in the substations and is therefore dependent on whether there is a higher net cooling or heating demand in the network. One of the possibilities to control the decentralised circulation pumps is to ensure that the temperature difference over the primary side of the heat exchanger is constant, therefore enabling the wanted return temperature [14].

Classical control strategies (PID and Rule based control) have as main advantage that it is robust, though there is only a limited capability to deal with the operating constraints of renewable sources [15]. [11] discusses multiple control strategies related to district heating networks and makes the distinction for control strategies suitable for 5GDHC since HPs are required and in the case of DHC bidirectional flow is used. Advanced control strategies

provide the ability of peak shaving and valley filling, interacting with the electricity grid and optimizing operation. Operational optimization can for example be accomplished with respect to a minimization of peak power or cost. Usually, it becomes a mixed-integer non-linear problem, non-linear because of the time delays and mixed-integer because of the ability to turn devices on/off. MPC can be a robust form as model mismatches will be visible in the feedback, however, the time delays should not be too large, to prevent oscillations. Distributed control is frequently applied by providing prices related to energy consumption and include multi-agent systems to ensure that constraints within each agent are met. Hybrid control is often also a multi-agent systems, a combination of MPC and distributed control, where the operation is optimized centrally after which the optimal loads are distributed to the agents.

As stated by [16] the better the model is performing, so the more detailed and close to reality it is, the better the system can be controlled, as it is more predictable, therefore resulting in a more stable system with less abrupt control actions resulting in oscillations. However, one should always keep in mind the effects of large disturbances and predictions.

[11] discusses multiple control strategies related to district heating networks and makes a distinction for control strategies suitable for 5GDHC since HPs are required and in the case of DHC bidirectional flow is used. Control strategies for traditional DH systems are generally classical control methods, which can be divided in Rule Based Control (RBC) or PID, and are mostly implemented in the production level. These include (minimum) supply temperature control, minimum pressure differential control, minimum/maximum pressure control and finally heat demand and flow control which is the only method used at the substation level. In 5GDHC there is not one central production location and the temperature can not simply be changed one sided, the pressure control is often distributed, since the flow is bidirectional and there should be no differential pressure. Possibilities and challenges of data-driven models and statistical time series forecasting methods are discussed. Advanced control strategies can be used in a centralized and decentralized manner which should work on top of the basic control strategies of individual components. Many variations of Model Predictive Control (MPC) have been researched, which allow for a reduced energy consumption, reduced CO<sub>2</sub> emissions, and/or energy and maintenance costs.

Control of substations is less widely discussed. As the substation consists of many different components that can be switched on/off or between discrete capacities, binary variables are of utmost importance. A switching logic, which is necessary when elements can be turned on/off, needs to be selected with great caution to prevent ‘chattering’, too fast switching. Two main strategies to prevent this are the hysteresis switching and the dwell time switching. The MLD model can for instance be used in mixed linear integer programming (MILP) to describe these systems and to solve optimization problems and find a proper control method [17].

The substation consists of many different components and that bring their own challenges and provide unique properties to the complete system, the combination of which are the cause of some of the problems and challenges faced in the control of 5GDHC substations. From control perspective these challenges and properties can be defined as [18]:

- Nonlinear dynamics
- Slow rise and settling times

- Time-varying system dynamics and set-points
- Time-varying disturbances from a multitude of sources
- Poor data availability
- Interacting and conflicting control loops
- Lack of supervisory control

[19] discusses an MPC to minimize energy costs for cooling of buildings. The system considered could be compared with a simplified substation with less components. Main differences would be the ability for heating and the considered horizon. The study concluded that a significant reduction in required energy is achieved compared to the baseline as the predicted weather conditions and building loads are implemented, however some of the control schemes suggested by MPC correlate largely with control profiles chosen by plant operators.

[20] develops a control strategy based on the optimisation problem to minimize the difference between the desired comfort and the realised comfort (reference tracking) and to minimize the cost related to the operation (mainly cost of the pumps and the HPs). The constraints on stored energy in the wells have been considered, however here only the effect of a single building has been taking into account and therefore the effects on the well temperature and the specific temperatures range in which heat/cold has to be delivered back are not taken into account. Furthermore, as the time step is one week, only the long-term effects are considered and non of the dynamic operational effects therefore are accounted for.

Finally there are also models which even consider the building dynamics its self and the heat load it can store using RC-models (resistor-capacitor), however this is general done for small buildings, with enough information and thus the ability to peak shave some of the demand.

It can be concluded from the literature survey that the control of substations in 5GDHC networks with bi-directional energy flows requires more attention. Focus on the short-term stability is a crucial aspect, as most of the literature is focussed on hourly or longer heat demands as well as the operational dynamics of a substation.

## 1-3 Problem statement and research objective

This thesis tackles the problems observed in the current design of the substations at the case study in Utrecht University, and for a more general substation design and defines potentials for improvements. It is researched by combining the fields of hydro- and thermodynamics and the control design.

The objective of this thesis based on the case study is: To improve the design of the substation and the control structure from a thermo-hydraulic and control perspective and provide guidelines for future designs.

Research questions:

- How can the substation be operated stably and how can the utilization of the ATES system be maximised, thus reducing the heat consumption from other sources, while maintaining building comfort and meeting the network restrictions?

Subquestions:

- How can the strict temperatures limits of the ATES network (better) be achieved?
  - What adaptations in the control system are required?
  - If needed, what adaptations in the thermo- and hydraulic design are needed?
- How can the heat pumps be operated on stable conditions while meeting the building demand?
  - What adaptations in the control system are required?
  - If needed, what adaptations in the thermo- and hydraulic design are needed?
- How can the control of the substation be improved to (better) meet the building demand and minimise the use of the conventional heater?
  - What adaptations in the control system are required?
  - If needed, what adaptations in the thermo- and hydraulic design are needed?
- Which improvements may Model Predictive Control introduce to the operational performance of the substation?

Hypotheses:

- The strict temperature limits of the ATES network can be better achieved by thorough simulations and determination of the hysteresis and PID control set points and goals.
- It is key that the components are chosen to match the building demand conditions, both in energy and temperature, to minimise the use of conventional heaters.
- Heat pumps (and the direct components) should be able to be operated such that the temperature on both sides of the heat pump can be controlled, irrespective of the capacity it is operating on.
- The substations ability to meet the demand is mainly based on the selection of the components and its ability to respond quickly.
- Model Predictive Control could improve the operation of the substation given that an accurate demand is provided and ideally large enough buffer capacities are available as it will accommodate for the (un)loading.

## 1-4 Methodology and outline

The methodology to reach the objective is the guide throughout this thesis. The outline of the chapters provide this methodology:

An introduction about 5GDHC networks and their substations together with the scope and objectives is provided in Chapter 1. The current design of substations, the case-study at Utrecht University and the differences with the standard are discussed in Chapter 2. Data analysis of the captured data at the case study are also discussed as this forms the basis to quantify and determine the problems/challenges on how to improve the substation design and control. Also from the data analysis, some cases have been extracted for simulations purposes later on. In Chapter 3 the model of the substation is introduced, simulations and verifications have been performed and some first thermo-hydraulic and low-level control improvements have been tested. Chapter 4 introduces the Model Predictive Control (MPC) controller design and simulations to determine whether this can improve the performance even further. In Chapter 5 the results of all the previous simulations are provided and the effects are considered in detail. The differences and performances are discussed and compared in Chapter 6. Finally in Chapter 7 the conclusions for the above stated objective and research questions is provided and recommendations for both the case study and future research are mentioned.



---

## Chapter 2

---

# System description

The 5th Generation District Heating and Cooling (5GDHC) substation is researched based on a case study at the University of Utrecht, where such a system is in use at a utility building and where they have encountered multiple problems and inefficiencies. Utrecht University has adopted an ATES system to deliver thermal energy from a renewable source, storing and upgrading the seasonal thermal energy. Hot and cold water storage wells are connected to a double ring network with a cold and hot flow. Multiple buildings at the campus of the University of Utrecht are connected to this ring network to extract thermal energy. The case study considers one substation connected to this heat network, located in the Victor J. Koningsberger building. Reason for choosing this substation is that the system design including hydraulics is closely related to the ISSO-39 standard [3], and that it is equipped with many sensors.

One of the challenges associated with this 5GDHC network, is the strict limitations on the return temperature to the grid as other buildings might be using the heated/cooled water directly and as well for the quality of the thermal wells, which was not a parameter for older generation heating grids. For the case study, the return temperature to the cold ring should remain below  $7.5^{\circ}\text{C}$  and to the warm ring above  $16^{\circ}\text{C}$  and below  $24^{\circ}\text{C}$ . These limits are often not met because of instabilities, inefficient control or complications in the substations, devaluating the quality of the storage wells and the system's efficiency and sustainability.

Besides the network side, the requirements for the building are not always achieved with the preferred components. The consumption of heat provided by the Heat Pump (HP) is preferred over a Conventional Heater or High Temperature source (HT). Yet the current operations of the heating system show that the HT is in operation even though the HP is not working at full capacity, or is even forced to reduce its capacity because of too high return temperatures from the building. To improve these issues, flaws in the (control) design must be identified and guidelines for thermodynamic and control design of these substation have to be improved, to maximize the effectiveness of the thermal storage and the utilisation of the HP. The goals are:

- to maximize the utilization of the ATES system

- to reduce the heat consumption from non sustainable sources
- to keep the return temperatures to the grid within the strict requirements
- to maximize the efficiency of the complete substation

## 2-1 System description

A schematic overview of the 5GDHC substation is provided in Figure 2-1. It consists of a Heat exchanger (HEX) for heating and a HEX for cooling. On the primary supply side of both heat exchangers there is a circulation pumps and a control valve, to control the flow over the HEX. The secondary sides of the network heat exchangers are connected in a different manner. The cooling heat exchanger using the return flow from the building cooling net as the secondary input and supplies the secondary output a bit further down stream, before the buffer, allowing the cooled water to flow over the cold buffer. The heating HEX is connected to the evaporator of the HPs in parallel to the cold buffer, taking the outflow of the evaporators as the secondary inflow of the heat exchangers and the evaporator inflow as the secondary outflow. It is important to notice that the secondary side of this heat exchanger also contains a connection with the Dry Cooler (DC) allowing to load additional cold to keep the ATEs wells in balance. An overview of the main component specifications to get a grasp of the size are stated in Table 2-1.

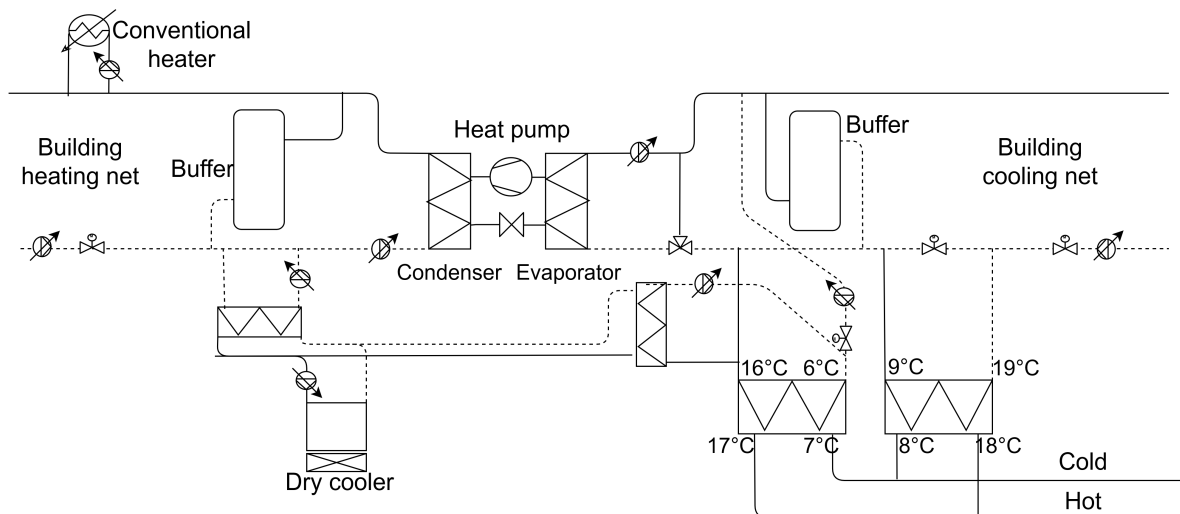


**Figure 2-1:** Main components of the substation at the VJK building. (Not hydraulically correct)

One of the key components in a 5GDHC substation is the HP. The substation of the case study contains two HPs of the same size and type in parallel, rated at a heating capacity of 250 kW each. It consists of four scroll compressors, allowing four capacity steps, over two liquid circuits using R-410A as a refrigerant. Pumps at both sides of the HPs operate to ensure a constant pressure drop over the evaporator and the condenser. The HPs can be either in heat leading or cold leading operation, both heat and cold are always produced, but this reflects the focus and the purpose for which the heat pump is running. The pump on the condenser side is controlled by a PI controller to ensure a constant pressure drop of

Component	Property	Value
Cold heat exchanger	Capacity	1200 kW
	$\dot{V}_{\text{HEX}_c, \text{sec}, \text{max}}$	$31.7 \text{ L s}^{-1}$
Warm heat exchanger	Capacity	470 kW
	$\dot{V}_{\text{HEX}_h, \text{sec}, \text{max}}$	$12.4 \text{ L s}^{-1}$
Heat pump (2x)	Heating capacity	250 kW
	Refrigerant	R410A
	COP	4.2
	Compressor type	scroll
	Compressor amount	4
Warm buffer vessel	Volume	1000 L
Cold buffer vessel	Volume	1000 L
Conventional heater	Capacity	1050 kW
Dry cooler	Capacity	500 kW

**Table 2-1:** Overview of substation component specifications

$\Delta p = 14.5 \text{ kPa}$  over the condenser, while the evaporator pump runs at 100% continuously. The three-way valve is designed such that the percentage of opening is linearly related to the mass flow through one inflow side and inversely related to the mass flow of the other inflow side.

During heat leading operation, the temperature setpoint of flow leaving the condenser is determined based on the temperature setpoint of the central heating supply and maximised at  $46^\circ\text{C}$  to ensure a reasonable Coefficient Of Performance (COP) and stay within operational limits ( $48^\circ\text{C}$ ). The temperature leaving the condenser is controlled by increasing/decreasing the heatpump capacity, while the flow leaving the evaporator is controlled at  $6.0^\circ\text{C}$  by the threeway valve and thus the temperature entering the evaporator. The minimum inflow temperature is limited at  $8.0^\circ\text{C}$  to ensure that the temperature leaving the evaporators does not fall too low in case of sudden temperature or capacity changes. During cold leading operation, the temperature setpoint of the flow leaving the evaporator is set between  $6.0^\circ\text{C}$  and  $12^\circ\text{C}$  depending on demand, but the maximum inflow temperature is controlled at  $19^\circ\text{C}$  and the temperature of flow leaving the condenser is set at a maximum of  $50^\circ\text{C}$ .

The start up procedure of the HP process is to first start up both the circulation pumps at the condenser and evaporator side of the HP and once flow is detected on both sides, the HP is started to prevent overheating or freezing of the HP. During shut down of the HP process, the HP is first turned-off after which the circulation pumps keep working up to 2 minutes to mitigate all heat. Therefore during start up and shut down there is always some energy transferred and the temperature setpoints are exceeded.

The DC is linked to two heat exchangers connecting, the warm network heat exchanger and the HPs. The first one to load additional cold to the ATES wells and the second to dissipate heat produced by the HPs when in cold leading operation. Important to note is that the small circuit between the DC and its two heat exchangers is not filled with process water, but with a ethylene glycol (30%) solution in water, reducing the freezing temperature of the fluid in the circuit to below  $-12^\circ\text{C}$ . The disadvantage of using this fluid mixture compared to water is that it has a smaller heat capacity ( $c_p = 3.6 \text{ kJ kg}^{-1} \text{ K}^{-1}$ ) than water ( $c_p = 4.2 \text{ kJ kg}^{-1} \text{ K}^{-1}$ ).

As the flow on both sides of the heat exchanger connecting the DC is controlled to be

the same, the temperature change on the ethylene glycol side is larger than on the process water side. Depending on the effectiveness and NTU of a heat exchanger, the glycol solution has to be cooled to a lower temperature for a smaller heat exchanger to ensure a certain outlet temperature at the secondary (process water) side. The temperature at the glycol solution can easily be calculated by equating the heat transfer in and out  $Q_{dc, sec} = Q_{dc, prim}$  which changes in  $\dot{m}_{glycol\ mix} c_{p, glycol\ mix} \Delta T_{glycol\ mix} = \dot{m} c_{p, water} \Delta T_{water}$ , since volumetric flows are the same, the density of the glycol mixture is 5% larger and given the above heating capacities,  $0.9 \Delta T_{glycol\ mix} = \Delta T_{water}$ . Depending on the heat exchangers the temperature jump is 1 °C to 2 °C, resulting in a glycol temperature entering the heat exchanger for cold loading at 3.0 °C to 4.5 °C, therefore the outside temperature should even be below this instead of below 5 °C to ensure a temperature returning to the HEX of 6.0 °C. Depending on what the DC is used for, a different setpoint in process water is required, 6.0 °C for loading cold to the wells while the setpoint for condenser heat dissipation is at 40 °C to 45 °C.

The cold and warm building side delivery is organised by multiple heat exchangers placed in parallel to provide the heating/cooling for different levels and sides of the building. Central distribution pumps provide the flow through these heat exchangers, which are individually controlled by a control valve. The position of the control valve of each heat exchanger also determines the temperature setpoint, of which the highest is used as the central temperature setpoint. The pressure drop over the warm building side delivery is controlled by the pumps at the return at  $\Delta p = 90$  kPa which is dependent on the pressure drop over the heat exchangers and their control valves as well as on the piping system to these interfaces. The cold building side delivery is controlled at  $\Delta p = 65$  kPa.

### 2-1-1 Control

The master controller defines the controller over-viewing all the component groups and the on and off switching between them under the appropriate circumstances (when the requirements are met). An overview of an idealised version of this controller is provided in Figure 2-2, any actions as a result of a broken or unavailable component are not considered as they are not a part of standard operation. This diagram depicts that the HT is turned on if both the HPs are turned on but the temperature setpoint is not achieved, while there is no condition on the capacity at which the HPs are operating. However, the state transition diagram does not show that the second HP can be turned off while the HT is still running. This happens when  $T_{HPs, conds, in}$  becomes too high, but the setpoint temperature is still above the maximum HP temperature or when there remains a difference in the temperature entering the building and the setpoint. Finally, the DC is also used to load additional cold to the grid, this occurs when the outside temperature is low enough ( $T < 6.0$  °C), when there is cold demand from the grid and  $\dot{V}_{evaps} - \dot{V}_{c, build} < 10$  L s<sup>-1</sup> for  $t > 15$  min.

Between the master controller and the low level PI controllers are some additional controllers that have multiple requirements before specific components of a group are turned on, a start-up or shut down procedure. For instance, when the group HPs are released in heat delivery operation, before a single HP starts up, first the pump at the condenser is started and the pressure difference controller is activated, after which the evaporator pump is started and its evaporator temperature out controller is activated with the three-way control valve in the minimum position. Finally if flow is detected on both sides the HP is started up.

Abbreviation	Component group name	binary variable
$Q_h$	Heat demand from the building	$\delta_{h, \text{ build}}$
$Q_c$	Cold demand from the building	$\delta_{c, \text{ build}}$
HP1	Heat pump 1	$\delta_{\text{HP1}}$
HP2	heat pump 2	$\delta_{\text{HP2}}$
$\text{HEX}_h$	Heat delivery, heat exchanger of the 5GDHC grid	$\delta_{\text{HEX}_h}$
$\text{HEX}_c$	Cold delivery, heat exchanger of the 5GDHC grid	$\delta_{\text{HEX}_c}$
HT	High temperature heater or conventional heater	$\delta_{\text{HT}}$
DC	Dry cooler cold loading	$\delta_{c, \text{ DC}}$
	Dry cooler dissipating condenser heat	$\delta_{h, \text{ DC}}$

**Table 2-2:** Substation component abbreviations explained

Variables	Variable explanation
$t$	Time
$t_{\text{HP1}}$	Time heat pump 1 is turned on
$T_{c, \text{ bt}}$	Temperature cooling network at the buffer top
$T_{c, \text{ set, buf}}$	Temperature set point, cooling network at the buffer
$T_{c, \text{ bb}}$	Temperature cooling network at the buffer bottom
$T_{c, \text{ set}}$	Temperature set point, cooling network
$T_{c, \text{ b, s}}$	Temperature cooling network, building supply
$T_{h, \text{ HP, o}}$	Temperature heating network, returning from heat pumps
$T_{h, \text{ set}}$	Temperature set point, heating network
$T_{h, \text{ b, r}}$	Temperature heating network, returning from building
$T_{h, \text{ b, s}}$	Temperature heating network, supplied to building
$T_{c, \text{ b, r}}$	Temperature cooling network, building return
$T_{c, \text{ HP, s}}$	Temperature cooling network, heat pump supply
$T_{c, \text{ HP, o}}$	Temperature cooling network, returning from heat pumps

**Table 2-3:** Variable definitions used in the state transition diagram of the case study (Figure 2-2)

During shut down the HP is shut down while the pumps rotate for 2 more minutes with the evaporator temperature outlet control turned off (three-way valve fully open) to ensure all heat and cold dissipated to prevent damage to HP.

The actively controlled components are listed in Table 2-4, most are controlled by PI(D) controllers, however the capacity of the HPs is based on reaching the temperature  $\pm$  a hysteresis. The PI(D) controller (2-1) is composed of a proportional gain  $K_p$ , an integral gain  $K_i = \frac{K_p}{T_i}$  and sometimes also a derivative gain  $K_d = K_p T_d$  and action. The derivative action is often not used in practice as it can result in an unstable behaviour of the system as it will even act extensively on noise.

$$u(t) = K_p e(t) + K_i \int_0^t e(\tau) d\tau + K_d \frac{de(t)}{dt} \quad (2-1)$$

The heat exchangers connecting the ring network and the substation are controlled by two cascade controllers. The primary side of the heat exchanger for heat delivery is controlled by a cascade controller of which the setpoint of the flow rate is determined on the minimum of three PI controllers. One controlling the maximum return temperature to the grid ( $T_{\text{HEX}_h, \text{ prim, out}} = 7.0^\circ\text{C}$ ), one controlling the supply temperature to the building ( $T_{\text{HEX}_h, \text{ sec, out}} = 14^\circ\text{C}$ ) and one the maximum allowable flow from the grid. The setpoint

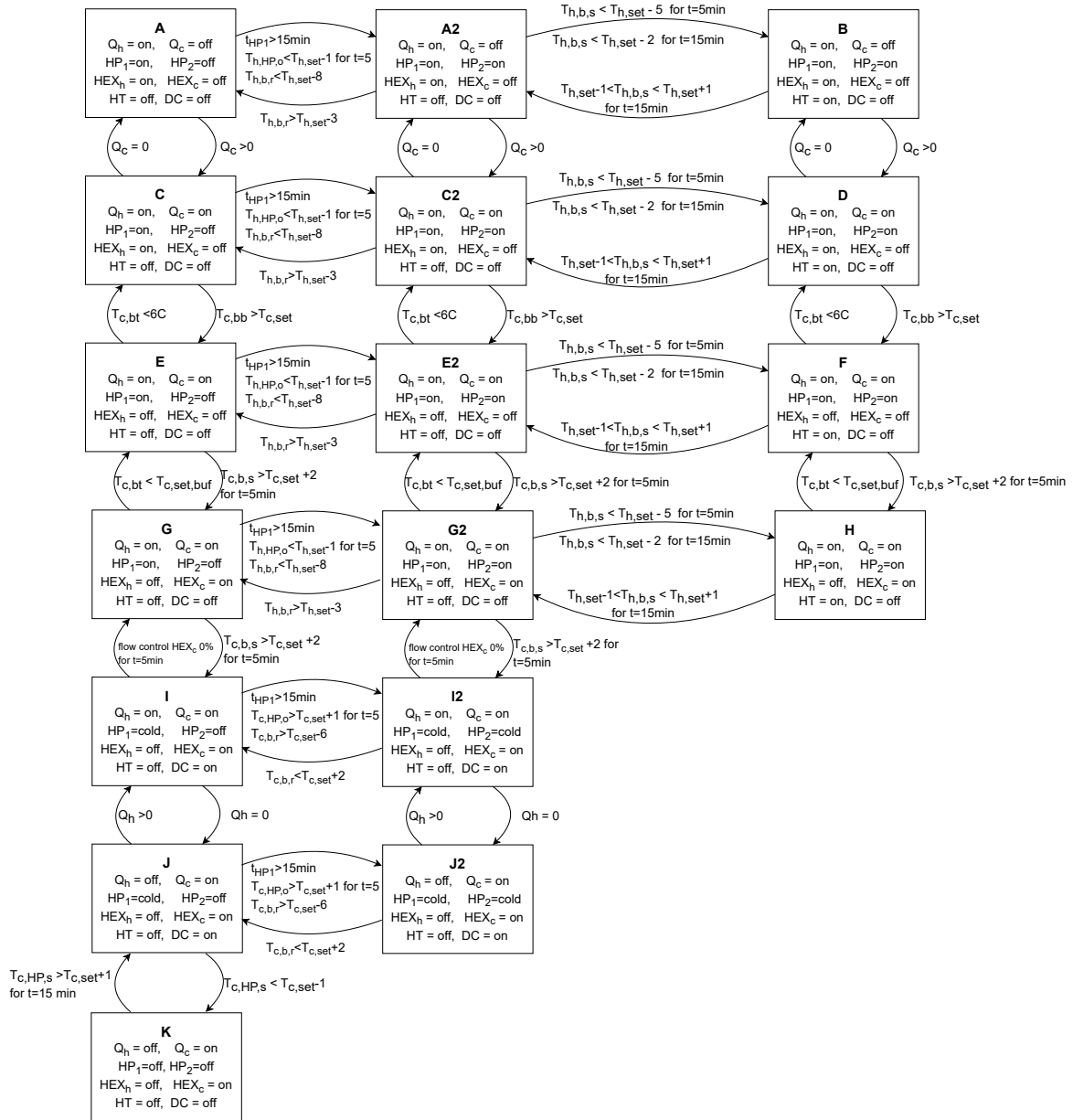


**Figure 2-2:** State transition diagram of the VJK building derived from the 'Regel Technische Omschrijving'. The abbreviations of the component groups and the variables are defined in respectively, Table 2-2 and 2-3.

Control components	State	Controlled variable	Setpoint
Heat pump	Heating	Capacity three-way valve	$T_{HP1, \text{cond, out}} = \min(T_{h, \text{set}}, 46^\circ\text{C})$ $T_{HP1, \text{evap, out}} = 6.0^\circ\text{C}$
	Cooling	Capacity three-way valve	
HEX prim pumps & control valves	Heating	$\dot{V}_{HEX_h, \text{prim}}$	$T_{HEX_h, \text{prim, out}} = 7.0^\circ\text{C}$
	Cooling	$\dot{V}_{HEX_c, \text{prim}}$	$T_{HEX_c, \text{sec, out}} = \max(9.0^\circ\text{C}, T_{HEX_c, \text{prim, in}} + 1.5^\circ\text{C})$
HEX <sub>h</sub> sec pump	Heating	$\dot{V}_{HEX_h, \text{sec, pump}}$	$\dot{V}_{HEX_h, \text{sec, pump}} = \dot{V}_{\text{evaps}} - \dot{V}_{c, \text{build}}$
Conventional heater	Heating	Capacity	$T_{h, \text{build, in}} = T_{h, \text{set}}$
Dry cooler	Dissipating heat	Capacity	$T_{h, \text{DC, out}} = 40^\circ\text{C}$
		Pump speed	$\dot{V}_{h, \text{DC}} = \dot{V}_{HPs, \text{conds}}$
	Loading cold	Capacity	$T_{h, \text{build, in}} = T_{h, \text{set}}$
		Pump speed	$\dot{V}_{c, \text{DC}} = \dot{V}_{HEX_h, \text{sec}} - \dot{V}_{\text{evaps}}$

**Table 2-4:** Actively controlled components in the substation

of the last controller can be adjusted as circumstances might occur where the maximum flow of all sources combined might be lower than the total demand of flow from all buildings. This cascade controller is used in the simulations as well, however, only the first controller is stated in the overview for clarity as this controller often takes over. For  $T_{HEX_h, \text{sec, out}} = 14^\circ\text{C}$  to be reached,  $T_{HEX_h, \text{prim, in}}$  should be above  $15^\circ\text{C}$  which only occurred 67% of the time and only 50% of the time  $T_{HEX_h, \text{sec, in}}$  was below  $6.5^\circ\text{C}$  so  $7.0^\circ\text{C}$  would be difficult to reach and the PI on  $T_{HEX_h, \text{sec, out}}$  would therefore dominate.

The main controller acts on the flow of the primary side by a split range output over the pump and the control valve (Figure 2-3). The controller output is the percentage of the absolute maximum flow, which is then split over the control valve and the pump. From 0% to 40% output of the cascade controller, the pump is working at minimum operation and the control valve opens from minimum to maximum position, with a linear increase in the flow. From 40% to 100% the control valve remains at the maximum position, while the pump increases the flow till the maximum in a linear fashion. Since revolutions per minute (RPM) and the flow rate are related in a linear fashion, the output of the controller can easily be transformed for the pump by the affinity laws.

A similar cascade and split controller is used for the cold HEX. The setpoint is determined by the maximum of the output flows of the controllers controlling the maximum return temperature to the grid ( $T_{HEX_c, \text{prim, out}}$ ) and the minimum of the flow setpoint provided by the controller controlling, the cold HEX secondary outlet temperature ( $T_{HEX_c, \text{sec, out}}$ ), the minimum return temperature to the grid ( $T_{HEX_c, \text{prim, out}}$ ) and the maximum allowable flow from the grid.

## 2-1-2 Comparison with ISSO39

The substation of the case study contains two separate heat exchangers for cooling and heating. In general this can be reduced to one heat exchanger with multiple valves to select the flows used. Furthermore, it is stated that the HP would require a three-way control valve at the evaporator side, but that at the condenser side this would generally not be necessary as the capacity is controlled on this leaving temperature. In the case study the DC circuit is connected with two different heat exchangers, while this can also be operated with just one

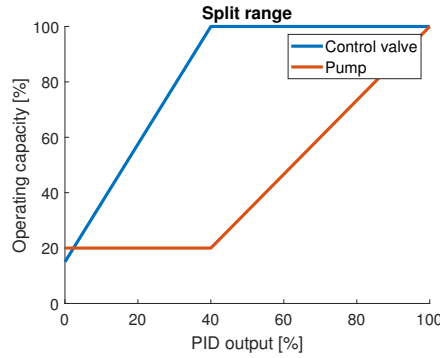


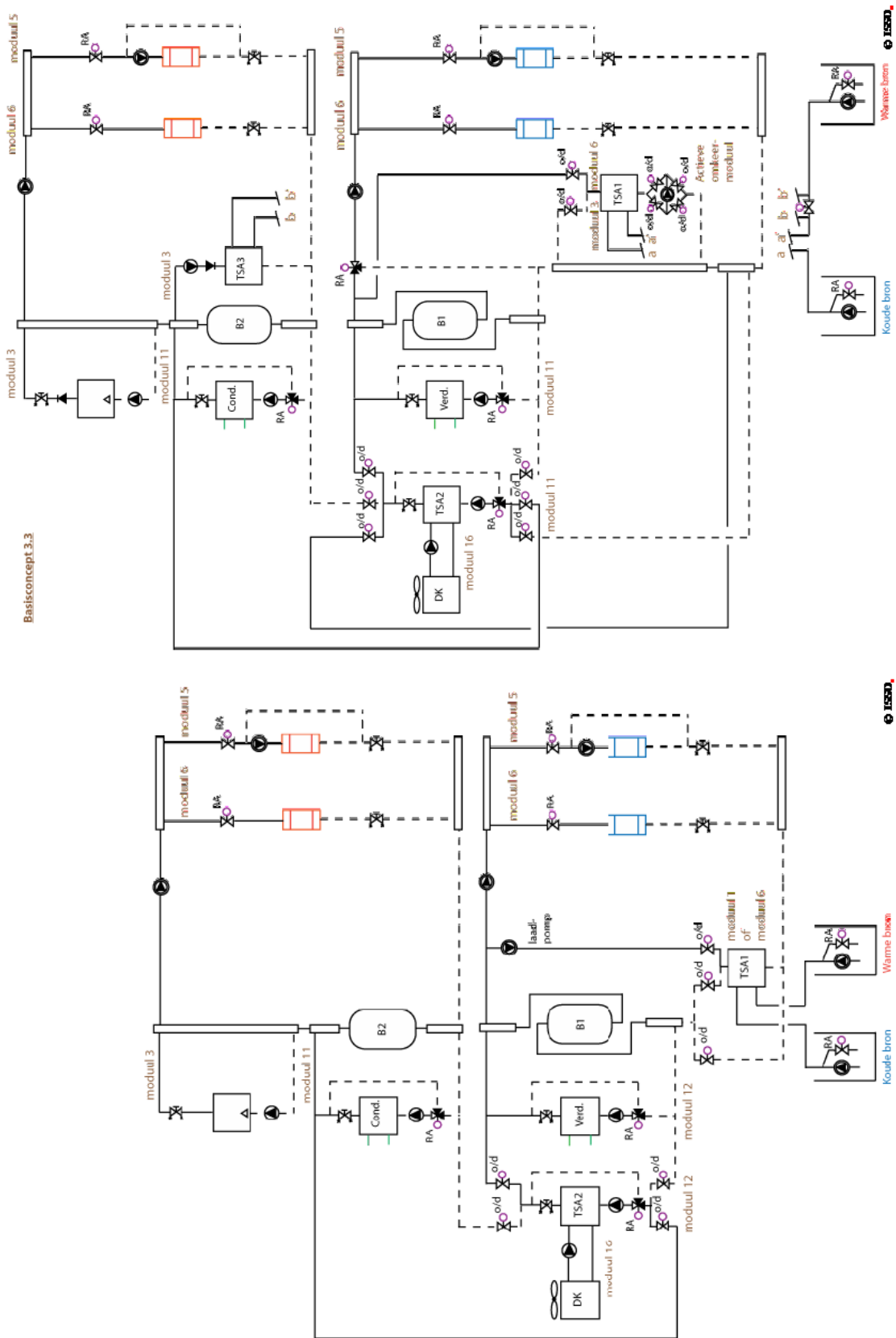
**Figure 2-3:** The split range for the PI controller over the valve and pump at the network heat exchangers.

	goal	min	max
$T_{\text{HEX}_h, \text{prim}, \text{out}}$	7.0 °C	6.0 °C	7.5 °C
$T_{\text{HEX}_h, \text{sec}, \text{out}}$	14 °C	-	18 °C
$\dot{V}_{\text{HEX}_h, \text{prim}}$	-	4 m <sup>3</sup> h <sup>-1</sup>	53 m <sup>3</sup> h <sup>-1</sup>
$T_{\text{HEX}_c, \text{sec}, \text{out}}$	max(9.0 °C, $T_{\text{HEX}_c, \text{prim}, \text{in}} + 1.5$ °C)	9	12
$T_{\text{HEX}_c, \text{prim}, \text{out}}$	17 °C	16 °C	24 °C
$\dot{V}_{\text{HEX}_c, \text{prim}}$	-	1.8 m <sup>3</sup> h <sup>-1</sup>	120 m <sup>3</sup> h <sup>-1</sup>

**Table 2-5:** The ranges and goals of the temperature and energy deliveries.

and using control valves to select the proper flows, like stated in the basic scheme 3.2 and 3.3 guidelines of ISSO-39 (Figure 2-4).

Important to notice, depending on the ISSO-39 basic scheme that is chosen the lay out may differ, the pumps required to operate the warm heat exchanger might also be operational for the cold heat exchanger. Also an additional operation point might be to add a line and three-way control valve parallel to the cold buffer, to accurately control the cold temperature entering the building, while keeping the HPs at a 6.0 °C setpoint. At maximum cold operation, when the cold building temperature setpoint is below the temperature the network can deliver, it prevents a flow over the cold buffer and thus uncontrolled mixing. This is again a difference between basic scheme 3.2 and 3.3. Therefore it is important to properly select the basic scheme depending on the demands of the building, whether there is also a strict temperature requirement at cold building side, or that temperature setpoints below 9.0 °C only occur when maximum cooling energy is demanded, thus no accurate control of the cooling temperature setpoint is required between 6 and 9.0 °C. Finally, basic scheme 3.3 has an additional advantage compared to basic scheme 3.2 as it also allows to regenerate the heat produced by the HP when operated in cooling mode as well as the loading of additional heat by a reversed operation of the DC. This is achieved by adding an additional heat exchanger after the first heat exchanger connecting the grid, where temperatures returning to the warm well are increased further.



(a) Basic scheme 3.2

(b) Basic scheme 3.3

Figure 2-4: Relevant basic schemes in ISSO-39 [3]

## 2-2 Data Analysis

Two types of data have been gathered and analysed to determine the shortcomings and problems of the current substation, the first one is 15 min yearly gathered data and the second is detailed high frequency data gathered online during the course of this research exercise. Yearly data provides an overview of the current status of the substation and the high frequency data is used to determine the causes of common problems into more depth, however these cannot be correlated as they are taken over different time frames.

The yearly data consists of time series gathered at the building Victor J. Koningsberger at Utrecht University over the year 2020, of which some sensor data is averaged over 15 minutes and others are momentary. Averaged data points consist of three values taken at a 5 minute interval, then averaged over time. The yearly gathered data are only the sensors of the energy meters, as all other sensors are only for live observation, monthly lookup and for the controllers. The energy meters are present at locations where energy is delivered or used, this is at the primary side of both heat exchangers connecting the grid, the combined secondary side of the heat exchangers, the drycooler (one is used for both loading cold and server room cooling), both sides of the heat exchanger groups, and at the delivery of the heat and cold to the building. The temperature in and out of these sections as well as the flow is saved, therefore allowing the energy to be calculated.

There are some limitations in the data. First of all, the data is an average over 15 minutes, therefore if a section is starting up or shutting down, the data doesn't present the real picture. The temperature at the cold side might rise as the section is turned down halfway the 15 minutes, therefore, there is still a measurement of the flow, and the average temperature is above the threshold, seeming like an improper operation, while in reality the operation might still be within the limits defined.

Data of the energymeter that registered the delivered heat to the consumers has issues, the data is saved under another energy meter name of which it could partially be retrieved. The saved energy and temperature entering the building seem correct, they have the right order of magnitude, and respectively correlate with data of the produced energy by the heat pumps and another temperature sensor. However the data of the flow is corrupt as it is saved as only 0 or  $0.01 \text{ m}^3 \text{ h}^{-1}$  and the return temperature from the building is too high, above  $60^\circ\text{C}$ , while these temperatures can never become as high in this part. The accuracy of the data of heat demand (energy used) is unfortunately low, it only registered in steps of 0.01 GJ for every 15 minutes. Assuming a constant heat demand in 15 minutes, as there is no way to determine the trend, the accuracy can only be set at 11 kW.

Observing the timeseries, a problem in the data can be observed from January 1st to January 30st 07.15h. For  $T_{c, \text{ build, in}}$ ,  $T_{c, \text{ build, out}}$ ,  $\dot{V}_{c, \text{ build}}$ ,  $T_{c, \text{ DC, in}}$ ,  $T_{c, \text{ DC, out}}$ ,  $\dot{V}_{c, \text{ DC}}$ ,  $T_{\text{evaps, in}}$ ,  $T_{\text{evaps, out}}$ ,  $\dot{V}_{\text{evaps}}$  and  $T_{\text{HEX}_h, \text{ sec, in}}$ ,  $T_{\text{HEX}_h, \text{ sec, out}}$ ,  $\dot{V}_{\text{HEX}_h, \text{ sec}}$  the values are constant for almost 24 hours, it seems that there is a problem with the saved data as it does not make sense to have the exact same value this long. Therefore this data is excluded.

Furthermore there is no energy meter for the HT connection, however there is a temperature sensor just before and after the HT connection that is monitored in the yearly data and the provided heat can be estimated by  $Q_{\text{HT}} = Q_{h, \text{ build}} - Q_{\text{HPs, conds}}$ . If there is a small difference between the production of the heat pumps and the consumption of the building, this does not necessarily mean that the HT is on as there is some delay. If the buffer is loaded

at a high temperature this energy can be extracted as well, therefore it is only considered if  $\Delta T$  over the HT is larger than  $2.0^\circ\text{C}$ . When  $Q_{\text{HT}}$  would be negative it could be caused by filling up the buffer or by using the DC to dissipate heat, the latter only applicable in the summer when the cold demand is larger.

In theory one could calculate the return temperature from the building and the flow, based on two cases where the flow over the condensers is larger or smaller than the flow over the building, by which the flow direction over the buffer is determined. For both the cases several equations can be set, where the third or fourth equation is selected based on the flow direction:

$$Q_{\text{h, build}} = c_p \dot{V}_{\text{h, build}} (T_{\text{h, build, in}} - T_{\text{h, build, out}}) \quad (2-2)$$

$$\dot{V}_{\text{HPs, conds}} = \dot{V}_{\text{h, build}} + / - \dot{V}_{\text{h, buffer}} \quad (2-3)$$

$$T_{\text{HPs, conds, in}} \dot{V}_{\text{HPs, conds}} = T_{\text{h, build, out}} \dot{V}_{\text{h, build}} + T_{\text{HPs, conds, out}} \dot{V}_{\text{h, buffer}} \quad \text{or} \quad (2-4)$$

$$T_{\text{h, build, in}} \dot{V}_{\text{h, build}} = T_{\text{HPs, conds, out}} \dot{V}_{\text{HPs, conds}} + T_{\text{h, build, out}} \dot{V}_{\text{h, buffer}} \quad (2-5)$$

These equations can not be solved as for the first flow direction,  $T_{\text{h, build, in}} = T_{\text{HPs, conds, out}}$  when the HT is off. All unknowns are cancelled out, resulting in a singularity. For the second flow direction, it is possible but this flow direction almost never occurs for longer periods as the mass flow of the condensers is relatively high. If the HT is on, the flow over the building can easily be calculated as both the energy and the temperatures before and after the HT connection are known.

Furthermore to determine the quality of the heat or cold delivery, it is important to notice that a small difference in temperature has a higher energetic impact when there are large flows compared to small flows. Therefore it is important to not focus solely on the temperature quality at the minimum flows or the large flows, but determine where the temperature quality is not met from the energetic perspective, thereby one can best improve the systems energetic operation. To determine how good the system is operating energetically, and therefore the temperature quality, the percentage of energy that is delivered within the desired temperature range is calculated. This way any settling times are partially considered as otherwise the temperature is too high and would not fall in the range. The temperature of the energy that is delivered with temperatures outside the desired range can be averaged over the energy to determine the temperature overshoot and how bad the quality really is.

One has to keep in mind that the energy is also dependent on the inlet temperature. If the inlet temperature is closer to the outlet temperature the energy is smaller eventhough a significant flow can occur and therefore it compromises the well's quality. If only the outlet temperature multiplied with flow is used, the temperature is compared to 0 which does not make sense, then the energy at higher outlet temperatures has a larger influence.

Using this temperature quality methods easily shows the impact of certain problems/inefficiencies. For the heat and cold delivered at the network heat exchangers and at the DC heat exchanger this can easily be done as the setpoint temperatures are known. However for the heat and cold delivery to the consumers this is more difficult as the setpoint temperature at which it should be delivered is not saved in the 15min data and is varying over time, therefore one can not properly determine the temperature quality.

Discussing the performance, one has to be able to tell how well certain limits are maintained or exceeded. The limit for instance can be the maximum temperature leaving the warm heat exchanger to the grid  $T_{\text{HEX}_h, \text{prim, out}}$  which has the goal be around  $7.0^\circ\text{C}$  with its

maximum temperatures to properly load cold, at 7.5 °C. One can simply count the amount of times that this maximum temperature is exceeded provided that there is a measured flow above the minimum possible flow. However, this does not provide real insight into the thermodynamic/energetic performance of the wells and the grid, as exceeding the limit has a larger influence when the flow is large. Therefore it is proposed to determine the influence of breaking the limits from an energetic point of view by determining the sum of energy for which the limit is broken as a percentage of the total sum of energy delivered. Hereby one implicitly considers the effect of a longer reaction or stabilizing time as the average temperature should only be affected minorly if it is a short overshoot.

In Section 2-2-1 correlation plots provide a nice overview of the operation of the system and under what conditions directives are breached. The data is split into 4 quarters, where each quarter shows 3 months, January - March, April - June, July-September and October-December. It has not been chosen to split them according to the seasons as than the January 2020 and December 2020 would be in the same plot, while the conditions of the well might be different each year. First of all it is important to determine the some guidelines for those plots, for instance only including the temperature data of a section when also a flow at this section is measured. An important decision has been made to only consider data where the 15 min averaged flow is above the minimum flow that is allowed in a section, therefore excluding some of the starting up/shutting down moments when the average flow is only a third of the minimum. To conclude more about the data one can for instance decide to only use data at very high/low flows/energies/temperatures at certain locations, to explore causes or results in the system.

The high frequency measurements can be saved when the system is monitored online and have been saved to get more detailed information about the switching and the responses of component groups. It is saved, based on a change of value requirement, however no influence can be executed on how large the change has to be in order to be saved again.

There are multiple ways to interpret the time series, in between the measured or saved values one can determine the value by interpolating or by keeping the value similar to the last measured value. Depending on the way the data is gathered, one of the two can be chosen. The detailed high frequency timeseries I gathered myself are saved on a change of value basis, therefore a new value is saved once there is a (significant) increase/decrease. At times a parameter might change very quickly and therefore have a value saved every 10 seconds or the parameter might stay around the same value for a long time before it significantly changes up/down again, therefore the value is then only saved when significantly changes or if it reaches its maximum time difference saving requirements. For this reason it makes sense to display the time series as stairs, e.g. similar values in between the measurements, instead of interpolation as this might give a wrong picture. This can most clearly be shown by the example where a parameter provides information if a system is on (1) or off (0), when interpolating it, one would have a decimal value which does not mean anything. Furthermore it is also important to notice that the stairs should be used to keep the value constant till a new value is measured.

The sensors and transmitters also have some limitations, which is of importance for both the yearly 15 min data as well as for the high-frequency data. Several flow sensors do not report a value between 0 and 1.6 Ls<sup>-1</sup>. When the data is frequently on a very short time switching between 0 and this value, it indicates a flow in between, but no specific value can

be determined as the sensor is not accurate in this area. In the 15min data one can therefore also see values of  $0.5 \text{ L s}^{-1}$  and  $1.0 \text{ L s}^{-1}$  as average values where there was only a flow for respectively 5 and 10 minutes.

The data is also used to calculate the energy consumption and production, it is important to note that small discrepancies in the measurements can result in larger deviations in the calculated energy. During start up or shut down of a section, there is the possibility that the water first has to be flushed through the section before a proper energy can be determined as for instance in the case of heating, when the system has been off for long, the outlet temperature of the heating system has reduced a lot.

### 2-2-1 Analysis of year data

Analysis of the yearly data shows numerous discrepancies in relation to desired operations and requirements.

The temperature requirements to the 5GDHC network are violated often. One of these violations is that the temperature returning to the cold network reaches above  $8.0^\circ\text{C}$ . Based on this data, the causes identified are the DC, which loads additional cold at too high temperatures, and a short-cut flow over the cold buffer when mass flows are small.

A discrepancy at the heat pumps is observed, where the energy measured at the condenser side is too small compared to the energy measured at the evaporator side and to the warm distribution network. As most measurements seem to correlate, the error is attributed to an error in the flow measurements over the condensers, which is confirmed by calculations of the high frequency data at the warm distribution network. Regarding the energy measurements at the evaporator side, it should be noted that one of the temperature sensors is slightly misplaced causing an underestimation of the evaporator energy when operated at small capacities, due to small buffer short-cut flows.

The heating energy demand of the building varies a lot, there is some correlation between the temperature setpoint and the energy demand, however, the spread is rather large. The cooling energy demand seems to be almost independent on the cold distribution building entering temperature except for low cooling demands there is a larger spread, indicating that the HPs are still operated for the warm distribution network. For high cooling demands the temperature is comparable to the temperature delivered by the 5GDHC network. Furthermore, the temperature returning from the building to the cold distribution network is high enough ( $T_{c, \text{build, out}} > 15^\circ\text{C}$ ) indicating a proper operation and tuning of the building systems.

Finally an expected correlation can be observed between the outside temperature and the building heating and cooling demand. There is a transition range in the outside temperature where both heating and cooling can occur, it is also based on whether it is night or day, rains, sun shines and the building occupation.

The above stated information in detail is in this section.

### Heat exchangers network

The analysis of the yearly data is started at the heat exchangers connecting the substation to the network.

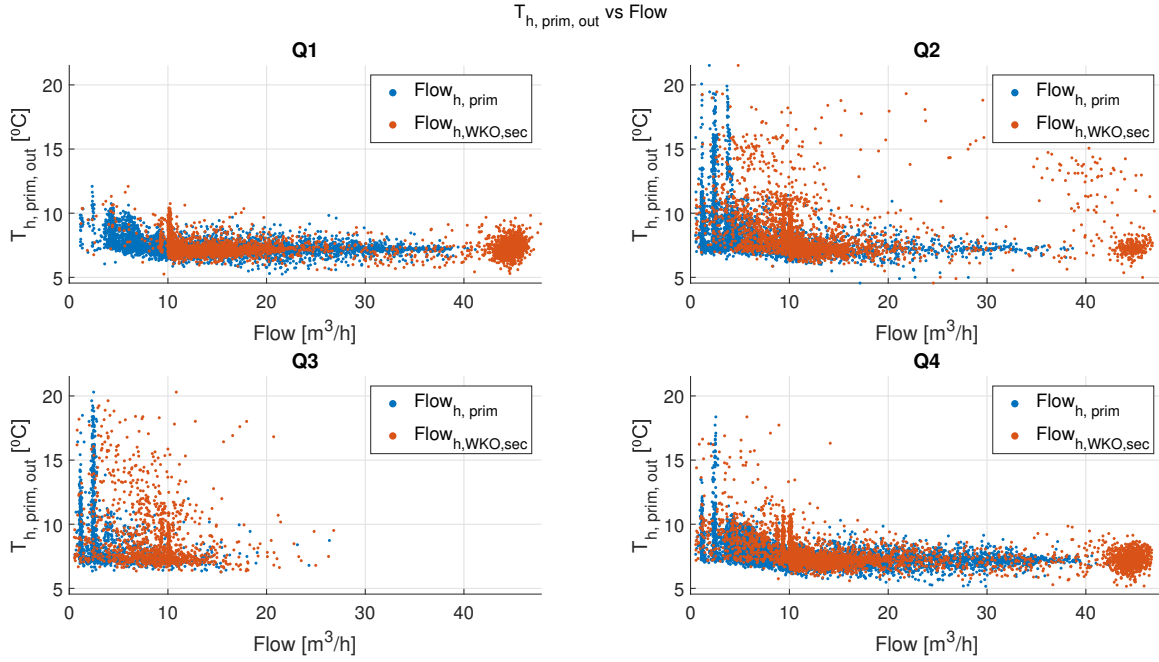


**Figure 2-5:**  $T_{\text{HEX}_h, \text{prim, out}}$  correlated with the flow on primary and secondary side of  $\text{HEX}_h$

The warm heat exchanger is operated for a large time of the year, however for  $\dot{V}_{\text{HEX}_h, \text{sec}}$ , between  $43 \text{ m}^3 \text{ h}^{-1}$  and  $46 \text{ m}^3 \text{ h}^{-1}$ , there is a thick cloud between  $6.0^\circ\text{C}$  and  $8.5^\circ\text{C}$  at the secondary flow (Figure 2-5). While between  $25 \text{ m}^3 \text{ h}^{-1}$  and  $40 \text{ m}^3 \text{ h}^{-1}$  there are just a few measurements and the flows on the primary side remain lower. This occurrence is caused by loading additional cold of the DC, which is only turned if the outside temperature and the flow at the warm heat exchanger ( $\dot{V}_{\text{HEX}_h, \text{sec}} \leq 36 \text{ m}^3 \text{ h}^{-1}$ ) are low enough. The flow at the warm heat exchanger is maximised at  $43 \text{ m}^3 \text{ h}^{-1}$  which is confirmed by the correlation between the DC and heat pump flow in Figure 2-6a, considering only flows at the secondary side above  $36 \text{ m}^3 \text{ h}^{-1}$ . It can clearly be observed that the high flowrates are caused by the DC loading additional cold or a high heat demand at the building, which occur at the same moment in time as they are related to the outside temperature.

Secondly, Figure 2-5 shows that above  $36 \text{ m}^3 \text{ h}^{-1}$ , the DC is on but  $T_{\text{HEX}_h, \text{prim, out}}$  is regularly too high ( $>8.0^\circ\text{C}$ ). It can be observed that these high flows do not occur at the primary side, indicating that the flow on the primary side is limited to try to ensure  $T_{\text{HEX}_h, \text{prim, out}} < 8.0^\circ\text{C}$  as a result of too high  $T_{\text{HEX}_h, \text{sec, in}}$ . Possible causes for the too high  $T_{\text{HEX}_h, \text{sec, in}}$  are; flow over the cold buffer,  $T_{\text{c, DC, out}}$  too high and  $T_{\text{evaps, out}}$  too high. Figure 2-6b shows the correlation between  $T_{\text{HEX}_h, \text{sec, in}}$  and  $T_{\text{c, DC, out}}$  and between  $T_{\text{HEX}_h, \text{sec, in}}$  and  $T_{\text{evaps, out}}$ , where only the data points are selected that correspond to  $\dot{V}_{\text{HEX}_h, \text{sec}} \geq 36 \text{ m}^3 \text{ h}^{-1}$  and  $T_{\text{HEX}_h, \text{prim, out}} \geq 8.0^\circ\text{C}$ . It is observed that  $T_{\text{HEX}_h, \text{sec, in}} > 6.0^\circ\text{C}$  is mostly caused by temperature exceedings that come from the DC as the water leaving the evaporators is below  $6.0^\circ\text{C}$  when the DC is on.

Finally, it can also be observed that particularly for small flows  $< 10 \text{ m}^3 \text{ h}^{-1}$  the temperature limits are more often and larger exceeded (Figure 2-5). This might be caused by the warm heat exchanger being on while it should not be, or the secondary flow through the

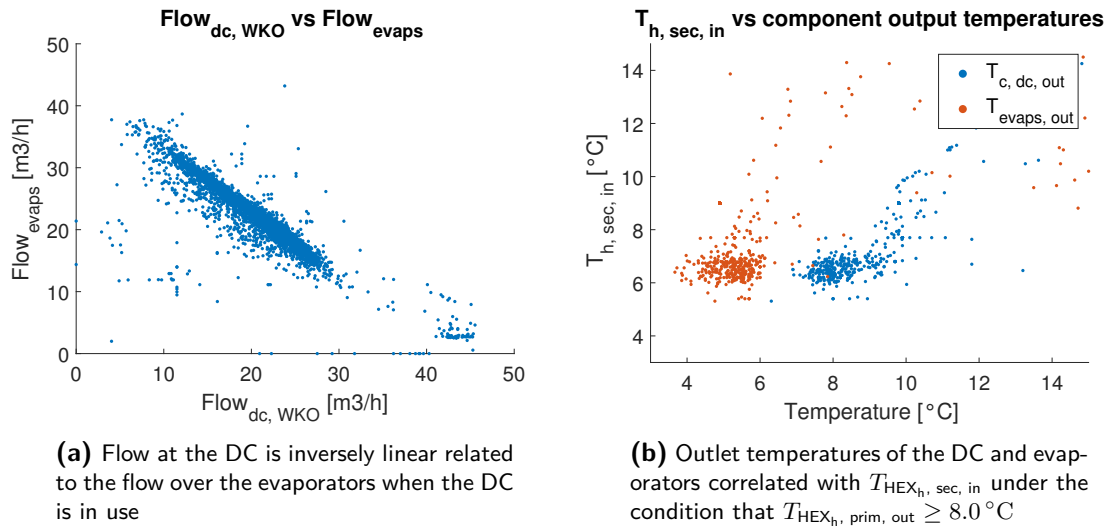


**Figure 2-6:** Correlation between the evaporator, DC and  $\text{HEX}_h$  at the secondary side

warm heat exchanger might not properly be matched with the evaporator flow of the heat pumps causing a short-cut cold buffer flow.

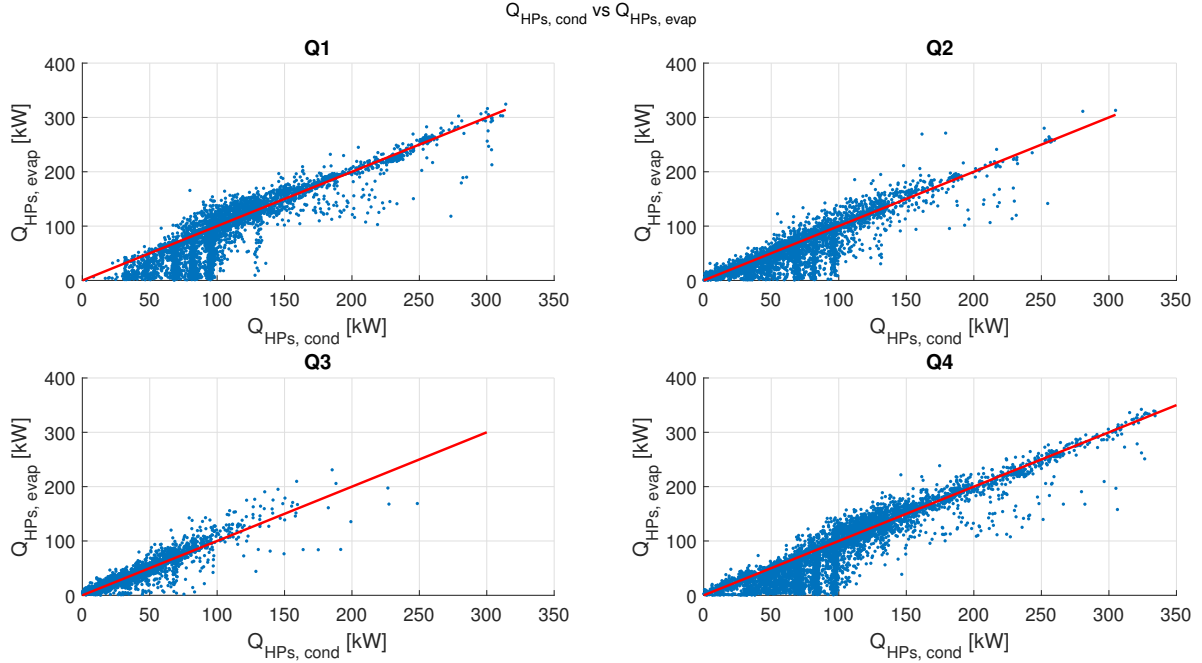
### Heat pump energies

Figure 2-7 shows the correlation between the energy extracted at the evaporators and added at the condensers. For most of the data points the production is correlated by  $Q_{\text{HPs, evap}} \approx Q_{\text{HPs, conds}}$ , while  $Q_{\text{HPs, evap}}$  should generally be lower than  $Q_{\text{HPs, conds}}$ . It should be noted that the energy at the condensers at low capacities ( $Q_{\text{HPs, evap}} < 100 \text{ kW}$ ) is somewhat lower, due to start up/shut-down effects. Technical specifications for these heatpumps state a COP of 4.2, since the temperature lift is slightly larger than for which the COP has been calculated, the COP will likely be lower. Including start-up the COP will be lower as the heating capacity is lower during the transient, since the compressor has to restore the pressure difference between both sides and thereby causing some delay before the desired pressure and temperature at the condenser are reached [21]. [22] provides a linear approximation of the COP for off-design cases, requiring the proper refrigerant selection a new COP can be approximated at the off-design conditions, this would still result in condenser energies well above the evaporator energies. This does not explain the poor energy production at the condensers.

The temperatures measured by the temperature sensors of the energy meters correspond to temperatures measured at other locations in the warm and cold building distribution network. The energy of the warm heat exchanger and the evaporator seem to correlate as  $Q_{\text{HPs, evap}}$  is slightly lower than  $Q_{\text{HEX}_h, \text{prim}}$ , therefore an error in the energy meter of the evaporators could not explain the one to one correlation with the condenser energy. The last possibility of the cause for the error in the condenser energy would be a measurement error of the condenser flow.

There are several ways to check if the flow measurement is approximately correct. It is assumed that all other measurements are correct/accurate.

The flow in the warm distribution network to the building is known, as well as the



**Figure 2-7:** Correlation between the measured condenser and evaporator energies.

condenser inlet temperature which is a mixture of flow over the warm buffer and the flow returning from the building of which the temperatures are known. If the DC is not dissipating any condenser heat, the flow over the buffer is equal to the difference of flow over the condensers and the building. Resulting in the following equation:

$$T_{\text{HPs, conds, in}} \dot{m}_{\text{HPs, conds}} = T_{\text{h, build, out}} \dot{m}_{\text{h, build}} + T_{\text{h, buffer, bottom}} (\dot{m}_{\text{HPs, conds}} - \dot{m}_{\text{h, build}}) \quad (2-6)$$

Unfortunately not all these sensors are saved in the yearly data, however, the live monitored and monthly data can be used. As all sensors might have a small error, there are limitations for the data that has been used for comparison. The data selected is based on  $\dot{m}_{\text{h, build}} \geq 1.6 \text{ L s}^{-1}$  as the sensor does not measure smaller flows and  $\dot{m}_{\text{HPs, conds}} \geq 2 \text{ L s}^{-1}$  for the old data as this indicates that at least one heat pump is running (which would be around  $4.5 \text{ L s}^{-1}$ ). Furthermore it is required that  $T_{\text{h, buffer, bottom}} > 40^\circ\text{C}$ , to ensure that there is flow over the buffer in the preferred direction and thereby ensuring the above stated equation is useful and  $T_{\text{h, build, out}} \leq 30^\circ\text{C}$  so that the temperature difference with the buffer is significant. These newly acquired condenser flows are plotted against the old flows and a fit is made to determine the correlation which seems to be around 1.5. There seem to be some values with a much higher mass flow ( $15 \text{ L s}^{-1}$  to  $20 \text{ L s}^{-1}$ ) at the moment where the old mass flow would be  $4.5 \text{ L s}^{-1}$  and vice versa, but these seem to be some discrepancies due to sensor inaccuracies, start up effects and time delays as these measurements are less than 5% of the total measurements.

During online monitoring of the system, the internal pump sensors can be observed and saved. Even though these might not be precisely calibrated, it can provide valuable information. This data combined with the data gathered from the flow sensor of the energy meter, is shown in Figure 2-8. Again it can be concluded that the real flow would be about 1.5 times

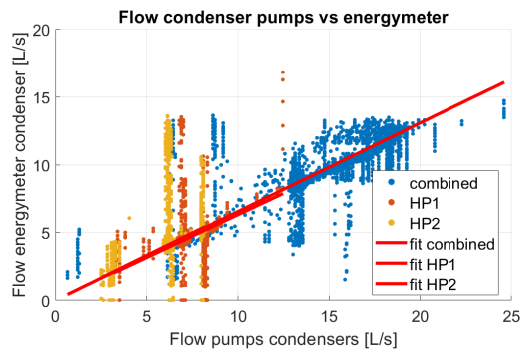


**Figure 2-8:** The flows measured by the energymeter of the condensers correlated with flow measurements of the pumps itself.

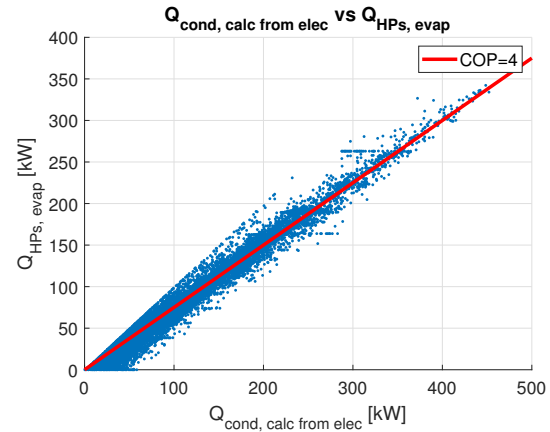


**Figure 2-9:** Correlation between the evaporator energies and the condenser energies when calculated according to  $Q_{\text{cond}} = Q_{\text{evap}} + W_{\text{comp}}$

the measured flow by the flow sensor of the energy meter. As these measurements are not completely accurate, combining this information with the above calculated flows, provides a proper indication.

There is yearly data available of the heat pump electric consumption. This can be correlated with the evaporator and condenser energy measurements and considering the basic energy equation  $Q_{\text{cond}} = Q_{\text{evap}} + W_{\text{comp}}$ , the new condenser energy can be calculated. In Figure 2-9 it can be observed that the correlation between this newly calculated condenser energy and the evaporator energy is around COP=4. Finally, as stated earlier and explained later, the evaporator energy might be a bit larger, especially at  $Q_{\text{HPs, evap}} < 100 \text{ kW}$ , which would result in also a slightly higher calculated condenser energy in this range, and thereby reducing the COP as the compressor energy remains the same. The result would be that the COP for  $Q_{\text{HPs, evap}} < 100 \text{ kW}$  would also move towards 4. Thus it can be concluded that the condenser energy would be about 30% higher than what has been measured.

Till  $Q_{\text{HPs, conds}} = 100 \text{ kW}$ , there is large variation in  $Q_{\text{HPs, evap}}$ , 0 kW to 100 kW, probably caused by start up effects, this is not observed in Q3 where the HPs generally only operate in cooling mode. This might also partially be caused by a displacement of the sensor measuring the evaporator outlet temperatures. As will be discussed later. The fact that  $Q_{\text{HPs, evap}}$  is similar  $Q_{\text{HPs, conds}}$  might be caused by a lot of losses on the condenser side and pipes but these losses have not been observed in other measurements.

Finally an important observation is that the energy of the condensers rarely reaches up to 300 kW, indicating that either the energy demand is only this low and therefore not the full capacity of the HPs is required and used, the HPs do not work on full capacity as a result of too high temperature setpoints or condenser inlet temperatures, or the HPs cannot deliver the capacity as stated in the specifications due to different settings, wrongly tuned parameters or other problems. This is seemingly exaggerated as a result of errors with the energymeters, the maximum measured condenser power would already be higher (400 kW to 450 kW). Therefore one has to consider the energy of the evaporator as that seems more accurate, which reaches up to 350 kW, 87.5% of the maximum evaporator energy, indicating it also operated at higher

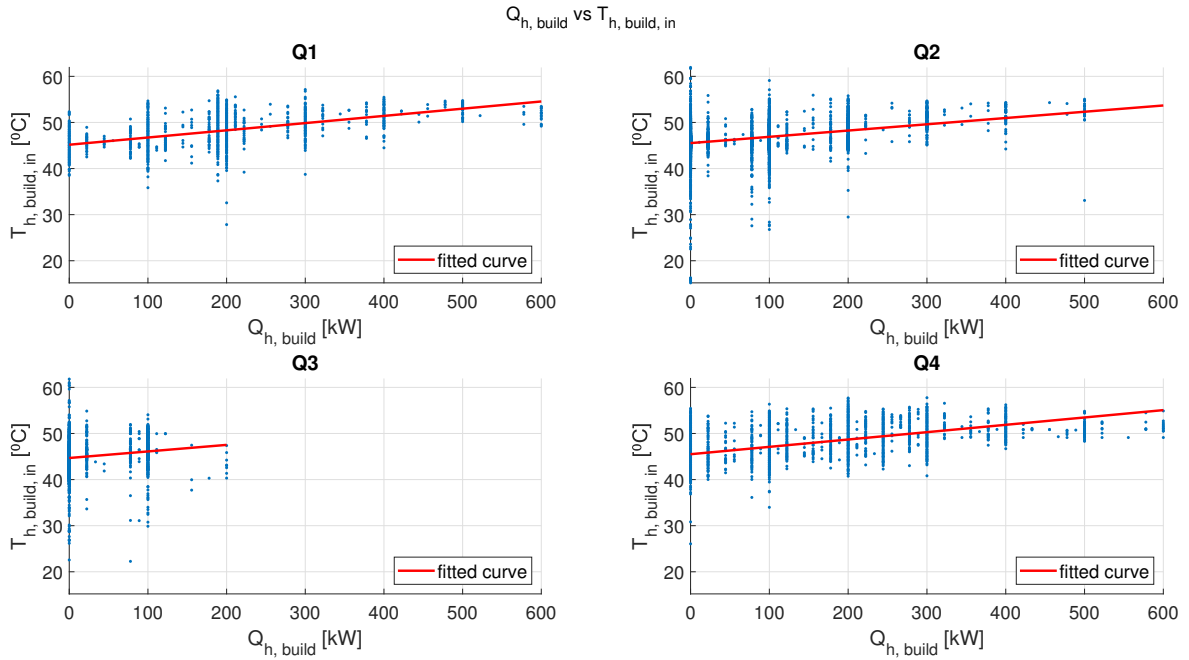


**Figure 2-10:** Energy heat demand correlated with the building supply temperature.

capacities.

## Energy demand

It can be observed that a large range of inlet temperatures at the warm building network occur at different heating demands (Figure 2-10). However when fitting a curve it can clearly be observed that an increasing heat demand relates to an increasing  $T_{h, \text{build, in}}$  on average. Above 300 kW there are almost no instances where  $T_{h, \text{build, in}}$  is below 45 °C and even at 100 kW the average inlet temperature seems to be above 45 °C. This clearly shows a problem with the selection of the heat pumps as they are only allowed to reach setpoint temperatures of 46 °C.  $T_{h, \text{build, in}}$  is used in this comparison as the temperature setpoint is not saved and this temperature should be closely related.

Figure 2-11 shows large differences in heat delivered to the building and heat produced by the condensers which are most likely caused by the error in the energy measurements at the condenser and the kick in of the conventional heater. The red line indicates the ideal location of the data points. Small differences that would still occur after the conversion, might be a result of buffer unloading. These differences will only be small as the buffers have a volume of 1000 L and thus a capacity of  $(T_{h, \text{build, in}} - T_{h, \text{build, out}})c_p V = 17.5 \text{ kW h}$  based on a reached temperature difference of 15 °C. If the buffer would have been fully unloaded in 15 minutes, the average energy difference between the building heating demand and the condenser production would be 70 kW. Which could cover the difference between two capacities, but due to the control design the buffers are almost never fully unloaded. Furthermore, combining it with Figure 2-10, it can be observed that  $T_{h, \text{build, in}}$  is above 50 °C from 200 kW onwards, which already partially explains the difference between the  $Q_{\text{HPs, conds}}$

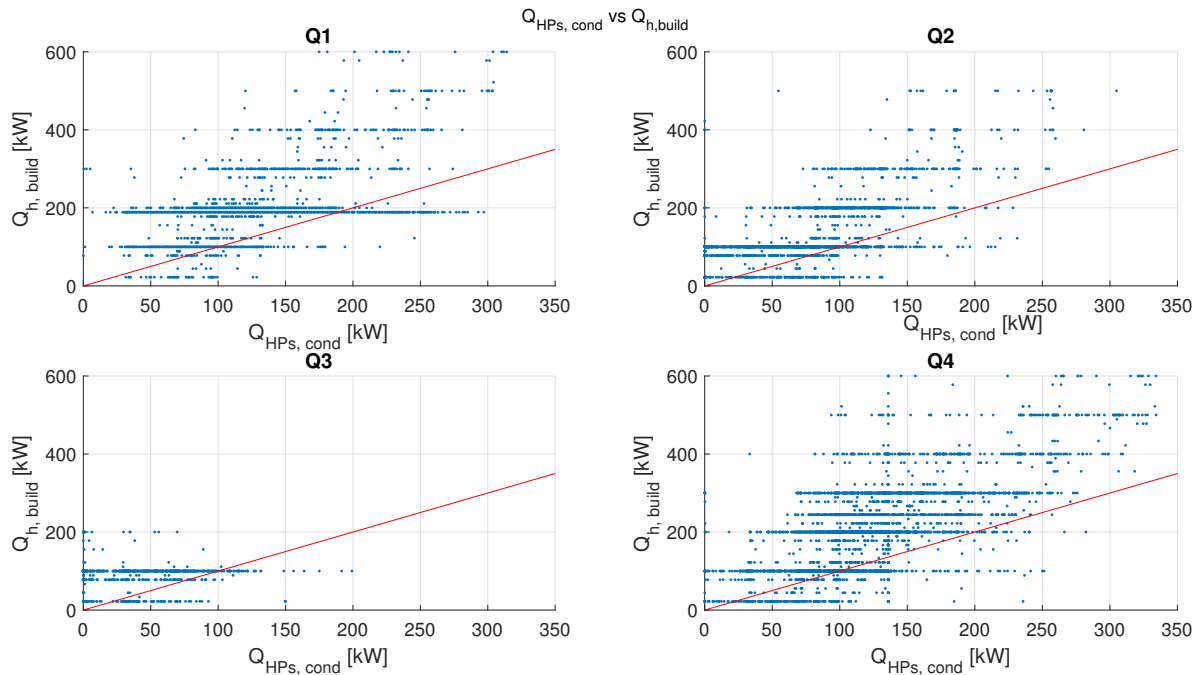


**Figure 2-11:** Measured condenser energy correlated with the building heat demand.

and  $Q_{h, build}$ , even though the HPs could deliver this capacity. Due to the high setpoint, the energy is partly delivered by the HT.

Heating demand in the building occurs 41% of the time. 14% of the time that heating energy is supplied  $Q_{h, build}$  is 300 kW or above of which 58% of the time  $T_{h, build, in}$  is above 50 °C. The heat demand is 27% of the time supplied with  $T_{h, build, in} \geq 50$  °C. The yearly heating demand is 2123 GJ, of which 586 GJ is for  $Q_{h, build} > 300$  kW, of which 353 GJ comprises  $T_{h, build, in} > 50$  °C. Considering the full heat demand and  $T_{h, build, in} > 50$  °C manifests for 760 GJ.

The total energy produced by the condenser side of the HPs is 1255 GJ under the assumption of heating demand and in total 1690 GJ (including for cooling). So the heating energy used by the building only consists at maximum 60-80% of energy produced by the HP. It should again be noted that there is some discrepancy at the HP energymeter, this energy might actually be slightly higher.

The temperatures entering and leaving the building cooling network are mostly independent from the cooling demand (Figure 2-12), with wide peaks for  $T_{c, build, in}$  around 10 °C and  $T_{c, build, out}$  around 17 °C.  $T_{c, build, out}$  generally remains above 15 °C, but it contains many values below 16 °C, eventhough this is the minimum temperature of  $T_{HEXc, prim, out}$ . The low  $T_{c, build, out}$  occurs for cooling demands below 400 kW, with varying inlet temperatures and flows. This might be caused by some groups at the buildings side that are not properly regulated. It should be noted that the width of the peaks especially of the  $T_{c, build, in}$  is wider for  $Q_{c, build} \leq 300$  kW.  $T_{c, build, in}$  can drop to 6.0 °C, which is a result of HP operation as the heat exchanger generally provides temperatures of 9 °C to 11 °C. Unfortunately there is no temperature setpoint available in the stored data, thus it can not be correlated whether this is based on the cold demand or that it occurs because of the balance between the heating

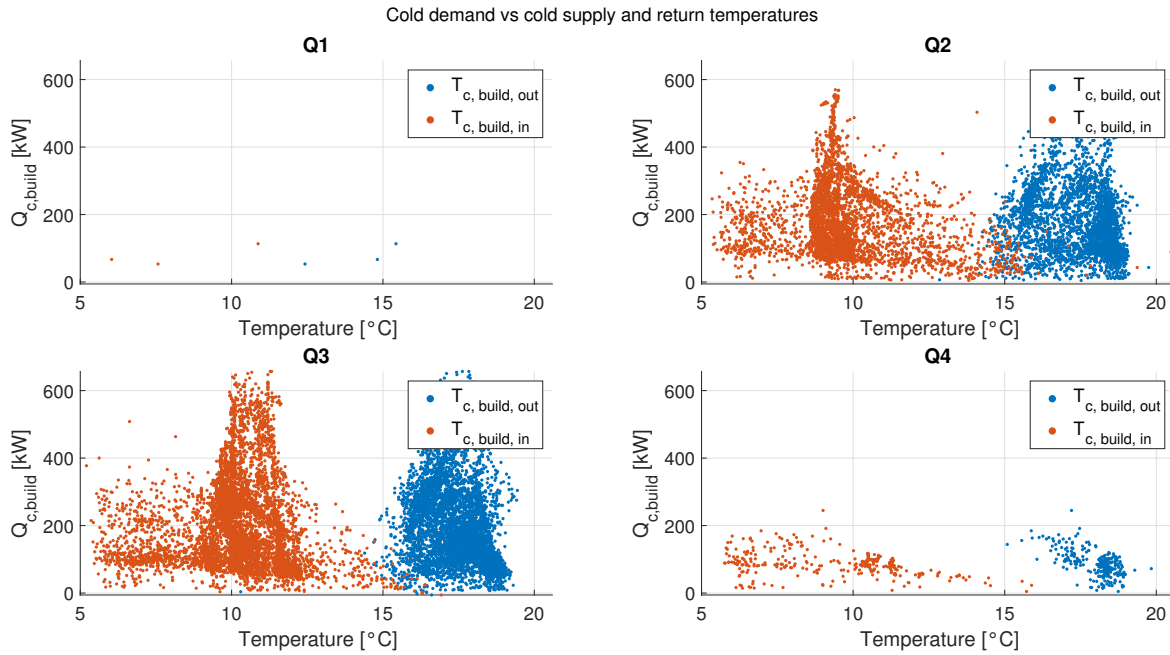


**Figure 2-12:** Correlation of the cold building distribution network entering and leaving temperatures with the cooling demand.

and cooling demand in the building. Important note, HP seems not to be necessary at high cooling demands, thus in general  $T_{c, set} \geq 9.0^\circ\text{C}$ .

In Figure 2-13 it can be observed that the evaporator outlet temperature can be much higher than the secondary temperature entering the warm heat exchanger, while this in reality is not possible. As the condition for these graphs is that the warm heat exchanger has a flow larger than  $3.0\text{ m}^3\text{ h}^{-1}$  and at least one heat pump is on, the evaporator outlet temperature should be lower than the temperature entering the warm HEX. This discrepancy can be explained by the displacement of the sensor for  $T_{\text{evaps, out}}$ , which is placed right after the connection with the warm heat exchanger instead of before, thus it does not properly represent the evaporator outlet temperature. This results in higher evaporator outlet temperatures thus a lower evaporator energy, due to a recirculation flow over the buffer when  $\dot{m}_{\text{evaps}} < \dot{m}_{\text{HEX}_h, \text{sec}}$  and when there is no cold demand. It becomes apparent that it mainly occurs for low energies as can be observed when comparing Figure 2-14 with Figure 2-15 where only the points are selected that comply with  $T_{\text{HEX}_h, \text{sec, in}} < 7.0^\circ\text{C}$  and  $T_{\text{evaps, out}} > 8.0^\circ\text{C}$  which clearly occurs at  $Q_{\text{HEX}_h, \text{prim}} < 100\text{ kW}$ . Thereby, the influence of the discrepancy of the evaporator outlet temperatures on the energy when operated at higher capacities is less significant as there is less short-cut flow over the buffer. The other temperatures and flows are measured at the proper location, therefore the energy removed by the evaporator can only be slightly larger.

### Correlation with outside temperature

The correlation of the energy consumption with the outside temperature provides information on how the consumption is distributed over the day and the year.

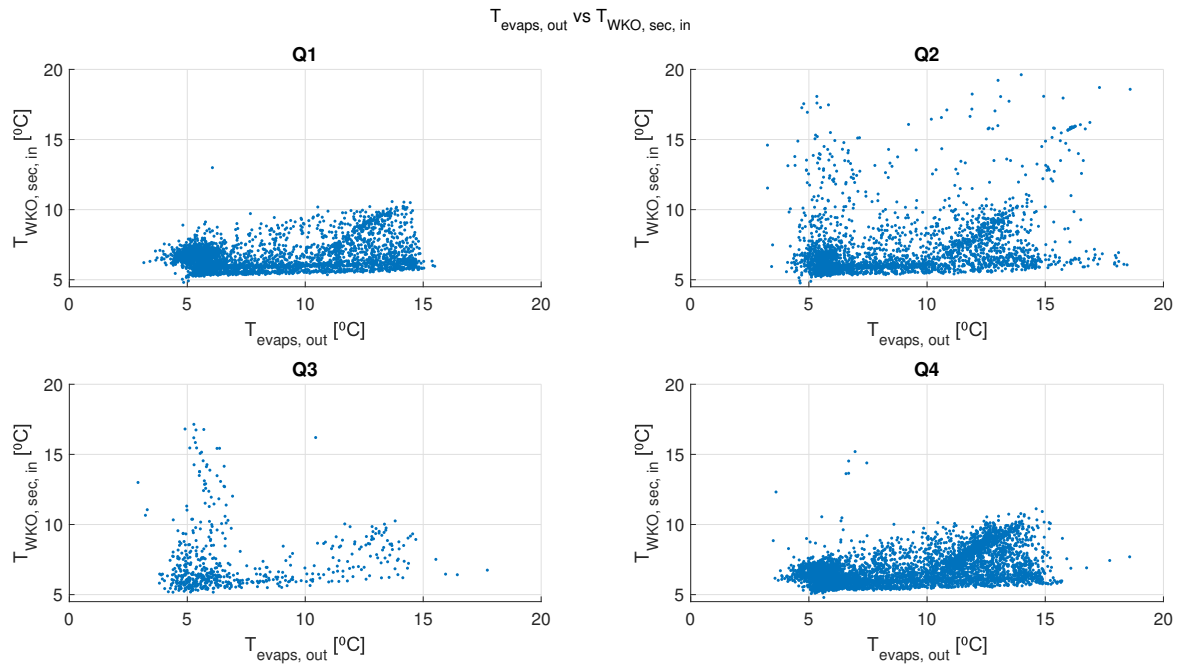


**Figure 2-13:** Temperature leaving the evaporators correlated with the temperature entering the secondary side of the warm heat exchanger.

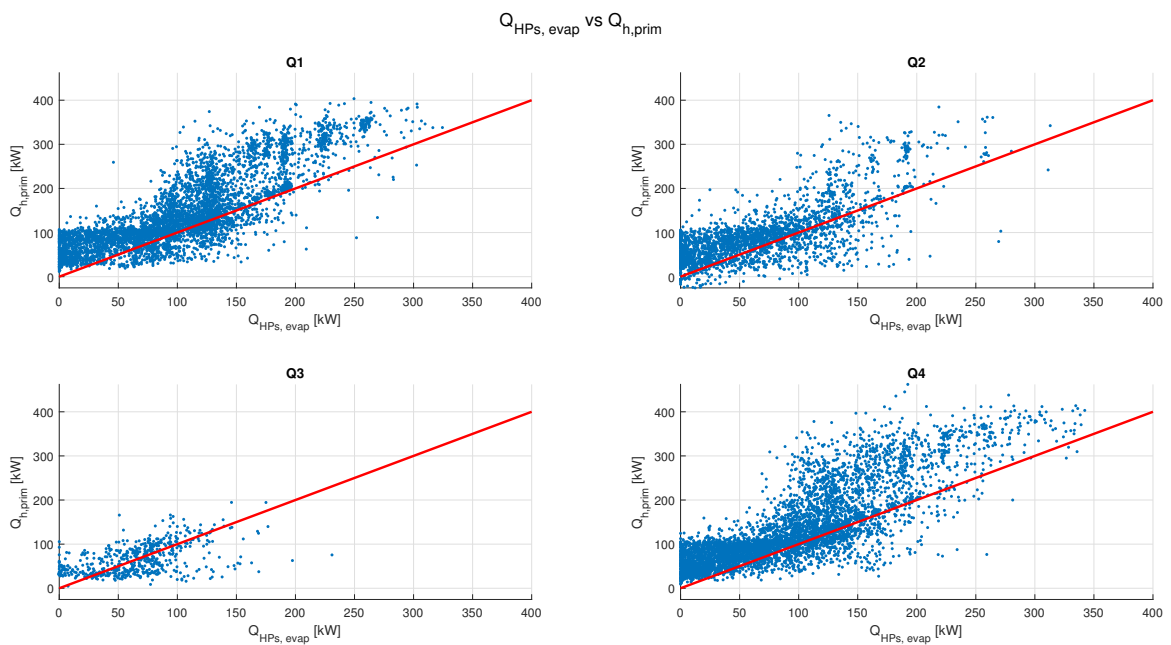


**Figure 2-14:** Correlation between the energy provided by the warm heat exchanger and the energy consumed by the evaporators of the heat pump.

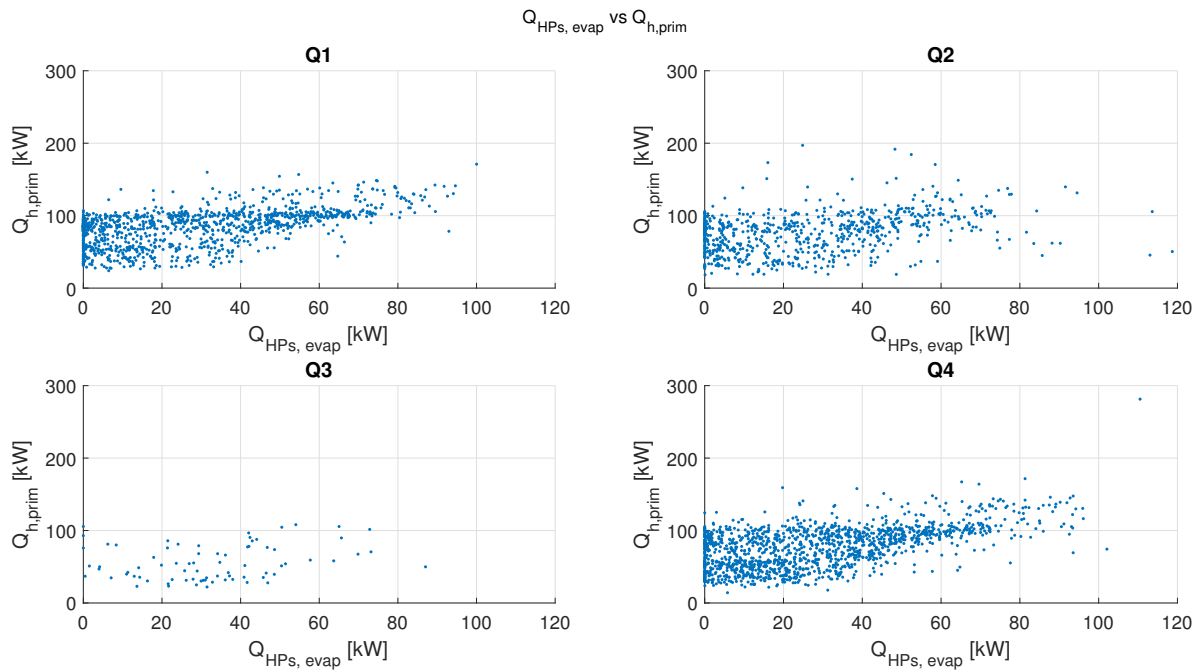


**Figure 2-15:** Correlation between the energy provided by the warm heat exchanger and the energy consumed by the evaporators of the heat pump under the condition  $T_{\text{HEXh, sec, in}} \leq 7.0^\circ\text{C}$  and  $T_{\text{evaps, out}} \geq 8.0^\circ\text{C}$

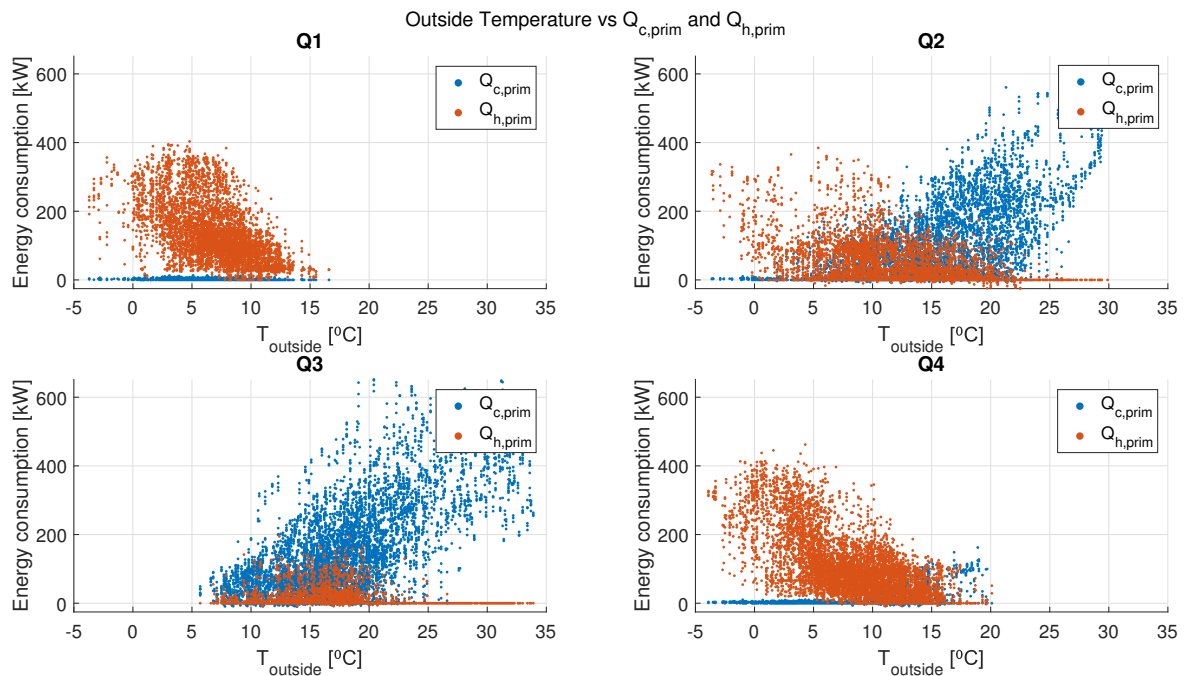


**Figure 2-16:** Correlation of the outside temperature with the cooling and heating energy extracted from the thermal storage.

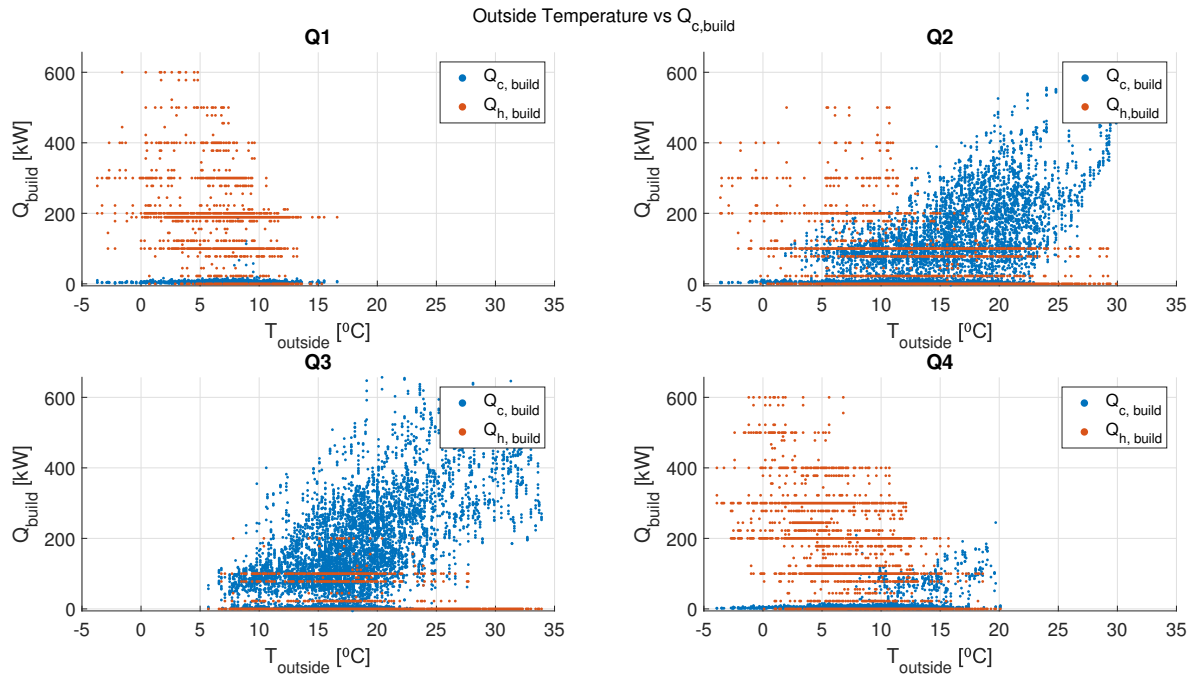


**Figure 2-17:** Correlation of the outside temperature with the heating and cooling demand of the building.

The energy provided at the heat exchangers shows the amount of energy that is recovered from the thermal seasonal storage and is the basis for the energy consumption of the building. Figure 2-16 shows that for outside temperatures below  $10\text{ }^{\circ}\text{C}$ , the cold heat exchanger delivers less than  $100\text{ kW}$  and often less than  $50\text{ kW}$ , as it is mainly on for server room cooling (Q1 and Q4), which is generally below  $20\text{ kW}$ . The higher the outside temperature the more heat the network is extracting from the building, completely within expectations. There is almost always cold delivery for temperatures of  $20\text{ }^{\circ}\text{C}$  and higher, while at temperatures between  $15\text{ }^{\circ}\text{C}$  to  $20\text{ }^{\circ}\text{C}$  there might be cold delivery, but that can also be facilitated by the heat pumps and therefore one can still see  $Q_{\text{HEX}_c, \text{prim}} = 0$  at these temperatures. The opposite occurs for heating energy provided by the network, the colder the outside temperatures the higher the energy.

Figure 2-17 compares the building energy consumption for cooling and heating with the outside temperature. It can be observed that  $Q_{c, \text{build}}$  increases with the outside temperature and for outside temperatures below  $15\text{ }^{\circ}\text{C}$ ,  $Q_{c, \text{build}}$  is generally below  $50\text{ kW}$  in Q1 and Q4. In Q2 and Q3 there are occasions where the outside temperature is between  $10$  and  $15\text{ }^{\circ}\text{C}$  and  $Q_{c, \text{build}} = 100\text{ kW}$  to  $200\text{ kW}$ , which might be explained by the fact that in Q1 and Q4  $15\text{ }^{\circ}\text{C}$  is the maximum temperature of the day, while in Q2 and Q3 these are the minimum temperatures of the day and therefore cooling still needs to be applied as the accumulated heat during the day has to be dissipated.

The heating energy used is higher when the outside temperature is lower, but it also depends on other variables like time of the day, sunshine, rain, inside temperature and building occupation. Selecting only the data with  $T_{h, \text{build}, \text{in}} > 50\text{ }^{\circ}\text{C}$  would show a similar distribution, indicating that a high temperature setpoint is not only the case with a high heat demand

and low outside temperatures, however below 100 kW it is less common. As a high  $T_{h, \text{build}, \text{in}}$  is not only the case for either high  $Q_{h, \text{build}}$  or low outside temperatures, there is room to improve the heat delivery at lower temperatures (45 °C), thus increasing the HP production.

### 2-2-2 Analysis of high-frequency measurements

The high-frequency day measurements are used for direct comparison with the model, as this provides a detailed overview in time and also to determine the causes and observe some of the problems that can not be observed solely with the 15 minute data. The problems that are shown in this section have been observed multiple occasions but are only shown here once to explain.

#### Network connection

**On/off switching cold heat exchanger** Frequent on/off switching of the cold heat exchanger when the top of the cold buffer reaches a temperature below the setpoint of the cold supply to the building is observed in Figure 2-18a. The switching itself might not be a big problem since only the heat exchanger is in use and therefore only the pump and valves switch on and off, but it can cause short irregularities in temperatures returning to the grid. The heat exchanger is controlled at  $T_{\text{HEX}, \text{c}, \text{sec}, \text{out}} = \max(9.0\text{ °C}, T_{\text{HEX}, \text{c}, \text{prim}, \text{in}} + 1.5\text{ °C})$ , but the off switching is also stated at 9.0 °C to prevent a too cold water flow to the heat pumps. This is more detailed shown in Figure 2-18b. Currently the heat pumps are off and the temperature returning from the building is still high (indicating the demand is still high), thus there would be no need for the cold heat exchanger to turn off.

**Drycooler cold-loading** The DC is turned on based on the outside temperature and on the request to load additional cold for the balance of the wells. However, as shown in Figure 2-19a the DC outlet temperature is often higher than 6.0 °C, resulting in an elevated  $T_{\text{HEX}, \text{h}, \text{sec}, \text{in}}$ . This can result in too high  $T_{\text{HEX}, \text{h}, \text{prim}, \text{out}}$ , specifically once the flow of the DC is a larger proportion of the total flow through the heat exchanger. Therefore the limitations on when additional cold can be loaded should be more strict (lower outside temperature), to ensure it does not cause a too high  $T_{\text{HEX}, \text{h}, \text{prim}, \text{out}}$ .

**Server room cooling** Server rooms demand cooling throughout the year at a low capacity. These rooms are at times cooled by the DC, the cold distribution network of the building or the cold heat exchanger directly. Ideally only the second and third option would be used as otherwise this heating energy is discarded. However, if there is an unbalance with heat excess, it is better to cool with the DC as the loading of additional cold can only be applied at lower temperatures and thus for a shorter period of the year. For these groups the order in which systems to use, should be reconsidered if additional buildings are added to the network and the unbalance is shifted to or from heat excess. In Figure 2-19b it is shown that the cooling demand of the server rooms is very low and thus it does not meet the temperature requirements for the warm well.

**Short-cut flow cold buffer** A too high  $T_{\text{HEX}, \text{h}, \text{sec}, \text{in}}$  is caused by a short-cut buffer flow as a result of the heat pump working at a low capacity and thus a small net flow ( $0.8\text{ L s}^{-1}$ ) over

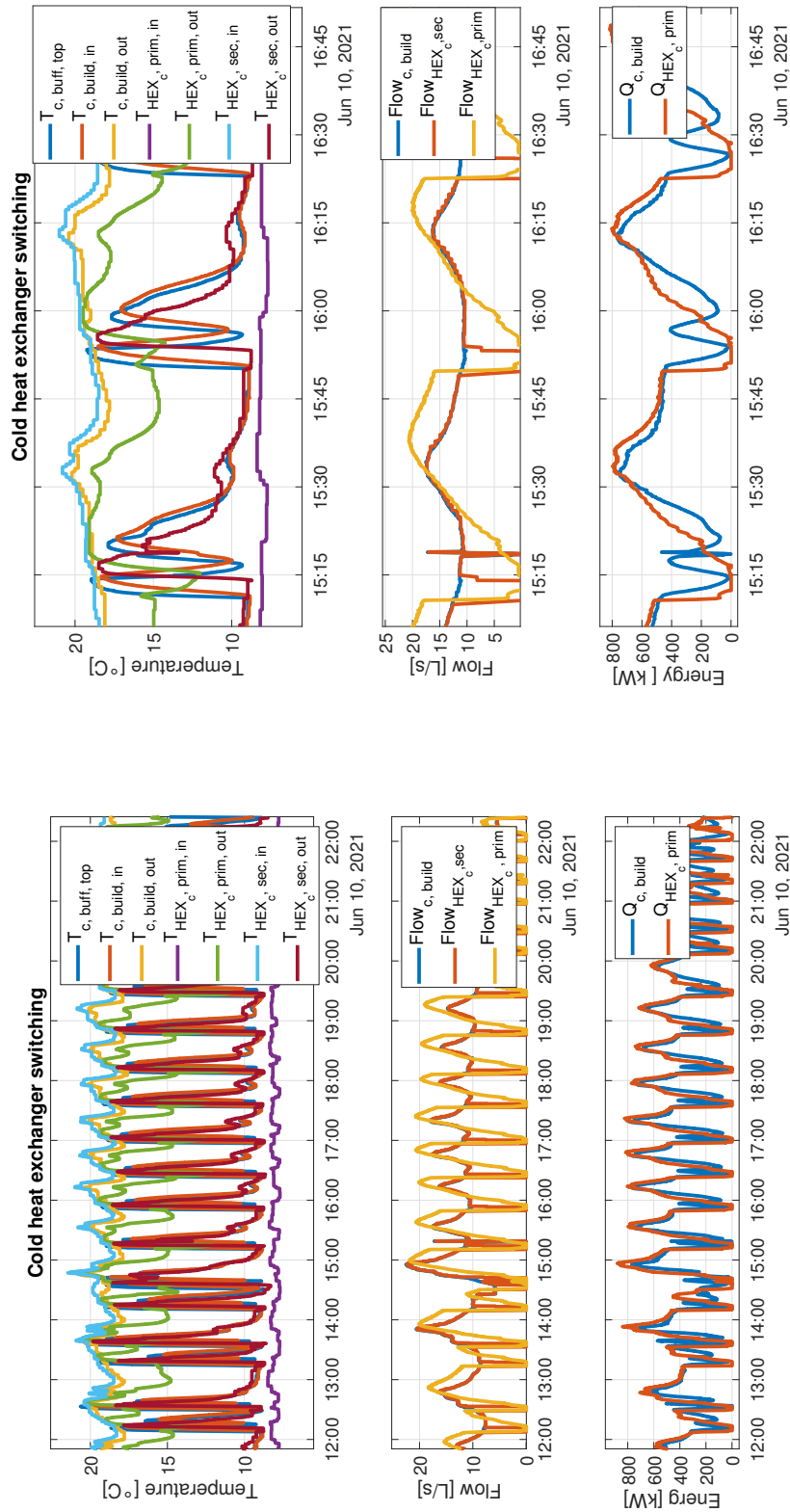


**Figure 2-18:** On/off switching of the cold heat exchanger as a result of  $T_{c, \text{buffer, bottom}} \leq 9.0^\circ\text{C}$

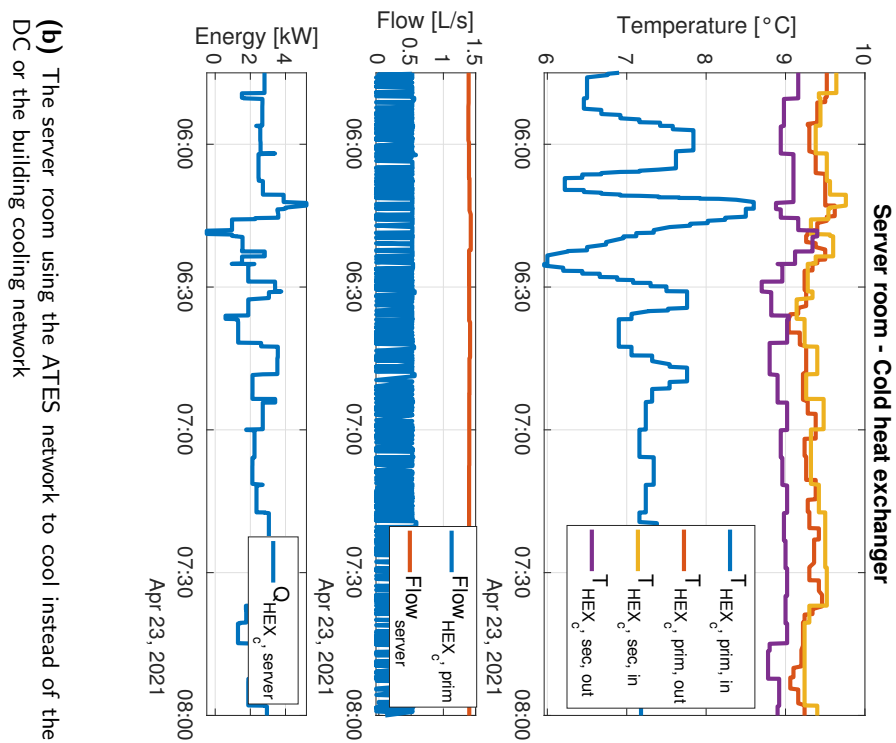
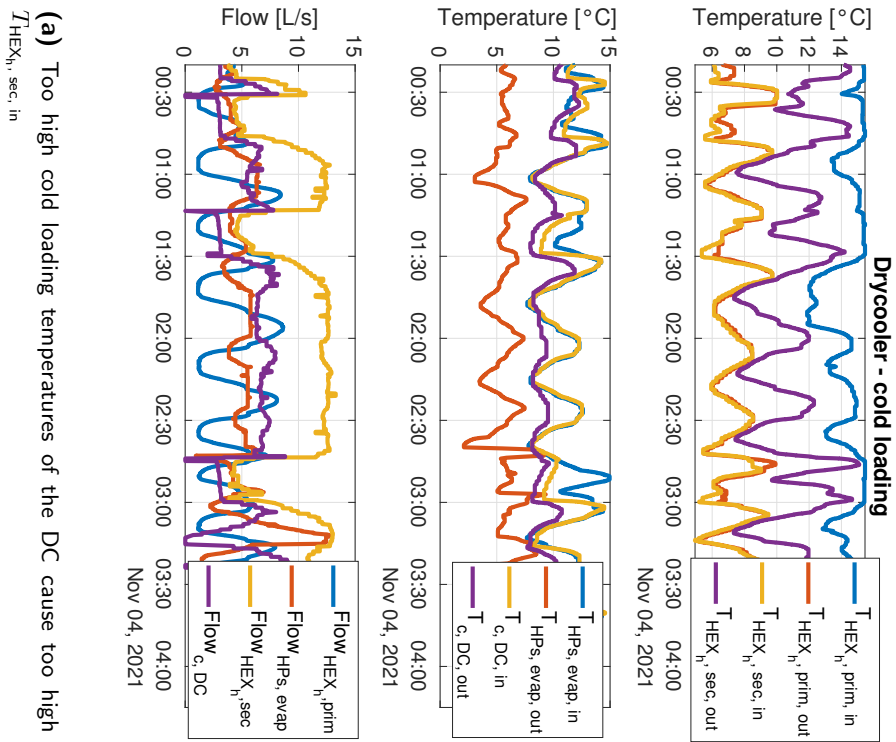


**Figure 2-19:** The effect of the drycooler and the server room on the temperatures to the grid

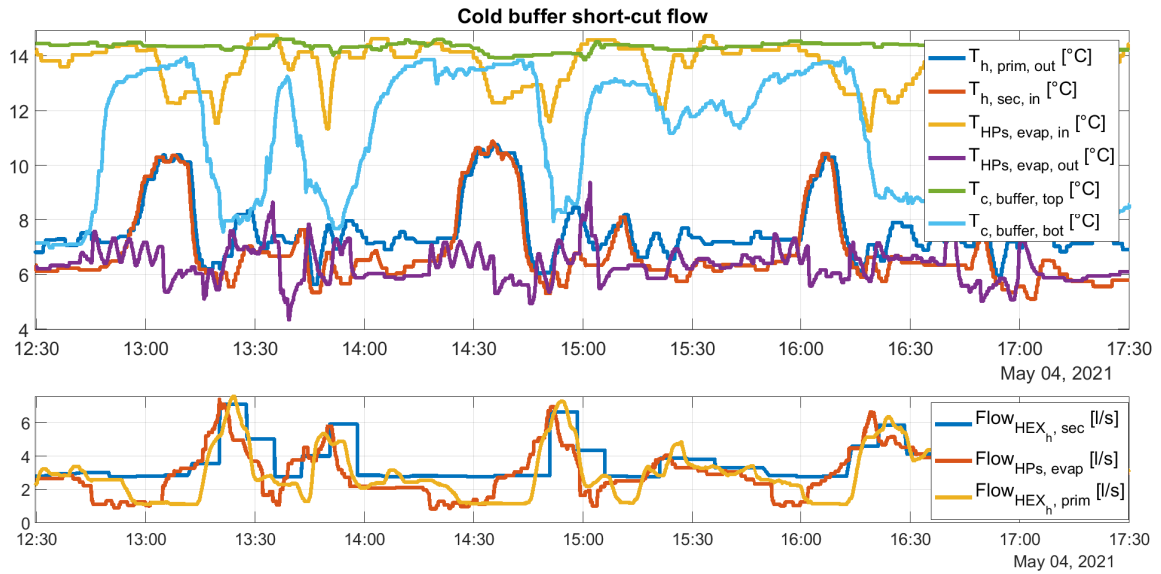


**Figure 2-20:** Short-cut flow over the cold buffer causing too high  $T_{HEX_h, sec, in}$

the evaporators. Since the pumps of the heat exchanger have a minimum flow of  $2.6 \text{ L s}^{-1}$  water leaving the evaporators and water from the cold buffer is mixed before it enters the heat exchanger (Figure 2-20) around 13.00h, 14.30h and 16.00h. The temperature at the secondary side of the heat exchanger only rises some time after the flow difference occurred eventhough the bottom buffer temperature might already have been high, due to the long distance between the buffer and the heat exchangers ( $> 20 \text{ m}$ ). As long as the buffer is fully cooled at  $6.0^\circ\text{C}$  this does not cause problems, however, the buffer will slowly heat up as the newly delivered water at the top which comes from the heat exchanger is about  $14^\circ\text{C}$ , resulting in higher  $T_{HEX_h, sec, in}$ . If the buffer is fully cooled it would take upto 9 minutes before the short-cut flow would cause too high  $T_{HEX_h, sec, in}$ . This is a result of the control system which only allows the warm heat exchanger to turn off when the heat pumps are on if, there is a cooling demand AND the temperature in the buffer is too high.

This problem could be solved by allowing the warm heat exchanger to also be turned off, if heat pumps are turned on AND  $\dot{V}_{evaps} \leq \min(\dot{V}_{HEX_h, sec})$  AND no cooling demand AND  $T_{c, buffer, bottom} \geq 12^\circ\text{C}$ . Or this could be solved by ensuring that pumps are selected that can reach this low flow as well if the heat exchanger are still able to properly operate turbulently.

**Substation instability** In general heat exchangers are only controlled at one outlet temperature by varying the flow [23], since for 5GDHC the return temperature to the grid is of importance, the flow on the primary side is also accurately controlled. This results in properly maintained temperature limitations, or only slight exceedings when the flow is low. It is based on a cascade controller controlling both the  $T_{HEX_h, sec, out}$  and the maximum  $T_{HEX_h, prim, out}$  as discussed before. However, the resulting return temperature to the substation can fluctuate a lot as shown in Figure 2-21, small oscillations in the secondary supply temperature of the heat exchanger are enlarged in the secondary return temperature. These fluctuations are reduced again by the HP controller, but are not directly strictly maintained at  $6.0^\circ\text{C}$  as the temperature slopes can be very sharp. Due to the size and frequency of the oscillations, the

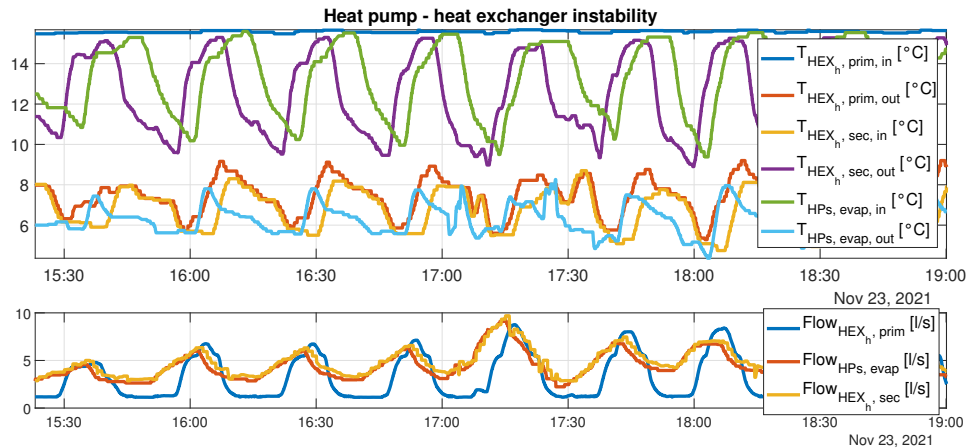


**Figure 2-21:** The instability of the complete substation

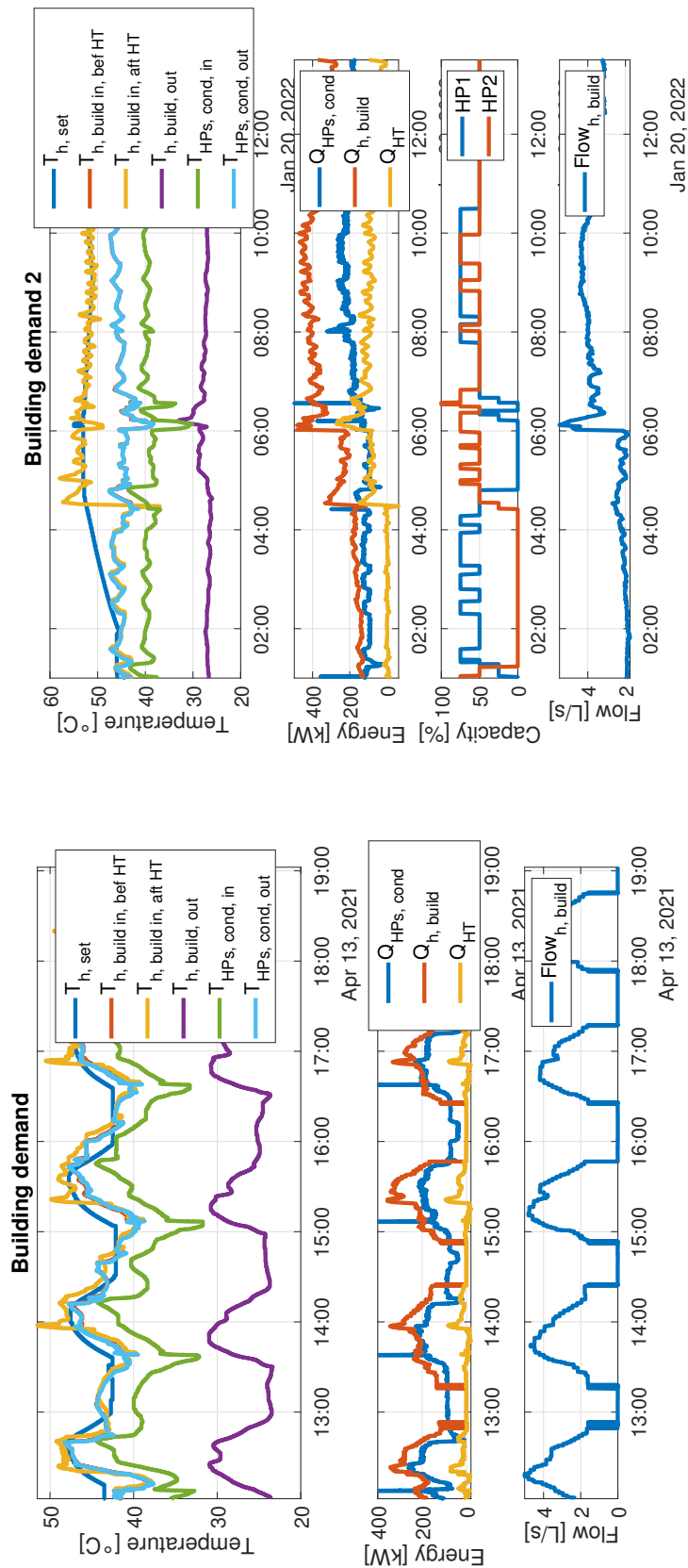
temperature to the heat exchanger fluctuates slightly with a small exceeding of the temperature limits, causing this process to continue. This instability of the substation is continued for longer periods of time and thus the return temperature limit to the grid is regularly exceeded. These instabilities can start suddenly due to small changes and occur for longer time periods. It is observed regularly for different heat demands, not specifically very small heat demands nor highly fluctuating heat pump capacities. This shows also the importance of observing the short term dynamics of such a substation as these oscillations happen every 30 minutes.

### Heating side substation

The heating demand can have several different profiles. Figure 2-22a shows a fluctuating profile where both the temperature setpoint and the flow fluctuate over time. Both the temperature setpoint and the flow increase simultaneously. As each group provides its own setpoint, the highest is taken. It should be noted that eventhough there is no measured flow and thus energy at certain times, in reality there is a flow, but the sensors do not register flows below  $1.6 \text{ L s}^{-1}$ . This can be verified by the fact that the heat pump produces energy, but the temperatures in the warm buffer do not increase, as well as an operation of the warm distribution network pumps. This profile is interesting for a case study as the substations behaviour should be able to work along side this.

Figure 2-22b shows a different type of building heat demand, during the night the demand is low, the flow is low and stable. The temperature setpoint is slowly increasing when suddenly at 6.00h the flow in the building increases significantly as the building is then starts to pre-heat. Furthermore, an important detail can be observed that the moment the second heat pump starts, the conventional heater also kicks in as the temperature difference is more than  $2^\circ\text{C}$  for more much more 15 minutes.

It can be observed that if there is a small building flow, the temperature entering the HPs will not be low enough for the second HP to go on, eventhough the setpoint, which can be above the HP maximum, is not reached. Once the second HP switches on, the HT immediately switches on as there is no minimum time for the second HP to be on, while there is the requirement that both HPs should be on. This is not a problem if  $T_{h, \text{set}}$  is above the HP maximum, however if it is not above the HP maximum, it will be an unnecessary HT kick



(b) Building demand and conventional heater kick in

(a) Fluctuating building demand

Figure 2-22: Various building energy demand curves

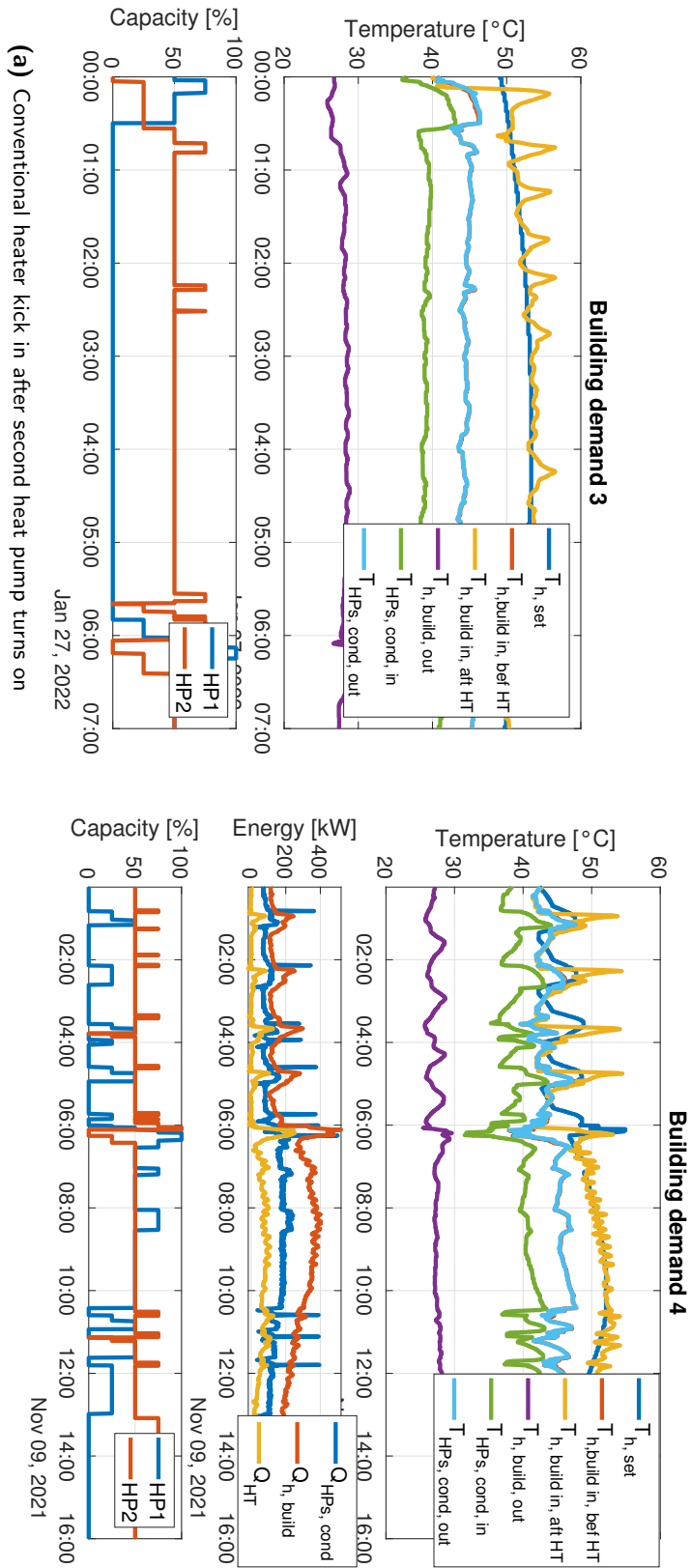


Figure 2-23: Various building heating demands responses including the HT

in.

In Figure 2-23a a fairly constant demand is shown, the temperature setpoint is not reached for a long time and once the second heat pump kicks in, the conventional heater also kicks in immediately and remains on, even though one of the heat pumps shuts down.

The choice of using multiple HPs also has an effect on deciding when a HP is switched on/off. Currently, turning on the second HP is based on the condenser inlet temperature and on the difference between the setpoint temperature and the building inlet temperature. Turning on the second HP quickly increased the temperature entering the condensers as more flow is recirculated over the buffer, this explains the large hysteresis between turning it on/off. However, the conventional heater turns on within 5.0 min of when the second HP is turned on (Figure 2-23b), even though the setpoint is still in reach of the HPs and the second HP only at 25% cap due to starting up. Therefore a time constraint on how long both HPs should be operational before the HT kicks in would be beneficial. Furthermore, quickly after the HT kicks in (20 min), the second HP shuts down because of a sharp  $T_{h, set}$  decrease, while conventional heater remains running for several minutes longer. Both inefficiencies are presented in Figure 2-23b. This adds to the conclusion that the conventional heater should shut down if the second HP shuts down.

From all the measurements several cases have been extracted, the data for these cases is shown once it is compared with the other methods.

## 2-3 Observations based on data analysis

The yearly data provides an overview of current status of the substation and the high frequency data is used to determine the causes of common problems into more depth. The most notable insights from the data analysis are:

- The DC is causing too high return temperatures to the cold ring when loading additional cold. This can be solved by reducing the outside temperature at which it turns on and especially when it turns off.
- Temperature requirements at the warm heat exchanger are violated at part-load conditions, specially for low flows. This is partially caused by start-up/shut-down produces, and short-cut flows over the buffer.
  - The short-cut over the buffer is a result of a mismatch between the flow over the evaporators of the HP and the flow from the heat exchanger connected to the network caused by the inability of the pump to accommodate smaller flows. This occurs when one HP is off and the other is operated at minimum capacity.
- The cooling of the building operates properly in terms of the demand being mostly covered by the 5GDHC and only a small part by the HPs.
- When only the server rooms are being cooled with the cold delivery heat exchanger, the return temperature to the grid is generally too low as the cold demand is low and this can not be matched with the flows to stay within the required temperature range.
- Frequent switching of the cold heat exchanger occurs, while the demand is continuous and there is no flow through the HPs. This is a result of slightly lower than  $9.0^{\circ}\text{C}$  while the cold heat exchangers tries to maintain  $T_{\text{HEX}_c, \text{sec}, \text{out}} = \max(9.0^{\circ}\text{C}, T_{\text{HEX}_c, \text{prim}, \text{in}} +$

1.5 °C). Resulting in short small flows returning to the warm ring just below 16 °C and a less continuous building operation.

- Frequent switching between the warm and cold heat exchanger connected to the grid, more than once an hour they switch, which cannot be explained by the changing heat and cold demand, but is a result of the control strategy of switching based on the cold buffer top/bottom temperatures. These seem to be too close and therefore keep changing in the same direction for a while after the HEX has been turned on/off, causing the other one to switch on/off as well.
- The design of the control strategy generates undesired system performance, such as
  - combined temperature and flow set-point variations from the demanders
  - frequent switching of heat and cooling supply resulting in a reduced share of energy produced by the HP and a violation of the temperature limits at the grid.
  - fluctuating temperatures at the warm heat exchanger are not stabilized, but enlarged at the secondary (building) side, as the control is mainly focussed on the primary (grid) side.
- The pumps of the HPs continue in operation for some time (2.0 min to 5.0 min) during shut-down to dissipate energy and prevent damage, even though the flow is relatively small, the temperature leaving the evaporator is too high. This can slightly increase the temperature at the warm heat exchanger, not allowing the  $T_{\text{HEX}_h, \text{prim, out}} < 7.5 \text{ °C}$ , however as it is a small flow and temperature increase, it can generally remain below 8.5 °C.
- At low building heat demand (< 200 kW), most of the energy is provided by the HPs, however at higher heat demands, the energy provided by the HPs does not match the demand and is generally lower, causing the unnecessary kick in of the conventional heater, even though the demand is still within the maximum HP capacity. This shows the problem of not maximizing the HP capacity for heating and is caused by:
  - setpoint temperatures for heat supply to the building that outsize the maximum temperature that can be produced by the HPs even though the energy demand is still below the maximum capacity of HPs.
  - higher building return temperatures due to the high building inlet temperatures and HT kick in causing a reduction in HP capacity and thereby the share of heat produced by the HPs.
- Heat pumps capacity fluctuations are caused by
  - Low heat demand flow, causing higher temperatures entering HP as there is a large short cut flow over the warm buffer.
  - Too high  $T_{h, \text{set}}$  while the flow remains low, causing slightly higher return temperatures from the building, and thereby when reducing the demand, causing HPs to reduce capacity as a result of higher  $T_{\text{HPs, conds, in}}$ .
- The heat demand of the building is determined by the valve position of the separate floors, opening the valve further increase the temperature setpoint and simultaneously increases the flow. Ideally the temperature setpoint should not be increased till the maximum flow in such a part is realised as only increasing the flow already influences

the heat transferred and increasing the setpoint temperature reduces the share of energy produced by the HP.

- $T_{h, set}$  officially ranges from 35 °C to 55 °C but, generally above 40 °C and often above 45 °C.  $T_{h, set}$  is the maximum of all the groups of heat demanders and the temperature setpoint of each group is based on the position of the control valve.

## 2-4 Summary

This chapter provides the information and system description of the implemented system and compares it with the current standards used. Furthermore an overview of the control system implemented is presented. This information is used to develop model of the current system as described in Chapter 3. The data analysis of the yearly data has provided some first observations and hypothesis of the causes of problems currently encountered. These correlations and causes of problems have been verified by the captured high frequency data, which provide an accurate overview of all the substation's variables. Based on these observations, insights have been gathered on what can be improved and should be considered as well as relevant cases were selected. In the upcoming chapter, after a verification that similar problems can occur in the model, some of the improvements and new control strategies are developed.



# Thermo-hydraulic modelling of the system

A model is made to verify causes of problems that have occurred and test adjustments of the control methods and their effects. This can not be tested on the building substation itself as a proper operation is required and no influence on the demand thus the testing conditions can be exerted on this. Nor is there the possibility to make a test set-up as it requires the dynamics of many components and especially their size and limitations are a big factor in this. Section 3-1 discusses how the model is build up, what is considered and what assumptions are made. Section 3-2 discusses validation of the model and Section 3-3 discusses the improvements for the substation based on the thermo-hydraulic and low-level control.

### 3-1 Modelling - WANDA

The system is modelled in an unsteady (transient) state, allowing for multiple variables to change upon time and observe the response of the system. The unsteady state modelling is performed in WANDA using quasi-steady calculations [24]. WANDA is a thermo-hydraulic simulation software that provides multiple standardised components for hydraulics and thermodynamics and also includes control components. To speed up calculations, WANDA's calculations are based on an explicit approach where the control values are evaluated at every time step once the hydraulics and thermodynamics of that timestep have been calculated. Thereby the controller output is only implemented a time step later. An implicit approach would integrate the control variables simultaneously in the simulation, however this increases the computational power required. The fact that the control components are evaluated with the output of the hydraulics and thermodynamics, and are solely updated in a straightforward, explicit approach, does not allow to build internal control loops (e.g. the output of a part of the control system is also a delayed input for that part of the control system) in the control strategy. This provides some difficulties with implementing the controllers, however in many cases this could be solved, by instead of taking the output of a certain control group, measuring the energy or the speed at the component where this output is provided, this does cause a delay of one time step. Python is used to connect with WANDA to allow for variable

inputs and in a later stadium to connect with advanced control methods.

Several simplifications, assumptions and choices have to be defined to allow the model to run smoothly. The advection velocity and time step together determine the grid. The number of cells is defined by:

$$n = \text{int} \left[ \frac{L}{\bar{u}_{ad} \Delta t} \right] \quad (3-1)$$

Where  $L$  is the pipe length,  $\bar{u}_{ad}$  the maximum advection velocity and  $\Delta t$  the timestep. First of all, if all pipe sections would be modelled with the approximate length between connections, there are sections that would be shorter than the distance travelled in that section at maximum velocity. Therefore higher velocities than the adapted wave speed (advection velocity) can occur, possibly resulting in modelling instabilities. This occurs for instance in the so-called hot water distributor, which is a large diameter pipe with a connection every 0.20 m, here multiple connections have been made at one location to lengthen the distance between the connectors. Adding these connections together, one has to ensure that the entering and leaving pipes to a certain component group are still separated with a pipe section in between. Also the pipe entering the secondary side of the warm heat exchanger which is only 80 mm in diameter and only 0.70 m long should be able to accommodate  $12.4 \text{ L s}^{-1}$ , thereby the length should at least be 2.5 m. Increasing the length of this pipe can be compensated by reducing the length of the pipe based on the change of volume of the connecting pipe. The pipe entering the secondary side of the cold heat exchanger is therefore also lengthened by the same volume to compensate the length reduction of the main pipe. The pipe between the exit of the three-way valve and the evaporator side of the heatpump was originally set at 0.8 m however a flow of  $7.8 \text{ L s}^{-1}$  is the maximum, resulting in a length of 1.0 m, which has therefore been adjusted. In general for pipes smaller than a 1.0 m in diameter the fluid velocity should be below  $3.0 \text{ m s}^{-1}$ . In this model all pipe diameters are smaller or equal to 0.25 m therefore the maximum advection velocity in this model has been set at  $3.0 \text{ m s}^{-1}$ , however if smaller cells/pipe sections are preferred, this maximum advection velocity could be reduced till  $1.0 \text{ m s}^{-1}$ .

The steel pipes theoretically have a wall roughness of  $R_w = 0.05 \text{ mm}$  however to also account for curved pipes and T/Y sections, which result in an additional pressure drop the wall roughness is set to  $R_w = 0.10 \text{ mm}$ . The wall roughness is required as it determines the friction and thus the pressure drop over a pipe section using the Darcy Weisbach equation (3-2) and the Darcy Weisbach friction factor  $f$  which is based on the relative roughness,  $R_w/D$  and the Reynolds number,  $\text{Re} = \frac{\rho u D}{\nu}$ .

$$\Delta H = \frac{f L u^2}{D 2g} \quad (3-2)$$

The heat loss of the pipes is modelled using a heat transfer coefficient, for which the exact pipe specifications have to be known, material, dimensions, type of insulation and surrounding temperature. Since not all this information is available, a set of measurements has been used, when there was no flow in the heating network nor in the HPs for a longer time. It is assumed that a flow does not significantly increase the heat transfer coefficient as all the pipes are well insulated. The change of the temperature in these pipes over time and the diameter of the pipe is used to determine the heat loss per second per meter pipe length. Furthermore using the diameter, the temperature in the pipe and the temperature of the surroundings (the technical room), the heat transfer coefficient for the heat loss to the surroundings can be determined. The temperature of this room is not known, but it is assumed that it will

always be above 20 °C as other rooms are heated till this temperature, and generally all the equipment also produces some heat. Using 20 °C as the surrounding temperature, a heat transfer coefficient of 1.1 W m<sup>-2</sup> K<sup>-1</sup> to 2.0 W m<sup>-2</sup> K<sup>-1</sup>. Finally, all pipes are modelled as a rigid column and thus not considering possible waterhammer as it is not a part of this study objective and it is not expected to arise here as pumps and valves are slowly closed.

Heat exchangers, heat suppliers and demanders, all require a pressure loss coefficient ( $C$ -value) to determine the pressure drop over these components, dependent on the mass flow (3-3). If data is available about the pressure drop and the mass flow over a certain component, it can easily be used to determine the pressure loss coefficient. Plate heat exchangers typically have a pressure drop between 10.0 kPa and 100 kPa, but as there was no measurement of the pressure drop available it has been estimated based on the equations described here. The total pressure drop on one side of a heat exchanger is the sum of the pressure drop in the ports and along the plates (the conduits) (3-4). The pressure drop in the conduit (3-5) is defined by  $f_w$ , the fanning friction factor of water, which is inversely proportional to the Reynolds number (3-6) and by  $L_p$  defining the plate length and  $d_e$  the hydraulic diameter. The pressure drop in the ports is based on the fluid velocity in the ports as well as on the number of passes  $N_p$  (3-7). [25, 26]

$$\Delta p = \rho g \left( C \frac{\dot{m}^2}{\rho^2} - \Delta z \right) \quad (3-3)$$

$$\Delta p_{\text{HEX}} = \Delta p_{\text{conduit}} + \Delta p_{\text{port}} \quad (3-4)$$

$$\Delta p_{\text{conduit}} = 2 f_w \rho u^2 \frac{L_p}{d_e} \quad (3-5)$$

$$f_w = 4.608 \text{Re}^{-0.287} \quad 400 \leq \text{Re} \leq 2500 \quad (3-6)$$

$$\Delta p_{\text{port}} = 1.3 \frac{\rho u_{\text{port}}^2}{2} N_p \quad (3-7)$$

The Dittus Boetler correlation (3-9) is used to determine the Nusselt number of a plate heat exchanger to allow a determination of the heat transfer coefficient (3-8). When there are large changes in the flow velocity, this might have an effect on the achieved heat transfer. The flow velocity is proportional to the Reynolds number and therefore if the velocity is only  $\frac{1}{3}$  of the design condition, the Reynolds number is also  $\frac{1}{3}$  of the design condition, depending on the value for  $n$  the Nusselt number also changes. Assuming the typical values for turbulent flow in a plate formation,  $C = 0.26$ ,  $n = 0.65$  and  $m = 0.40$ , if the velocity is only  $\frac{1}{3}$ , the Nusselt number and therefore the heat transfer coefficient of the water is on a side is 48.9% of the design condition, therefore the overall heat transfer coefficient is only 58% of the design condition, assuming it remains a turbulent flow. Using Wanda for the simulation does not allow to change all values in operation mode (transients), for instance the heat transfer coefficients remain constant. As WANDA assumes that it is independent of the operation, based on the assumption that heat transfer coefficients should only change when there is air trapped in the column or when the mass flow changes largely such that the turbulence

becomes laminar or is reduced significantly.

$$\text{Nu} = \frac{h_{\text{conv}}}{k/L} \quad L = d_e = 2\delta_p \quad (3-8)$$

$$\text{Nu} = C\text{Re}^n\text{Pr}^m \quad (3-9)$$

The effective heat transfer area of a plate heat exchanger can generally be calculated by the number of channels multiplied by the area of a plate ( $A = L_p B_p$ ) however the effective area as a result of the chevron profile can generally be approximated by multiplying it by  $\Phi = 1.22$

The HPs with cooling, respectively heating, capacities of 200 kW, respectively 250 kW have an extensive commissioning report, covering the pressure drop, temperature and flow rates of the cooled and cooling water as well as refrigerant properties during the Heat Pump (HP) cycle at maximum capacity. Using these measurements the heat transfer coefficient and area,  $UA$ , as well as the pressure loss coefficient,  $C$  can be determined.

$$\dot{Q} = UA\Delta T_m \quad (3-10)$$

The pump characteristics provided by the manufacturer sometimes contain a small rise in the head before it starts to drop with increasing flows. As WANDA is a numerical program, to find the operation point the pump characteristic has to be flattened on the left side of the maximum to ensure a monotonously decreasing curve (negative derivative) to ensure no instabilities arise during the optimization. In general the operation of the pump should also not be on the left side of the maximum as the efficiency there is very low.

Each pump can operate at different rotational speeds, depending on the requirements it has a certain operational range and pump curves are provided for the maximum, minimum and often multiple other rotational speeds. In WANDA only one pumpcurve has to be provided, the flow, head and efficiency, and using the affinity rules (3-11), WANDA can calculate the pumpcurve at another RPM. However it should be remembered that the affinity rules imply a constant efficiency and pump diameter, therefore if there is a major difference in the top efficiency at different RPM, it is wise to chose the pumpcurve at the maximal or 100% RPM, as the minimum RPM is often less efficient and not very often used if the pumps have been dimensioned properly for the system.

The circulation pumps located to circulate the water in the cold and heat distribution net are placed with two in parallel, as well as the pumps circulating the water from the HPs to the warm heat exchangers connected to the 5GDHC networks. One individual pump can allow for the maximum flow, however the parallel pump is there as a back up in case the other pump has an error or is broken, this way the heat and cold delivery can still be maintained. The control system switches between the two pumps every week to determine the primary pump, ensuring an equal amount of operating hours thus wear and chance of breaking down. In the WANDA model, both the pumps have been modelled, however during the simulations the controller has only been implemented on one of the pumps and the other one is shut down. There is no use to switch the operation between the two pumps in the simulation as there is no simulation of the wear or internal pump errors.

$$\dot{m} \propto n \quad H \propto n^2 \quad P_{\text{pump}} \propto n^3 \quad (3-11)$$

Many valves in the substation are solely used to open/close the pipe flow and therefore the valve characteristic is not very important. Butterfly valves of the same manufacturer

and type are used so that the  $K_v$  value only depends on the nominal diameter. The control valves are of the same type and have a linear characteristic, however the motors driving the valve contain a function to change it into an equal percentage characteristic with the ability to change the  $\alpha$  value and therefore fit it with the respective application (heat exchanger). Resulting in a linear control characteristic to allow the heat exchange or flow to be linear with the valve position. Furthermore these valves contain a pressure difference control to ensure an authority of 1 (100%) as the characteristic does not change its shape as a result of a change in pressure.

It should be noted that, when modelling the building delivery side, the same flowrate can be obtained by either changing the opening of one control valve and therefore adjusting the flowrate through a specific heat exchanger, or by changing multiple control valves and therefore requiring a smaller opening change. Since these systems are connected in parallel, the pressure drop over each system is the same and the mass flow is the sum. When only one system (control valve and heat exchanger) is in use, the valve is more open, resulting in a smaller pressure drop, the pump will work harder (higher RPM) to obtain the predefined pressure drop of  $\Delta p = 90$  kPa over the system. If multiple systems would be in use while maintaining the same flowrate over the combined system, the flowrate of each connection is smaller, indicating that the control valve is more closed and the pressure drop over the control valves is larger, to maintain the same pressure drop, the pumps have to work less hard (lower RPM). To model the correlation of the pump's power with the mass flow, the separate groups would have to be modelled and the position of the control valve for all these groups would have to be considered, as this is not known, it is simplified to one heat node with a given flow. This does not have to be a problem, the demanders can be modelled with one heat node, one control valve controlled on the flow and a long pipe as most of the head loss is caused by the pipes and the heat exchanger.

The heating, cooling and air treatment groups determine the supply temperature setpoint to these groups as well as the flow. As these groups and the building it self are not modelled in detail, the flow generated by these groups are used as inputs for the model by opening/closing the control valve connected to a heat generator/extractor while the pumps ensure a pressure drop over the building side. The heat generator/extractor is used to model the heat exchanger that is in place between the distribution network and the inner floor network and air treatment groups cooling/heating the air, as the heat flux that is generated can easily be modelled using it as an input to the model. A lower limit on the return temperature from building to the heating distribution network is set at  $T = 25^\circ\text{C}$  as below this temperature the distribution network can not provide heat to the floor network. An upper limit is set on the temperature of the flow returning from the building to the cold distribution network at  $T = 20^\circ\text{C}$  as above this temperature it can no longer provide cooling. These limits are important to provide simulations that are as close to reality as possible. In case not the full heat flux can be obtained due to the temperature limitations, the heat flux that is not provided, is accumulated and is added to this heat flux when the temperature limitations are not exceeded. Figure 3-1 provides the scheme of the modelled substation in WANDA.

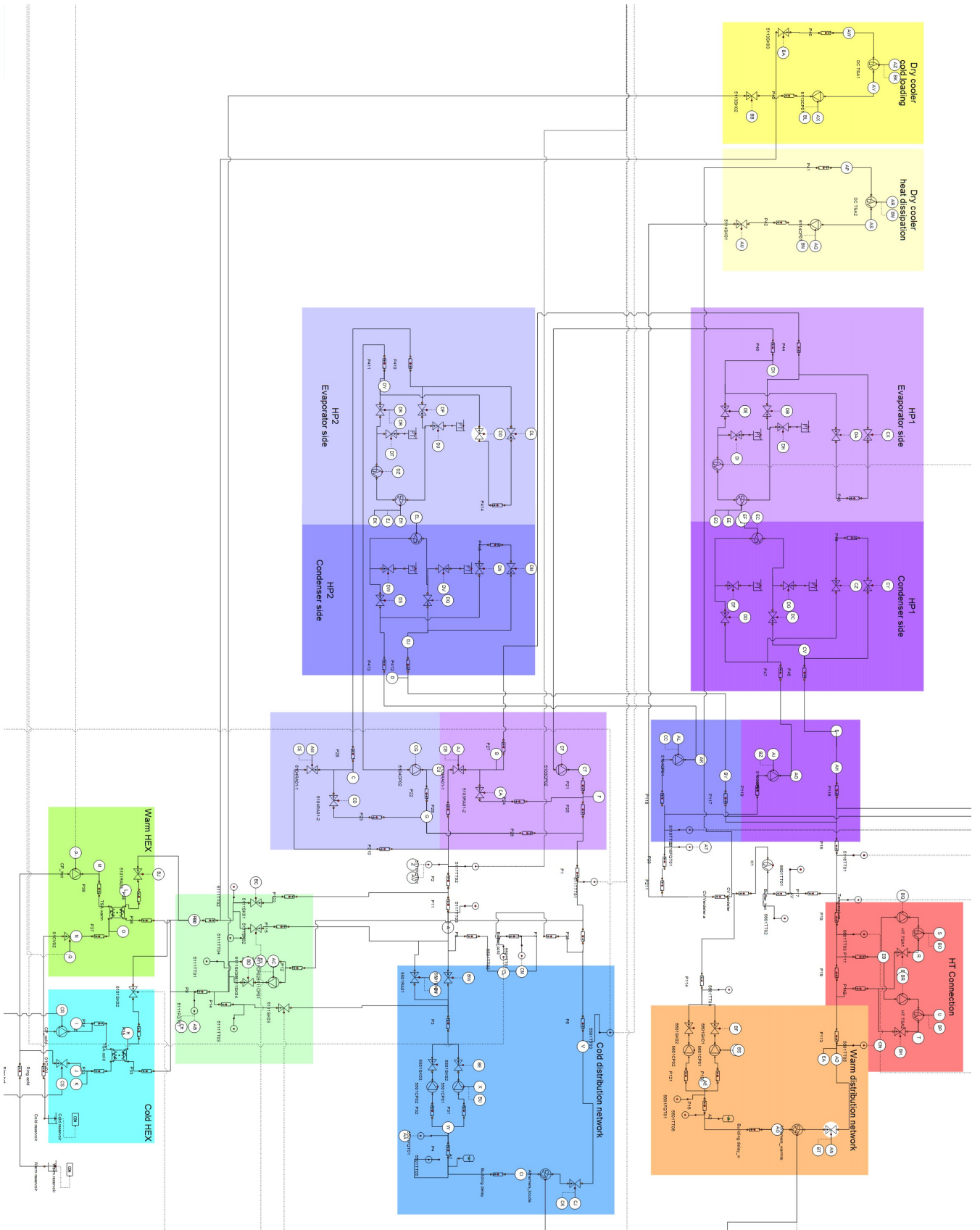


Figure 3-1: WANDA model of the substation

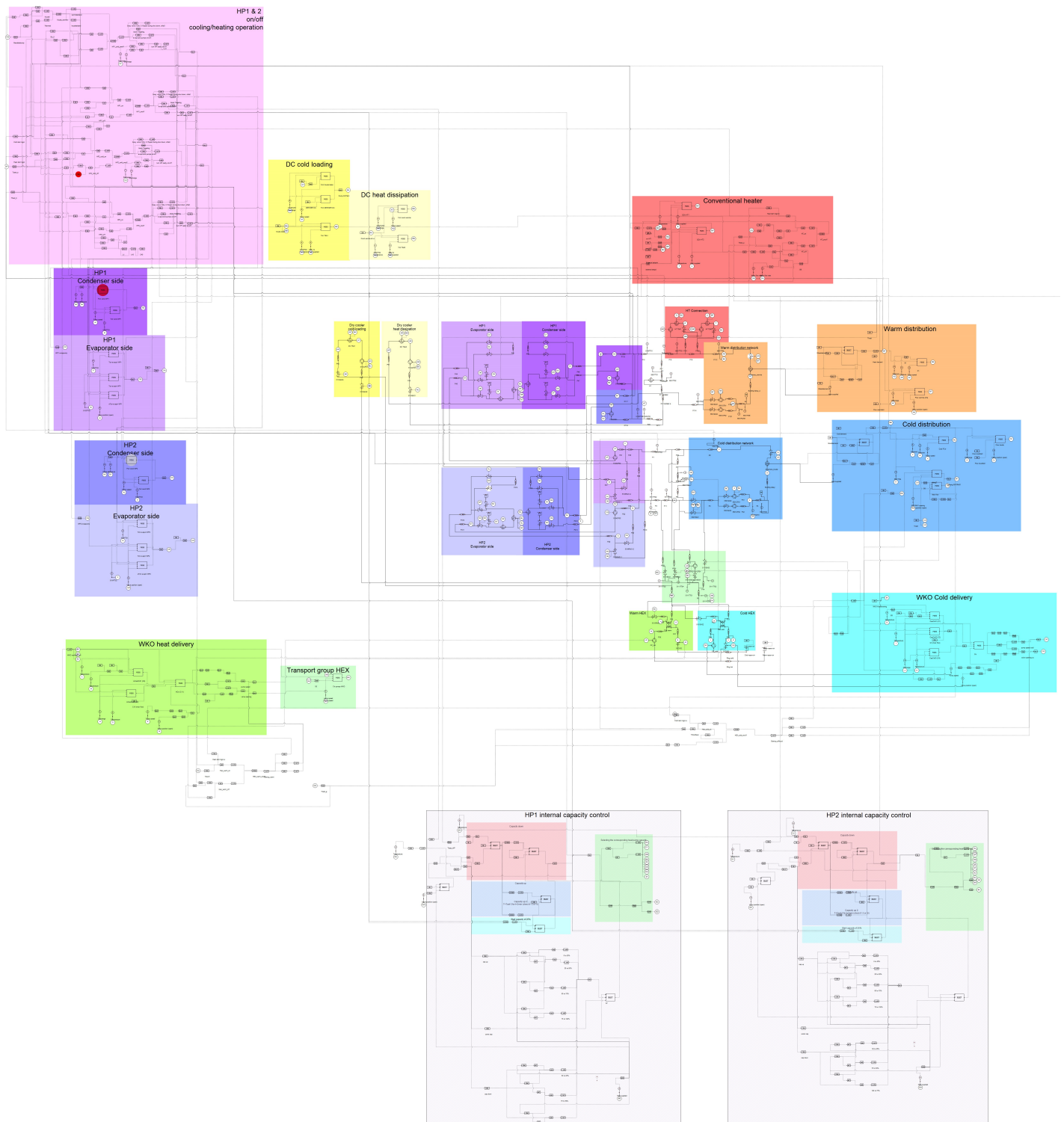


Figure 3-2: WANDA model of the substation including the control systems

Component	Property	Value
General	Ambient temperature	$T_{sur} = 20\text{ }^\circ\text{C}$
Steel pipes	Wall roughness	$R_w = 0.05\text{ mm}$
	Heat transfer coefficient	$h = 1.1 - 2.0\text{ W m}^{-2}\text{ K}^{-1}$
	Maximum advection velocity	$v_{ad, max} = 3\text{ m s}^{-1}$
	Calculation mode	Rigid column
Heat exchanger 5GDHC cold	Pressure loss coefficient	$C = 5490\text{ s}^2\text{ m}^{-5}$
	Heat transfer coefficient Area	$UA = 300\,000\text{ W K}^{-1}$
Heat exchanger 5GDHC warm	Pressure loss coefficient	$C = 3835\text{ s}^2\text{ m}^{-5}$
	Heat transfer coefficient Area	$UA = 240\,000\text{ W K}^{-1}$
Heat exchanger DC	Pressure loss coefficient	$C = 5000\text{ s}^2\text{ m}^{-5}$
Heat exchanger HT	Pressure loss coefficient	$C = 10\,000\text{ s}^2\text{ m}^{-5}$
Heat pump	Pressure loss coefficient evaporator	$C = 36\,000\text{ s}^2\text{ m}^{-5}$
	Heat transfer coefficient evaporator	$UA = 82\,380\text{ W K}^{-1}$
	Pressure loss coefficient condenser	$C = 31\,300\text{ s}^2\text{ m}^{-5}$
	Heat transfer coefficient condenser	$UA = 29\,340\text{ W K}^{-1}$
Heat consumers	Minimum return temperature	$25\text{ }^\circ\text{C}$
Cold consumers	Maximum return temperature	$20\text{ }^\circ\text{C}$

**Table 3-1:** Overview of the assumptions

Some general assumptions have been made regarding the model. The ambient temperature of the substation, the temperature of the room where all the components are located has been assumed at  $T_{sur} = 20\text{ }^\circ\text{C}$  because the room itself is heated and temperature controlled, however, the apparatus present would produce enough heat to atleast have a temperature of  $20\text{ }^\circ\text{C}$  most days. On warm days, this might be higher, and thus heat losses would be lower on the warm side of the substation and 'cold losses'/heat additions on the cold side of the substation would be higher, however on the short time dynamics this is of small importance due to the low heat transfer coefficients of the pipes.

The controllers in WANDA are defined in SI units, therefore the controllers as installed in the system should be changed to the SI units this is especially important for the setpoint and gains, while the integration time is already in seconds. If the setpoint is in kPa the setpoint in WANDA has to be multiplied with  $1.0 \cdot 10^3$  to change it to Pa, the gain should therefore be divided by  $1.0 \cdot 10^3$ . Furthermore the outputs of the controllers in the system are often provided in % of the maximum, while the input for components is for instance the pump speed, therefore the gain has to be multiplied by the maximum speed divided by 100%, furthermore while the speed is often provided in RPM, the SI units are  $\text{rad s}^{-1}$  therefore the gain also has to be multiplied by  $\frac{2\pi}{60}$ . Finally, the gain of the PI controller measuring the pressure difference over the building should be multiplied with  $\frac{1}{1000} \frac{\max\text{ RPM}}{100} \frac{2\pi}{60}$ . Figure 3-2 provides the scheme of the modelled substation in WANDA including the modelled control systems.

Concluding, the external inputs to the model are the flow and heat flux demand for cooling and heating the building and it is stated whether additional cold should be loaded to the wells. The temperature of the warm and cold ring network are important inputs as they might fluctuate over the year or as a result of a return flow from another building.

The model also needs to be initialised, stating the temperature in the nodes which correspond to temperatures measured, the initial pump speeds, valve positions, operating capacities and controller on/off states. It should be noted that if there is no mass flow through a pipe at

Case	Energy demand			$T_{h, set}$		HT kick in		
	Fluctuating	High	Low	Fluctuating	> HP max	High $T_{h, set}$	Slow HP	HP shut down
0		x	x	x	x	x		
1	x		x	x	x	x	x	x
2		x			x	x		x
3			x	x	x	x	x	
4					x	x		x
5					x	x		x
6		x		x	x	x	x	x
7		x		x	x	x	x	x
8					x	x		x
9	x				x	x		x
10	x			x	x	x	x	
11	x	x	x	x			x	x

**Table 3-2:** The selection of the cases and their warm distribution building network properties

$t = 0$ s, the initial water temperature in that pipe is set to the ambient temperature instead of the temperature at one of the connecting nodes. Furthermore, WANDA simulations start from a steady state while the substation is dynamic. The starting conditions can therefore not always be copied from the measured conditions due to controllers needing to start in a steady state.

Finally, it should be noted that parts can be broken or unavailable during the operation of the substation. As this is not the standard operation, the system and its controllers have only been modelled under the assumption that all the components are available and not broken. In reality the controllers consider the fact, that one component, for instance a HP might not be available as a result of an internal error and therefore the HT connection might be activated even though only one HP is on. The overview of all the values that are based on certain assumptions for the WANDA model is shown in Table 3-1.

## 3-2 Simulations

All the simulations in WANDA are simulated with a time step of 1.0 s. The model first had to be verified, to ensure that similar behaviour occurs for the thermo- and hydrodynamics and the control systems. Verification is done both on (group of) component(s) level, as well as for the complete substation system. The validation shows that the behaviour is similar, however, some values can be slightly different and thus cause a different response of the control system. Small changes in demand or temperature can have a completely different effect. Inaccuracy and lack of data due to earlier explained causes in Section 2-2 can have a significant effect on the validation, and thus those cases can not be used for validation but only for testing purposes.

Based on the data analysis, several cases have been derived to determine the response of the system and to determine the effect of the proposed improvements. Some cases are almost similar in response, but as stated before slight changes in the demand profile can have completely different effects and thus all profiles have been tested. The considered cases based on the warm distribution side operation are shown in Table 3-2.

Furthermore, some specific cases have been selected based on observed problems by the

data analysis that occur at the heat exchangers connecting the ring network. These cases are based on the descriptions in Section 2-2-2. The substation instability is considered, but also other events, like cold heat exchanger switching, cold buffer short-cut flow and the Dry Cooler (DC) conditions and server room influence which have simple improvements.

### 3-3 Low level control and thermodynamic improvements

Based on the observations in Chapter 2 several adjustments in the system are proposed. The improvements regarding the thermodynamics as well as the control system are discussed here.

A relative easy amendment for modelling purposes would be to increase the maximum temperature of the HPs as it is expected that if a HP is used with a higher maximum operating temperature, the energy produced by the conventional heater can be reduced significantly. The other option would be to change the demand profile provided by the building, such that the temperature setpoint of each group would only reach upto the maximum temperature that the HPs can provide after which the flow over the group is increased till its maximum (control valve fully open) before it increases the temperature setpoint further.

#### 3-3-1 Matching components with building demand

The thermodynamic properties of the substation should be better aligned with thermal and hydraulic demand. This can be improved by changing the demand profile, such that the flow is first increased to its maximum before the temperature setpoint is increased above the maximum temperature that can be reached by the heatpumps. The other possibility would be to ensure that the heatpumps can provide temperatures up to the maximum setpoint such that the conventional heater would only be switched on if the demand exceeds the heatpump's capacity. Still, the demand should be managed properly to minimize the energy consumption, by ensuring that the temperature setpoint does not become too high, as this requires a larger electricity demand from the heatpump to reach the setpoint (the COP reduces with an increased temperature lift), but simultaneously a high flow will also cause additional pumping power. Ensuring that the heatpumps can reach the maximum setpoint temperature shows the improvements in terms of reduction of conventional heater usage, thus a reduction in the CO<sub>2</sub> production.

If similar sizes of heat exchangers are required, one heat exchanger and primary pump can be removed and the water flow can be circulated using control valves to select the appropriate pipe. This would reduce the system by one heat exchanger and one pump.

Furthermore, it should be noted that also other components and sensors should be properly determined based on the range in which they should be able to operated. The minimum flows of the pumps should align with the minimum flow of the substation section in which it is installed and sensors should be able to register small flows that can occur.

#### 3-3-2 Peak shaving

Peak shaving can be accomplished on two sides, at the substation or at the demand side. Demand-Side Management (DSM) can reduce a peak in heat demand, for example by starting to heat up a building earlier in the morning, or reducing the night setback. This can also be organised in a more advanced manner by model predictive control methods that consider

the buildings heat loss. Peak shaving in the substation itself can be organised by heating up a large buffer, which can be drained when the demand is at its peak and the HPs are already working at full capacity or at their best point of operation from an energy efficiency perspective. It is important that the buffer has a decent size, such that it can really shift some of the peak load. Currently in many of these substations, the buffers installed are only there to hydraulically decouple the substation from the building network and to stabilize the operation of the HPs, thus ensuring that the HPs do not switch between capacities more often than 5 minutes and preferably 15 minutes and do not turn on or off for shorter than 15 minutes to reduce compressor wear.

In this thesis the demand, including the temperature setpoint and the mass flow are considered to be given and thus peak shaving by DSM is not considered in this work. Furthermore peak shaving at the substation could be of interest, however the buffer vessels currently implemented are too small (1000 L). If one HP is working at its smallest heating capacity (60 kW), and a temperature difference over the building of at least 15 °C (generally higher for the buildings considered) upto 25 °C (depends on temperature setpoint) is reached, the buffer can only store  $1000 * .998 * 4.2 * 15 = 63 \text{ MJ}$  upto 105 MJ, which translates to about 17.5 kWh to 29 kWh. Building flows generally being between 1.5 and 6.0 L s<sup>-1</sup> one can imagine these buffers would be drained quickly between 3.0 min and 10 min if used stand alone. Also the buffer can be completely filled with one HP at its smallest capacity in about 20 min and since the buffer generally is not fully drained, there is some dead weight in the bottom and top, there is always some mixing and the temperature setpoints would not be reached before it is fully drained, resulting in an even shorter time. Therefore these buffers are only to be used for stabilising the HPs, the controls and to hydraulically disconnect the substation from the building network.

### 3-3-3 HEX - heat pump instability

Previously it was discussed that the primary flow at the heat exchanger is controlled based on a cascade controller. Hereby, it is preferred that the heat exchanger is controlled at both outlet temperatures, to ensure that this influence of both component groups (HPs and HEX) performance, which continues the fluctuations and temperature exceedings, is smoothed out. Possibilities would be to reduce the gain, changing the flow setpoint such that a minimum return temperature to the substation is maintained or changing the setpoint of the return temperature to the grid such that this setpoint does not become lower than the supply temperature from the substation. A reduction of the gain is not preferred as the effect will be a slower response during normal operation.

The choice to change the setpoint of the controller from 7 °C to  $\max(7^\circ\text{C}, T_{\text{HEX}_h, \text{sec}, \text{in}})$  on the primary (grid) side of the HEX, avoids that the setpoint of the temperature returning to the grid is lower than what is entering on the secondary side. Thus resulting in a slower reduction/increase of the primary flow and keeping the return temperature to the substation higher. Another possibility is to add a PI controller to the cascade, for the minimum temperature  $T_{\text{HEX}_h, \text{sec}, \text{out}}$  at for instance  $\min(12^\circ\text{C}, T_{\text{HEX}_h, \text{prim}, \text{in}} - 1.5^\circ\text{C})$ , this will ensure the minimum temperature on the secondary side if the maximum of this controller and the  $T_{\text{HEX}_h, \text{prim}, \text{out}}$  controller is taken.

### 3-3-4 Cold buffer short-cut network

The short-cut flow over the cold buffer occurs when the HPs are working at low capacity and is caused by the control system which only allows the warm heat exchanger to turn off:

- if there is a cooling demand and the temperature in the buffer is too high
- or if there is no cooling demand and the HPs are turned off.

This is done to prevent too low temperatures entering the evaporator and preventing freezing as it requires time before warmed water at the heat exchanger can arrive at the evaporator. This problem could be solved by allowing the warm heat exchanger to also be turned off, if only one heat pump is turned on at 25% capacity AND  $\dot{V}_{\text{evaps}} - \dot{V}_{\text{c, build}} \leq \dot{V}_{\text{HEX}_h, \text{sec}} - 0.20 \text{ L s}^{-1}$  AND  $T_{\text{c, buffer, bottom}} \geq 12^\circ\text{C}$ . A deviation of  $0.20 \text{ L s}^{-1}$  is chosen as this is about 10% of  $\dot{V}_{\text{HEX}_h, \text{sec}}$  and 10% of buffer short-cut flow would keep the temperature still within limits. This is different from the current case as there is still no cooling demand but one HP is now on at its lowest capacity, therefore also the flow and buffer temperatures have to be considered.

Or the primary pump should be turned off if  $T_{\text{HEX}_h, \text{sec, in}}$  is larger than  $9^\circ\text{C}$  for more than one minute, but this might cause only a short shut down of the pump as it should turn on again once it is below  $9.0^\circ\text{C}$  to prevent freezing of the HPs. The downside for this option compared with the previous option is that the evaporator inlet temperature before the three-way valve will quickly decrease as the secondary side of the HEX is still operated and thus this flow is short-cutted instead of fully emptying the cold buffer.

Generally, for both options the buffer will be filled up quickly  $\left(\frac{1.0 \cdot 10^3 \text{ L} \cdot (14 - 9.0)^\circ\text{C} \cdot 4.2 \text{ kJ kg}^{-1} \text{ K}^{-1} \cdot 0.998 \text{ kg m}^{-3}}{50 \text{ kW}} \approx 8.0 \text{ min}\right)$  till below  $9.0^\circ\text{C}$  thus the warm heat exchanger would have to operate quickly again to prevent freezing.

Finally, this could also be solved by ensuring that pumps are selected which can reach this low flow and if the heat exchanger are still able to operate properly turbulent at these flows.

### 3-3-5 On/off switching cold heat exchanger

Switching parameters for cold/heat delivery of the 5GDHC network should be chosen with a wider hysteresis and ensuring that during cold delivery, the cold HEX is not shut down if the buffer is just below the desired supply temperature and if the HPs are turned off. This desired supply temperature might be higher than the  $T_{\text{HEX}_c, \text{sec, out}}$  and would otherwise cause a sudden increase in the  $T_{\text{c, build, in}}$ , having to be immediately turned on again. This can not be implemented if at least one HP is on as it might then cause a too low evaporator inlet temperature.

### 3-3-6 Capacity and temperature control heat pumps

Currently the outlet temperature of the HPs is solely based on the condenser inlet temperature, which is a mixture returning from the building and the buffer, and on the operating capacity. This does not allow for a strict temperature control as there are only discrete capacity steps to be made and the mass flow over the condenser side of the HP is constant.

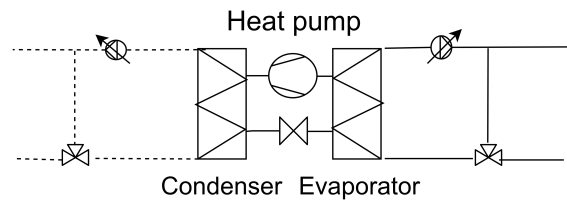


**Figure 3-3:** The added 3way valve at the condenser side of the heat pump to improve the temperature control

### Temperature control

To allow for such control, a proposal in this thesis is to add a three-way valve connecting the condenser outlet and inlet in a similar manner as on the evaporator side, shown in Figure 3-3. This three-way valve could be controlled with a PI controller based on the error of the condenser outlet temperature compared to the temperature setpoint. The three-way valve would always have a minimum opening of 15% to ensure that overheating is not able to happen as always some lower temperature water is added. This allows for a reduced net flow over the condenser, while the flow over the condenser is still the same, a different temperature can enter the condenser. The temperature before the three-way valve is lower than without this control method as the net flow is lower. The warm buffer is now not continuously flushed through and thus there is less mixing from the buffer and the building resulting in lower temperatures entering the three-way control valve.

Ideally one would also be able to variate the flow over the condenser, thus reducing the pump speed, allowing for a reduced pumping energy consumption and possibly even a higher COP as the temperature jump over the condenser is larger. The pump and three-way valve control would then have to be combined, the pump would have to be started at its minimum rotational speed, in correspondence with the minimum flow required by the HP for the heat exchanger to work properly. The three-way valve would have an active/fast control based on the condenser outlet temperature, the control on the pump needs to be slower as it can not change its rotational speed very quickly and it will increase the wear.

Ideally, one would want the pump to be at the lowest rotational speed while reaching the demand, as this reduces energy consumption, thus the three-way control valve should be almost fully open (minimizing the short cutting/mixing flows). Therefore, the pump should be controlled with a PI controller where the speed is only increased if the three-way valve is open for more than 80%, as the pump responds slowly, a higher percentage might result in an overshoot at the outlet temperature. Furthermore the speed should be reduced when the three-way valve is open for less than 60%. A 20% hysteresis ensures that the speed can stabilize, and allowing the three-way valve to be in a position between these two values ensures a wide range in which it can respond quickly, which is a trade off with the pumping power required.

Another option to control the condenser pump speed would be to ensure a constant temperature difference over the condenser. If the temperature difference is smaller, the pump speed would decrease and if the temperature difference is larger, the pump speed would increase. A slow PI controller, to ensure it does not interact with the fast three-way valve dynamics and not continuously adjust the pump speed, could be implemented with a minimum pump speed. This option might result in a higher inlet temperature than the previous

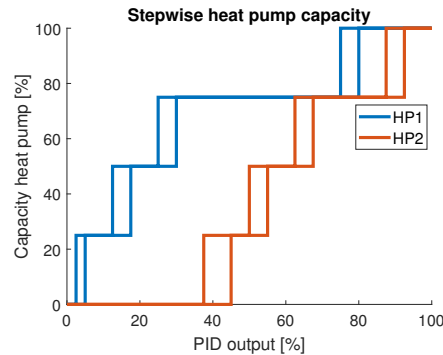


**Figure 3-4:** The distribution of the heat pump capacity steps over the PI controller output

option, depending on the temperature difference that is chosen ( $\Delta T$ ). Again a minimum is set on the pump speed to ensure a minimum flow. Also it should be noted that if there is a high temperature entering the three way valve from the buffer and building, the temperature difference can not be achieved without overshooting the temperature setpoint. Thus, the minimum of the chosen temperature difference and the difference between the temperature setpoint and temperature entering the condenser before the 3way valve has to be chosen ( $\min(\Delta T, T_{h, set} - T_{HPs, conds, in})$ ) as the setpoint. The larger the standard temperature difference that is chosen the larger the reduction in pumping energy will be, however a too large temperature difference might result in difficulties regarding the tuning as it will more often be influenced by changes in  $T_{HPs, conds, in}$  and thus be controlled more actively. One should be careful to prevent interactions between the pump and the three-way valve.

Lastly, there is the option to control the three-way valve and the pump using a split range controller as discussed before and applied at the network heat exchangers. This would minimise the pumping power however, when even small changes occur in the condenser outlet temperature this would result in changing the pumping power. As it should only be controlled slowly to prevent wear and large fluctuations, this does not allow for the most accurate control, especially regarding large changes.

These improvements for the pump and three-way valve control can also be used on the evaporator side, however, the range of operation for the pumps might be limited more as one wants to prevent too low evaporator entering temperatures due to freezing effects.

### Capacity control

The heat pump's capacity can now no longer be controlled based on the condenser outlet temperature, but the temperature entering the building would be a good parameter as this will also indicate if the 'net flow' over the condenser is large enough. If it is too small, the flow entering the building will mix with the water from the buffer. A PI controller could be used, and based on the output, one or two HPs would be operated at specific capacities, a hysteresis is implemented to ensure that no continuous switching between two capacities occurs due to the dynamics when changing capacity. This procedure is shown in Figure 3-4.

Besides measuring the temperature entering the building it is also possible to measure the energy produced by the HPs and use the energy consumed by the building as a setpoint as energy combines both the temperature and the flow. The problem is that the energy steps of the HPs are discrete and have to properly include the buffers volume and energy potential.

Furthermore, one has to determine to either use the temperature setpoint or the temperature entering the building to determine its demand. The advantage of using the energy based on  $T_{h, \text{build, in}}$  is that the production is compared to what is really being used, however if the temperature setpoint is increased and the flow not, the HPs would still produce the correct temperature, but now some mixing might occur causing the new temperature setpoint not to be reached at the building entrance. Thus it seems like the energy demand remains the same as long as the return temperature from the building does not significantly decrease. If the energy is based on the temperature setpoint, it provides us with a better estimate of the energy demand and thus PI capacity control setpoint. A downside could be that a similar energy production could occur as the demand, yet it is possible that the temperature setpoint is not reached and the buffer is solely heated up, which would later ensure that the temperature increases again and thus the temperature setpoint will be reached. This delay would particularly be relevant if at small capacities the minimum net flow is used, while this is larger than the demand flow of the building.

Finally, regarding using the energy for the PI capacity control, one could also use the energy demand as a setpoint and the energy consumption as the manipulated variable. The manipulated variable is now not a discrete value, however, this does not have the ability to consider the energy in the buffers and thus the PI output will only start to decrease once  $T_{h, \text{build, in}}$  exceeds  $T_{h, \text{set}}$ . This operation would be similar to the temperature setpoint PI operation, but it now also considers the difference in flow, such that at larger flows, the temperature difference is more important.

One might think it would be wise to control the capacity based on the difference in flow between the building and the condensers, thus the flow over the buffer. However a too tight control on this, might result in not fully filling up/emptying the buffer and too frequent switching between capacities as the buffer capacity would than not fully be used to stabilize the HPs. It should be a slow control with especially an important factor for the integrator. This might also result in the temperature setpoint not to be met at the building entrance as there is some flow from the buffer, yet small, and not yet increasing the capacity. The dynamics should carefully be considered. As temperature setpoints might vary the temperature would seem like a safer option as it should not be a problem to take some water from the buffer when the temperature is decreasing. Also the net flow over the HPs might be minimal (pump and three-way valve), yet the temperature setpoint might not be possible as the temperature entering is too low, if the flow over the HPs is still larger than the flow over the building, the capacity will not be increased, eventhough the temperature setpoint can not be reached. Therefore the minimal net flow over the condenser should be larger than the minimal flow over the building, for this to work. This typically becomes a problem when the temperature difference over the building (10 - 25 °C) is larger than the temperature difference that can be reached over the HP (minimal capacity/minimal net flow =  $65 \text{ kW} / (0.15 * 6.0 \text{ L s}^{-1} * 4.2)$ ). So temperature or heat demand would be better, however the heat demand would have to be based on  $(T_{h, \text{set}} - T_{h, \text{build, out}})c_p \dot{m}_{h, \text{build}}$  and not on the temperature entering, otherwise the setpoint might not be reached and due to not reaching the setpoint, the energy consumed by the building would also not be the real demand.

For continuous capacity controlled HPs (stepless), the options to use a PI controller based on the energy are easier as the buffers are of less influence and the change in capacity can be smaller.

The control system has been implemented in the simulation with a three-way control

valve and a constant speed pump as the current HP investigated can not handle a wide range in mass flows. The corresponding PI values for the three-way control valve and the capacity controller are shown in Table 3-3, also it shows the PI output at which it switches between capacities. Currently it has been chosen that the second HP will be turned on after the first HP is at 75% capacity as the capacity changes where than easier to implement in WANDA, the hysteresis between the on/off of the second HP is also set the largest to ensure that the HP does not switch on/off too often. If the second HP would already be turned on when the other one is at 25% capacity, this doubling in capacity could become problematic for the temperature control, as it might become more difficult to manage within the range. Also the buffer could be filled up too quickly if the demand/temperature setpoint would decrease again, causing it to shut down again. Yet it would provide greater flexibility in a capacity change, tracking faster energy demand ramps as two heat pumps can increase their capacity almost simultaneously.

### Capacity control including buffer

The capacity control based on the temperature setpoint seems to work properly in every case besides case 11, where there is a strong fluctuation in the flow and the temperature setpoint. Eventhough these fluctuations have also been encountered in other cases, there the problems did not arise, but only some comfort limits were exceeded.

The response of the PI capacity control takes some time before it reaches a new capacity level and there is also a non constant time delay between the water leaving the condensers and entering the building. The result is that the capacity can go down too late or too slow under certain conditions, this was particularly visible in case 11. It could be estimated earlier in time that the difference between the setpoint temperature and the temperature entering the building would become negative as the three-way valves at the HPs would already be almost fully open due to a high condenser inlet temperatures compared to the setpoint. Therefore instead of using the temperature setpoint as the setpoint for the PI capacity control, it is added with a negative gain multiplying:

$$\max(0, o_{HP1,3\text{-way}} - 0.90) + \max(0, o_{HP2,3\text{-way}} - 0.90) + \min(0, o_{HP1,3\text{-way}} - 0.25) + \min(0, o_{HP2,3\text{-way}} - 0.25).$$

This will result in an earlier detection of the HPs running at a too high or too low capacity. The gain should not be chosen too high as it will influence the operation at maximum capacity when maximum heat demand occurs.

When the control of the three-way valve has been substituted with a controller for both the pump and the three-way valve, the opening of the three-way valve can no longer simply be used to determine the whether the capacity will soon have to be reduced or increased. As the position of the three-way control valve in the standard case basically tells us something about the net condenser mass flow, the same procedure can be applied, but now the valve opening is replaced by the net condenser mass flow ( $\dot{m}_{HP1, \text{cond}, \text{net}}$  and  $\dot{m}_{HP2, \text{cond}, \text{net}}$ ) and 0.90 replaced with  $0.90\bar{m}_{HP1, \text{cond}}$  and 0.25 with  $0.25\bar{m}_{HP1, \text{cond}}$  and the gain is adjusted properly.

Another method that could also be considered, would be to use the buffer temperatures to determine a reduced or increased setpoint for the capacity controller. The condenser inlet temperature increases quickly once the capacity has to be reduced as a result of the buffer being fully loaded. The bottom of the buffer would have a temperature ranging anywhere from the temperature at which water returns from the building and maximum setpoint tempera-

PI controller	Proportional gain	Integration time constant
Three-way valve control	$0.065 \text{ } ^\circ\text{C}^{-1}$	15.0 s
Capacity control	$0.001042 \text{ } ^\circ\text{C}^{-1}$	8.0 s

**Table 3-3:** PI-control values, 3-way control valve and capacity

ture. As the temperature at the buffer bottom is a strong indication, an elevated temperature should reduce the setpoint of the capacity controller. This is determined based on the difference between  $T_{h, \text{buffer, bottom}}$  and  $T_{\text{HPs, set}}$  which should be smaller than  $10 \text{ } ^\circ\text{C}$  to be of effect. A similar action with opposite control, increasing the setpoint, can be taken based on a difference larger than  $10 \text{ } ^\circ\text{C}$  between  $T_{h, \text{buffer, top}}$  and  $T_{\text{HPs, set}}$ , indicating the buffer is fully unloaded. But this last difference should not be considered as even a slightly lower temperature and mixing before the building entrance would already have the effect to increase the capacity and could thus destabilise as this would result in a too large capacity change response.

### 3-4 Summary

A hydro- and thermodynamic model of the substation is made in WANDA including all the control components that are currently applied. Simulations are performed for all standard cases. Several thermodynamic and control improvements are proposed for the different problems that occur.

It is important that all components are selected for the complete range in which they should be able to operate, thus all the minima and maxima of that specific substation section. Furthermore the use of larger buffers can result in fewer capacity changes of the heat pumps and if large enough, even some in building storage for peak shaving. Peak shaving can also be organised by DSM, but is not considered in this study.

The instability of the substation regarding the interaction between the Heat exchanger (HEX) and HP can be prevented by changing the temperature control of the HEX to prevent it from responding inadequately and too rapidly on temperature changes. This could be achieved by changing the temperature setpoint of  $T_{\text{HEX}_h, \text{prim, out}}$  based on  $T_{\text{HEX}_h, \text{sec, in}}$  or by adding a PI controller to ensure a minimum temperature returning to the grid  $T_{\text{HEX}_h, \text{sec, out}}$ .

The cold buffer short-cut flow causing too high  $T_{\text{HEX}_h, \text{sec, in}}$  and thus  $T_{\text{HEX}_h, \text{prim, out}}$  could be averted by shutting the warm HEX down under special conditions such that it does not affect normal operation, if it cannot be averted by ensuring that proper pumps are chosen. For the cold HEX the unnecessary on/off switching can be reduced by reducing the buffer temperature for which to shut down if there is a cooling demand and the heat pumps are not in operation.

Finally a different approach for the capacity and temperature control of the heat pumps is proposed. The physical system for the temperature control to be implemented is changed with an added three-way valve. The capacity control can be based on the temperature entering the building or on the energy demand, which is based on the flow, temperature setpoint the temperature returning from the building.



# Model Predictive Control

As observed in previous cases, large fluctuations in the temperature setpoint and in the energy demand can occur. As Model Predictive Control (MPC) has the ability to consider the system dynamics and a prediction of the demand it can optimise the control inputs for the future and thus start up a heat pump earlier in time or change its capacity. First the theory behind MPC is shortly introduced in Section 4-1 after which the substation model required is described in Section 4-2. Finally the MPC strategy is discussed including the constraints and objectives in Section 4-3.

## 4-1 MPC theory

MPC utilizes a model to predict the future states and to determine the optimal control inputs for a given objective function. Compared to PID and the basic hybrid control methods for switching this is an advanced control method. It can consider the system dynamics to provide an optimal control while handling the constraints of the given system. The constraint handling is an important feature as it considers the limits of the system instead of just trying to increase the speed further or the temperature higher while it is not possible, this is especially important for physical systems. The disadvantage is that an accurate model is required to ensure that the optimality can also be executed and the computation time can become problematic for large systems of equations especially for non linear problems. Finally, a main advantage of MPC is that it can predict the systems response and thus anticipate on future events, once again, the anticipation is only as good as the prediction of future events provided. Examples of those future events are for instance weather conditions or energy demands.

MPC consists of a prediction model of the system and an optimisation algorithm. The model consists of the state/manipulated variables (dependent variables) and of the decision/-controlled variables (independent variables). The optimisation algorithm optimises over a finite horizon for a given reference/trajectory and cost/objective function. It is based on a receding horizon principle, meaning, that the at time  $k$ , the system states are measured and the previously decided input is given. Using this, the prediction of the systems state at the next time time step  $k + 1$  are determined and from here on, the optimisation algorithm can compute the optimal control inputs to achieve the reference/trajectory or setpoints. Once

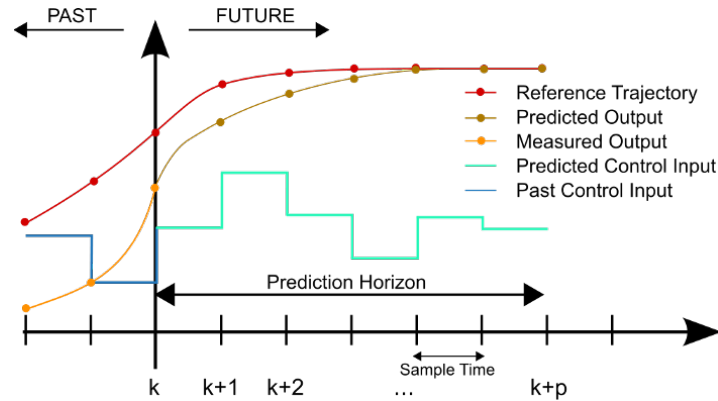


Figure 4-1: MPC receding horizon policy [5]

the time step's time in real time is over, the first time step computed control inputs are given as an input to the real system and the other control inputs are discarded. The process starts over again, with just one time step ahead and the updated measurements. An overview of this process is shown in Figure 4-1. The optimisation algorithm continuously optimises over the same length, the prediction/control horizon  $N_p$ . The control horizon can be smaller than the prediction horizon to reduce the computational expense or because of internal model delays, then the controlled variables remain constant after the control horizon is finished and for the remainder of the prediction horizon.

The objective function sums the weight values and penalty values multiplied with the respective variables, that can be the error of state variables compared to the trajectory or the change in value in decision variables. Besides constraint handling there is also the possibility to handle binary variables, these optimisation algorithms are named Mixed Integer Programming (MIP) problems. These optimisation algorithms are generally based on a branch and bound method possibly combined with cutting planes, and can be come computationally intensive as the number of possible binary variable combinations grows exponentially with the number of binary values. If both the objective and the constraints are linear it is referred to as Mixed Integer Linear Program (MILP), which is the least computationally intensive form of the MIP group.

Finally the control of the 5GDHC networks is mainly influenced by the demand and therefore the control can also be focused on Demand-Side Management (DSM), either modifying the demand side by incentives and information or using demand response programs for peak shaving and load management. Besides control strategies, faults in the entire system, the network, the substations and building, have a great effect on the operational stability and efficiency [27]. Therefore [11] also discusses the possibilities for fault detection and diagnosis. These methods can be divided in physical model-based methods and data-driven methods. The latter has the advantage they can be very accurate and represent complex phenomena, however they require a large data set.

## 4-2 Mathematical system model

This system consists of many bilinear and nonlinear equations. The bilinear equations arise for instance when multiplying the mass flow with temperature to get the energy, which are

both variables that are influenced and controlled and can thereby not be assumed constant. A bilinear system is defined as a system where for a fixed input the system is linear in the state and for a fixed state the system is linear in the input [28]. The mathematical representation of such a continuous system (4-1), can also be described by the Kronecker product  $F(u \otimes x)$  instead of the summation.

$$\begin{aligned}\dot{x} &= Ax + Bu + \sum_{j=1}^p u_j F_j x \\ y &= Cx + Du\end{aligned}\tag{4-1}$$

The complete model can be described by connecting the separate component. It has been decided that the mass flow will be considered an input as it is directly based on the pumps and the controllers, while the temperature is only indirectly influenced.

The incompressible energy equation for heat transfer (4-2) is described by  $Q$  which can be used for the heat transfer with the surroundings and for energy consumption/production of components and by  $q = \frac{\dot{Q}}{A} = -k \frac{\partial T}{\partial x}$  which is the diffusion represented by Fourier's law where  $A$  is the cross sectional area. MPC works with discrete models and to produce a convex optimisation problem, the model would normally be linearised, but as discussed before, this is a bilinear model and other methods are available as a linearisation would significantly reduce the accuracy due to the large range of both the manipulated and process variable.

The model for the MPC is written using the Finite Volume Method (FVM), which integrates the energy equation over the cell volume (4-4). The advantage of using FVM compared to a Finite Difference Method (FDM) is that it ensures the conservation of energy, however, here only one flow dimension will be considered, the flow direction. To apply FVM, it is assumed that the density and heat capacity are constant and there is a uniform temperature distribution over the cross sectional area. Several numerical schemes are available to model these systems, however they are not all appropriate. In general one would prefer a central difference method over the upwind method, as the central difference is a second order method and upwind only a first order. The Peclet number is defined as  $Pe = \frac{uL}{\alpha}$ , where  $u$  is the velocity typically  $0.10 - 1.0 \text{ m s}^{-1}$ ,  $L$  the characteristic length (for pipes, the hydraulic diameter) typically  $0.10 - 0.25 \text{ m}$  and  $\alpha$  the thermal diffusivity with  $\alpha = \frac{k}{\rho c_p} 0.143 \cdot 10^{-6} \text{ m}^2 \text{ s}^{-1}$ . This results in  $Pe \approx 7.0 \cdot 10^4 - 1.75 \cdot 10^6$ , thereby much larger than 1, showing the dominance of the convection. For large Peclet numbers ( $>2$ ), the central difference scheme is not used as it does not consider the direction of the flow for the influence of the temperature and does not converge, is unstable, resulting in physically impossible solutions and exploding oscillations near sharp gradients. Upwind can handle the flow direction and is stable (4-5), however, it does have numerical diffusion and therefore the grid should be chosen as fine as possible, this is especially evident near sharp gradients/jumps. To further reduce numerical diffusion, a flux limiter can be used as they can handle sharp gradients/jumps, however, this does make the system of equations nonlinear, so for computational effort of the MPC it is not advised. If the model is used for other purposes for instance to simulate the system, it would be an interesting option. A viable flux limiter is Superbee (4-7) by Phil Roe [29]. Furthermore, explicit Euler (4-6) is used as this ensures the (bi)linearity of the system, while implicit (backward) Euler is always stable, the linearity is lost.

$$\frac{\partial}{\partial t}(\rho c T) = -\nabla(\rho c T u) + \nabla q + \nabla^3 \dot{Q} \quad (4-2)$$

$$\rho c \frac{\partial T}{\partial t} = -\rho c u_x \frac{\partial T}{\partial x} + \frac{\partial q}{\partial x} + \frac{\partial q}{\partial y} + \frac{\partial q}{\partial z} + \frac{\partial^3 \dot{Q}}{\partial x^3} \quad (4-3)$$

$$\frac{\partial}{\partial t} \int \int \int_{CV} (\rho c T) dV = - \int \int \int_{CV} \nabla(\rho c T u) dV + \int \int \int_{CV} \nabla \cdot (k \nabla T) + \int \int \int_{CV} \nabla^3 \dot{Q} dV \quad (4-4a)$$

$$= - \int \int_{CS} (\rho c T u) \hat{n} dS - \int \int_{CS} q \hat{n} dS + \dot{Q}_{\text{cell}} \quad (\text{divergence theorem}) \quad (4-4b)$$

$$= (\rho c u A_{\text{cross}})(T_{i-\frac{i}{2}} - T_{i+\frac{i}{2}}) + \frac{\Delta T}{\Delta x} \Big|_{i-\frac{i}{2}}^{i+\frac{i}{2}} k A_{\text{cross}} - T_{\text{outside}}^i U A_{\text{eff}} + \dot{Q}_{\text{cell}} \quad (\text{constant geometry, density and heat capacity and mass continuity}) \quad (4-4c)$$

$$\rho c V \frac{\partial T_i}{\partial t} = (c_p \dot{m})(T_{i-1} - T_i) + \left( \frac{T_{i+1} - 2T_i + T_{i-1}}{\Delta x} \right) k A_{\text{cross}} - (T_i - T_{\text{outside}}) U A_{\text{eff}} + \dot{Q}_{\text{cell}} \quad (\text{convection/advection upwind, diffusion central difference}) \quad (4-5)$$

$$\rho c_p V \frac{T_i^{k+1} - T_i^k}{\Delta t} = (c_p \dot{m})(T_{i-1}^k - T_i^k) + \left( \frac{T_{i+1}^k - 2T_i^k + T_{i-1}^k}{\Delta x} \right) k A_{\text{cross}} - (T_i^k - T_{\text{outside}}^k) U A_{\text{eff}} + \dot{Q}_{\text{cell}} \quad (4-6)$$

$$\sigma_i^n = \text{maxmod}(\sigma_i^{(1)}, \sigma_i^{(2)})$$

with

$$\sigma_i^{(1)} = \text{minmod} \left( \frac{q_{i+1}^n - q_i^n}{\delta x}, 2 \frac{q_i^n - q_{i-1}^n}{\delta x} \right) \quad (4-7)$$

$$\sigma_i^{(2)} = \text{minmod} \left( 2 \frac{q_{i+1}^n - q_i^n}{\delta x}, \frac{q_i^n - q_{i-1}^n}{\delta x} \right)$$

$T_{\text{outside}}$  is the ambient temperature for pipes and  $A_{\text{eff}}$  is the surface area of the pipe, but it can also be used for heat exchangers, then  $T_{\text{outside}}$  is the temperature of the cell on the other side and  $A_{\text{eff}}$  is the effective heat exchanger area. Since upwind is used the flow direction has to be defined, which is from  $i - 1$  to  $i$ .

### 4-2-1 Components

#### Pump

As the dynamics of the pump are nonlinear, the power, head and mass flow are correlated with the rotational speed according to the affinity law (4-8), not all the dynamics can be incorporated in the bilinear model. The rotational speeds is proportional to the mass flow for constant head and pump power, therefore the mass flow can be considered and the all the other factors can be determined by post processing, as the power is only of consideration for the power consumption but does not influence the mass flow and the change in head does only has a minor influence the mass flow. The PI controller of the pump provides the pump with a rotational speed, thereby this can easily be changed to the mass flow, assuming similar head values. The measured value and the setpoint of the controllers are either the mass flow or the pressure drop over a certain section. The mass flow is already incorporated in the model and thereby this controller can easily be added, however the pressure drop and thereby the pressures are not yet incorporated. The model on which the MPC is based, does not need to consider the pumps of with a pressure drop as these pumps are either there to ensure a fixed pressure drop over the building delivery system and thus the mass flow is already defined as an input. Furthermore the pumps that ensure a fixed pressure drop over the condenser side of the heat pumps are also not considered, but solely a constant mass flow is considered here, as this is should be approximately constant during normal operation.

$$\dot{m} \propto n \quad H \propto n^2 \quad P_{\text{pump}} \propto n^3 \quad (4-8)$$

#### Pipes and buffer tanks

Pipes are used to transport warm or cold water, as they are well insulated, they mainly cause a delay in the temperature delivery (advection). When the mass flows are zero for a longer period of time, heat flux with the ambient air (conduction (through pipe wall) & convection (between wall and fluid & wall and air)) as well as diffusion (heat transport by molecular movement) can cause the temperature to rise/reduce. Buffer tanks are basically very wide pipes, ensuring a low ratio surface area-to-volume, reducing the total heat flux over the volume, however as there might be temperature gradients in the buffer tanks this can result in convection, when for instance warmer water enters at the bottom. Both the pipe and buffer can be divided into several segments to provide more accurate calculations. As the mass flows can vary a lot the maximum mass flow has to be smaller than the internal mass of a pipe segment, to ensure that the temperature of the pipe segment can be calculated (4-9). The heat transfer between the fluid, wall and air is summarised using an overall heat transfer coefficient  $U$  and  $A_{\text{cir}}$  is the circumference area.

$$\rho c_p V_{\text{cell},i} \frac{T_i^{k+1} - T_i^k}{\Delta t} = (c_p \dot{m}^k)(T_{i-1}^k - T_i^k) + \left( \frac{T_{i+1}^k - 2T_i^k + T_{i-1}^k}{\Delta x} \right) k A_{\text{cross}} - (T_i^k - T_{\text{amb}}^k) U A_{\text{circ, cell}} \quad (4-9)$$

The previously stated equations can also be written in a bilinear version (4-10). Since mass continuity in a pipe holds,  $\frac{\Delta t}{c_p V_{\text{cell},i}} \frac{c}{2} (m_{i-1/2}^k - m_{i+1/2}^k)$  should cancel out for the equations of a pipe cell. Thereby, one can also shorten the input vector to one mass flow for each pipe

as it should be the same throughout the pipe, as long as there are no other connections, due to mass continuity.

$$\begin{aligned}
 x^k &= \begin{bmatrix} T_{i-1}^k \\ T_i^k \\ T_{i+1}^k \end{bmatrix} & u^k &= \begin{bmatrix} \dot{m}_{i-1}^k \\ \dot{m}_i^k \\ T_{\text{amb}}^k \end{bmatrix} \\
 T_i^{k+1} &= \frac{\Delta t}{c_p V_{\text{cell},i}} \left[ \frac{k A_{i-1/2}}{\Delta x} \quad -\frac{k(A_{i-1/2} + A_{i+1/2})}{\Delta x} \quad -U p_{\text{circ}} \Delta x + \frac{c_p \rho V_{\text{cell},i}}{\Delta t} \quad \frac{k A_{i+1/2}}{\Delta x} \right] x^k \\
 &+ \frac{\Delta t}{c_p V_{\text{cell},i}} \begin{bmatrix} 0 & 0 & U p_{\text{circ}} \Delta x \end{bmatrix} u^k \\
 &+ u_1^k \frac{\Delta t}{c_p \rho V_{\text{cell},i}} \begin{bmatrix} c_p & 0 & 0 \end{bmatrix} x^k \\
 &+ u_2^k \frac{\Delta t}{c_p \rho V_{\text{cell},i}} \begin{bmatrix} 0 & -c_p & 0 \end{bmatrix} x^k \\
 &+ u_3^k \begin{bmatrix} 0 & 0 & 0 \end{bmatrix}
 \end{aligned} \tag{4-10}$$

### Heat pump

The heat pump contains interesting internal dynamics that influence the dynamics of the system. One could decide to model all these internal dynamics which are nonlinear and depend on the refrigerant properties, however, it can also be simplified completely till only the energy transferred between the refrigerant and the water on both the evaporator and condenser side is used (4-11). Using the Coefficient Of Performance (COP) and defining only for instance the evaporator energy one can determine the condenser energy (4-12), currently the same COP for all operating capacities is considered. The evaporator energy would then solely be based on the capacity at which the heat pump is operating, and thus the influence of operating temperatures would not be considered. The heat pump cannot instantly produce the energy correlated with the capacity when it increases its capacity from 25% to 50% or reduces. Thereby, constraining the change of energy per second, is an efficient and easy method to mimic the dynamics of the energy increase/reduction.

The resulting equation for FVM (4-13) is fairly simple, but it should be reminded that for the evaporator energy, the sign is negative and for the condenser energy positive. The considered properties of the heat pump are shown in Table 4-1.

$$Q_{\text{evap}} = Q_{\text{cond}} - W_{\text{comp}} \tag{4-11}$$

$$COP = \frac{Q_{\text{cond}}}{Q_{\text{cond}} - Q_{\text{evap}}} \tag{4-12}$$

$$\rho c_p V \frac{T_i^{k+1} - T_i^k}{\Delta t} = (c_p \dot{m})(T_{i-1}^k - T_i^k) + \left( \frac{T_{i+1}^k - 2T_i^k + T_{i-1}^k}{\Delta x} \right) k A_{\text{cross}} + \dot{Q}_{\text{HP,cell}} \tag{4-13}$$

Property	Unit	Evaporator	Condenser
COP			4.17
Refrigerant			R410A
$p_{\text{ref}}$	MPa	0.85	3.0
Heat loss coefficient C	$\text{s}^2 \text{m}^{-5}$	32500	27000
$\dot{Q}_{\text{max}}$	kW	190	250
$V$	$\text{m}^3$	0.0324	0.0341
$\dot{V}_{\text{max}}$	$\text{m}^3 \text{s}^{-1}$	0.008	0.008
$n_{\text{cell}}$	-	4	4
$V_{\text{cell}}$	$\text{m}^3$	0.0081	0.0085

**Table 4-1:** Properties of the heat pump.

### Heat exchanger

The heat exchanger can be modelled in great detail and thereby cut into several cells as, has been done for the heat pipes. However, this would also require a detailed knowledge of the heat exchanger lay-out. Since only estimates of the overall heat transfer coefficient and the water volume of the heat exchanger are known, one can determine the heat transfer between both fluids (4-14) and one can consider the delay, by adding additional volume section for advection (heat transport by bulk mass transport).

The heat transfer is based on the logarithmic mean temperature difference (4-15), however this cannot be put in a bilinear model. Besides the logarithmic mean temperature difference, the mean temperature difference can be used. As the difference with the logarithmic mean temperature difference is generally small, it seems a reasonable assumption to use the mean temperature difference  $\Delta T_m = \frac{1}{2}(T_{h, \text{in}} - T_{c, \text{out}} + T_{h, \text{out}} - T_{c, \text{in}})$ . The Finite Volume Method is also used on the heat exchanger, where it has been assumed that heat losses of the heat exchanger with the environment and stored heat in the plates are neglected.

A uniform temperature of the water in a cell in direction of the heat transfer through the plates (perpendicular to the flow) can be assumed as within plate heat exchanger the flow is turbulent there is mixing and therefore one can still assume a uniform temperature. (Large nusselt and  $\text{Pr} > 1$ )

$$\dot{Q} = U A_{\text{eff}} \Delta T_m = \dot{m}_h c_{p_h} (T_{h, \text{in}} - T_{h, \text{out}}) = \dot{m}_c c_{p_c} (T_{c, \text{out}} - T_{c, \text{in}}) \quad (4-14)$$

$$\Delta T_m = F_t \Delta T_{\text{lm}} = F_t \frac{(T_{h, \text{in}} - T_{c, \text{out}}) - (T_{h, \text{out}} - T_{c, \text{in}})}{\ln \frac{(T_{h, \text{in}} - T_{c, \text{out}})}{(T_{h, \text{out}} - T_{c, \text{in}})}} \quad (4-15)$$

$$q = -U \Delta T \quad (4-16)$$

$A_{\text{eff}}$  is the effective area of heat exchanger

The energy equation can be written in a bilinear state space format, where the temperatures are the states and the mass flow is the input. It should be noted that since the heat exchangers are in countercurrent flow, the index  $i$  indicates the location in the heat exchanger. If one is at the bottom,  $i=1$ , the cold flow is entering while the hot flow is leaving the heat exchanger. Therefore on the other side of the heat exchanger the cells are numbered in the

Property	unit	Warm HEX	Cold HEX
$\dot{V}_{\max}$	$\text{m}^3 \text{s}^{-1}$	0.0124	0.0317
$V_{\text{one side}}$	$\text{m}^3$	0.15385	0.33615
$A_{\text{eff}}$	$\text{m}^2$	148.6	261.4
$U_o$	$\text{W m}^{-2} \text{K}^{-1}$	1500	2500
$n_{\text{cell}}$	-	12	10
$V_{\text{cell}}$	$\text{m}^3$	0.0128	0.0336
$A_{\text{eff, cell}}$	$\text{m}^2$	12.38	26.14

**Table 4-2:** Heat exchanger properties

Property	Unit	HEX <sub>dc, WKO</sub>	HEX <sub>dc, HPs</sub>	HEX <sub>HT1</sub>	HEX <sub>HT2</sub>
$\dot{V}_{\max}$	$\text{m}^3 \text{s}^{-1}$	0.0170	0.0242	0.0024	0.0048
$V_{\text{one side}}$	$\text{m}^3$	0.1323	0.0828	0.004	0.0078
$n_{\text{cell}}$	-	7	3	1	1
$V_{\text{cell}}$	$\text{m}^3$	0.0189	0.0276	0.004	0.0078

**Table 4-3:** Drycooler connection properties. The energy added/removed in a cell is the total energy divided by the number of cells

opposite order, to coincide with the direction of the flow, therefore the cell number of the warm side is  $n + 1 - i$  where  $n$  is the total number of cells (4-17).

$$\rho c_p V \frac{T_{c,i}^{k+1} - T_{c,i}^k}{\Delta t} = (c_p \dot{m}_c)(T_{c,i-1}^k - T_{c,i}^k) + \left( \frac{T_{c,i+1}^k - 2T_{c,i}^k + T_{c,i-1}^k}{\Delta x} \right) k A_{\text{cross}} - (T_{c,i}^k - T_{h,n+1-i}^k) U A_{\text{eff}} \quad (4-17)$$

In reality the heat transfer coefficient might vary as the flow has a wide range of operation. In the model it would be possible to incorporate this by using the overall heat transfer as another model input or as a linearised function of the flow, therefore making this term also bilinear. The resulting properties of the heat exchanger are shown in Table 4-2.

## Drycooler/HT

The drycooler/conventional heater or high temperature connection are modelled such that the primary side is not considered, only the secondary side (the distribution network) is considered and the added/removed energy is provided as an input which is controlled by a PI(D) controller. Furthermore the mass flow on the secondary side is also an input as it is based on the mass flow in the network through the different groups which are again controlled by controllers. A partial differential equation is again used with a Finite Volume Method and Forward Euler to allow the calculations for the next time step (4-18). Here it has been assumed that diffusion is not significant nor is the heat flux with the ambient air in these apparatus.

$$T_i^{k+1} = \frac{\Delta t}{\rho c V_{\text{cell}}} \left( c_p \dot{m}_i^k (T_{i-1}^k - T_i^k) + \frac{\dot{Q}^k}{n_{\text{cell}}} \right) + T_i^k \quad (4-18)$$

## Valves

Several types of valves are used, to include/exclude a group of components, to determine the flow and temperature setpoint of consumers and to regulate the temperature inflow of the evaporators using three-way valves. The first does not require any detailed modelling as it just allows mass flow or not. The second type, being the consumers, are modelled as an input for both the mass flow and the temperature setpoint and therefore these valves can also be excluded. Finally the third type of valve is important as it mixes two flows. A three-way valve, combines two streams into one, such that the sum of the percentages at which the valve is open is 100%. Generally equal percentage valves (4-20) are used, in combination with a heat exchanger device, this results in a linear correlation of the flow with the valve opening. The mass flow leaving the three-way valve and entering the evaporator is an input of the system as it is a result of the speed at which the evaporator pump is running. The valve opening is an output of the temperature controller. Considering the position also as a state allows to multiply the mass flow of the three way valve output with opening to determine the other mass flows (4-21).

$$\dot{V} = K_v \sqrt{\frac{\Delta p}{\rho} 1000} \quad (4-19)$$

$$\frac{K_v}{K_{vs}} = \frac{K_{v0}}{K_{vs}} \exp + \left[ \frac{h}{h_{100}} \ln \left( \frac{K_{vs}}{K_{v0}} \right) \right] \quad (4-20)$$

$$\dot{m}_3 T_3 = \dot{m}_1 T_1 + \dot{m}_2 T_2 \quad (\text{Energy conservation}) \quad (4-21a)$$

$$\dot{m}_3 = \dot{m}_1 + \dot{m}_2 \quad (\text{Mass continuity}) \quad (4-21b)$$

$$\dot{m}_1 = \dot{m}_3 o_{v1} \quad \dot{m}_2 = \dot{m}_3 o_{v2} = \dot{m}_3 (1 - o_{v1}) \quad (4-21c)$$

$$T_3 = \frac{\dot{m}_1}{\dot{m}_3} T_1 + \frac{\dot{m}_2}{\dot{m}_3} T_2 = o_{v1} T_1 + o_{v2} T_2 \quad (4-21d)$$

For the mass flow over the condenser and evaporator, the net mass flow could be considered as long as only the energy input of the heat pump is considered as the detailed temperature inside the heat pump is now not of influence.

### 4-2-2 Nodes

The nodes between different component groups can be connected as shown below. It should be noted that for the cold building distribution network, there are two options, based on whether the ring network is providing heat or cold. Furthermore, the buffer mass flows, both for the warm and cold building distribution network, can also have negative values indicating a reversed flow. The reversed flow will be modelled differently, as a negative value can not be used for the upwind method which has a defined flow direction.

Warm distribution network:

$$\dot{m}_{h, \text{ build}} = \dot{m}_{\text{HPs, conds}} + \dot{m}_{h, \text{ buffer}} \quad (4-22)$$

$$\dot{m}_{\text{HPs, conds}} = \dot{m}_{\text{HP1, cond}} + \dot{m}_{\text{HP2, cond}} \quad (4-23)$$

Heat pumps:

$$\dot{m}_{\text{evaps}} = \dot{m}_{\text{HP1, evap, new}} + \dot{m}_{\text{HP2, evap, new}} \quad (4-24)$$

$$\dot{m}_{\text{HP1, evap, new}} = \dot{m}_{\text{HP1, evap}} o_{v1} \quad (4-25)$$

$$\dot{m}_{\text{HP2, evap, new}} = \dot{m}_{\text{HP2, evap}} o_{v2} \quad (4-26)$$

Cold distribution network: cold HEX

$$\dot{m}_{c, \text{ build}} = \dot{m}_{\text{evaps}} + \dot{m}_{c, \text{ buffer}} \quad (4-27)$$

$$\dot{m}_{c, \text{ build}} = \dot{m}_{\text{HEX}_c, \text{ sec}} + \dot{m}_{c, \text{ HEX}_c \text{ shortcut}} \quad (4-28)$$

Cold distribution network: warm HEX

$$\dot{m}_{\text{HEX}_h, \text{ sec}} = \dot{m}_{\text{evaps}} + \dot{m}_{c, \text{ WKO - buffer}} + \dot{m}_{c, \text{ DC}} \quad (4-29)$$

$$\dot{m}_{c, \text{ buffer}} = \dot{m}_{c, \text{ WKO - buffer}} + \dot{m}_{c, \text{ build}} \quad (4-30)$$

$$(4-31)$$

## 4-3 MPC strategy

### 4-3-1 Constraints

Some of these input variables first have to be transformed before they can be used. Furthermore other constraints related to the system are described here.

#### Heat pump

The heat pump can operate at discrete capacities defined as the operating capacities at the evaporator (4-32) from which the condenser heating capacity can be determined using the COP (4-33). The mass flow over the condenser and evaporator side are nearly constant when the HP is on ( $\delta_{\text{HP1}} = 1$ ) and the input can be simplified (4-35 and 4-34), where  $c$  denotes constants.

$$Q_{\text{HP1, evap}} = \left\{ 0 \quad Q_{\text{HP1, evap, 25\%}} \quad Q_{\text{HP1, evap, 50\%}} \quad Q_{\text{HP1, evap, 75\%}} \quad Q_{\text{HP1, evap, 100\%}} \right\} \quad (4-32)$$

$$Q_{\text{HP1, cond}} = \frac{\text{COP}}{\text{COP} - 1} Q_{\text{HP1, evap}} \quad (4-33)$$

$$\dot{m}_{\text{HP1, evap}} = \left\{ 0 \quad c\dot{m}_{\text{HP1, evap}} \right\} = c\dot{m}_{\text{HP1, evap}} \delta_{\text{HP1}} \quad (4-34)$$

$$\dot{m}_{\text{HP1, cond}} = \left\{ 0 \quad c\dot{m}_{\text{HP1, cond}} \right\} = c\dot{m}_{\text{HP1, cond}} \delta_{\text{HP1}} \quad (4-35)$$

$$(4-36)$$

The heat pumps can only operate at 1 capacity at a time (4-37).  $\oplus$  denotes the exclusive or (XOR). Furthermore, the heat pump can only be operated at a capacity if it is on, but if it is on, it does not mean it is also running at a capacity, as a result of start up conditions, first requiring a flow (4-38). The input vector for heat pump 1 can be replaced by the new matrices consisting of constants and the new binary variables (4-39). The second heat pump requires a similar transformation.

$$\delta_{\text{HP1}, 0\%} \oplus \delta_{\text{HP1}, 25\%} \oplus \delta_{\text{HP1}, 50\%} \oplus \delta_{\text{HP1}, 75\%} \oplus \delta_{\text{HP1}, 100\%} \quad (4-37a)$$

$$0 \leq \delta_{\text{HP1}, 25\%} + \delta_{\text{HP1}, 50\%} + \delta_{\text{HP1}, 75\%} + \delta_{\text{HP1}, 100\%} \leq 1 \quad (4-37b)$$

$$Q_{\text{HP1}, \text{evap}} \neq 0 \implies \delta_{\text{HP1}} = 1 \text{ is equivalent to} \quad (4-38)$$

$$\delta_{\text{HP1}, 25\%} + \delta_{\text{HP1}, 50\%} + \delta_{\text{HP1}, 75\%} + \delta_{\text{HP1}, 100\%} - \delta_{\text{HP1}} \leq 0$$

$$\begin{bmatrix} \dot{m}_{\text{HP1}, \text{evap}} \\ \dot{m}_{\text{HP1}, \text{cond}} \\ Q_{\text{HP1}, \text{evap}} \\ Q_{\text{HP1}, \text{cond}} \end{bmatrix} = \begin{bmatrix} c\dot{m}_{\text{HP1}, \text{evap}} & 0 & 0 & 0 & 0 \\ c\dot{m}_{\text{HP1}, \text{cond}} & 0 & 0 & 0 & 0 \\ 0 & \frac{Q_{\text{evap}, 25\%}}{\text{COP}-1} & \frac{Q_{\text{evap}, 50\%}}{\text{COP}-1} & \frac{Q_{\text{evap}, 75\%}}{\text{COP}-1} & \frac{Q_{\text{evap}, 100\%}}{\text{COP}-1} \\ 0 & \frac{Q_{\text{evap}, 25\%}}{\text{COP}-1} & \frac{Q_{\text{evap}, 50\%}}{\text{COP}-1} & \frac{Q_{\text{evap}, 75\%}}{\text{COP}-1} & \frac{Q_{\text{evap}, 100\%}}{\text{COP}-1} \end{bmatrix} \begin{bmatrix} \delta_{\text{HP1}} \\ \delta_{\text{HP1}, 25\%} \\ \delta_{\text{HP1}, 50\%} \\ \delta_{\text{HP1}, 75\%} \\ \delta_{\text{HP1}, 100\%} \end{bmatrix} \quad (4-39a)$$

$$\begin{bmatrix} -1 & 1 & 1 & 1 & 1 \\ 0 & 1 & 1 & 1 & 1 \\ 0 & -1 & -1 & -1 & -1 \end{bmatrix} \delta_{\text{HP1}, \text{cap}} \leq \begin{bmatrix} 0 \\ 1 \\ 0 \end{bmatrix} \quad (4-39b)$$

### Component on/off

There are several components that can be turned on/off and thereby switch the mass flow of a variable from 0 to an equation or another value. An example here is provided on how these constraints have to be written. First one starts with the massflow and defining what the value will be if the component group is turned on or off (4-40). These conditions can be defined by an auxiliary variable  $v$  which is the multiplication of a continuous and binary variable, which can then also be transformed in linear constraints (4-41).

$$\dot{m}_{c, \text{DC}} = \left\{ 0 \quad [\min(\dot{m}_{c, \text{DC}}), \overline{\dot{m}}_{c, \text{DC}}] \right\} \quad (4-40a)$$

$$\delta_{c, \text{DC}} = 0 \implies \dot{m}_{c, \text{DC}} = 0 \quad (4-40b)$$

$$\delta_{c, \text{DC}} = 1 \implies \dot{m}_{c, \text{DC}} = [\min(\dot{m}_{c, \text{DC}}), \overline{\dot{m}}_{c, \text{DC}}] \quad (4-40c)$$

is equivalent to

$$v = \dot{m}_{c, \text{DC}} \delta_{c, \text{DC}} \quad \text{can be translated in:} \quad (4-41a)$$

$$v \leq \overline{\dot{m}}_{c, \text{DC}} \delta_{c, \text{DC}} \quad (4-41b)$$

$$v \geq \underline{\dot{m}}_{c, \text{DC}} \delta_{c, \text{DC}} \quad (4-41c)$$

$$v \leq \dot{m}_{c, \text{DC}} - \underline{\dot{m}}_{c, \text{DC}} (1 - \delta_{c, \text{DC}}) \quad (4-41d)$$

$$v \geq \dot{m}_{c, \text{DC}} - \overline{\dot{m}}_{c, \text{DC}} (1 - \delta_{c, \text{DC}}) \quad (4-41e)$$

This procedure can be used for all variables that combine continuous and discrete values, where  $\dot{m}_{c, DC}$  can also be replaced by a function.  $\underline{\dot{m}}_{c, DC}$  indicates a minimum and  $\overline{\dot{m}}_{c, DC}$  indicates a maximum.

All the components groups that can be turned on or off have a binary variable. These binary variables are connected using multiple constraints, based on the way a component is operated. The drycooler can only load cold or dissipate heat, this can not occur simultaneously (4-42). The cold heat exchanger and the warm heat exchanger connecting the building, can not be operated simultaneously to supply the the building network (4-43). When the drycooler is loading additional cold, this implies that the warm heat exchanger connecting the grid is also used to supply heat to the building (4-45). If the cold heat exchanger (4-48) connecting the grid is on, this implies that there is a cold demand from the building. If the warm heat exchanger connecting the grid is on, this implies that there is heat demand (4-46) and that at least one heat pump is in operation for this (4-47), if there is no heat demand the warm heat exchanger will not be on, but it does not necessarily need to be on if there is heat demand, the heat could also be delivered by the cooling of other building parts to allow the HP working. The HT and the DC for dissipating heat should not be operated simultaneously as they would counteract each other (4-44). The HT in operation implies that there is heat demand (4-49) as well as that both heat pumps should be on (4-50), however currently there is no condition on the capacity at which the HPs should be operated. Finally the drycooler dissipating heat, only implies that at least one of both heat pumps is on (4-51).

$$\delta_{c, DC} + \delta_{h, DC} \leq 1 \quad (4-42)$$

$$\delta_{HEX_c} + \delta_{HEX_h} \leq 1 \quad (4-43)$$

$$\delta_{HT} + \delta_{h, DC} \leq 1 \quad (4-44)$$

$$\delta_{c, DC} - \delta_{HEX_h} \leq 0 \quad (\delta_{c, DC} = 1 \implies \delta_{HEX_h} = 1) \quad (4-45)$$

$$\delta_{HEX_h} - \delta_{h, build} \leq 0 \quad (\delta_{HEX_h} = 1 \implies \delta_{h, build} = 1) \quad (4-46)$$

$$\delta_{HEX_h} - \delta_{HP1} - \delta_{HP2} \leq 0 \quad (\delta_{HEX_h} = 1 \implies \delta_{h, build} = 1) \quad (4-47)$$

$$\delta_{HEX_c} - \delta_{c, build} \leq 0 \quad (\delta_{HEX_c} = 1 \implies \delta_{c, build} = 1) \quad (4-48)$$

$$\delta_{HT} - \delta_{h, build} \leq 0 \quad (\delta_{HT} \implies \delta_{h, build}) \quad (4-49)$$

$$\left. \begin{array}{l} \delta_{HT} - \delta_{HP1} \leq 0 \\ \delta_{HT} - \delta_{HP2} \leq 0 \end{array} \right\} (\delta_{HT} \implies (\delta_{HP1} \wedge \delta_{HP2})) \quad (4-50)$$

$$\delta_{h, DC} - (\delta_{HP1} + \delta_{HP2}) \leq 0 \quad (\delta_{h, DC} = 1 \implies (\delta_{HP1} = 1 \vee \delta_{HP2} = 1)) \quad (4-51)$$

An overview of all the input variables with their corresponding constraint and conditions are shown in Table 4-4 which are the basis for the transformations with auxiliary variables as described above.

## PI controllers

There are several locations where a PI controller is used for the mass flow using the temperature as a process variable. These controllers are located at the three-way valve on the evaporator side of both components, and on the primary side of the heat exchanger connecting the grid. The PI controller (4-52) contains the error, defined as the difference between

Input	Values	Conditions
$\dot{m}_{c, DC}$	$\left\{ 0 \left[ \underline{\dot{m}}_{c, DC}, \overline{\dot{m}}_{c, DC} \right] \right\}$	$\delta_{c, DC} = 0 \implies \dot{m}_{c, DC} = 0$ $\delta_{c, DC} = 1 \implies \dot{m}_{c, DC} = \left[ \underline{\dot{m}}_{c, DC}, \overline{\dot{m}}_{c, DC} \right]$
$\dot{m}_{h, DC}$	$\left\{ 0 \left[ \underline{\dot{m}}_{h, DC}, \overline{\dot{m}}_{h, DC} \right] \right\}$	$\delta_{h, DC} = 0 \implies \dot{m}_{h, DC} = 0$ $\delta_{h, DC} = 1 \implies \dot{m}_{h, DC} = \left[ \underline{\dot{m}}_{h, DC}, \overline{\dot{m}}_{h, DC} \right]$
$\dot{m}_{c \text{ to } HEX_h}$	$\left\{ 0 \left[ \underline{\dot{m}}_{c \text{ to } HEX_h}, \overline{\dot{m}}_{c \text{ to } HEX_h} \right] \right\}$	$\delta_{HEX_h} = 0 \implies \dot{m}_{c \text{ to } HEX_h} = 0$ $\delta_{HEX_h} = 1 \implies \dot{m}_{c \text{ to } HEX_h} = \left[ \underline{\dot{m}}_{c \text{ to } HEX_h}, \overline{\dot{m}}_{c \text{ to } HEX_h} \right]$
$\dot{m}_{HEX_h, sec}$	$\left\{ 0 \left[ \underline{\dot{m}}_{HEX_h, sec}, \overline{\dot{m}}_{HEX_h, sec} \right] \right\}$	$\delta_{HEX_h} = 0 \implies \dot{m}_{HEX_h, sec} = 0$ $\delta_{HEX_h} = 1 \implies \dot{m}_{HEX_h, sec} = \left[ \underline{\dot{m}}_{HEX_h, sec}, \overline{\dot{m}}_{HEX_h, sec} \right]$
$\dot{m}_{HEX_c, sec}$	$\left\{ 0 \left[ \underline{\dot{m}}_{HEX_c, sec}, \overline{\dot{m}}_{HEX_c, sec} \right] \right\}$	$\delta_{HEX_c} = 0 \implies \dot{m}_{HEX_c, sec} = 0$ $\delta_{HEX_c} = 1 \implies \dot{m}_{HEX_c, sec} = \left[ \underline{\dot{m}}_{HEX_c, sec}, \overline{\dot{m}}_{HEX_c, sec} \right]$
$\dot{m}_{HEX_h, prim}$	$\left\{ 0 \left[ \underline{\dot{m}}_{HEX_h, prim}, \overline{\dot{m}}_{HEX_h, prim} \right] \right\}$	$\delta_{HEX_h} = 0 \implies \dot{m}_{HEX_h, prim} = 0$ $\delta_{HEX_h} = 1 \implies \dot{m}_{HEX_h, prim} = \left[ \underline{\dot{m}}_{HEX_h, prim}, \overline{\dot{m}}_{HEX_h, prim} \right]$
$\dot{m}_{HEX_c, prim}$	$\left\{ 0 \left[ \underline{\dot{m}}_{HEX_c, prim}, \overline{\dot{m}}_{HEX_c, prim} \right] \right\}$	$\delta_{HEX_c} = 0 \implies \dot{m}_{HEX_c, prim} = 0$ $\delta_{HEX_c} = 1 \implies \dot{m}_{HEX_c, prim} = \left[ \underline{\dot{m}}_{HEX_c, prim}, \overline{\dot{m}}_{HEX_c, prim} \right]$
$\dot{m}_{5501SK01}$	$\left\{ 0 \left[ \dot{m}_{c, build} \right] \right\}$	$\delta_{HEX_c} = 0 \implies \dot{m}_{5501SK01} = \dot{m}_{c, build}$ $\delta_{HEX_c} = 1 \implies \dot{m}_{5501SK01} = 0$
$\dot{m}_{h, HT}$	$\left\{ 0 \left[ c\dot{m}_{h, HT} \right] \right\}$	$\delta_{HT} = 0 \implies \dot{m}_{h, HT} = 0$ $\delta_{HEX_c} = 1 \implies \dot{m}_{h, HT} = c\dot{m}_{h, HT}$
$\dot{m}_{HP1, cond}$	$\left\{ 0 \left[ c\dot{m}_{HP1, cond} \right] \right\}$	$\delta_{HP1} = 0 \implies \dot{m}_{HP1, cond} = 0$ $\delta_{HP1} = 1 \implies \dot{m}_{HP1, cond} = c\dot{m}_{HP1, cond}$
$\dot{m}_{HP2, cond}$	$\left\{ 0 \left[ c\dot{m}_{HP2, cond} \right] \right\}$	$\delta_{HP2} = 0 \implies \dot{m}_{HP2, cond} = 0$ $\delta_{HP2} = 1 \implies \dot{m}_{HP2, cond} = c\dot{m}_{HP2, cond}$
$\dot{m}_{HP1, evap}$	$\left\{ 0 \left[ c\dot{m}_{HP1, evap} \right] \right\}$	$\delta_{HP1} = 0 \implies \dot{m}_{HP1, evap} = 0$ $\delta_{HP1} = 1 \implies \dot{m}_{HP1, evap} = c\dot{m}_{HP1, evap}$
$\dot{m}_{HP2, evap}$	$\left\{ 0 \left[ c\dot{m}_{HP2, evap} \right] \right\}$	$\delta_{HP2} = 0 \implies \dot{m}_{HP2, evap} = 0$ $\delta_{HP2} = 1 \implies \dot{m}_{HP2, evap} = c\dot{m}_{HP2, evap}$
$\dot{m}_{HP1, evap, 3way}$	$[0.0, 0.9] \dot{m}_{HP1, evap}$	
$\dot{m}_{HP2, evap, 3way}$	$[0.0, 0.9] \dot{m}_{HP2, evap}$	
$Q_{HP1, evap}$	$\left\{ 0 \left[ Q_{evap, 25\%}, \dots, Q_{evap, 100\%} \right] \right\}$	
$Q_{HP2, evap}$	$\left\{ 0 \left[ Q_{evap, 25\%}, \dots, Q_{evap, 100\%} \right] \right\}$	
$Q_{HT}$	$\left[ 0, \overline{Q}_{HT} \right]$	$\delta_{HT} = 0 \implies Q_{HT} = 0$ $\delta_{HT} = 1 \implies Q_{HT} = \left[ 0, \overline{Q}_{HT} \right]$
$Q_{c, DC}$	$\left[ \underline{Q}_{c, DC}, 0 \right]$	$\delta_{c, DC} = 0 \implies Q_{c, DC} = 0$ $\delta_{c, DC} = 1 \implies Q_{c, DC} = \left[ \underline{Q}_{c, DC}, 0 \right]$
$Q_{h, DC}$	$\left[ \underline{Q}_{h, DC}, 0 \right]$	$\delta_{h, DC} = 0 \implies Q_{h, DC} = 0$ $\delta_{h, DC} = 1 \implies Q_{h, DC} = \left[ \underline{Q}_{h, DC}, 0 \right]$

**Table 4-4:** The input variables and the corresponding constraints and conditions, from which the implementable auxiliary variables and constraints can be introduced

the setpoint and the process variable and the output value, the proportional gain  $K_p$  and the integral gain  $K_i = K_p/T_i$ . The controller has to be discretised (4-53) after which the input can be substituted by the mass flow and the process variable by the temperature. Since these mass flows are multiplied with a temperature in the model, the terms where the mass flow is determined based on a PI controller will remain bilinear. The time step of the discrete controllers is 1.0s, thus this would also not allow a larger time step for the model. If a larger timestep for the model is considered, the PI equation could simply be replaced with a constraint on the temperature and using a slack variable which is highly penalised to provide similar, longer time dynamics.

The energy provided by the HT and dissipated by the DC are in reality a function based on the mass flow on the other side of the heat exchangers, which are PI controlled. As this side is not considered in this work and the energy is considered an input, the PI controller has been converted to the energy units and it remains to consider the temperature outlet as process variable.

$$u(t) = K_p \left( e(t) + \frac{1}{T_i} \int_0^t e(\tau) d\tau \right) \quad (4-52)$$

$$u(k) = u(k-1) + (K_p + K_i \Delta t) e(k) - K_p e(k-1) \quad (4-53)$$

$$\begin{aligned} \dot{m}_{\text{HEX}_h, \text{prim}}(k) &= \dot{m}_{\text{HEX}_h, \text{prim}}(k-1) + (K_p + K_i \Delta t) (T_{\text{HEX}_h, \text{prim, out}}(k) - T_{\text{set}}(k)) \\ &\quad - K_p (T_{\text{HEX}_h, \text{prim, out}}(k-1) - T_{\text{set}}(k-1)) \end{aligned} \quad (4-54)$$

### Combined mass flow determination

$\dot{m}_{\text{HEX}_h, \text{sec}} = \dot{m}_{\text{c to HEX}_h} + \dot{m}_{\text{c, DC}}$  does not need to be its own variable as it is simply the sum of the two. Since the minimum and maximum of  $\dot{m}_{\text{c to HEX}_h}$  and  $\dot{m}_{\text{HEX}_h, \text{sec}}$  are the same and  $\dot{m}_{\text{c, DC}}$  is based on the maximum flow through the heat exchanger and the flow from the cold distribution network, the requirements on the flow through the heat exchanger are met. Therefore the following conditions are only needed besides the conditions on  $\dot{m}_{\text{c to HEX}_h}$ :

$$\dot{m}_{\text{c, DC}} \leq \dot{m}_{\text{c to HEX}_h} - \underline{\dot{m}}_{\text{HEX}_h, \text{sec}} (1 - \delta_{\text{c, DC}}) \quad (4-55a)$$

$$\dot{m}_{\text{c, DC}} \geq \dot{m}_{\text{c to HEX}_h} - \overline{\dot{m}}_{\text{HEX}_h, \text{sec}} (1 - \delta_{\text{c, DC}}) \quad (4-55b)$$

Since the mass flow from the cold distribution network to the warm heat exchanger ( $\dot{m}_{\text{c to HEX}_h} = \dot{m}_{\text{evaps}} - \dot{m}_{\text{c, build}}$ ) is constrained as a consequence of the pump's limited range of operation. Besides solely determining whether it is on or off, and leaving it as freely determined variable within these limits. The setpoint ( $\dot{m}_{\text{c to HEX}_h} = \dot{m}_{\text{evaps}} - \dot{m}_{\text{c, build}}$ ) of the PI of these pumps is set as a condition, which is described as a saturation function (4-56).

$$\dot{m}_{\text{c to HEX}_h} = \begin{cases} \dot{m}_{\text{c to HEX}_h} & \dot{m}_{\text{evaps}} - \dot{m}_{\text{c, build}} \leq \underline{\dot{m}}_{\text{c to HEX}_h} \\ \dot{m}_{\text{evaps}} - \dot{m}_{\text{c, build}} & \\ \overline{\dot{m}}_{\text{c to HEX}_h} & \dot{m}_{\text{evaps}} - \dot{m}_{\text{c, build}} \geq \overline{\dot{m}}_{\text{c to HEX}_h} \end{cases} \quad (4-56)$$

It is described using additional equations and auxiliary variables. The first case is defined

with  $\delta_1 = 1$  and the last case is defined with  $\delta_2 = 1$  and  $\delta_1 + \delta_2 \leq 1$ . Furthermore  $\dot{m}_{c \text{ to HEX}_h}$  becomes an auxiliary variable such that

$$\begin{aligned} \dot{m}_{c \text{ to HEX}_h} - (\bar{m}_{\text{evaps}} - (-\bar{m}_{c, \text{ build}}))\delta_1 &\leq \dot{m}_{\text{evaps}} - \dot{m}_{c, \text{ build}} \\ \dot{m}_{c \text{ to HEX}_h} + (\bar{m}_{\text{evaps}} - (-\bar{m}_{c, \text{ build}}))\delta_2 &\geq \dot{m}_{\text{evaps}} - \dot{m}_{c, \text{ build}} \end{aligned} \quad (4-57)$$

with

$$\begin{aligned} \dot{m}_{c \text{ to HEX}_h} &\geq \underline{\dot{m}}_{c \text{ to HEX}_h}, \\ \dot{m}_{c \text{ to HEX}_h} - (\bar{m}_{\text{evaps}} - \underline{\dot{m}}_{c \text{ to HEX}_h})(1 - \delta_1) &\leq \underline{\dot{m}}_{c \text{ to HEX}_h}, \\ \dot{m}_{c \text{ to HEX}_h} &\leq \bar{m}_{c \text{ to HEX}_h}, \\ \dot{m}_{c \text{ to HEX}_h} + (\bar{m}_{c \text{ to HEX}_h} - (-\bar{m}_{c, \text{ build}}))(1 - \delta_2) &\geq \bar{m}_{c \text{ to HEX}_h}. \end{aligned} \quad (4-58)$$

There are two possible ways to combine the above saturation with the on/off condition. Either a new auxiliary variable is created that is defined as  $v = \delta_{\text{HEX}_h} \dot{m}_{c \text{ to HEX}_h}$  which can be rewritten as stated in 4-3-1 or one could define the above stated equation (4-56) with all three entries being multiplied with  $\delta_{\text{HEX}_h}$ . The first approach would only result in one additional auxiliary variable and 4 constraints, while the second approach would result in 3 additional auxiliary variables ( $\delta_1 \delta_{\text{HEX}_h}$ ,  $\delta_2 \delta_{\text{HEX}_h}$  and  $\delta_{\text{HEX}_h}(\dot{m}_{\text{evaps}} - \dot{m}_{c, \text{ build}})$ ) and the thereby 10 additional constraints, thus the first option is preferred.

$$\delta_3 = \delta_1 \delta_2 \quad \text{is equivalent to} \quad \begin{cases} -\delta_1 + \delta_3 \leq 0 \\ -\delta_2 + \delta_3 \leq 0 \\ \delta_1 + \delta_2 - \delta_3 \leq 1 \end{cases} \quad (4-59)$$

A similar choice has to be made for the PI controller on the threeway valve. First of all they have to be inserted in a saturation function, which should be limited by 0 and  $0.9\dot{m}_{\text{HP1, evap}}$ , afterwhich it also has to be turned on/off by  $\delta_{\text{HP1}}$ . Again the first approach of just one auxiliary variable is advised as otherwise a multitude of auxiliary variables and their constraints are required.

An overview of input variables that rely on the binary on/off variable as well as on other variables or statements are listed in Table 4-5. The limitations on the lower or upper bound of the mass flow for  $\dot{m}_{c \text{ to HEX}_h}$ ,  $\dot{m}_{\text{HEX}_h, \text{ prim}}$  and  $\dot{m}_{\text{HEX}_c, \text{ prim}}$  are caused by limitations on the pump capacity

The energy provided by component groups is generally a continuous variable, except for the energy provided by the heat pumps as already defined before.  $Q_{c, \text{ build}}$  and  $Q_{h, \text{ build}}$  are external inputs and  $Q_{\text{HT}}$  is a continuous variable which can therefore be described by an auxiliary variable to consider if it is in operation. Furthermore the energy dissipated by the drycooler is not a free variable. The condenser heat is dissipated such that the temperature leaving the dry cooler is  $40^\circ\text{C}$ .

## Reversed flow

The selection of upwind numerical scheme, allows for only one flow direction. This can be a problem if the flow in certain sections is reversed as it does not simply mean an opposite sign of the mass flow, another variable has to be used. Instead of  $T_{i-1}$  the temperature of the cell on the opposite is required  $T_{i+1}$ , therefore the equations have to be adjusted.

The reversed flow can be modelled using the opposite upwind scheme and adding them

Input variable	Methods in applied order	Important variable
$\dot{m}_{\text{HP1, evap, 3way}}$	PI control	$T_{\text{HP1, evap, out}}$
	Saturation	$\bar{\dot{m}}_{\text{HP1, evap, 3way}} = 0.9c\dot{m}_{\text{HP1, evap}}, \underline{\dot{m}}_{\text{HP1, evap, 3way}} = 0$
	On/off	$\delta_{\text{HP1}}$
$\dot{m}_{\text{HP2, evap, 3way}}$	PI control	$T_{\text{HP2, evap, out}}$
	Saturation	$\bar{\dot{m}}_{\text{HP2, evap, 3way}} = 0.9c\dot{m}_{\text{HP2, evap}}, \underline{\dot{m}}_{\text{HP2, evap, 3way}} = 0$
	On/off	$\delta_{\text{HP2}}$
$\dot{m}_{\text{c to HEX}_h}$	Equation	$\dot{m}_{\text{evaps}} - \dot{m}_{\text{c, build}}$
	Saturation	$\underline{\dot{m}}_{\text{c to HEX}_h}, \bar{\dot{m}}_{\text{c to HEX}_h}$
	On/off	$\delta_{\text{HEX}_h}$
$\dot{m}_{\text{c, DC}}$	Equation	$\bar{\dot{m}}_{\text{HEX}_h, \text{sec}} - \dot{m}_{\text{c to HEX}_h}$
	Saturation	$\underline{\dot{m}}_{\text{c, DC}} = 0, \bar{\dot{m}}_{\text{c, DC}} = \bar{\dot{m}}_{\text{HEX}_h, \text{sec}}$
	On/off	$\delta_{\text{c, DC}}$
$\dot{m}_{\text{HEX}_h, \text{prim}}$	PI control	$T_{\text{HEX}_h, \text{prim, out}}$
	Saturation	$\underline{\dot{m}}_{\text{HEX}_h, \text{prim}}, \bar{\dot{m}}_{\text{HEX}_h, \text{prim}}$
	On/off	$\delta_{\text{HEX}_h}$
$\dot{m}_{\text{HEX}_c, \text{prim}}$	PI control	$T_{\text{HEX}_c, \text{sec, out}}$
	Saturation	$\underline{\dot{m}}_{\text{HEX}_c, \text{prim}}, \bar{\dot{m}}_{\text{HEX}_c, \text{prim}}$
	On/off	$\delta_{\text{HEX}_c}$
$Q_{\text{c, DC}}$	PI control	$T_{\text{c, DC, out}}$
	Saturation	$\underline{Q}_{\text{c, DC}}, \bar{Q}_{\text{c, DC}} = 0$
	On/off	$\delta_{\text{c, DC}}$
$Q_{\text{h, DC}}$	PI control	$T_{\text{h, DC, out}}$
	Saturation	$\underline{Q}_{\text{h, DC}}, \bar{Q}_{\text{h, DC}} = 0$
	On/off	$\delta_{\text{h, DC}}$
$Q_{\text{HT}}$	PI control	$T_{\text{h, build, in}}$
	Saturation	$\underline{Q}_{\text{HT}} = 0, \bar{Q}_{\text{HT}}$
	On/off	$\delta_{\text{HT}}$

**Table 4-5:** List of input variables that require multiple methods to determine the input

and subtracting the current upwind scheme from the equation. This part, has to be multiplied with a binary value that determines when the reversed flow has to be selected (4-60). The value of all mass flows have to be positive (due to upwind), yet the way a value is calculated might result in different signs for the mass flows. For instance,  $m^k = \dot{m}_{\text{evaps}} - \dot{m}_{\text{c to HEX}_h}$  is the standard flow, through the pipe section between the buffer and the entrance of the HP evaporators, where the heat exchanger connection is made. When  $\dot{m}_{\text{evaps}} - \dot{m}_{\text{c to HEX}_h} < 0$  the flow is reversed, resulting in a negative mass flow value, therefore the reversed flow equations have to be selected and the new mass flow is  $m_{\text{new}}^k = \dot{m}_{\text{c to HEX}_h} - \dot{m}_{\text{evaps}}$ .

Sections where reversed flow is possible:

- Warm buffer  $m = \dot{m}_{\text{HPs, conds}} - \dot{m}_{\text{h, build}} \rightarrow m = \dot{m}_{\text{h, build}} - \dot{m}_{\text{HPs, conds}}$  with the condition  $\dot{m}_{\text{HPs, conds}} - \dot{m}_{\text{h, build}} \leq 0 \iff \delta_{\text{h, buff, rev}} = 1$
- Warm building in, parallel to HT,  $m = \dot{m}_{\text{h, build}} - \dot{m}_{\text{h, HT}} \rightarrow m = \dot{m}_{\text{h, HT}} - \dot{m}_{\text{h, build}}$  with the condition  $\dot{m}_{\text{h, build}} - \dot{m}_{\text{h, HT}} \leq 0 \iff \delta_{\text{h, HT, rev}} = 1$
- Cold buffer  $m = \dot{m}_{\text{c, build}} - (\dot{m}_{\text{evaps}} - \dot{m}_{\text{c to HEX}_h}) \rightarrow m = \dot{m}_{\text{evaps}} - \dot{m}_{\text{c, build}} - \dot{m}_{\text{c to HEX}_h}$  with the condition  $\dot{m}_{\text{c, build}} - (\dot{m}_{\text{evaps}} - \dot{m}_{\text{c to HEX}_h}) \leq 0 \iff \delta_{\text{c, buff, rev}} = 1$

Besides the reversed flow in the pipes and components, these reversed flows also have an effect on the connecting cells. Here once again this method has to be applied and carefully considered which mass flows would be added/subtracted and which temperatures are used as inflow temperatures. For instance, a reverse flow in the warm buffer results a change of composition of the flow entering the warm distribution network.

$$\begin{aligned} \rho c_p V_{\text{cell}, i} \frac{T_i^{k+1} - T_i^k}{\Delta t} = & (c_p \dot{m}^k)(T_{i-1}^k - T_i^k) + \left( \frac{T_{i+1}^k - 2T_i^k + T_{i-1}^k}{\Delta x} \right) k A_{\text{cross}} \\ & - (T_i^k - T_{\text{amb}}^k) U A_{\text{circ, cell}} + \left( c_p \dot{m}_{\text{new}}^k (T_{i+1}^k - T_i^k) - c_p \dot{m}^k (T_{i-1}^k - T_i^k) \right) \delta_{\text{rev}} \end{aligned} \quad (4-60)$$

### Time constraints

Certain components have a minimum running time and minimum off time to reduce the component wear as a result of frequent shut down/start up as well as to provide them the time to reach their operational point. The constraints to model the minimum on/off time are listed below where to additional binary variables  $\delta_{\text{HP1}}^{\text{start}}$  and  $\delta_{\text{HP1}}^{\text{stop}}$  are used to define the starting and stopping moment and  $t_{\text{HP, on/off}}$  is the minimum running/off time.

$$\delta_{\text{HP1}}(k) - \delta_{\text{HP1}}(k-1) = \delta_{\text{HP1}}^{\text{start}}(k) - \delta_{\text{HP1}}^{\text{stop}}(k) \quad (4-61)$$

$$\sum_{k-t_{\text{HP, on/off}}}^k (\delta_{\text{HP1}}^{\text{start}}(n) + \delta_{\text{HP1}}^{\text{stop}}(n)) \leq 1 \quad (4-62)$$

If the minimum running time is different from the minimum off time, than the the last equation (4-62) needs to be split in two equations, one for the minimum running time and

one for the minimum off time.

$$\sum_{k-t_{\text{HP, on}}}^k \delta_{\text{HP1}}^{\text{start}}(k) \leq \delta_{\text{HP1}}(k) \quad (4-63)$$

$$\sum_{k-t_{\text{HP, off}}}^k \delta_{\text{HP1}}^{\text{stop}}(k) \leq 1 - \delta_{\text{HP1}}(k) \quad (4-64)$$

Time constraints are also implemented for the capacity changes as it can put a lot of stress on the compressor and to allow the system, time to adjust. The start/stop moments are defined (4-65) and these variables are constrained similarly to the heat pump turning on/off with a minimum capacity time  $t_{\text{cap, change}}$ .

$$\begin{bmatrix} 1 & 0 & 0 & 0 \\ 0 & 1 & 0 & 0 \\ 0 & 0 & 1 & 0 \\ 0 & 0 & 0 & 1 \end{bmatrix} \left( \begin{bmatrix} \delta_{\text{HP1}, 25\%} \\ \delta_{\text{HP1}, 50\%} \\ \delta_{\text{HP1}, 75\%} \\ \delta_{\text{HP1}, 100\%} \end{bmatrix} (k) - \begin{bmatrix} \delta_{\text{HP1}, 25\%} \\ \delta_{\text{HP1}, 50\%} \\ \delta_{\text{HP1}, 75\%} \\ \delta_{\text{HP1}, 100\%} \end{bmatrix} (k-1) \right) = \begin{bmatrix} \delta_{\text{HP1}, 25\%}^{\text{start}} \\ \delta_{\text{HP1}, 50\%}^{\text{start}} \\ \delta_{\text{HP1}, 75\%}^{\text{start}} \\ \delta_{\text{HP1}, 100\%}^{\text{start}} \end{bmatrix} (k) + \begin{bmatrix} \delta_{\text{HP1}, 25\%}^{\text{stop}} \\ \delta_{\text{HP1}, 50\%}^{\text{stop}} \\ \delta_{\text{HP1}, 75\%}^{\text{stop}} \\ \delta_{\text{HP1}, 100\%}^{\text{stop}} \end{bmatrix} (k) \quad (4-65)$$

The capacity steps that can be taken also have to be constrained as once again the heatpump needs time to adapt and also the change in capacity is rather slow as the pressure has to be increased or reduced or the massflow of circuit has to be adjusted. Therefore the heatpump can only go up one capacity step every time(4-66) and go down two capacity steps (4-67).

$$\begin{bmatrix} -1 & 0 & -1 & -1 \\ 0 & -1 & 0 & -1 \\ 0 & 0 & -1 & 0 \end{bmatrix} \begin{bmatrix} \delta_{\text{HP1}, 25\%}^{\text{stop}} \\ \delta_{\text{HP1}, 50\%}^{\text{stop}} \\ \delta_{\text{HP1}, 75\%}^{\text{stop}} \\ \delta_{\text{HP1}, 100\%}^{\text{stop}} \end{bmatrix} (k) + \begin{bmatrix} 0 & 1 & 0 & 0 \\ 0 & 0 & 1 & 0 \\ 0 & 0 & 0 & 1 \end{bmatrix} \begin{bmatrix} \delta_{\text{HP1}, 25\%}^{\text{start}} \\ \delta_{\text{HP1}, 50\%}^{\text{start}} \\ \delta_{\text{HP1}, 75\%}^{\text{start}} \\ \delta_{\text{HP1}, 100\%}^{\text{start}} \end{bmatrix} (k) \leq 0 \quad (4-66)$$

$$\begin{bmatrix} -1 & -1 & 0 & -1 \\ 0 & -1 & -1 & 0 \end{bmatrix} \begin{bmatrix} \delta_{\text{HP1}, 25\%}^{\text{start}} \\ \delta_{\text{HP1}, 50\%}^{\text{start}} \\ \delta_{\text{HP1}, 75\%}^{\text{start}} \\ \delta_{\text{HP1}, 100\%}^{\text{start}} \end{bmatrix} (k) + \begin{bmatrix} 0 & 0 & 1 & 0 \\ 0 & 0 & 0 & 1 \end{bmatrix} \begin{bmatrix} \delta_{\text{HP1}, 25\%}^{\text{stop}} \\ \delta_{\text{HP1}, 50\%}^{\text{stop}} \\ \delta_{\text{HP1}, 75\%}^{\text{stop}} \\ \delta_{\text{HP1}, 100\%}^{\text{stop}} \end{bmatrix} (k) \leq 0 \quad (4-67)$$

### State variable constraints

The state variables are all temperatures and should therefore always be above  $0^\circ\text{C}$ , however since the temperature could only drop below  $6.0^\circ\text{C}$  after the evaporator and short fluctuations are possible due to capacity changes, the lower bound on all temperatures is set to  $4.0^\circ\text{C}$ . All temperatures are well below  $60^\circ\text{C}$ . One could even make a distinction between the temperatures in the cold side of the substation and the warm side, maximising the cold side at  $25^\circ\text{C}$  and minimizing the warm side at  $20^\circ\text{C}$ . Furthermore it is key to not set too strict limits on the temperature limitations if no slack is allowed as it could make the model infeasible.

In Table 4-6 is an idealised list of the limits on the state variables. Some of these limitations have been derived from the considerations of the substation design, where for example, it is desired that the temperature leaving the primary side of the cold heat exchanger remains between 16 and 24 °C. If these are imposed as hard constraints, this might result in an infeasible solution as it sometimes is impossible to remain between these values, for instance during switching, when some of the pipes to the heat exchanger first have to be flushed before it can actively control. Some constraints can be considered as hard as they should pose problems with starting too high/low but do help with the choice for switching like the conditions on the HP temperatures. Adding the constraints if the problem remains solvable improves the computation time as there is a smaller range of possible values, especially important for variables that are multiplied with continuous variables (bilinear terms).

There are two special state variables constraints, on the return temperature from the building cooling and heating devices. Generally, as a result of the systems used to provide the heat/cold to the rooms, the minimum/maximum temperature returning is constraint,  $T_{h, \text{build, out}} \geq 23.5 \text{ °C}$  and  $T_{c, \text{build, out}} \leq 19 \text{ °C}$ . As the heat/cold demand is an external input, the mass flow is as the external input and the temperature entering is a state variable, this could result in lower/higher temperatures returning. This can occur when the setpoints are not met by the model, or when the temperature during the measurements exceeded the setpoint. Setting these variables as hard constraints could result in an insolvable problem, however, allowing an exceeding of the constraints would result in physically unrealistic temperatures and thereby system responses.

Therefore, the equation where the energy is added/extracted from the building can be added with a slack variable (4-68). The energy slack variable ( $\epsilon^k$ ) needs to have the opposed sign of  $\dot{Q}$  so in the case shown below, it should be positive. The slack variable should only ensure that the temperature is within the constraints, therefore the slack variable should be added to the cost function with a large penalty value. However, some of the heat demand will therefore not be delivered, and should be delivered at a later moment in time, this results in the summation of values of the slack variable, which will then again have to be subtracted ( $\epsilon^{k-1}$ ). As  $\epsilon^k$  has to ensure that the temperature stays in range it automatically adds the previous time step to its new value, when the current time step heat demand would be within the temperature limits, the slack variable would be reduced in value again, till it is zero, its minimum. For the cold demand the statement is the same, only the energy slack variable  $\epsilon^k$  should then be negative.

$$T_{h, \text{build, out}}^{k+1} = \frac{\Delta t}{\rho c_p V_{\text{cell}}} \left( -c_p \dot{m}^k (T_{h, \text{build, out}}^k - T_{h, \text{build, in}}^k) + \dot{Q}^k \right) + T_{h, \text{build, out}}^k + \frac{\Delta t}{\rho c_p V_{\text{cell}}} (\epsilon^k - \epsilon^{k-1}) \quad \epsilon^k \geq 0 \quad (4-68a)$$

$$\min(\epsilon^k)^2 \quad (4-68b)$$

State variable	Constraint	Hard \ soft
$T_{HP1, \text{ cond, out}}$	$\leq 47^\circ\text{C}$	S
$T_{HP2, \text{ cond, out}}$	$\leq 47^\circ\text{C}$	S
$T_{HP1, \text{ evap, out}}$	$\geq 4.0^\circ\text{C}$	H
$T_{HP2, \text{ evap, out}}$	$\geq 4.0^\circ\text{C}$	H
$T_c, \text{ build, out}$	$\leq 19^\circ\text{C}$	H slack variable on energy
$T_h, \text{ build, out}$	$\geq 23.5^\circ\text{C}$	H slack variable on energy
$T_{HEX_c, \text{ prim, out}}$	$\leq 24^\circ\text{C}$	S
$T_{HEX_c, \text{ prim, out}}$	$\geq 16^\circ\text{C}$	S
$T_{HEX_c, \text{ sec, out}}$	$\leq 12^\circ\text{C}$	S
$T_{HEX_h, \text{ sec, out}}$	$\geq 10^\circ\text{C}$	S

**Table 4-6:** Constraints linked to state variables

### 4-3-2 Move blocking

The MPC controller would ideally be designed with time steps of 30 s or 60 s as this would provide small enough steps to regularly adjust the on/off and capacity inputs. Smaller would be an unnecessary computational burden as the on/off/capacity inputs should also be on/off or at a certain capacity for respectively 15 min or 5.0 min. If larger time steps would be chosen, it could provide problems with the switching.

The model constructed earlier, ideally uses as small as possible cell volumes, to limit numerical diffusion. The volume is set to the maximum volumetric flow it can handle in a second. Thereby, the time step required by the model is 1.0 s. This would increase the number of free variable inputs significantly, even though this would not be necessary for the system itself. Thereby it is chosen to have an optimization algorithm with a time step of 15 s, but where the binary input variables for the on/off/capacity remain constant for 60 s. This is achieved using the so called Move blocking procedure (4-69) [30], where  $\hat{U} \in \mathbb{R}^{Mm}$  where  $M$  is the number of times the input variables are updated/changed,  $U \in \mathbb{R}^{Nm}$  and  $T \in \mathbb{Z}^{Nm \times Mm}$  where  $T$  is the blocking matrix, with  $N$  the horizon and  $m$  the number of free input variables per time step.  $T$  is a zero matrix which contains at least one 1 in each column and only one 1 in each row with  $M \leq N$ .

$$U = (T \otimes I_m) \hat{U} \quad (4-69)$$

### 4-3-3 Cost function

The cost function is an overarching function that minimises or maximises the system cost by optimisation techniques. Examples of minimising costs are a minimal use of energy or financial expenses, or a maximum in revenue or energy generation. To define a cost function, it is of utmost importance to know the goals and constraints within one or multiple ranges of variables for the controller to optimise:

- Maintain building comfort, reference tracking of  $T_{h, \text{ set}}$  with  $T_{h, \text{ build, in}}$  within a  $1.0^\circ\text{C}$  band.
- Minimise the energy delivered by the HT.
- Keep the return temperatures to the grid within its limits for both heat exchangers.

- Reduce component wear by reducing the amount of unnecessary switching.

The MPC model would consist of many binary variables if it is setup like stated above. There is a clear distinction between two parts of the system, the heating part of the substation and the cooling part which also connects the ring network. As the operation of the cooling part of the substation during the heating season is mainly dependent on the heating part (the HP operating capacities), the system for the optimization could be split in two. One MPC for the heating part of the substation and another one for the cooling part, where the heatpump operating capacities are used as inputs. In the next subsections the different MPC cost function options are discussed for the heating and the cooling part of the substation

### Substation heating part

As stated above one goal is to track the setpoint temperature and minimise the use of the conventional heater. This can be achieved with different objective functions.

As the temperature setpoint should be tracked, the building managers provide a guideline of a  $1.0^{\circ}\text{C}$  band, the square of the error ( $e = T_{h, \text{set}} - T_{h, \text{build, in}}$ ) could be used as the objective function (4-70). If all the constraints and model equations would be linearised this would still result in a simple Quadratic Programming problem. However, the model equations are quadratic (bilinear) equality equations, thereby this would result in a Non-Convex Programming problem, as the quadratic equality equations are non-convex. This will make it computationally intensive and there is no guarantee the optimal solution will be found. There are several possibilities to simplify, one could state the equality as an inequality constraint, such that the maximisation/minimization would also lie on the equality, resulting in a Quadratically Constrained Quadratic Programming (QCQP) problem. This is prone to problems, as the equality might not be reached or the inequality might be non-convex.

Another option would be to linearise these model equations as linear equalities are allowed for QCQP problems. There are no other quadratic (inequality) constraints than the model dynamics, thus this would result in a standard Quadratic Programming (QP) problem. The current case of the heating part of the substation, this is possible as the mass flows through certain sections is either provided (building demand) or only depends on whether the component group is turned on. The multiplication of a binary variable with a continuous variable, can also always be written linearly as shown before (4-41).

Since binary variables are used to determine whether a component group is switched on/off, the optimization will always be a MIP program. A MIP problem is generally computationally intensive as there are  $2^{n \cdot N_p}$  possible binary combinations, where  $n$  is the number of binary variables and  $N_p$  the control horizon. Therefore it is key to keep the number of binary variables and its control horizon small while also ensuring a convex description. Limits on how often a binary variable in this control horizon is allowed to change, does reduce the computational burden, as it rules out several combinations.

Furthermore to track the temperature setpoint, instead of an quadratic objective function one could also use a linear objective function (4-71). It is important to notice that a slack variable  $v_{\text{Thset}}$  is used to take a  $1.0^{\circ}\text{C}$  band around the setpoint as this small temperature difference does not influence the operation (4-72). This linearisation allows for a MILP problem if all other constraints are linearised. As the penalty for the  $v_{\text{Thset}}$  is set to 1, it allows to determine the other penalties in terms of temperature differences.

$$\min \left( \sum_{k=0}^{N_p-1} e^2(k) \right) \quad (4-70)$$

$$\min_{\delta} \left( \sum_{k=0}^{N_p-1} \max(|T_{h, \text{set}}(k) - T_{h, \text{build, in}}(k)| - 1, 0) \right) = \min_{\delta} \left( \sum_{k=0}^{N_p-1} v_{\text{Thset}} \right) \quad (4-71)$$

$$v_{\text{Thset}} \geq 0 \quad (4-72a)$$

$$v_{\text{Thset}} \geq T_{h, \text{set}}(k) - T_{h, \text{build, in}}(k) - 1 \quad (4-72b)$$

$$v_{\text{Thset}} \geq -T_{h, \text{set}}(k) + T_{h, \text{build, in}}(k) - 1 \quad (4-72c)$$

Besides tracking the temperature setpoint, the use of the conventional heater should be minimized such that it is only used if there are no other options to maintain building comfort. A constraint is set on the minimum time the conventional heater is on as it otherwise would not allow for a proper start up and a very short on time might result in unnecessary start if not penalised. It also helps the optimisation as it reduces the number of free binary variables.

The part of the objective to penalise the conventional heater can be set it two ways, either a penalisation on the conventional heater being on (4-73) or on the additional temperature difference it adds to the flow entering the building (4-74). It should be noted that the mass flow in the building is an external variable, thus provided, therefore the objective remains linear. The weight factors  $w_{p, \text{HT}}$  and  $w_{p1, \text{HT}}$  can be tuned to set the sensitivity. It is also possible to use a combination of both penalising methods. It should be noted that  $w_{p, \text{HT}}$  can be chosen depending on the preferred temperature difference one would want the conventional heater to kick in.  $w_{p1, \text{HT}}$  should always be smaller than 1, otherwise the error in tracking ( $v_{\text{Thset}}$ ) will always be preferred over the conventional heater kicking in. But if used separately and the weight would be smaller than 1, the HT will kick in almost all the time even for very small and short violations and the effect of turning on is not penalised as the MPC might set the energy to 0 for all other time steps that it remains on. Ideally the combination of both penalising methods would be preferred, as it penalises the fact that the HT has to turn on, but also minimizes the use of the conventional heater energy as the temperature difference it achieves is also penalised. If it is only penalised for being on, once it is on and the HPs could never reach the setpoint temperature it could also result in the HPs running at lower capacities and the HT maximising its consumption.

At times it is possible that the temperature setpoint is properly tracked, however the heat demand can not fully be extracted, due to small fluctuations or overshoots in the gathered data. As the minimum temperature returning from the building is constrained at 23°C a slack variable is added to these dynamics to cover the temperature decrease, that could not be achieved. The slack variable is then added again to the time step as this energy is demanded and has to be extracted. This slack variable ( $v_{\text{Qh}}$ ) is penalised in the objective function as it should only be larger than 0 when the setpoint temperatures are reached and the energy can not fully be extracted.

$$\min_{\delta} \left( \sum_{k=0}^{N_p-1} w_{p, \text{HT}} \delta_{\text{HT}} \right) \quad (4-73)$$

$$\min_{\delta} \left( \sum_{k=0}^{N_p-1} w_{p1, HT} \frac{Q_{HT}}{c_p \dot{m}_{h, build}} \right) \quad (4-74)$$

$$\min_{\delta} \left( \sum_{k=0}^{N_p-1} \left[ v_{T_{hset}} + w_{p, HT} \delta_{HT} + w_{p1, HT} \frac{Q_{HT}}{c_p \dot{m}_{h, build}} + w_{Qh} v_{Qh} \right] \right) \quad (4-75)$$

Furthermore, the temperature leaving the heat pumps was constrained at 47.5 °C, however very small excesses should not be a problem and also if the temperature in the real system has exceeded, this should not result in an infeasible model. Thus a slack variable ( $v_{T, HP1}$ ) was added with a large penalty as this is definitely not desirable, but it can sometimes not be avoided (as it is the measurement from the real system). The conventional heater in reality is controlled by a PID controller tracking the setpoint temperature and the MPC only decides the on/off condition.

Therefore an additional constraint has to be added to prevent the MPC from deciding that it might shortly heat up the stream a lot, to above the setpoint temperature, such that afterwards it can shut down and use the additional provided energy. If the conventional heater is on, the temperature entering the building should be below the  $T_{h, set} + 1$  (4-76). As it in reality is controlled by a PID and during start up some old (cooled down) water first is flushed, this can result in a short but sharp spike in the temperature not meeting this constraint. When this value is used as an initial condition for the time cycle, it would make the model infeasible, thus this is mitigated by adding a slack variable with a high penalty in the cost function (4-77).

$$\begin{aligned} T_{HP1, cond, out} &\leq 47.5 + v_{T, HP1} \\ T_{HP2, cond, out} &\leq 47.5 + v_{T, HP2} \end{aligned} \quad (4-76)$$

$$T_{h, build, in} - \left( \bar{T}_{h, build, in} - \left( \bar{T}_{h, build, in} - T_{h, set} \right) \cdot \delta_{HT} \right) \leq 1 + v_{T, HT}$$

$$\min_{\delta} \left( \sum_{k=0}^{N_p-1} [w_{T, HP} (v_{T, HP1} + v_{T, HP2}) + w_{T, HT} v_{T, HT}] \right) \quad (4-77)$$

The main objective is to track the setpoint temperature while minimising the energy consumption of the conventional heater. The tracking of the setpoint temperature is done within a 1.0 °C bound, thus whenever the temperature is within this bound for the full horizon, seemingly unnecessary actions could happen. For instance, the time constraint for switching between capacities is 5 minutes and turning on or off a heat pump is 15 minutes, and thus it could occur that the minimum objective of 0 is reached but one heat pump is turned down in the process and the other one is turned on, while the same objective could be reached with keeping the first heat pump on and the second off. This can also occur with the capacities, thus a small penalty for the change in capacity  $w_{HP, cap}$  or the starting or stopping heat pump  $w_{HP, on/off}$  is added. It is important to keep the penalty small as it should not effect the standard operation, to try and maintain the temperatures. If both a penalty on the change of capacity and a start of the heat pump are chosen it is important to notice, that this might lead to first maximising the capacity of one, before the other heat pump will be turned on.

As for a heat pump to stop/start, there will also be a change in capacity at some point, from or to zero, therefore this action is already penalised. Yet the penalty will be smaller than a capacity change between other operating capacities, as now only a start or a stop of capacities occur and not both, thus the HP start or stop could still be used.

$$\min_{\delta} \left( \sum_{k=0}^{N_p-1} \sum_{j=1}^2 \left[ w_{\text{HP, on/off}} \left( \delta_{\text{HP } j}^{\text{start}} + \delta_{\text{HP } j}^{\text{stop}} \right) + w_{\text{HP, cap}} \sum_{i=1}^4 \left( \delta_{\text{HP } j, \text{ cap } i}^{\text{start}} + \delta_{\text{HP } j, \text{ cap } i}^{\text{stop}} \right) \right] \right) \quad (4-78)$$

### Substation cooling part

The MPC for the cooling part of the substation is a subpart of the total MPC. The HP capacity will be used as inputs as well as the dry cooler's status and thus solely the operation of the heat exchangers ( $\delta_{\text{HEX}_h}$  and  $\delta_{\text{HEX}_c}$ ) has to be considered for this section. This results in a significant reduction of the binary decision variables, however, there are more bilinear terms as a result of more flows that are variable.

The prediction and control horizon for the optimisation can be relatively short, 5.0 min as this is the minimum on/off time of the heat exchanger, which should preferably be longer. The time steps need to be much shorter as the temperature limitations at both the heat pumps and the heat exchangers connecting the grid are more strict and thus the numerical diffusion should be limited.

The cost function can be based on the temperature returning to the grid. The evaporator leaving temperatures should be largely penalised for temperatures above 6.0 °C as this is the setpoint of the three-way valve PI controllers.

### 4-3-4 MPC variable flow

The warm side of the substation can be modelled and controlled based on the current design, but also on a design where the temperature control at the condenser side is operated using a three-way control valve. The last option possibly also using pump speed control results in a variable net flow over the condensers and thus the variable flow section should be considered.

Optimisation problems with bilinear functions (4-79) are a special class of the nonlinear optimisation problems, these have widely been described as pooling problems and several relaxations have been studied in literature to linearise it efficiently. The McCormick relaxation is discussed in [31], where a linearisation based on the McCormick envelope (4-80) is used to estimate the bilinear function. This can result in under- or overestimations due to the convexification, and it transforms a problem with bilinear equality constraints into a MILP. As the problem considered is already a MIP, this does not degrade the optimisation. However to reduce the error, the envelope can be reduced in size by partitioning it either in univariate (one variable) or bivariate (both variables), this will increase the number of binary and continuous variables as well as the number of constraints and therefore a trade-off has to be made between the computation time and the accuracy.

Bilinearity is considered to be the mass flow multiplied with the temperature. This bilinearity occurs at all cells where the mass flow over one of the two heat pumps influences the net mass flow, thus all cells and temperatures besides the cells regarding the building distribution network. The mass flow would be the partitioned variable as there are less

mass flow variables in the bilinear terms combined than there are temperature variables, and the number of binary variables scales linearly with the number of the partitioned variables and the number of partitions. The partitions are formed on a linear scale and the bilinear variable is defined by the partitioned McCormick envelope (4-81), where  $N_{\text{McC}}$  is the number of partitions and  $n_{\text{McC}}$  is the partition number selected.

Implementing these partitions in an optimisation program requires some adjustments and additional variables, binary switch variables  $\lambda \in \{0, 1\}^{N_{\text{McC}}}$  and continuous switch variables  $\Delta T \in [0, T^U - T^L]^{N_{\text{McC}}}$ . The selection of a partition is constrained by  $\sum_{n_{\text{McC}}=1}^{N_{\text{McC}}} \lambda(n_{\text{McC}}) = 1$ .

$$z = \dot{m} \cdot T \quad (4-79)$$

$$z \geq \dot{m} \cdot T^L + \dot{m}^L \cdot T - \dot{m}^L \cdot T^L \quad (4-80a)$$

$$z \geq \dot{m} \cdot T^U + \dot{m}^U \cdot T - \dot{m}^U \cdot T^U \quad (4-80b)$$

$$z \leq \dot{m} \cdot T^L + \dot{m}^U \cdot T - \dot{m}^U \cdot T^L \quad (4-80c)$$

$$z \leq \dot{m} \cdot T^U + \dot{m}^L \cdot T - \dot{m}^L \cdot T^U \quad (4-80d)$$

$$n_{\text{McC}} \in \{1, \dots, N_P\} \left[ \begin{array}{l} z \geq \dot{m} \cdot T^L + \left( \dot{m}^L + a \cdot (n_{\text{McC}} - 1) \right) \cdot (T - T^L) \\ z \geq \dot{m} \cdot T^U + \left( \dot{m}^L + a \cdot n_{\text{McC}} \right) \cdot (T - T^U) \\ z \leq \dot{m} \cdot T^L + \left( \dot{m}^L + a \cdot n_{\text{McC}} \right) \cdot (T - T^L) \\ z \leq \dot{m} \cdot T^U + \left( \dot{m}^L + a \cdot (n_{\text{McC}} - 1) \right) \cdot (T - T^U) \\ \dot{m}^L + a \cdot (n_{\text{McC}} - 1) \leq \dot{m} \leq \dot{m}^L + a \cdot n_{\text{McC}} \\ T^L \leq T \leq T^U \end{array} \right] \quad (4-81)$$

The reversed flow which was previously defined separately will now also have a McCormick variable, for which just simply the value of the 'normal flow' McCormick variable is multiplied with the binary variable for reversed flow.

The adjustment of the bilinear terms to McCormick variables with linear relaxations can result in significant under- or overshoot, thus besides increasing the number of partitions, which will improve it significantly, also some additional constraints can be added. These additional constraints are based on the energy flow of the system. For instance the mass flow is in one direction based on  $\dot{m}_{\text{h, build}} \leq \dot{m}_{\text{HP1, cond}} + \dot{m}_{\text{HP2, cond}}$  and since there is only one temperature in a cell, this would also mean that for that specific cell  $\dot{m}_{\text{h, build}} T \leq \dot{m}_{\text{HP1, cond}} T + \dot{m}_{\text{HP2, cond}} T$ . Thus this is added as an additional constraint as due to the McCormick relaxations, this might otherwise not always hold for the optimal values. The constraint including the condition for reversed flow has to be added for all cells that compose the buffer as they consist of the reversed flow part (4-82).  $z_{\text{HP1, } i}$  is the McCormick variable where HP1 indicates the mass flow of the condenser of the first heat pump and  $i$  indicates the cell number for the temperature. It should also be noted that  $\dot{m}_{\text{h, build}}$  is an external input, thus the first term is also linear.

$$\dot{m}_{\text{h, build}} T_i + \dot{m}_{\text{h, build}} \delta_{\text{rev}} T_i \leq z_{\text{HP1, } i} + z_{\text{HP2, } i} - (z_{\text{HP1, rev, } i} + z_{\text{HP2, rev, } i}) \quad (4-82)$$

Furthermore, the equation to determine the temperature of the combined flows of the heat pumps, requires some adjustments. As  $z_{\text{HPs, HPsout}} \leq z_{\text{HP1, HP1out}} + z_{\text{HP1, HP2out}} = z_{\text{HP1, HPsout}} + z_{\text{HP2, HPsout}}$  should not only hold, because the combined temperature resulting from this could be higher than both the temperature of the first and second heat pump as a result of relaxations. Especially, if only one heat pump is on, the combined temperature should be the same as that specific heat pump, and if both are on, the combined temperature should be lower than the maximum of both heat pumps (4-83).

$$T_{\text{HPs, conds, out}} \geq T_{\text{HP1, cond, out}} (\delta_{\text{HP1}} - \delta_{\text{HP1}} \delta_{\text{HP2}}) \quad (4-83a)$$

$$T_{\text{HPs, conds, out}} \leq \bar{T}_{\text{HP1, cond, out}} - (\bar{T}_{\text{HP1, cond, out}} - T_{\text{HP1, cond, out}}) (\delta_{\text{HP1}} - \delta_{\text{HP1}} \delta_{\text{HP2}}) \quad (4-83b)$$

$$T_{\text{HPs, conds, out}} \geq T_{\text{HP2, cond, out}} (\delta_{\text{HP2}} - \delta_{\text{HP2}} \delta_{\text{HP1}}) \quad (4-83c)$$

$$T_{\text{HPs, conds, out}} \leq \bar{T}_{\text{HP2, cond, out}} - (\bar{T}_{\text{HP2, cond, out}} - T_{\text{HP2, cond, out}}) (\delta_{\text{HP2}} - \delta_{\text{HP2}} \delta_{\text{HP1}}) \quad (4-83d)$$

$$T_{\text{HPs, conds, out}} \leq \max(T_{\text{HP1, cond, out}}, T_{\text{HP2, cond, out}}) \quad (4-83e)$$

The net flow through the heat pump is controlled by a PI controller on the added three-way valve with a setpoint ( $\min(T_{\text{h, set}}, 46^\circ\text{C})$ ) for the temperature leaving the heat pump. Therefore a constraint (4-84) is added to ensure the MPC will also decide the flow based on this temperature with a slack variable ( $v_{\text{HP1, set}}$ ) in case it is impossible to reach it.

$$(T_{\text{HP1, cond, out}} - \min(T_{\text{h, set}}, 46)) \delta_{\text{HP1}} - v_{\text{HP1, set}} = 0 \quad (4-84)$$

## 4-4 MPC variations

## 4-5 Summary

This chapter described the design of the MPC controller and the mathematical system model using the FVM on which it is based. Constraints for the system model to accurately describe the systems behaviour are provided as well as constraints providing the operational conditions.

Important to note is that the mass flows at multiple sections can generally be based on a few free variables as mass continuity should be maintained. The FVM model is set up using the upwind method, where reversed flow cannot simply be applied by changing the sign of the mass flow as water and the corresponding energy would now arrive from a different cell, thus binary variables are used to select the correct equations based on the flow direction. Time constraints for the on/off conditions have been provided with an additional group of binary variables, stating the start/stop behaviour. A move blocking strategy is used, to keep the inputs constant within the timestep of the MPC and thus for multiple timesteps of the model as the timestep of the MPC is 60s and of the model 15s, reducing the number of free input variables and thus the computational burden.

Finally the cost function to be minimised is determined, to track the temperature setpoint and where a penalty is applied on the violation of temperature constraints, the switching operations, the operation of the Conventional Heater or High Temperature source (HT) and

on the energy that cannot be extracted at the demander group.

Besides the current system design, the MPC is also applied for the variable net flow over the condensers, using the three-way valve. This results in a bilinear continuous system model which is thus non-convex for the optimisation and has thereby been relaxed using the (partitioned) McCormick envelope, resulting in a convex MILP problem.

In the next chapter the results of the simulations of the standard cases, the hydro- and thermodynamic and low-level control improvements and the effect of the MPC on the operation are shown.



---

# Chapter 5

---

## Results

The validation of the model will be shown here in Section 5-1. These will be the simulations in WANDA using the current control system implemented. In Section 5-2 simulations of some of the thermo-hydraulic improvements will be shown as well as improvements on the low-level control, including the proposed temperature and capacity control strategy. Finally in Section 5-3 the results of the MPC control, both for a constant flow over the condensers and for a variable flow over the condensers, thus with a three-way valve temperature control, are shown. The results of these different control methods will afterwards be compared and discussed in Chapter 6.

### 5-1 Validation WANDA model

As the whole system is modelled with several uncertainties in the information provided, or solely based on assumptions and educated estimations, it is important to verify that the model provides similar component and system behaviour. This also allows for an estimation of discrepancies, what needs to be considered if changes were implemented and how and when the model behaves differently. Once this is validated, improvements can be modelled and the effects can be determined. The validation of the individual component behaviour is not shown here as it is not as complex. The validation of the system itself is more difficult as a small difference in starting conditions or sensor inaccuracies can show a different response.

The selected cases for the validation are 5,7,8,9 and 10 as they show a wide variety of energy demands.

First the performance of the warm side of case 5 of the model is compared with the captured data. It can be noted that in general a similar performance is observed, however there are some differences. In the model one heat pump is set to be the first and the other the second heat pump. This order is not changed in the model, while in reality this is changed. This can for instance be observed in case 5, where if one heat pump has been turned on, the other heat pump is turned off a bit later instead of the newly turned on heat pump. In the model, the same heat pump as the one that has been turned on the latest is here turned down.

Furthermore, the operation is in reality slightly smoother, the temperature slopes are less

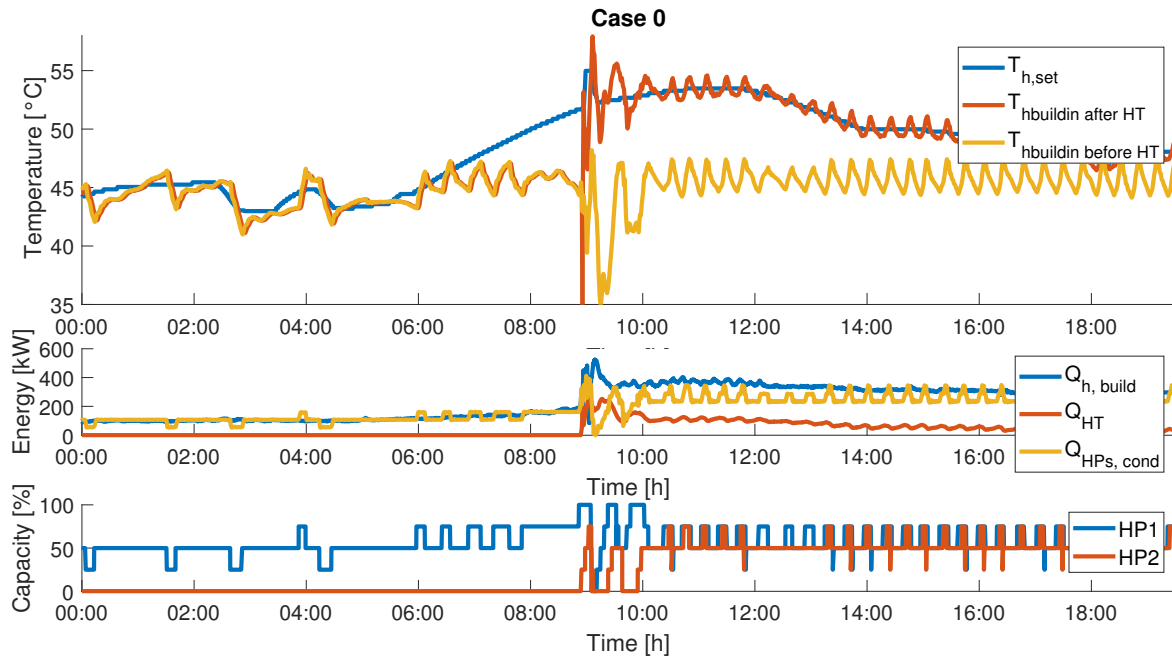


**Figure 5-1:** Case 0: warm building network modelled with the standard control methods

sharp as there might be more mixing and the energy provided by the heat pump would not be exactly constant as the internal heat pump control can cause slightly different pressures and condensing temperatures. The higher the condenser entering temperature gets, there might be a slight reduction in the heat transferred due to a lower temperature jump across the heat exchanger.

The comparison of case 9 with the measurements is particularly interesting as in reality the temperature entering the warm distribution network of the building is much higher than the setpoint. The energy extracted by the building is based on this measurement and thus in the simulation, where the setpoint is followed, not all energy demanded by the building could be extracted, thus resulting in a return temperature at its minimum.

In general for most cases, the moment where a second heat pump turns on or off, or when the conventional heater kicks in is almost the same. Even a very small temperature difference between the simulation and the reality can result in them kicking in or not, so sometimes, when it is just on the verge, it might not occur. If a section is turned on for the first time in the simulations, one might see a temperature jump, as this section is set to the ambient temperature during the initialisation. Throughout this report one should keep in mind that this occurs and thus might cause some unexpected behaviour.

Similar temperatures are leaving the warm building distribution network and are entering the condensers, as long as the same number of heat pumps is on, therefore indicating that the newly chosen mass flows for the condensers are in a similar region. Furthermore, both in the simulation and in reality the temperatures at the warm buffers are similar to the condenser leaving temperatures.

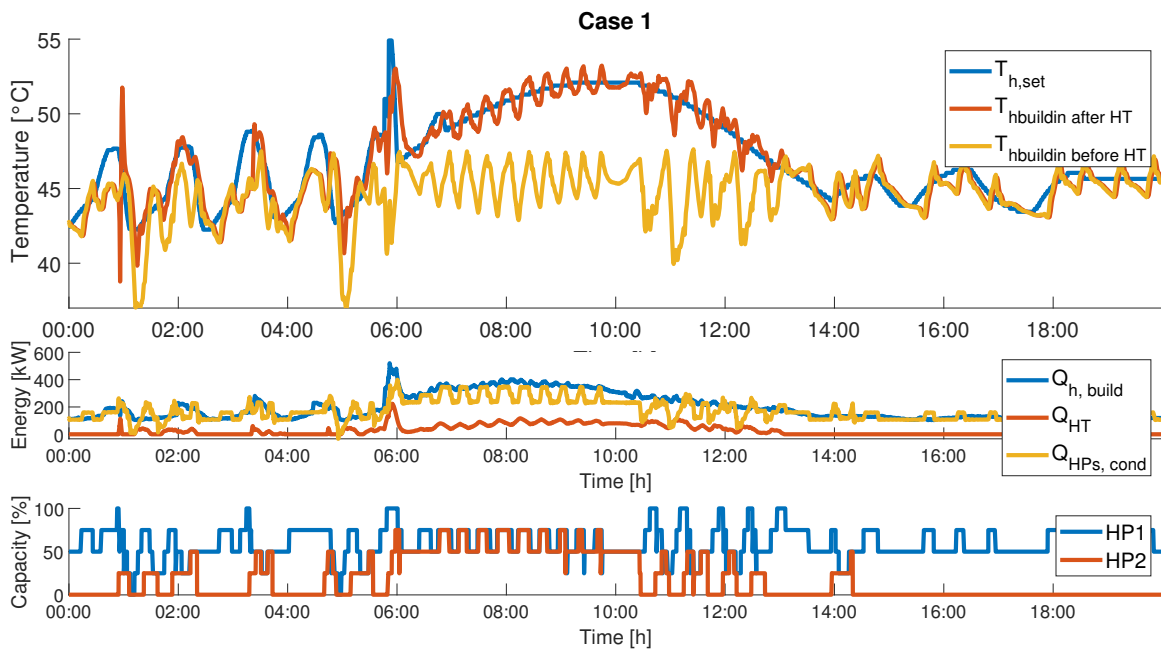


Figure 5-2: Case 1: warm building network modelled with the standard control methods

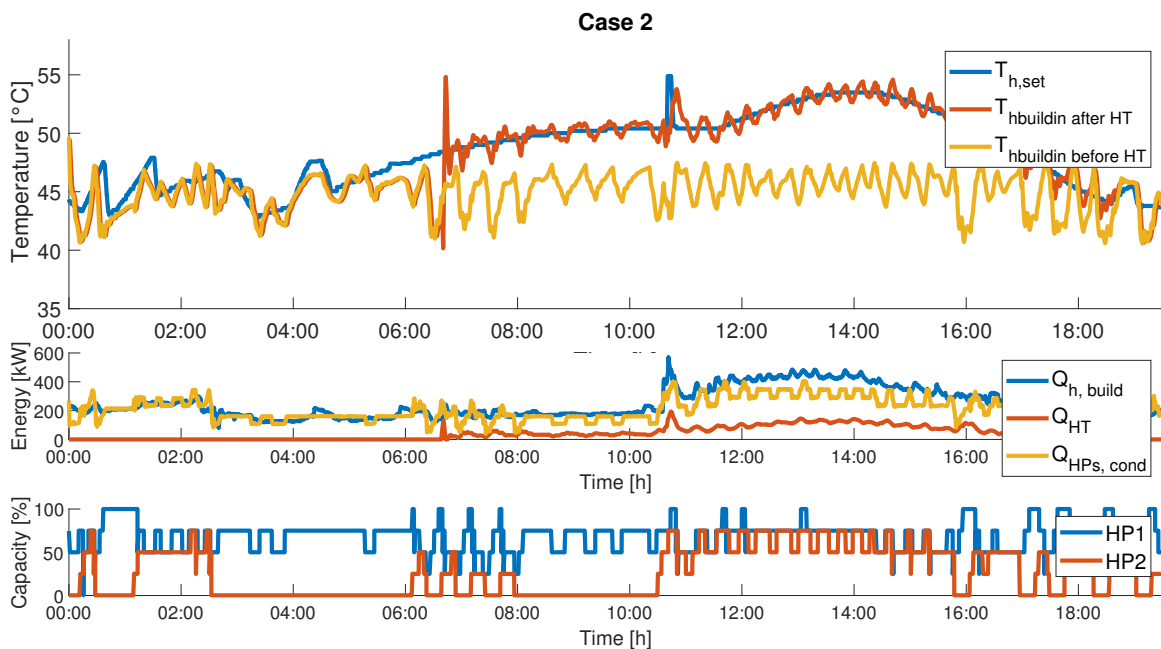
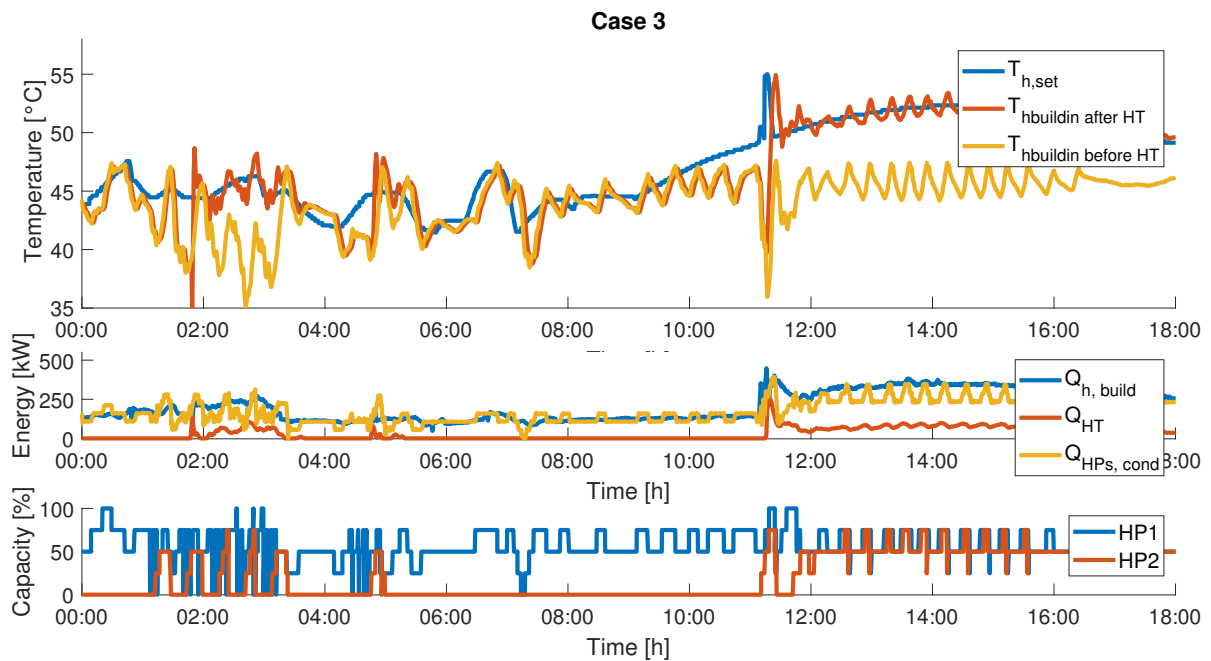
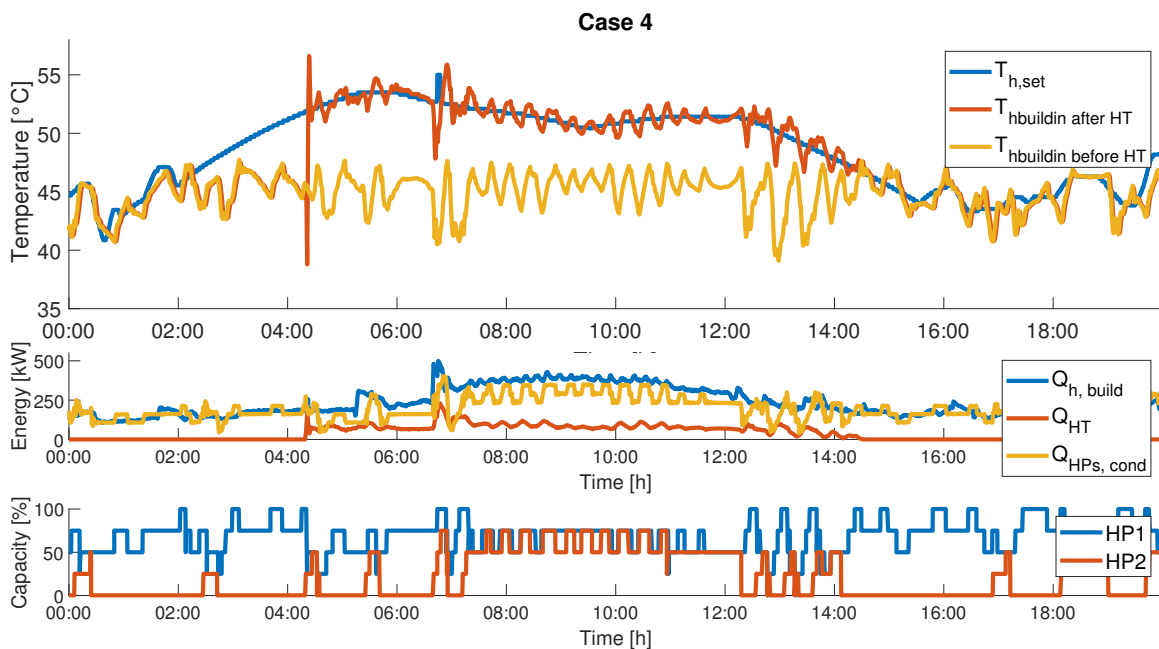


Figure 5-3: Case 2: warm building network modelled with the standard control methods



**Figure 5-4:** Case 3: warm building network modelled with the standard control methods



**Figure 5-5:** Case 4: warm building network modelled with the standard control methods

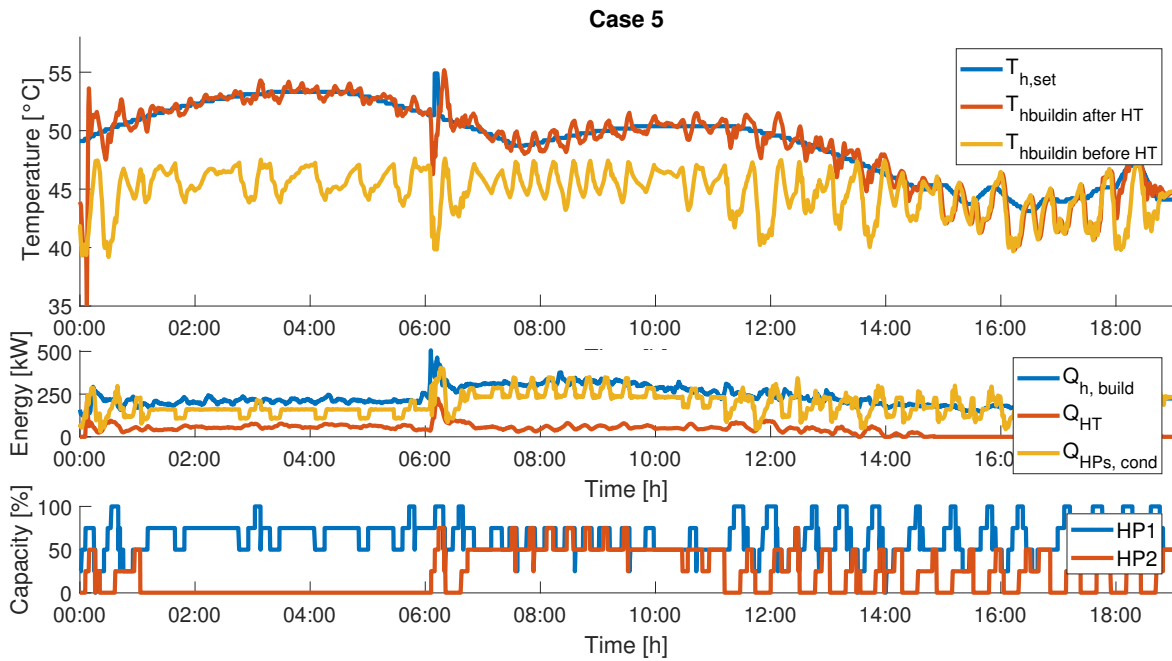


Figure 5-6: Case 5: warm building network modelled with the standard control methods

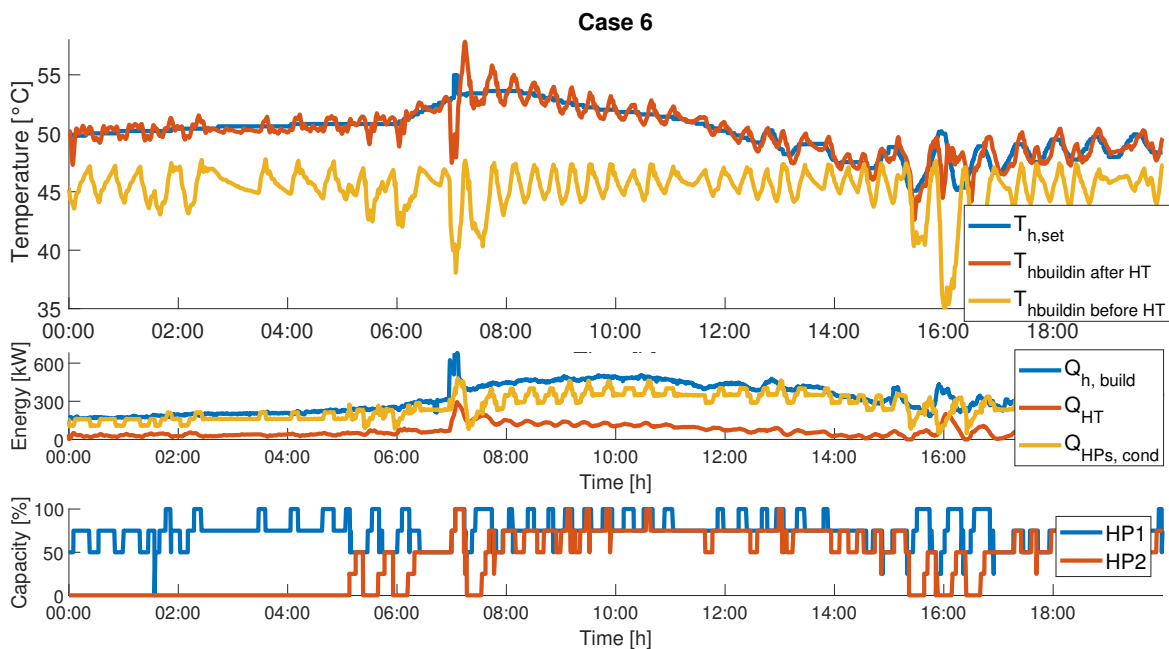


Figure 5-7: Case 6: warm building network modelled with the standard control methods

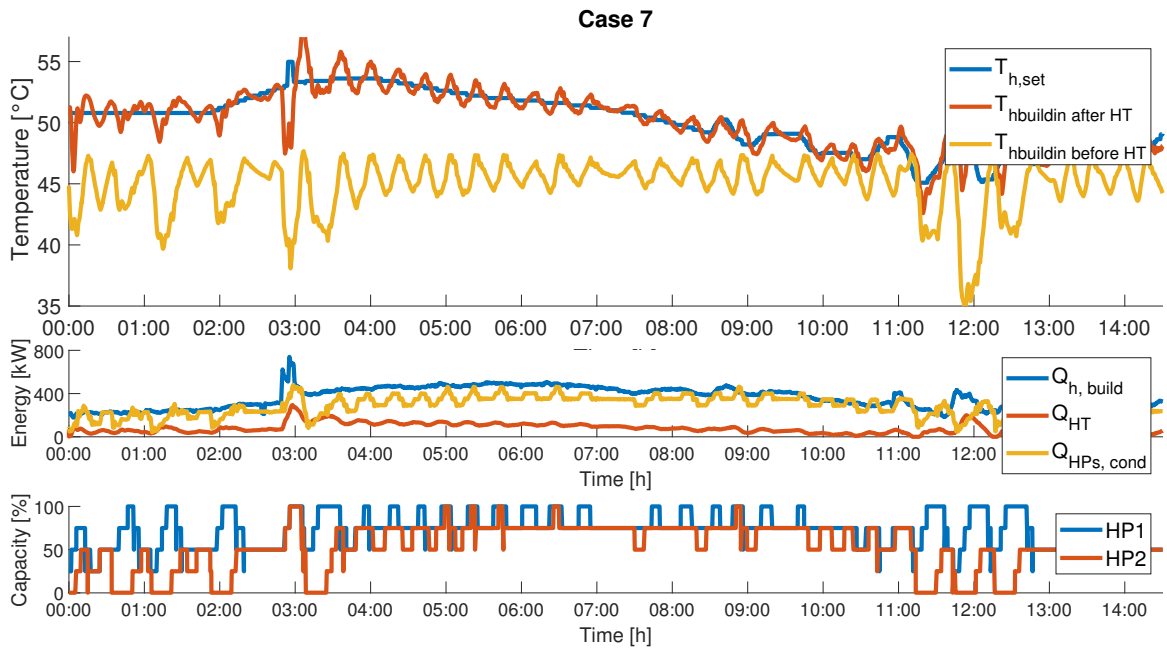


Figure 5-8: Case 7: warm building network modelled with the standard control methods

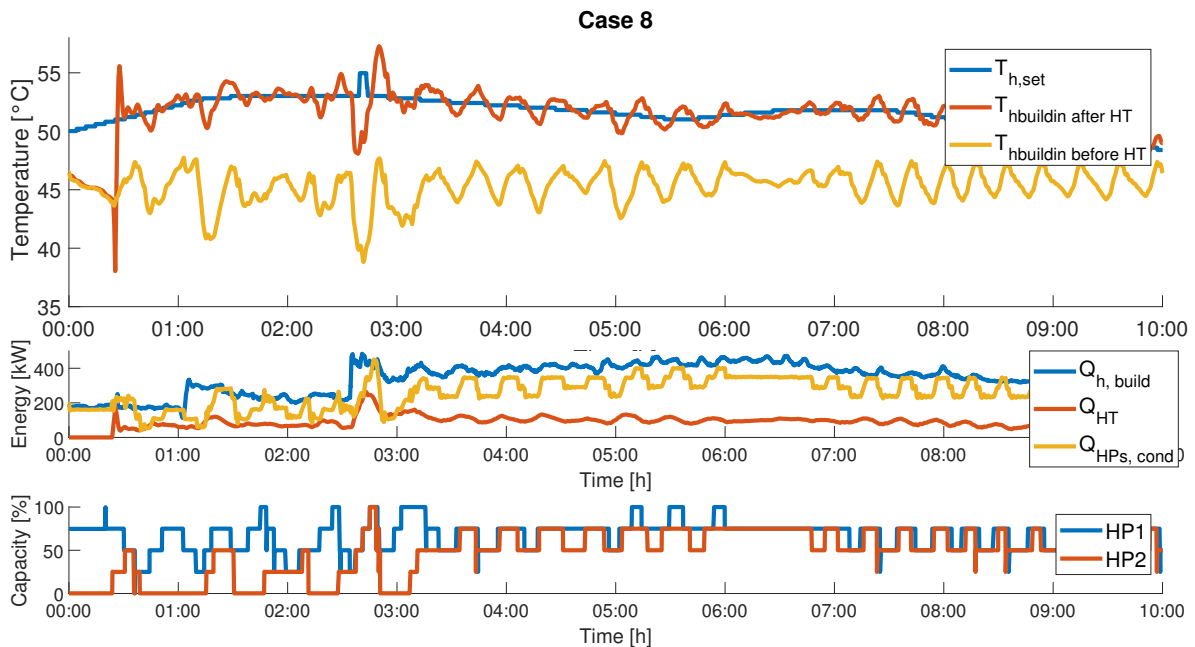


Figure 5-9: Case 8: warm building network modelled with the standard control methods

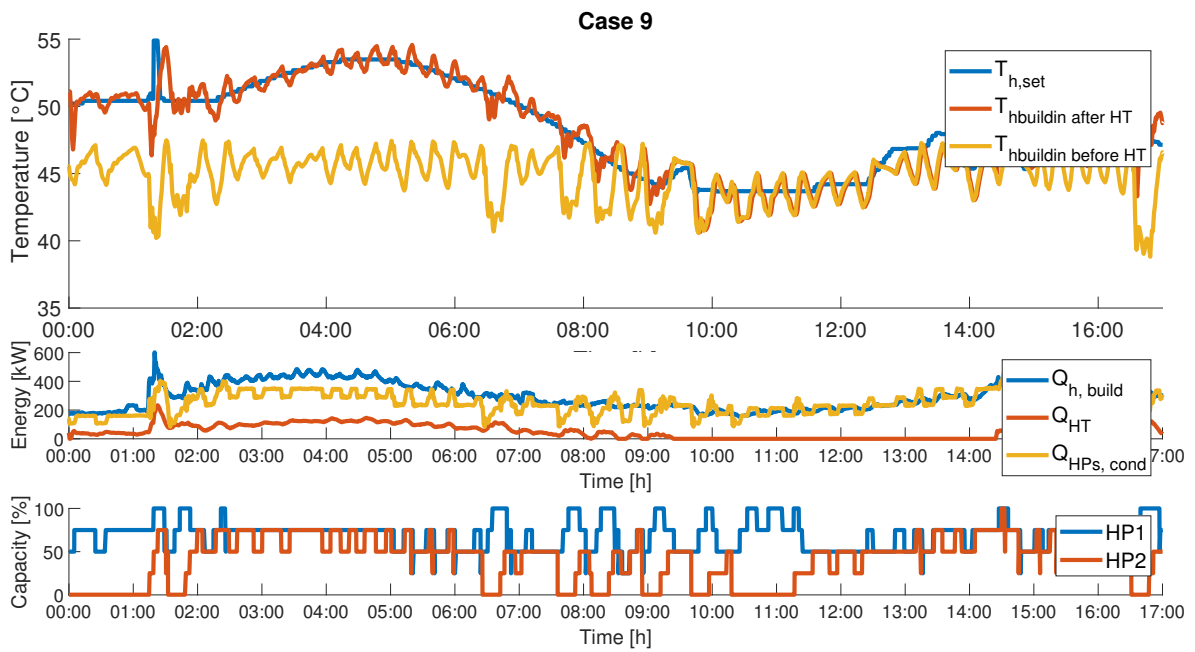


Figure 5-10: Case 9: warm building network modelled with the standard control methods

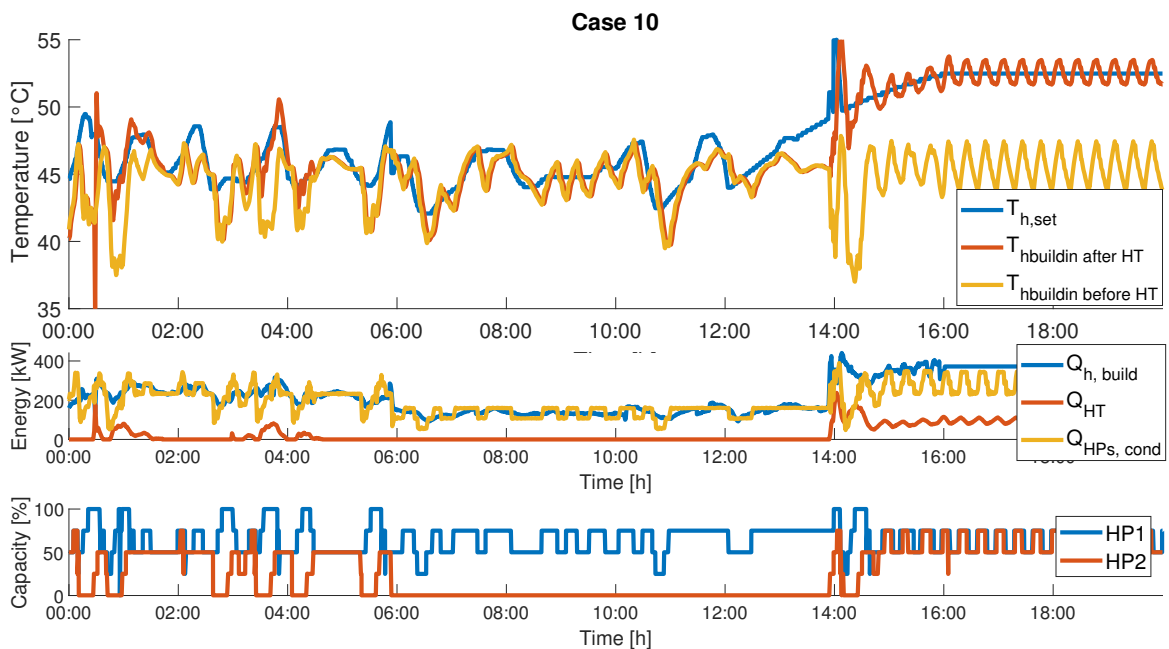
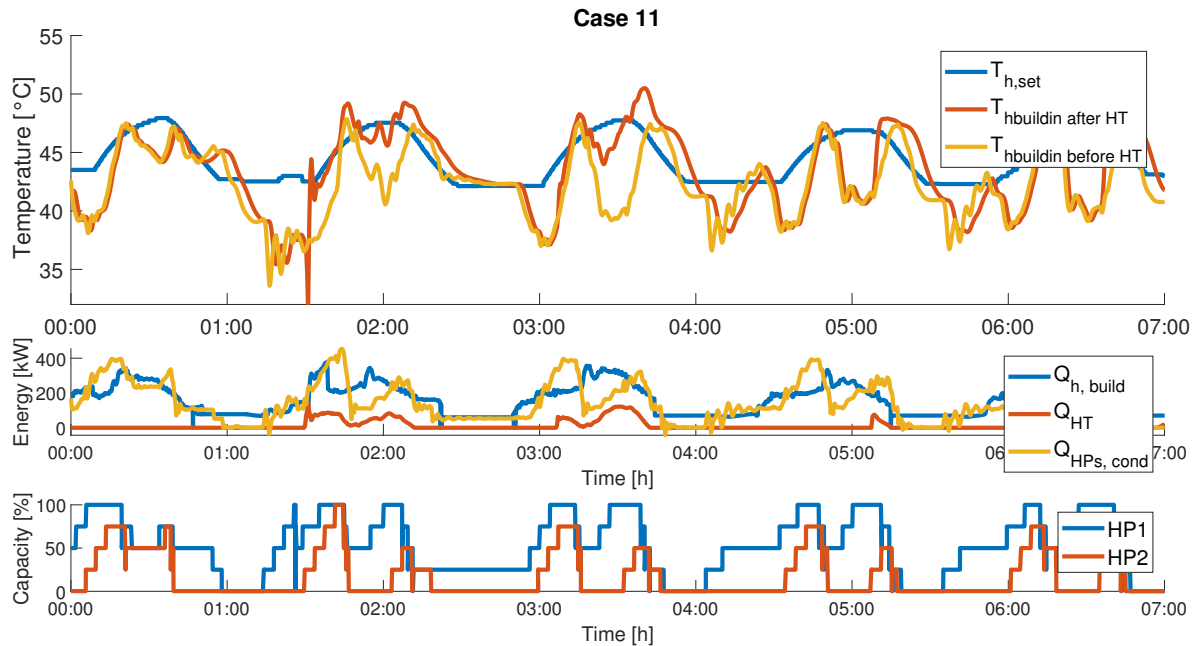


Figure 5-11: Case 10: warm building network modelled with the standard control methods



**Figure 5-12:** Case 11: warm building network modelled with the standard control methods

## 5-2 Low level control and thermodynamic improvements

Several simulations of the previously proposed improvements (Section 3-3) are shown in this section. The change of temperatures for which the loading of additional cold by the Dry Cooler (DC) should be turned on/off is not shown here as this is solely of influence on the outlet temperature of the drycooler and is mainly based on the outside temperature. Furthermore, the peak shaving is not simulated either as strategies for peak shaving on the demand side are not part of this study and most buildings considered, do not have enough space to install large water buffer vessels. Other forms of storage are not considered as this would again require additional equipment to transfer the heat to the substation. To prevent the short-cut network flow by installing pumps on the secondary side of the heat exchanger that can manage these small flows, is also not shown as this effect is rather obvious. Finally, the same reason is applied for not modelling the on/off switching condition of the cold heat exchanger.

### 5-2-1 Matching components with building demand

Selecting a heat pump that can reach the required temperature setpoints, can have a significant effect on the consumed energy by the Conventional Heater or High Temperature source (HT). Two cases have been selected to illustrate this simple improvement. Figure 5-13 shows the increasing temperature setpoint far above the maximum temperature  $48^{\circ}\text{C}$  (setpoint maximum is  $46^{\circ}\text{C}$ ). It can be observed that after about 40 minutes in the simulation, the conventional heater kicks in, furthermore the temperature entering the heat pumps, fluctuate around  $40^{\circ}\text{C}$  as a result of mixing of the building return and the warm buffer, which is

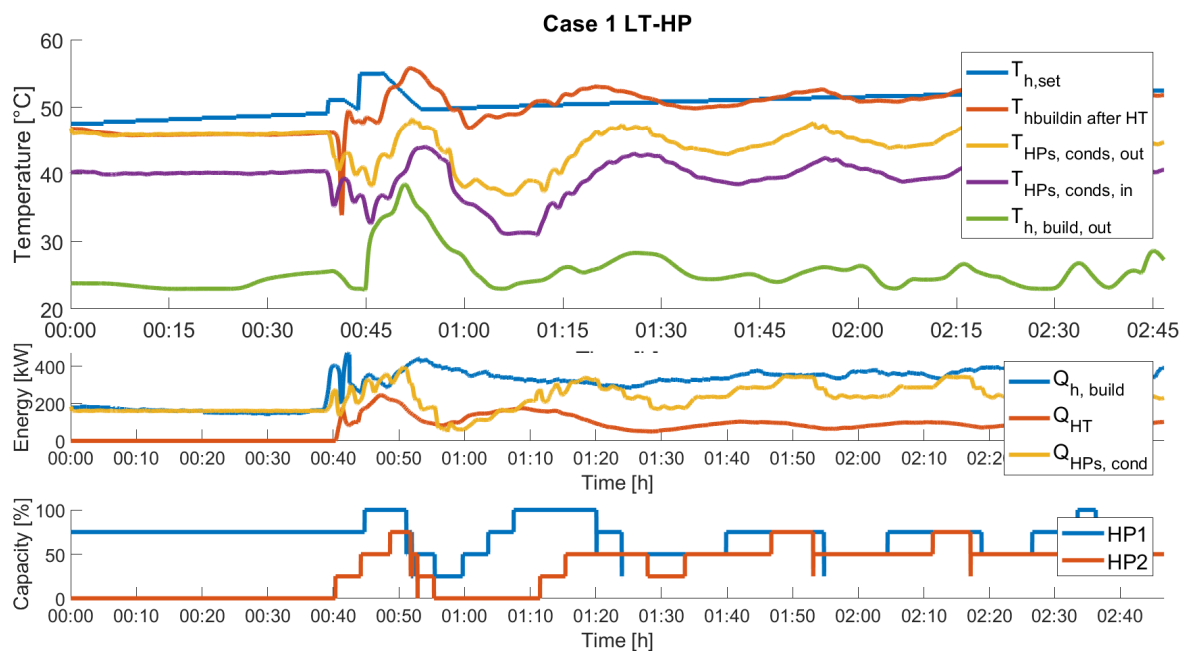


**Figure 5-13:** A simulation of the response of the current heat pumps (LT-HP) to the temperature and energy demand with a significant response of the HT

at the same temperature as the flow leaving the condenser.

The effect of an increased maximum temperature of the heat pump till  $58^{\circ}\text{C}$  (high temperature heat pump (HT-HP)) can be observed in Figure 5-14. The condenser leaving temperature and thus the building entering temperature before the conventional heater, now more closely follows the setpoint temperature and also an increased condenser entering temperature can be observed as the buffer temperature is now higher. The conventional heater still shortly kicks in as a result of a sudden sharp increase in the temperature setpoint and some time is required before the second heat pump can operate at a high capacity. However, the comparing the energy provided by the conventional heater, it quickly reduces once the second heat pump is up and running and reaches the desired capacity. It can also be observed that the capacities at which it is operated are more stable as the condenser inlet temperatures also fluctuate in a slightly smaller range.

The second case is similar in profile, yet some other aspects become better visible. The setpoint increases slowly and as a result of the limited temperature that can be reached with the low-temperature heat pump (LT-HP), the conventional heater kicks in after 20 minutes Figure 5-15. As the HT-HP can still reach these temperatures the conventional heater does not kick in at this moment (Figure 5-16), yet one and half hour later, it does kick in as a result of a rather slow response of heat pumps as the second heat pump had to remain turned down for 15 minutes and the time constraint for the HT starts to count before the second Heat Pump (HP) is on. The energy the conventional heater added in the case of the HT-HP is still small as it quickly turned down once the heat pump reaches the proper capacity. Here similarly to the previous case a reduction in the capacity changes and in the energy of the conventional heater can be observed.

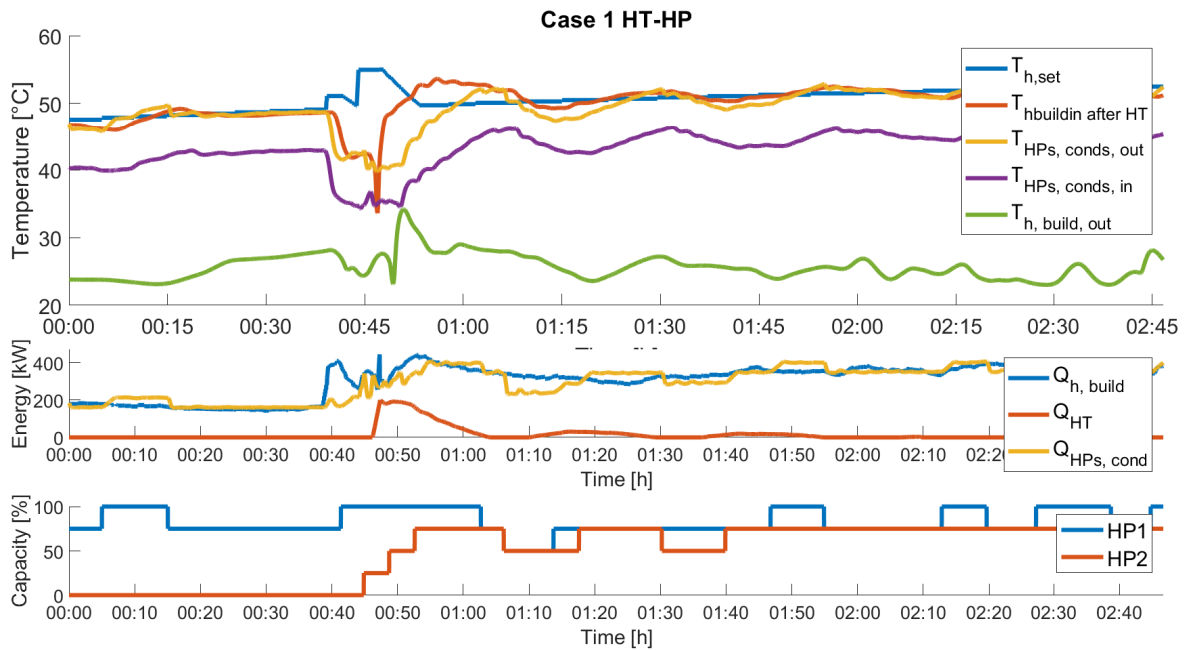


**Figure 5-14:** A simulation of the response of heat pumps that can reach higher temperatures (HT-HP), where there is only a short response of the HT due to the slow HP response.

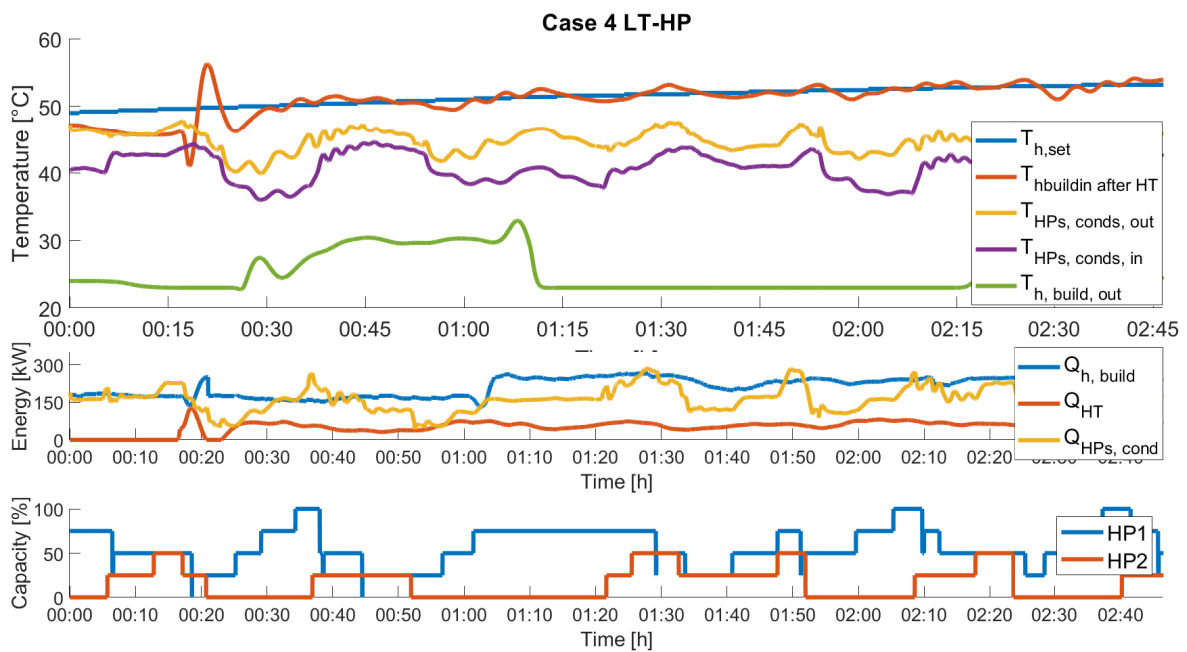


**Figure 5-15:** A simulation of the response of the current heat pumps (LT-HP) to the temperature and energy demand with a significant response of the HT

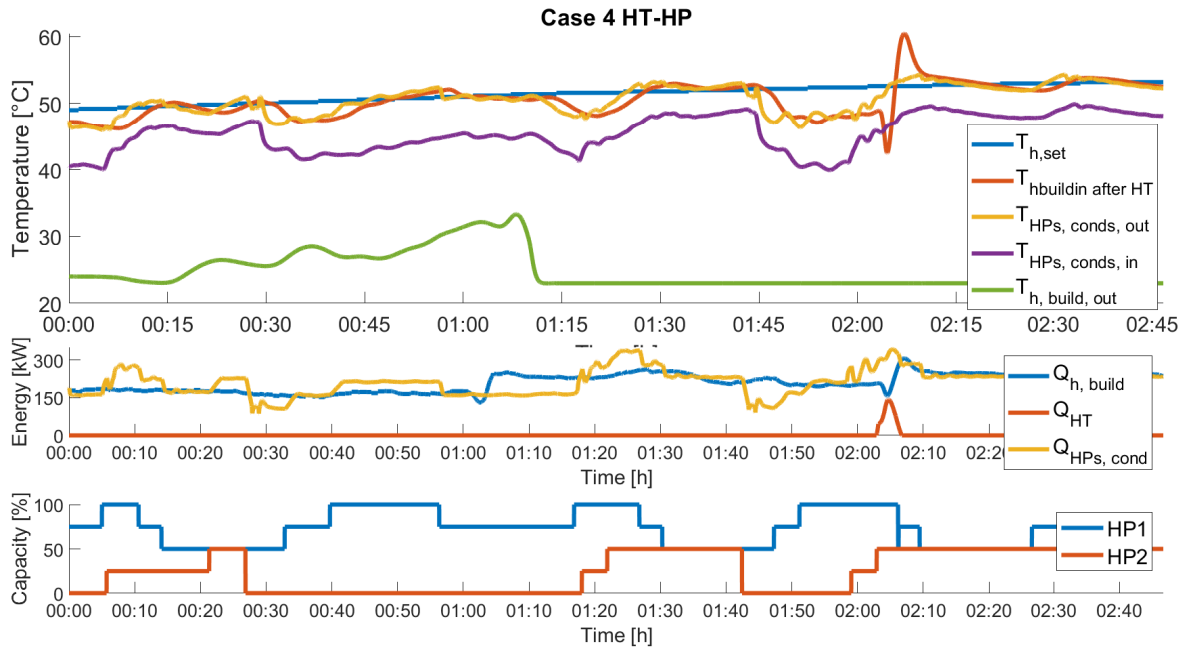


**Figure 5-16:** A simulation of the response of heat pumps that can reach higher temperatures (HT-HP), where there is only a short response of the HT due to the slow HP response.

### 5-2-2 HEX operation

Figure 5-17 shows the effect of the proposed controllers on the temperature leaving the heat exchanger on both the primary grid and secondary substation side to prevent the substation instability. Here it is observed that both controller options show similar temperatures on the primary side compared to the standard case, from which it can be concluded that these controllers do not cause unnecessary high return temperatures to the grid ( $T_{HEX_h, prim, out}$ ). In Figure 5-17 differences on the secondary side between both controllers are clear; the adjusted setpoint causes a higher  $T_{HEX_h, sec, out}$  and a shallower slope, while the additional controller on  $T_{HEX_h, sec, out}$  causes the temperature to stay above 12°C, but the slope remains steep.

Adaptation in the controllers will also affect normal operation when temperature limits are exceeded and when they do not necessarily cause a fluctuating returning problem. This has to be considered in choosing between these measures.

Larger mass flows are observed when temperature limits are exceeded for the controllers compared to the standard case, thereby carrying a larger energy quantity with exceeding temperatures. Mass flow should be minimised as much as reasonably possible, keeping all objectives in mind. Figure 5-17 presents that for both controller design, the primary flow does increase, but still remains at a low value. The flow is lower for  $T_{HEX_h, sec, out}$  controller, however the sharp temperature slopes remain in place, which might be another disadvantage. In all, both controllers have a similar effect on the temperature leaving the evaporator. The heat exchanger secondary output temperatures are used as an input value for the complete substation system. In Figure 5-18 the temperatures leaving the HP as a result of  $T_{HEX_h, sec, out}$  and the different controllers are shown, here it can clearly be observed that that the newly

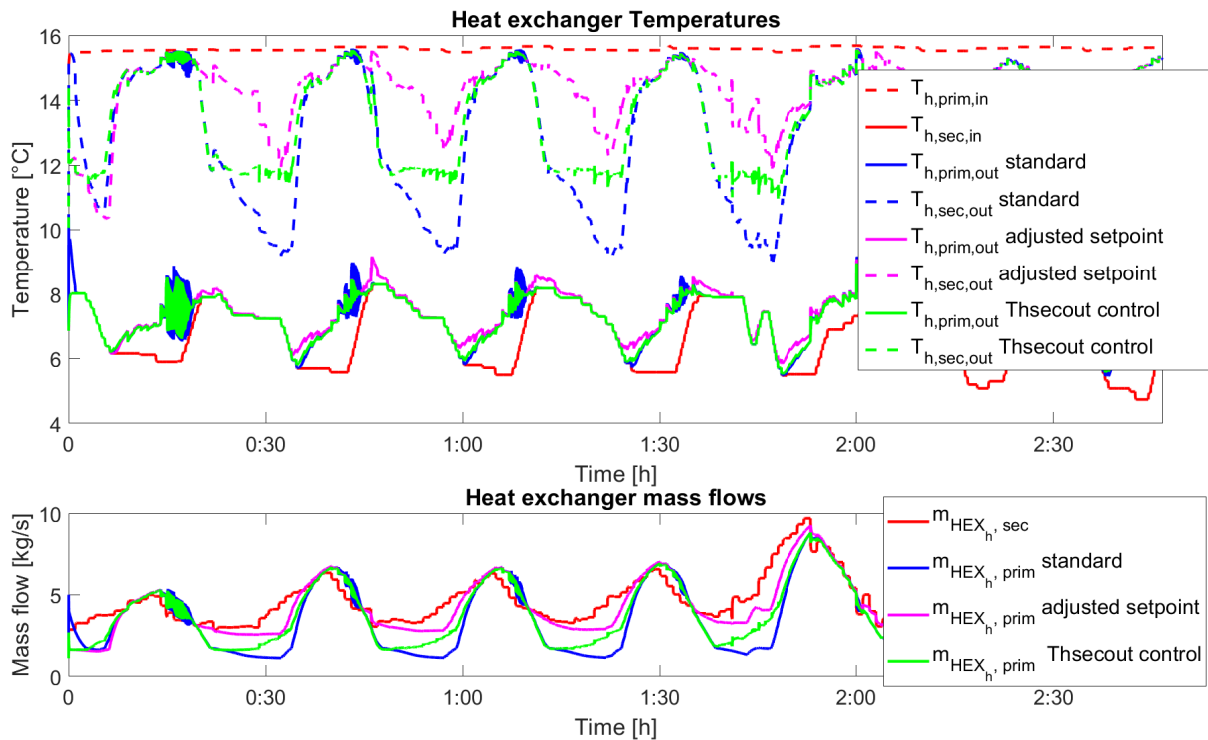


**Figure 5-17:** The effect of the proposed changes on the control of the warm heat exchanger.

designed controllers in most cases enable to reduce  $T_{evaps, out}$ , keeping it closer to  $6.0^{\circ}\text{C}$ , resulting in a smoother heat exchanger operation. The temperature violation just after 2.0 h is a result of a HP shut down.

### 5-2-3 Capacity and temperature control heat pumps

#### Temperature control

Different control methods discussed in Section 3-3-6 to accurately provide a temperature control and also reducing the pump energy are shown in this section.

The response of these different methods on a change in capacity, temperature setpoint or condensers inlet temperature are shown in Figure 5-19. The capacity is changed from the minimum to the maximum capacity with the maximum ramp, while in reality at each or every two capacity steps the, the capacity is kept constant for at least 5.0 min, thus the maximum change is smaller which might reduce the overshoot or the settling time. The ramp on the condenser inlet temperature and the temperature setpoint are larger than largest measured ramps.

The first method is solely the control on the three-way valve while the pump operates at a constant speed and thus requires a constant amount of pumping energy. Furthermore, the temperature entering the condenser after the mixing of the three-way valve will be higher as the opening for the three-way valve will be smaller compared to other methods. Thus the temperature jump over condenser will be smaller which might negatively impact the heat

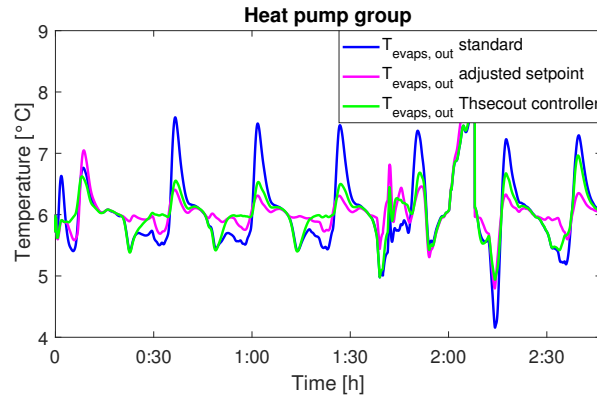


**Figure 5-18:** The effect of the proposed changes on the control of the warm heat exchanger at the heat pump group.

pumps performance and cause a higher energy cost.

The second method of a split range over the three-way valve and pump, first maximizes the three-way valve opening before it increases the pump's speed. Thereby the pump speed is always minimal and thus the pumping energy, yet the flexibility is smaller as the pump's speed ramp is relatively small and shouldn't fluctuate too much. This can be observed in the response, where  $T_{HP1, \text{cond}, \text{out}}$  has the largest over- or undershoots for this type of control and the settling time is also the largest.

The third method is based on a constant  $\Delta T$  over the condenser. The temperature difference can be set at different setpoints, influencing the pumping energy consumption. If  $T_{HPs, \text{conds}, \text{out}} - T_{h, \text{set}} \leq \Delta T$ , the setpoint of the pump controller would be adjusted to  $T_{HPs, \text{conds}, \text{out}} - T_{h, \text{set}}$  to ensure that the maximum outlet temperature of the condenser would not overreach its maximum. If  $\Delta T$  is kept constant and the temperature difference can not be reached, the mass flow over the condenser would be reduced, however even the three-way valve would be fully open, yet  $T_{HP1, \text{cond}, \text{out}}$  would become higher than  $T_{h, \text{set}}$ . In many cases the pumping energy is similar to the pumping energy of the split range control, but some cases it is higher, for instance when it is operated at maximum capacity and the entering temperature is very low.

Finally there is the adjusted pump control, where the pump speed is changed based on the position of the three-way valve. Thereby the position of the three-way valve is almost never maximised and thus the pumping energy is not fully minimised. The response is generally good, not always the best, but not problematic either.

### Capacity control

The capacity and temperature control inserted as discussed before (Section 3-3-6) can be observed with several cases. It should be noted that for these cases the capacity control is based on the temperature setpoint and the temperature entering the building, this could also be replaced by the energy as discussed before (Section 3-3-6), but this is for the discrete capacity steps less suitable as the tuning becomes more difficult.

The different cases show different responses for similar demand behaviour. Case 0 (Figure 5-20), contains slowly changing temperature setpoints and thus is a nice case to start testing the capacity control. It can be observed that the temperature setpoint is followed

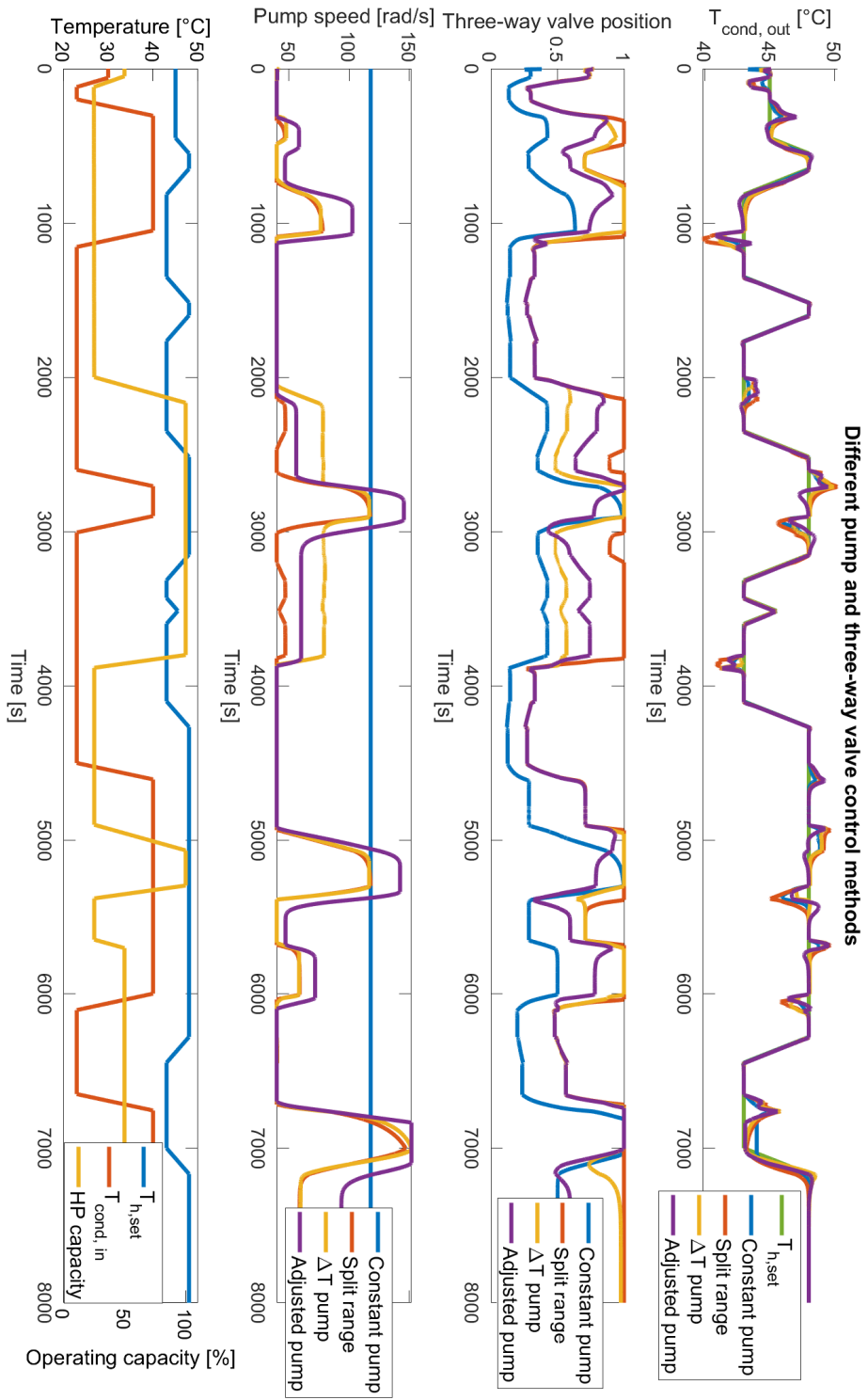


**Figure 5-19:** The response on different changes with different pump and three-way operations to control  $T_{HP1, cond, out}$

closely, however at some moments small spikes can be observed, right before the capacity changes, as the capacity controller acts on these changes. Generally during these spikes the temperature is within  $1.0\text{ }^{\circ}\text{C}$  of the setpoint, thus still meeting the requirements. These spikes are caused by the buffers being completely filled and thus the temperature entering the condensers is increased to a point, where even if the three-way valves are completely open, the setpoint temperature of  $46\text{ }^{\circ}\text{C}$  is exceeded and thus the capacity has to be reduced. Furthermore, it can be observed that when the second heat pump turns on, the temperature is shortly not met by a large percentage as a result of first the flow being start up before the heat pump is started up. Also here it can be observed that the conventional heater kicks in immediately after the second heat pump as the temperature difference and time required before the second HP kick in is already long before met. It should be noted, that due to design of the capacity control, that only the second heat pump will turn on if more than 37.5% of the total maximum heat pump capacity is required and thus also limiting the kick in of the conventional heater as it now can not kick in for lower demands.

Case 1 (Figure 5-21) starts with a fluctuating temperature setpoint and a slightly fluctuating energy demand as a result of some fluctuations in the mass flow. Again some small temperature spikes deviating from the setpoint can be observed before a capacity change occurs. This is also the case when the temperature is operated at a steady  $46\text{ }^{\circ}\text{C}$  while the setpoint is very high. These spikes are slightly larger than  $1.0\text{ }^{\circ}\text{C}$  yet the temperature leaving the condensers remains within their save limitations. This is not the case for one occurrence, right after the HT kicks in, where the temperature spikes till  $50\text{ }^{\circ}\text{C}$  due to a sharp energy demand and a temperature increase after which it decreased quickly again, on which the PI capacity control responded with an overshoot. It is worth noting that during the fluctuating part, the HT does not kick in as the setpoint is closely followed and thus the temperature difference remains below the minimum for which the HT kicks in. Also the reduction in oscillations and maintaining the  $46\text{ }^{\circ}\text{C}$ , reduces the energy provided by the conventional heater from 2.0 GJ to 1.5 GJ, a 25% decrease.

Case 3 (Figure 5-22) contains some temperature setpoint fluctuations, but the energy does not always similarly oscillate with it. Important to note is the sharp increase in temperature around 3:30h, where the setpoint is simultaneously decreasing. This is caused by a completely filled buffer and thus high temperatures entering the condenser as the building mass flow has also significantly reduced from  $2.3\text{ L s}^{-1}$  to  $1.6\text{ L s}^{-1}$  as can be seen in Figure 5-4. The reduction in conventional heater energy is 19%, yet it should be noted that there is a large overshoot of the condenser temperatures around 11:30h, thus the part of the energy that provides the temperatures above  $46\text{ }^{\circ}\text{C}$  should also be considered. Considering this energy as energy that would normally also have been added by the conventional heater, still a reduction of 16% compared to the standard case is shown, thus a significant improvement if this peak can be removed.

Case 5, 9 and 10 show similar responses compared to other cases, the HT energy reduced by 22%, 23% and 23% respectively.

Case 7 similar behaviour with the HT energy reduced by 32% This large reduction is a result of reduced capacity or heat pump shut down while the HT is on, causing even lower building inlet temperatures before the conventional heater.

Case 11 (Figure 5-27) is interesting as here the temperature setpoint fluctuates at a rate of  $0.29\text{ }^{\circ}\text{C min}^{-1}$  while also the building mass flow and thus the heat demand decreases from 280 kW to 80 kW at a rate of  $15\text{ kW min}^{-1}$ . As the buffer is seemingly fully filled up

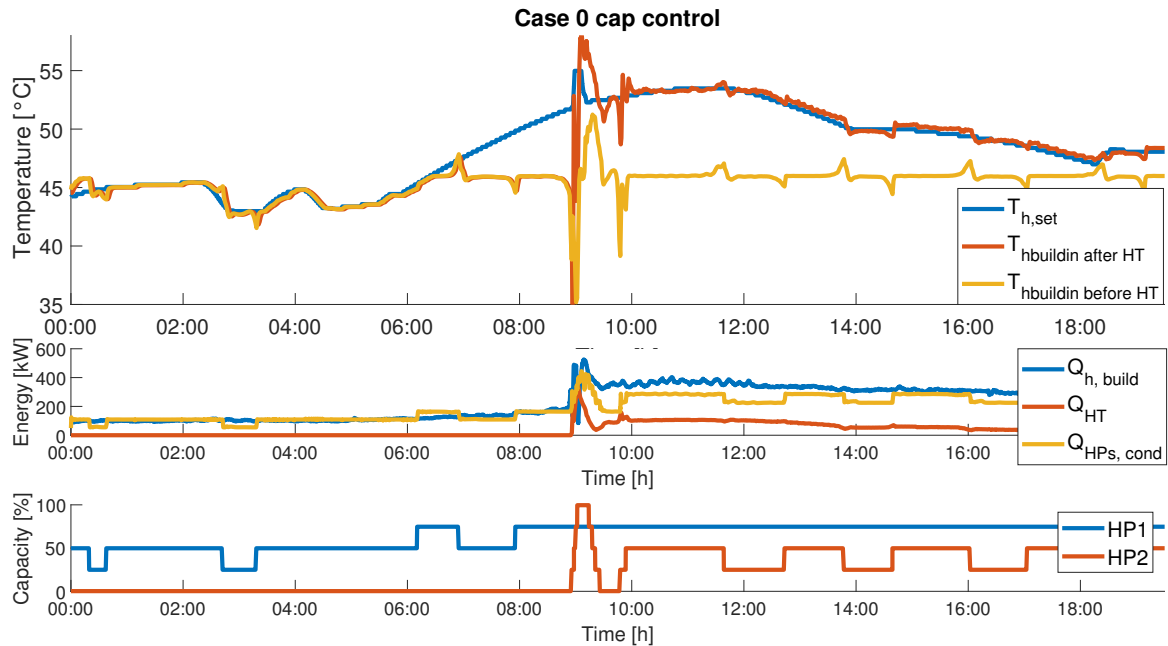


**Figure 5-20:** Case 0: warm building network modelled with the temperature and capacity PI control

just after the setpoint starts to decrease, this also causes a much higher condenser entering temperature due to the simultaneously increased buffer temperature and the reduced flow from the building, thus a higher flow over the buffer. The total heat pump capacity used needs to be reduced from 67.5% to 12.5% or even 0%. The additional security of the heat pump being shut down if temperatures reach above 48 °C is also removed, to determine the effects of the controller itself as a normal control action is preferred over a safety control action which causes a hard shut down and thereby might remove too much capacity and intervenes with normal operation.

### Capacity control including buffer

The capacity control is not always optimal as the buffer might be fully filled or the mass flow through the building might be significantly reduced. Thereby some adjustments to the setpoint are advised in Section 3-3-6. Two options are discussed, a setpoint adjustment based on the mass flow over the condensers or the bottom and top temperatures of the buffer compared to the heat pump setpoint.

The first option shows improvements on how the temperature setpoint is followed. Figure 5-28 has smaller peaks and specifically after the fast temperature setpoint increase between 6:00h and 8:00h, the overshoot of the temperature leaving the condensers is smaller. Also the small peaks during the oscillatory part have reduced in size as well as the peaks during the high temperature setpoints. Figure 5-29 shows the effect of the adjustment based on the mass flow over the condensers for case 11, which previously showed high temperature overshoot. These temperature overshoots would even be as high that they might be harmful for the heat

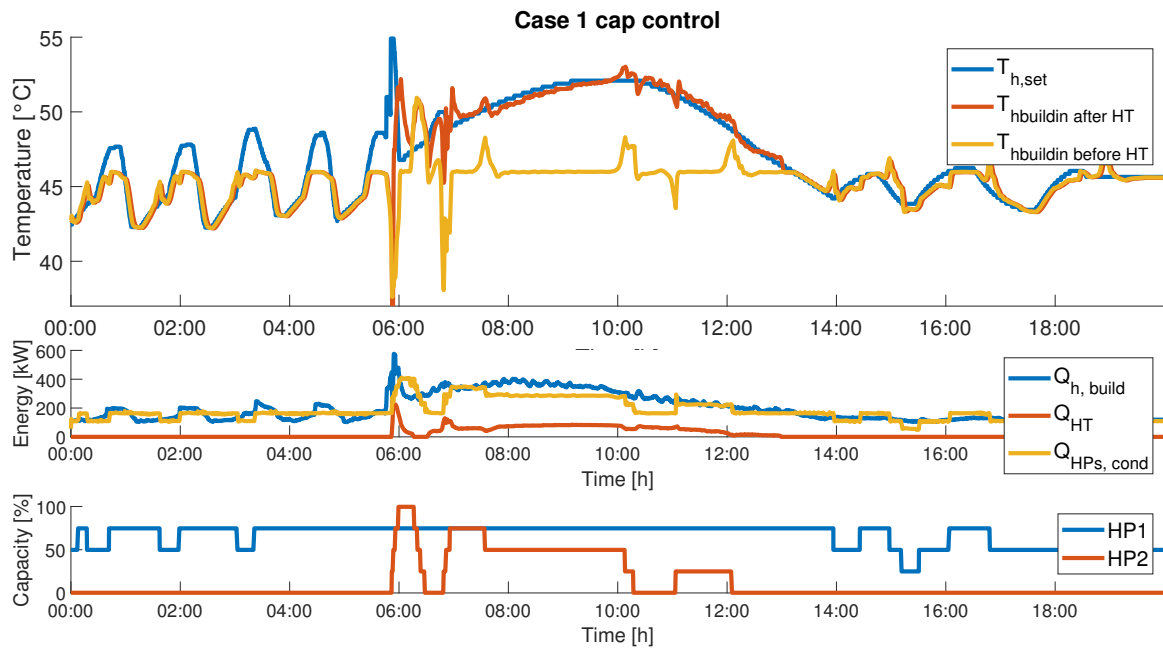


**Figure 5-21:** Case 1: warm building network modelled with the temperature and capacity PI control

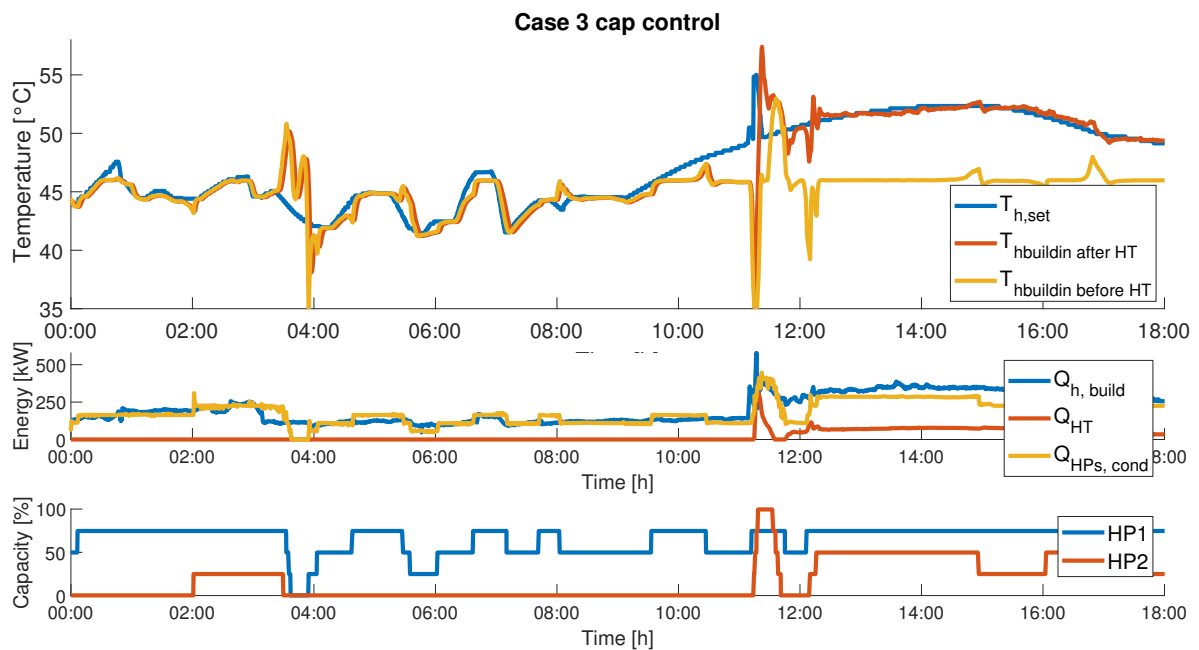


**Figure 5-22:** Case 3: warm building network modelled with the temperature and capacity PI control

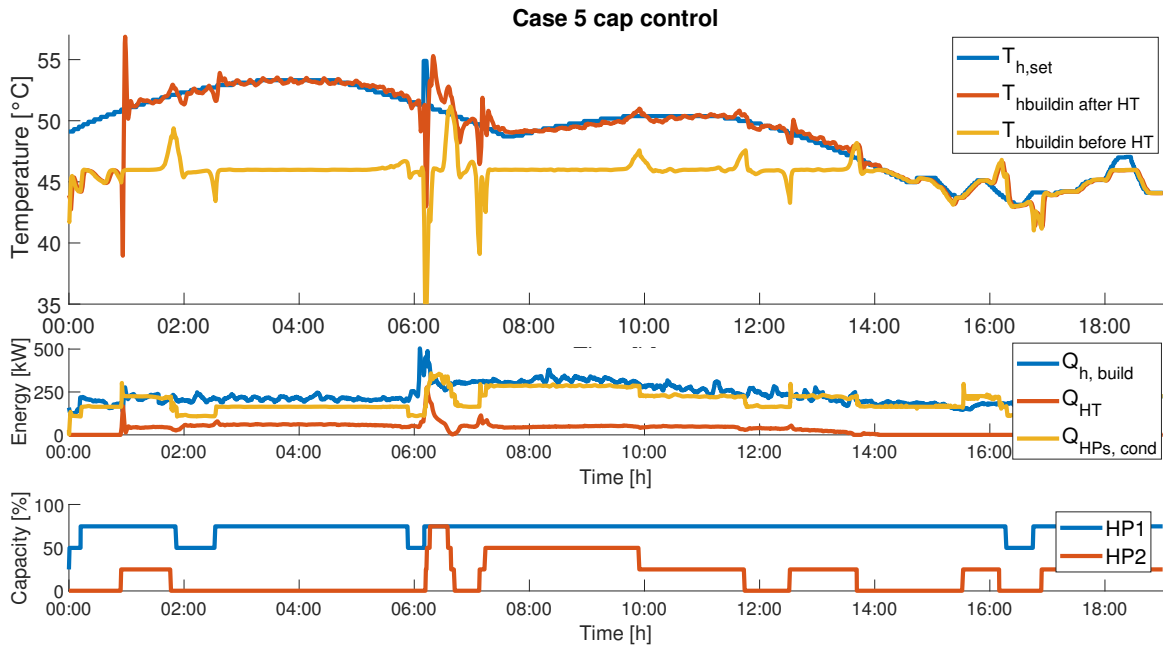


**Figure 5-23:** Case 5: warm building network modelled with the temperature and capacity PI control

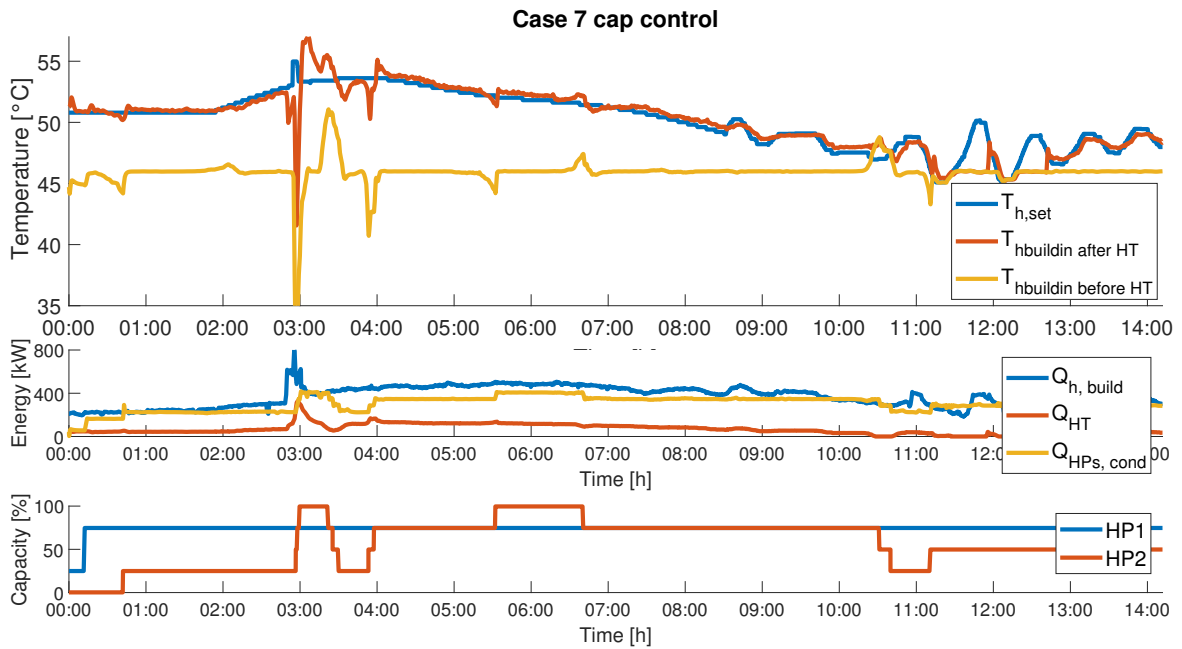


**Figure 5-24:** Case 7: warm building network modelled with the temperature and capacity PI control

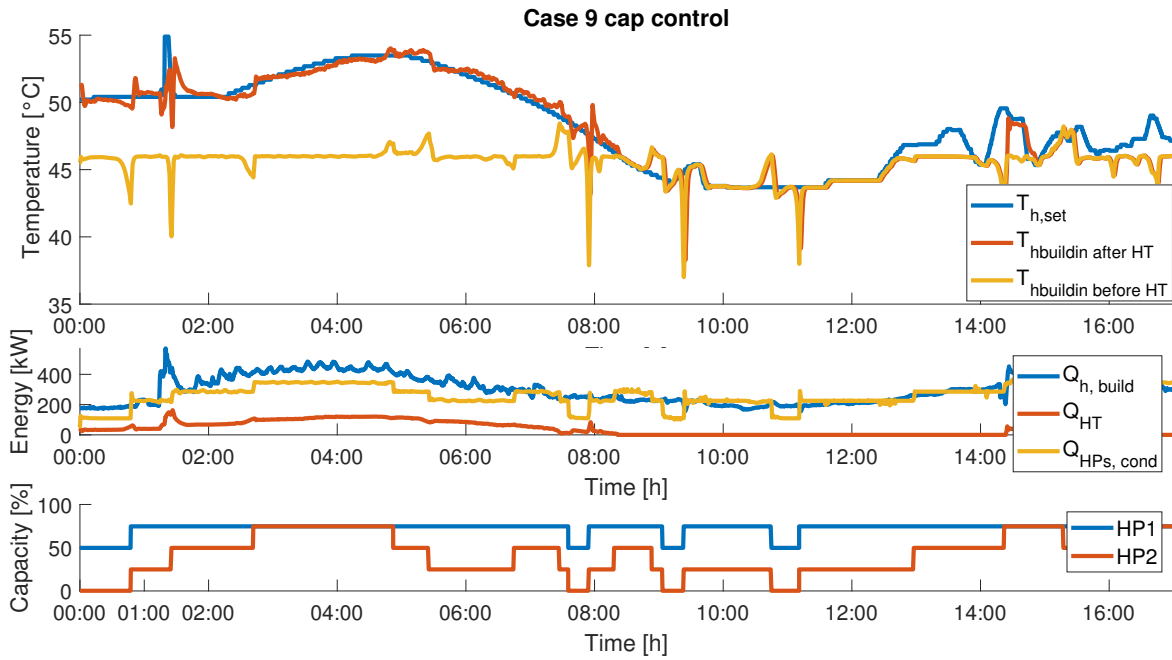


**Figure 5-25:** Case 9: warm building network modelled with the temperature and capacity PI control

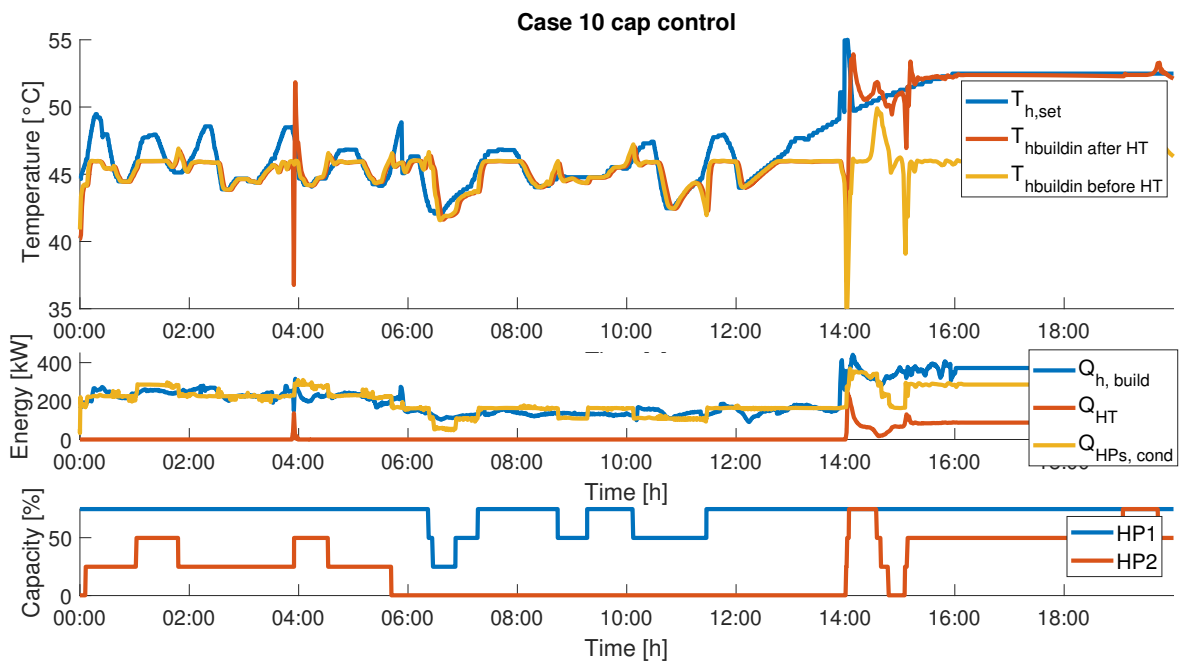


**Figure 5-26:** Case 10: warm building network modelled with the temperature and capacity PI control

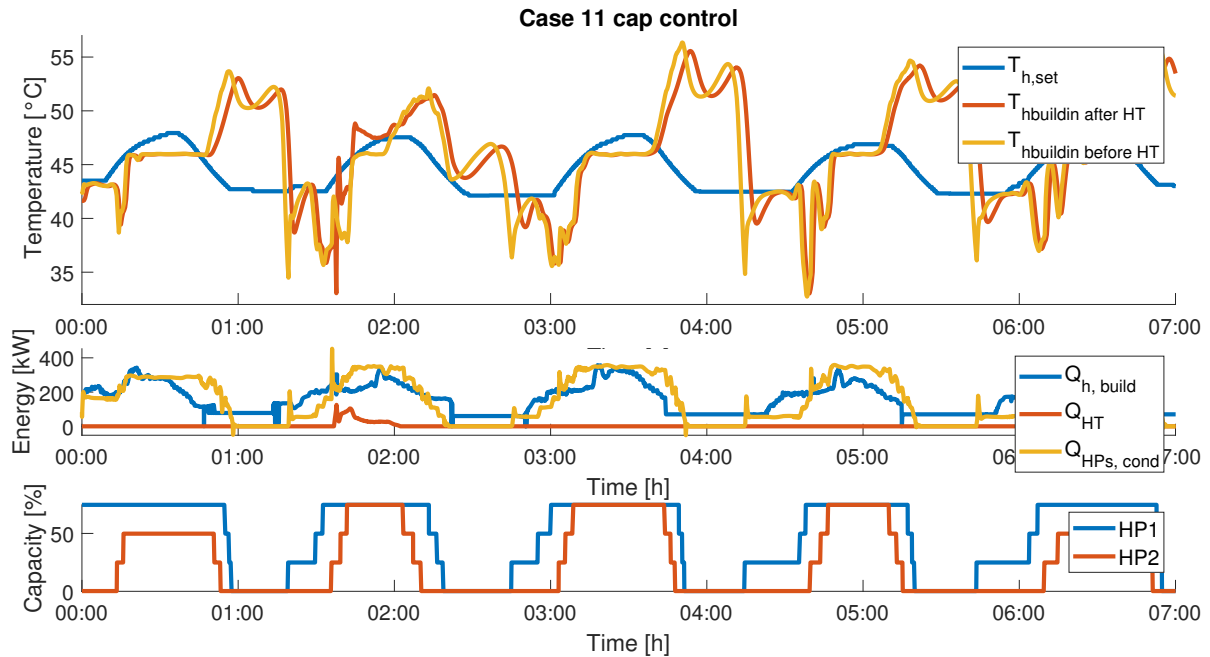


**Figure 5-27:** Case 11: warm building network modelled with the temperature and capacity PI control

pumps. The adjustment of the setpoint shows an improvement regarding the high temperatures, yet there is still overshoot present with respect to the setpoint and some undershoot.

The second option requires proper tuning, but can also significantly reduce the temperature overshoots. The undershoot is something which tends to be difficult to tune compared to the overshoot. Figure 5-30 shows the effect on case 1, where it can be observed that the overshoot in temperature is largely reduced, yet the undershoot is increased as there is also generally an aggressive adjustment made by the temperatures of the buffer. This can be observed as often two capacity steps are taken at those locations. Figure 5-31 shows a similar behaviour where the overshoot is significantly reduced, yet the undershoot is having large effects.

Both options are difficult to tune to have a positive impact for case 11 with its highly fluctuating demand while not negatively impacting the other cases too much. Both options are possible to use for all the other cases, but small gains are required, to prevent undesired and unnecessary switching between capacities. It remains best, to shut the second heat pump down if the temperature entering the condensers before the three-way valve is higher than  $T_{h, set} - 6.0^{\circ}\text{C}$  as this indicates that there is a significant amount of recirculation over the buffer. A value of  $6.0^{\circ}\text{C}$  can safely be chosen as this indicates that when  $T_{h, set}$  is at its lowest value of  $42^{\circ}\text{C}$  and the return temperature from the building remains below  $30^{\circ}\text{C}$ , half of the flow is recirculated over the buffer and therefore only half of the energy is being used by the building. A higher setpoint would result in a higher temperature for the second heat pump before it shuts down, thus indicating a larger amount of the flow recirculating over buffer before it is shut down.

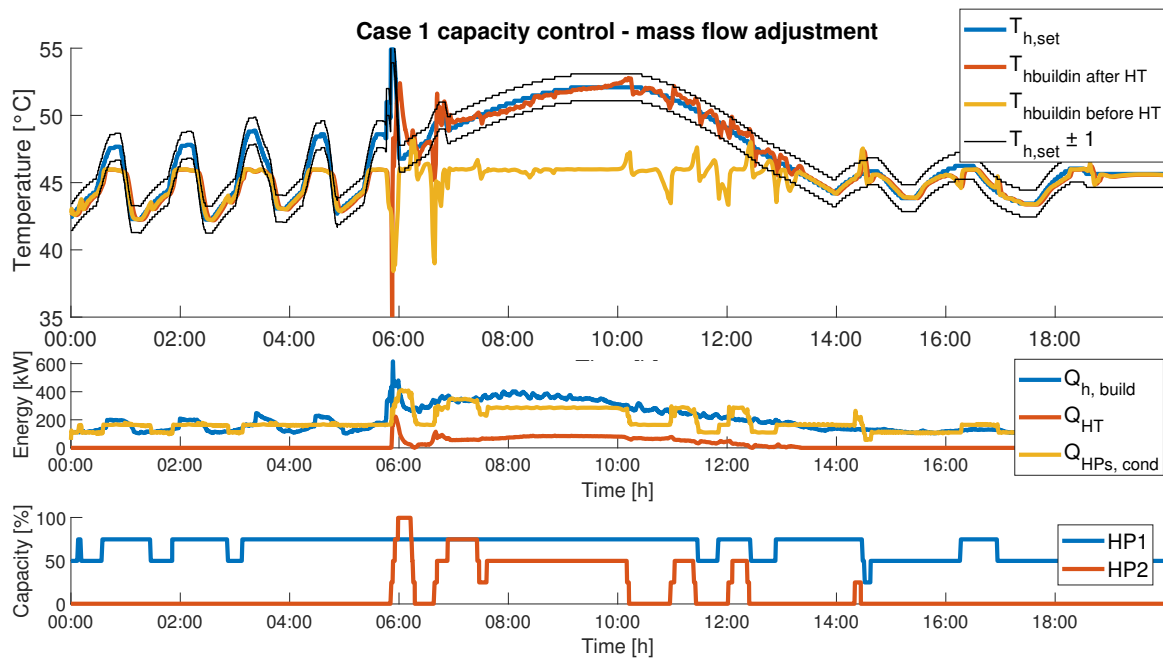


**Figure 5-28:** Case 1: warm building network modelled with the temperature and capacity PI control with setpoint adjustment based on the net condenser mass flow

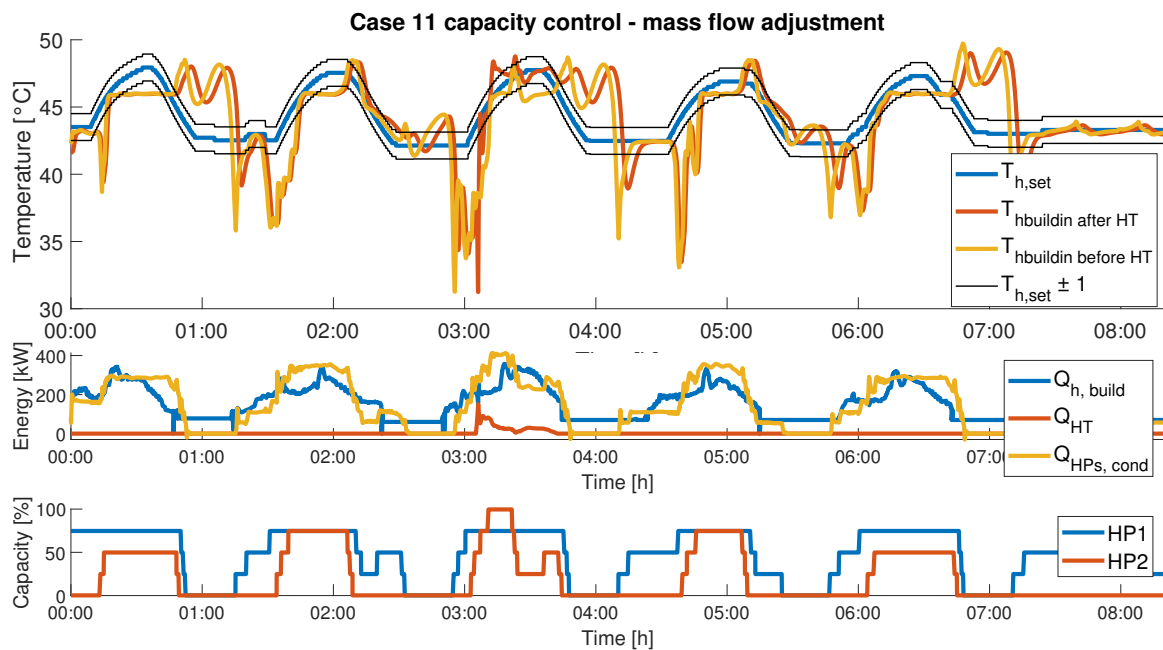


**Figure 5-29:** Case 11: warm building network modelled with the temperature and capacity PI control with setpoint adjustment based on the net condenser mass flow

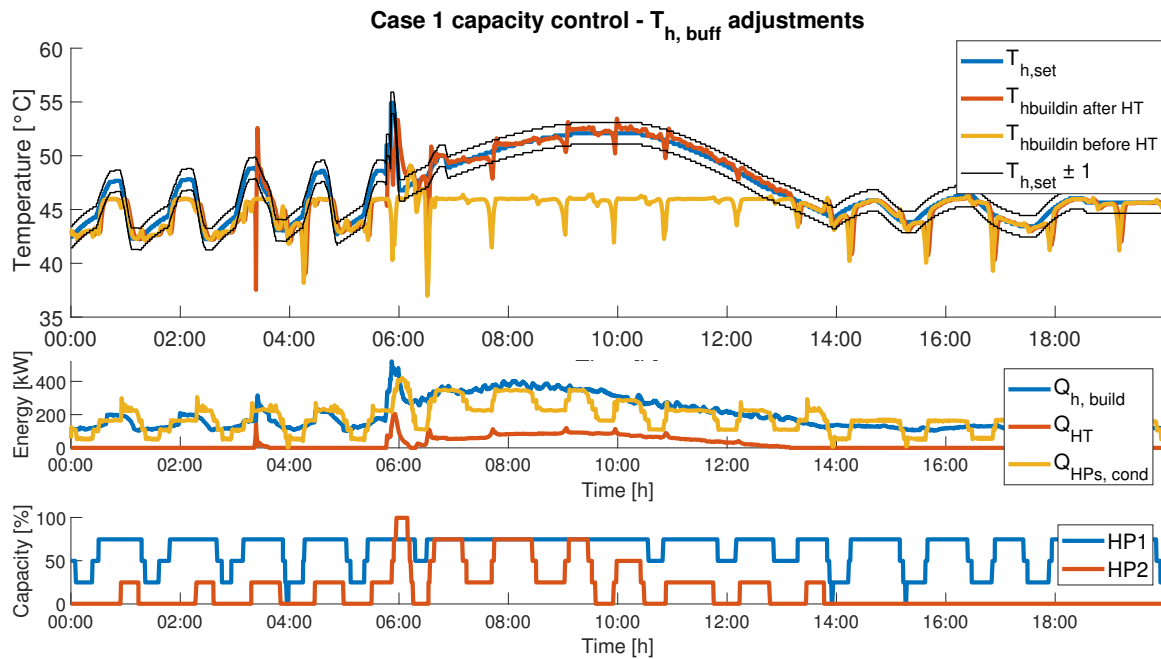


**Figure 5-30:** Case 1: warm building network modelled with the temperature and capacity PI control with setpoint adjustment based on buffer temperatures

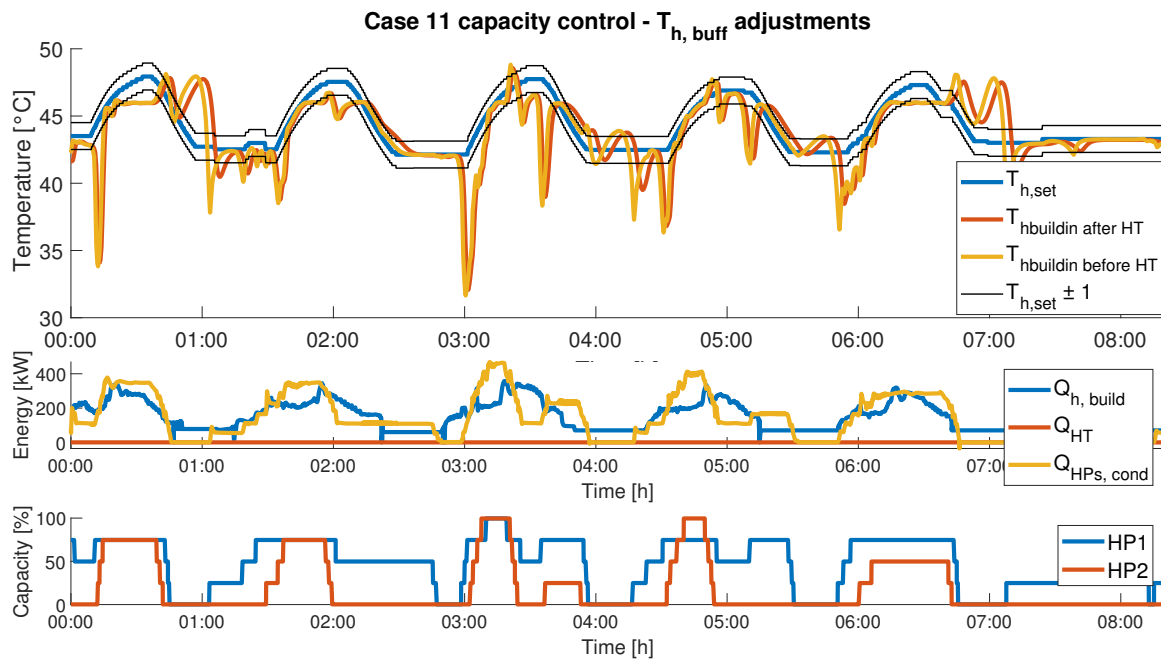


**Figure 5-31:** Case 11: warm building network modelled with the temperature and capacity PI control with setpoint adjustment based on buffer temperatures

MPC strategy variables	$N_h$	$N_p$	$N_t$	$t_{HP, on/off}$	$t_{cap, change}$	$t_{HP, diff on/off}$	$t_{HT, on/off}$
Unit	min	-	-	min	min	min	min
Value	15	15	4	15	15	5	5
MPC strategy variables	$w_{p, HT}$	$w_{p1, HT}$	$w_{HP, cap}$	$w_{HP, on/off}$	$w_{Qh}$	$w_{T, HP}$	$w_{T, HT}$
Unit	-	-	-	-	-	-	-
Value	0.8	0.2	0.02	0.05	10	10	100

**Table 5-1:** The values that determine the MPC strategy

## 5-3 MPC

The theory and design of Model Predictive Control (MPC) controllers are discussed in Section 4-3. For the controllers to be implemented in reality they need to be solved within the timestep considered for the decision variables. During the research it has been chosen to not limit the computational power of the optimisation algorithm and to reach its real optimal solution, however in reality a limit would have been placed. For some cases a comparison has been made to determine how much the solution is effected if a working limit is installed. Furthermore, branching priority and a warm start have been used to speed up the optimisation, this is particularly of importance if a worklimit is used.

An overview of the values chosen to determine the MPC strategy are shown in Table 5-1. The control horizon is set at 15 min as this is also the minimum on/off time for a HP and thus the MPC can determine whether it is indeed practical to turn it on or off. Furthermore, the timesteps of the model are 15s thus a move blocking strategy of four steps is chosen as this allows to determine capacity or on/off changes every minute while keeping the number of binary variables to a minimum. Besides the weighing values, also the minimum time of the HT can be of influence for its performance. It currently is set at 5.0 min as any shorter would not make any sense because of start up and shut down procedures, but it could be lengthened to 10 min as one could argue that if the HT is only on for 5.0 min it might just as well have stayed off.

Currently there are many binary variables that have to be decided on as a result of the discrete capacity steps of the heat pumps. If a continuously capacity controlled heat pump is used, the binary variables for the capacity control could be substituted by a continuous variable, which would increase the optimisation speed as it is also just a linear relation and less binary combinations are possible.

### 5-3-1 Constant flow

All the cases with their current set-up, where the flow over the heat pumps is constant, have been simulated with an MPC controller. Three of these cases are shown here as they provide an interesting view on the performance of MPC controllers.

The first case is Case 0, where there is a fairly constant heat demand at the start after which, the temperature setpoint quickly increases till highly above the maximum temperature the heat pump can reach (Figure 5-32). At the start the capacity regularly fluctuates, but for the most part the temperature entering the building remains within the 1.0 °C band of the setpoint temperature. The temperature leaving the condensers remains below 47.5 °C at

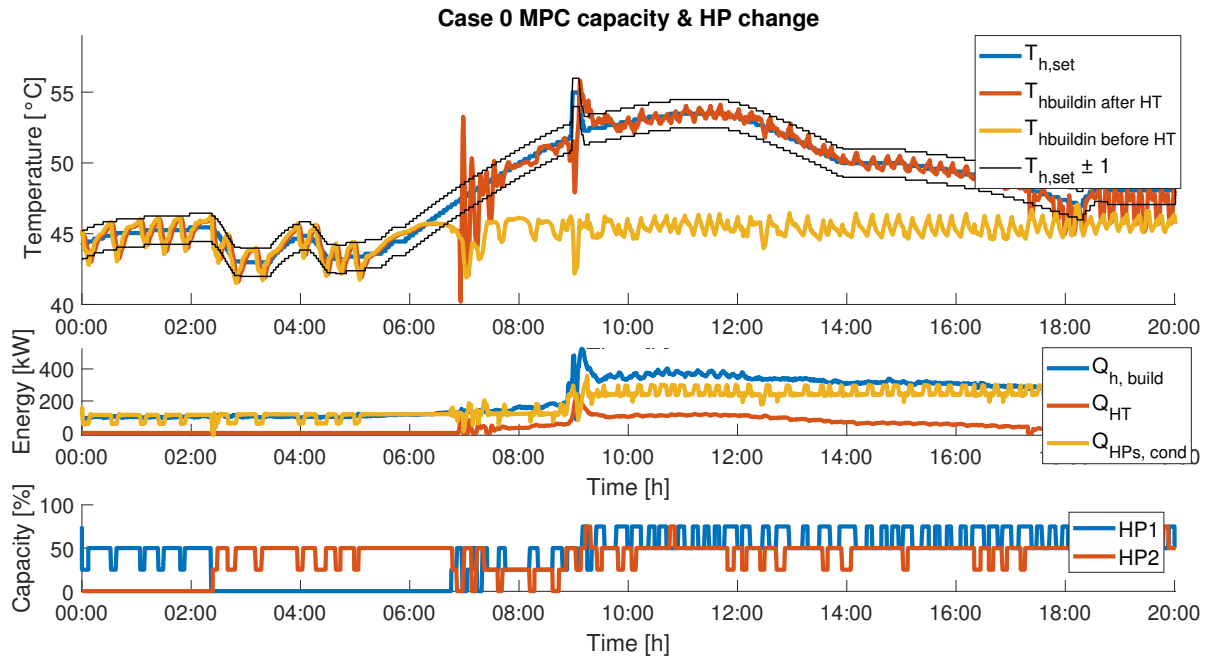


**Figure 5-32:** Case 0 using the MPC controller with a fixed mass flow over the condensers according to the strategy described in Table 5-1

all times. Furthermore, the temperature entering the building before the HT is generally also within a band of  $44.7^{\circ}\text{C}$  to  $46.6^{\circ}\text{C}$  when the temperature setpoint is above the HP maximum. This has the result that the capacity tends to fluctuate, as the condenser leaving temperatures have to remain below  $48^{\circ}\text{C}$  and the amount of energy by the HT is minimised in the cost function.

It should be noted that around 7:00h, the HT is started, but the temperature fluctuates largely. As discussed before, since this is the first time the HT is turned on, the temperature in the pipes of the model is still at  $20^{\circ}\text{C}$  and thus causing the large temperature fluctuation. Furthermore, there are a few occasions where the HT is turned down, resulting in the temperature setpoint not being reached as can be observed around 12:00h, as well as after 18:00h. For these occasions, the cost of keeping the HT on must have been higher, than turning it off, causing  $T_{h, set}$  not to be reached. If the model is more accurate, smaller timesteps of 1.0 s instead of 15 s, this potentially would not have occurred as then the diffusion would have been less and the gradients thus sharper. Another possibility to prevent this from potentially happening would be to increase the time to be on/off and reduce the maximum gradient of the energy provided by the HT. This last option is particularly interesting as currently, this gradient is based on the maximum gradient output that the PI controller of the HT could provide, however, this would in reality not occur as it would also require a very large temperature difference for a longer moment.

Case 1 (Figure 5-33) starts off with a fluctuating capacity and temperature setpoint. Once again, the first time the HT is turned on in this simulation, the temperature spikes both up and down as discussed before, this causes the MPC to have more problems to determine the

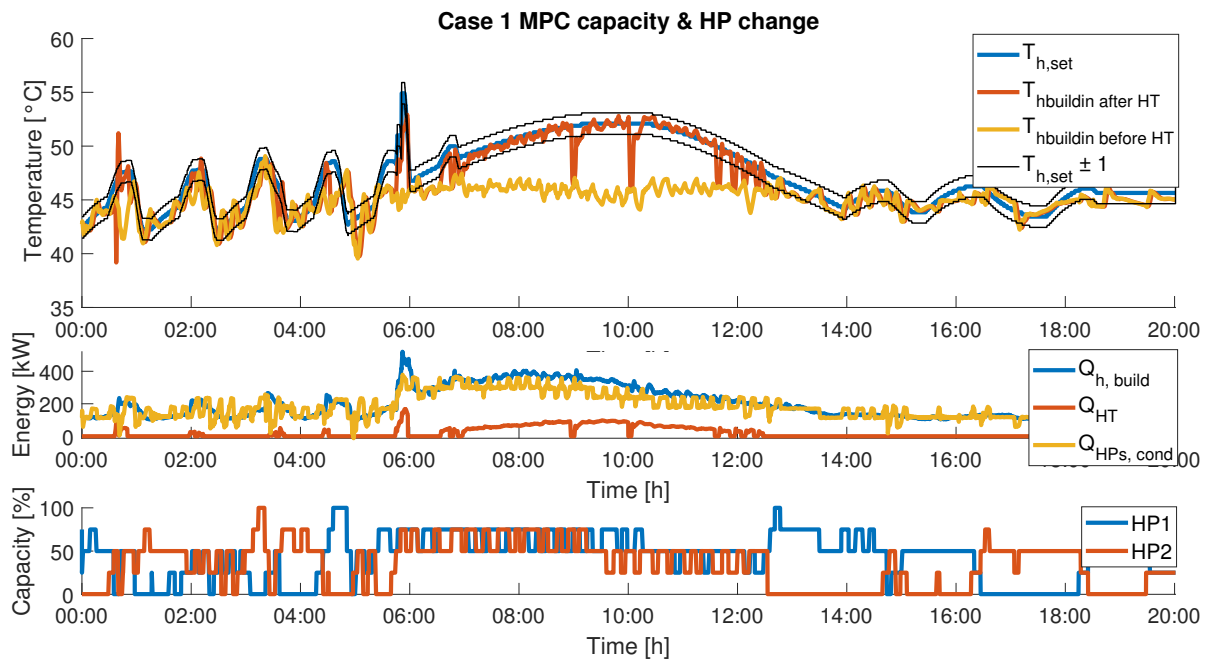


**Figure 5-33:** Case 1 using the MPC controller with a fixed mass flow over the condensers according to the strategy described in Table 5-1

optimal control strategy. It can therefore also be observed that in the first oscillation, the temperature before the HT is significantly reduced as a result of a HP capacity reduction. The other oscillation, show a better performance in tracking the temperature setpoint also before the HT kicks in. The last oscillation, shows that before the HT, the temperature remains around  $45^{\circ}\text{C}$  to prevent too high condenser outlet temperatures, but also a larger undershoot is observed. The temperature entering the building before the HT fluctuates between  $45.0^{\circ}\text{C}$  to  $46.7^{\circ}\text{C}$  mostly. Only after the HT shuts down there are some hiccups in the temperatures. Once again in this situation the on/off switching of the HT is observed when the temperature setpoint and heat demand are decreasing till below  $50^{\circ}\text{C}$ .

Case 11 shown in Figure 5-34, depicts a different heat demand and setpoint trajectory. The repetitive oscillation occurs every one and a half hour. The MPC controller tracks the setpoint properly. At the start it deviates due to the initialisation and later it generally remains within the  $1.0^{\circ}\text{C}$  bound of the setpoint temperature and only slightly exceeds it in the regions where there is a very low demand.

### 5-3-2 Variable flow

The MPC with variable flow has a significant amount of additional binary and continuous variables as discussed in Section 4-3-4. Thereby the time to solve the optimisation algorithm increases considerably for the moments where not most of the binary variables are time constrained.

The simulations have been provided with different number of McCormick variable par-

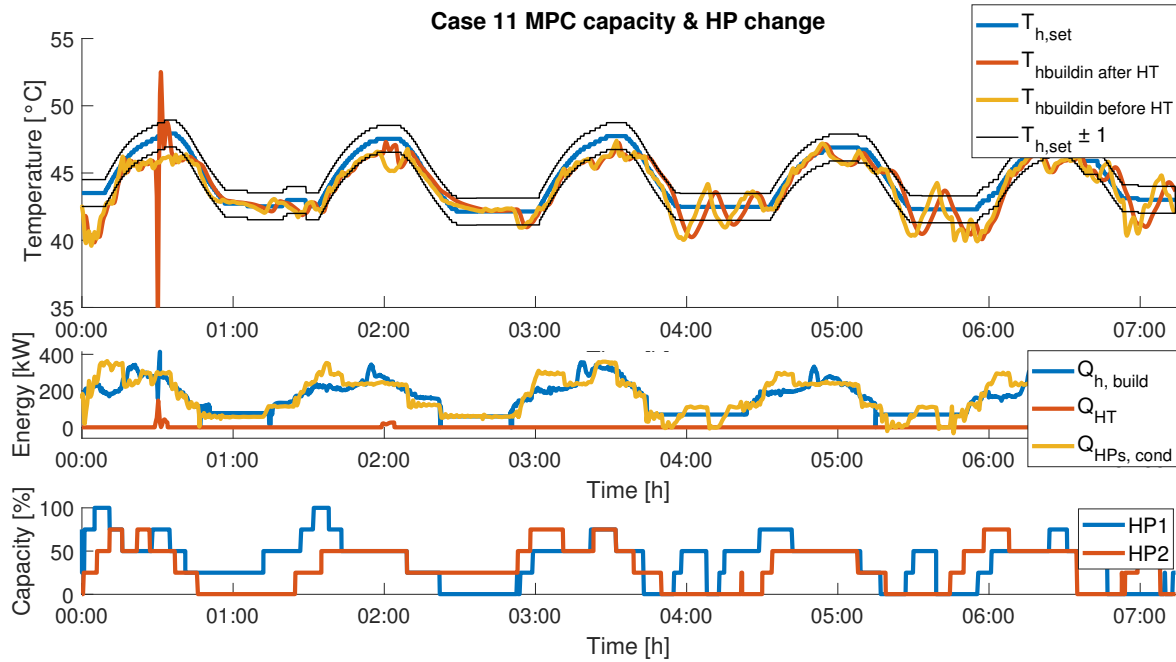


**Figure 5-34:** Case 11 using the MPC controller with a fixed mass flow over the condensers according to the strategy described in Table 5-1

titions. Figure 5-35 and Figure 5-36 show the simulation of case 1 and 11 with a variable mass flow over the condensers. The penalty on the capacity change and HP switching is kept and furthermore, the McCormick relaxations only have a partition of one, thus the mass flow variables are not split up, leaving a large range for the mass flow. This can result in larger over- and under- estimations of the bilinear variable.

In case 1, the effect of the over- and underestimations can be observed by the fact that the conventional heater starts up and shuts down frequently. These over- and under estimations cause a larger freedom in the energy provided by the heat pumps. Therefore, it is wise to increase the minimum on/off time of the conventional heater to 10 min as then it is more likely that the MPC controller will predict that the shutting down of the conventional heater at these high temperature setpoints causes more harm than good. Besides the the on/off switching of the conventional heater, the temperature before the HT follows the setpoint within the  $1.0^{\circ}\text{C}$  band and a maximum of  $46^{\circ}\text{C}$ .

In case 11, it can be observed that the temperature is not always strictly followed. This is a result of the over- or underestimation where the temperatures entering and leaving the condensers might correspond with different mass flows and thus also different temperatures that would occur in the buffer. Around 4:00h the undershoot is caused by the start up of a HP continuously being pushed back by one time step or failing to get an objective within  $8.0 \cdot 10^3\text{s}$  (objective= Inf).

The number of McCormick variable partitions would have to be increased to reduce the under- or over estimation, however, this results in more binary variables and thus a higher computational burden. Therefore a balance between the computational burden and

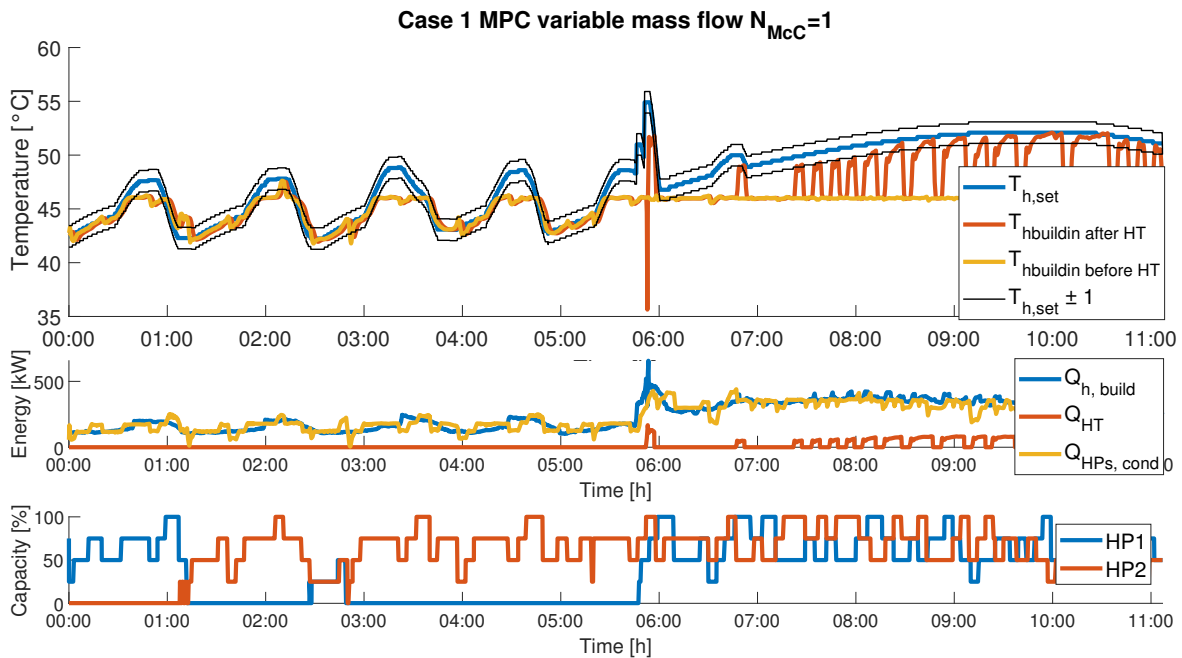


**Figure 5-35:** Case 1 using the MPC controller with a variable mass flow over the condensers. ( $N_{McC}=1$ )

the accuracy has to be considered. The total time to simulate and optimise this case required about 1.5 times the time simulated. While most optimisations (90%) remain within the time limit of a time step, the ones that exceed this optimisation time, exceed it significantly. The average computation time for the optimisations within the timelimit is about 15 s, while for the ones exceeding it is 1000 s.

In Figure 5-37 the same simulation has been performed but with a maximum computation time of 60 s. The under- and overshoots of the system are significant, the temperature control is less accurate. Yet there is no occasion where the temperature undershoots for more than 10 °C as there it found a solution every optimisation, and has not enough computational possibilities to postpone the HP start.

The number of McCormick variable partitions has been increased to three, to determine the effect of a more accurate model. This resulted in much longer optimisation times and my computer crashed or restarted during multiple simulations. Therefore, for some of these simulations only a part of the results is shown.

Case 1 is shown in Figure 5-38 where it can be observed that the simulation has stopped just before 7:00h. The fluctuating part behaves properly and the HT is shortly turned on around the peaks of 2:00h, 4:30h and 6:00h, which results in a closer tracking of the setpoint temperature while the energy of the HT is still minimal. As the optimisation times are high, much larger than the timestep, a simulation is run with a limit on the optimisation time of 60 s to observe the difference in response. In Figure 5-39 the response with a limit on the optimisation is shown. It can be observed that in general the performance is good, the temperature setpoint is tracked properly. However, with the sudden rise of the temperature

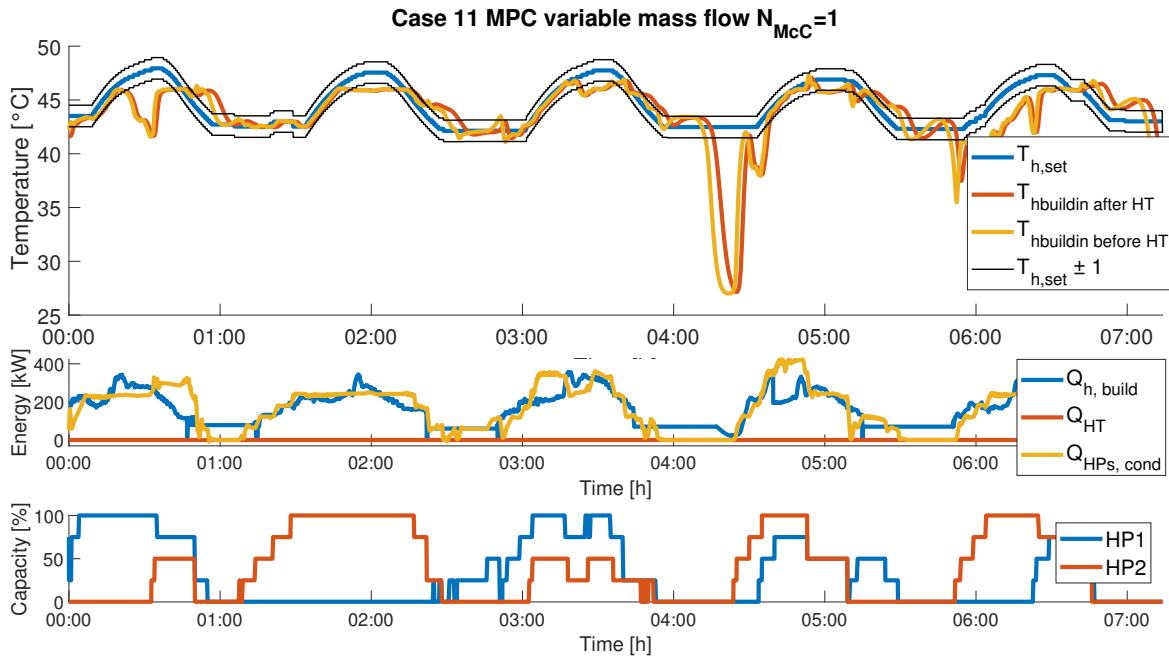


**Figure 5-36:** Case 11 using the MPC controller with a variable mass flow over the condensers. ( $N_{McC}=1$ )

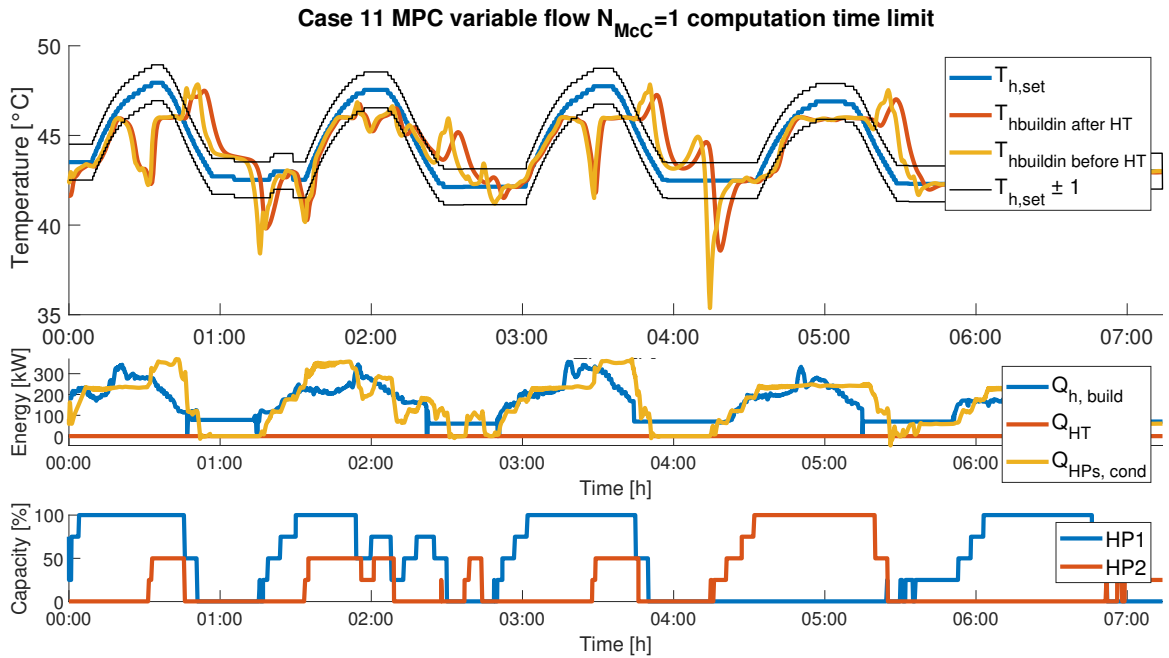


**Figure 5-37:** Case 11 using the MPC controller with a variable mass flow over the condensers and a maximum computation time of 60°C. ( $N_{McC}=1$ )

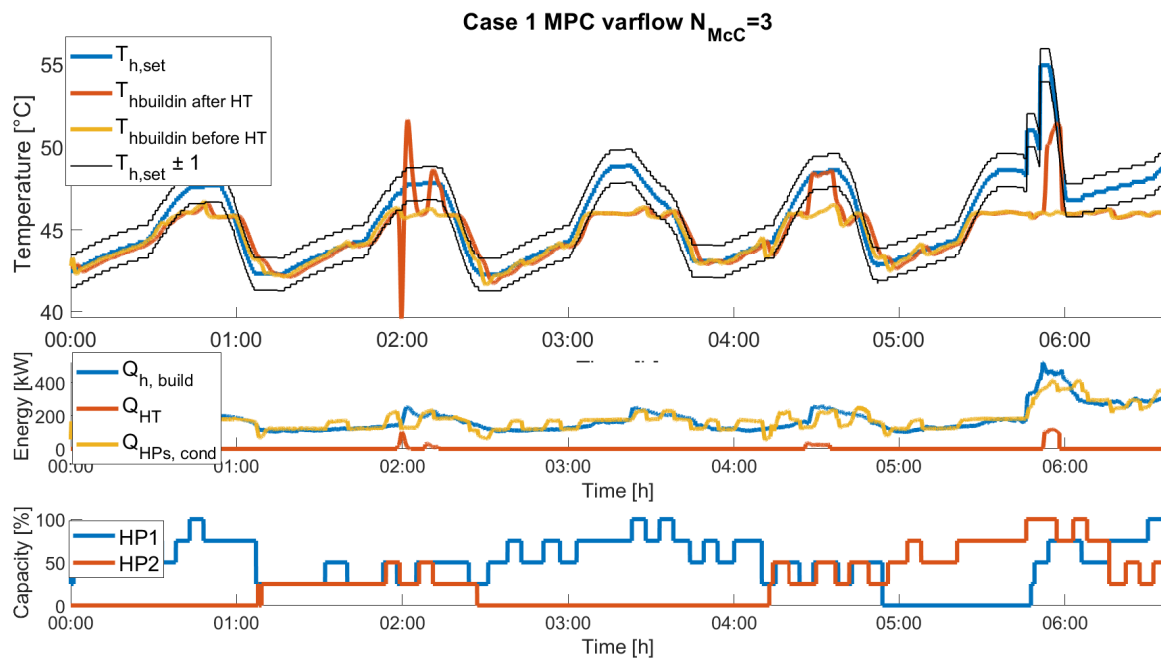


**Figure 5-38:** Case 1 using the MPC controller with a variable mass flow over the condensers. ( $N_{McC}=3$ )

setpoint and mass flow at 6:00h, there is a drop in the building inlet temperature before the HT.

The increased number of McCormick partitions has also been tested on case 11, Figure 5-40. The temperature tracking remains good till just after 4:00h, where again, the system pushes back the start of the HP every timestep. Once again, if a time limit is set on the computation time, the result is worse for case 11 (Figure 5-41). It can be observed that it more frequently contains large undershoots, however, it does not significantly overshoot.

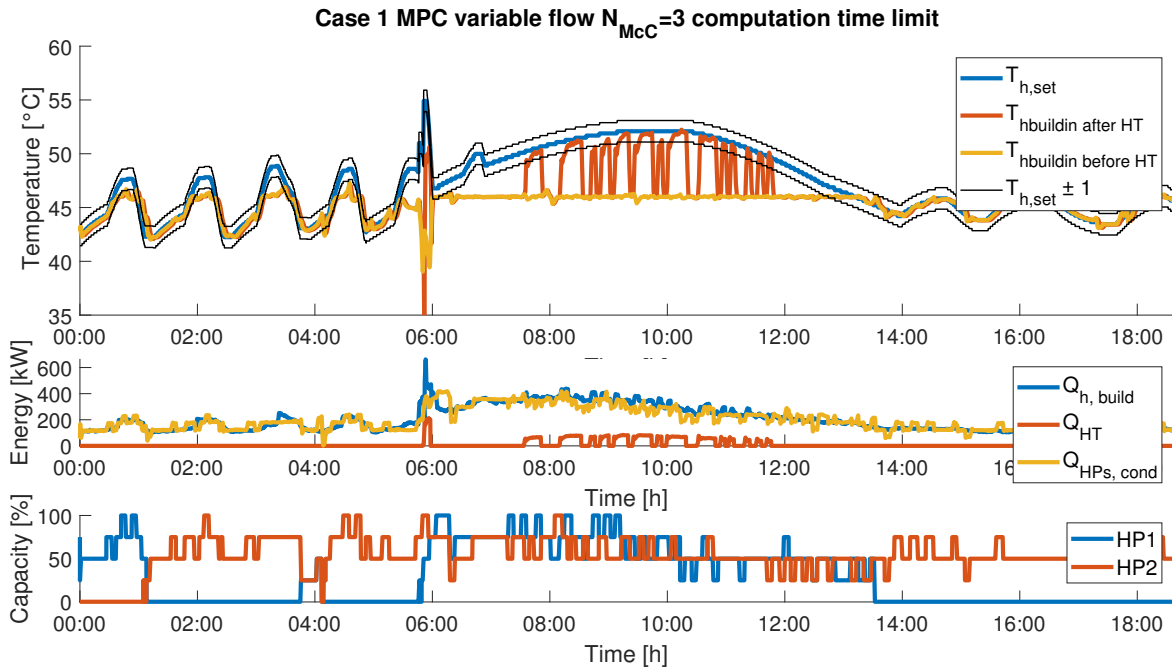


**Figure 5-39:** Case 1 using the MPC controller with a variable mass flow over the condensers and a maximum computation time of 60 °C. ( $N_{McC}=3$ )

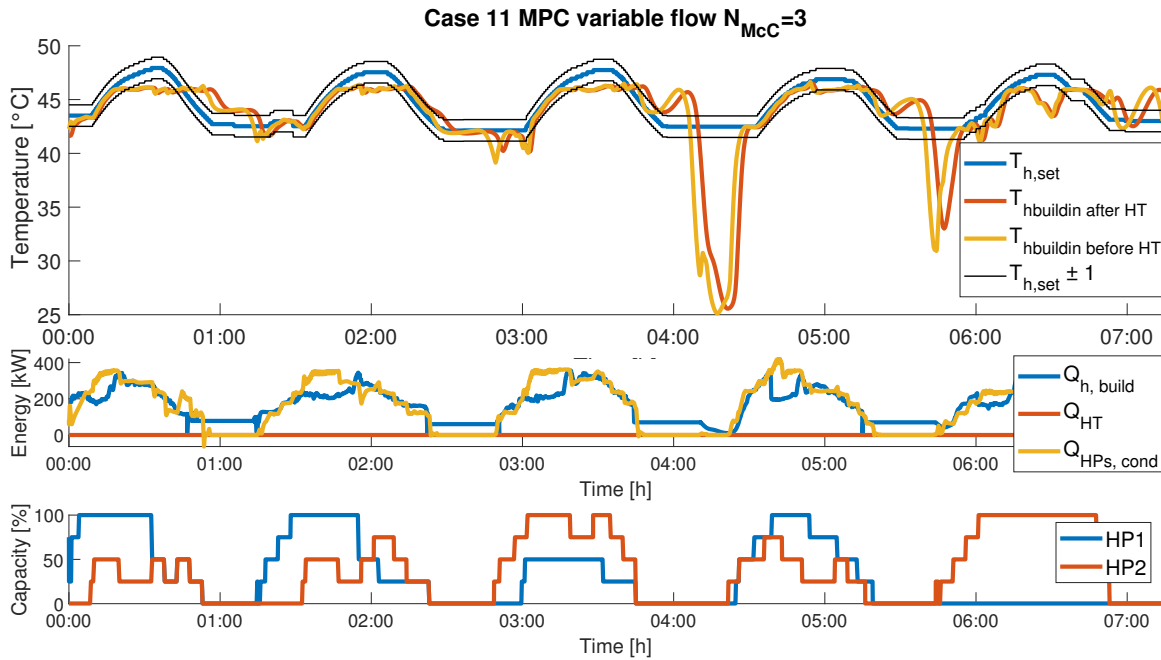


**Figure 5-40:** Case 11 using the MPC controller with a variable mass flow over the condensers. ( $N_{McC}=3$ )

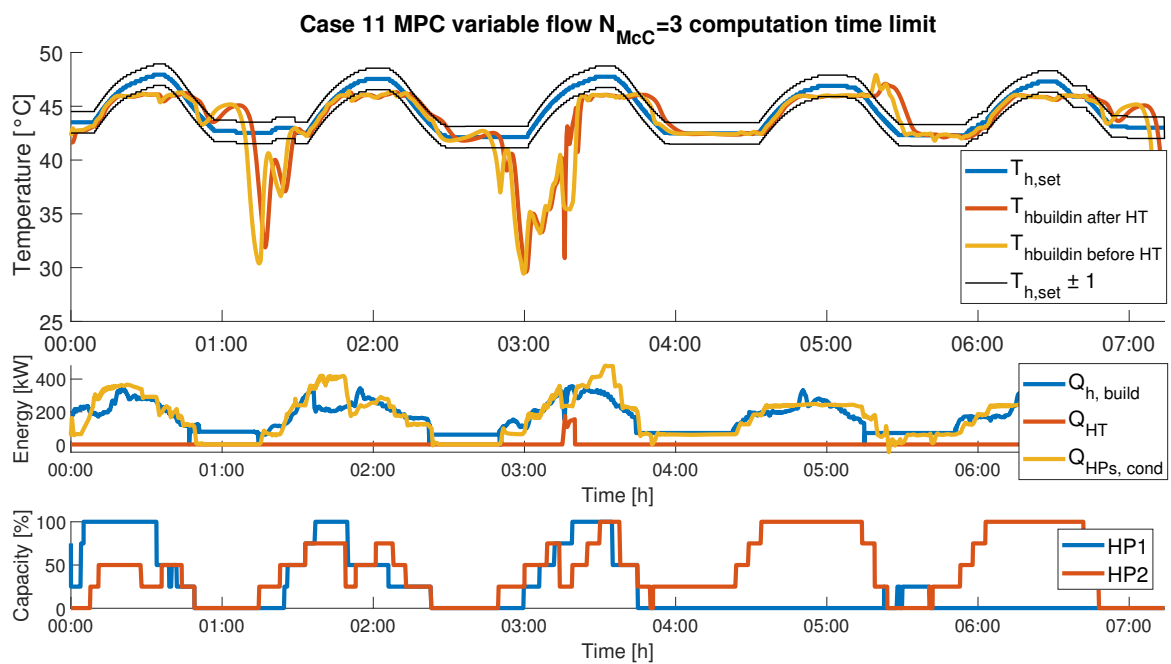


**Figure 5-41:** Case 11 using the MPC controller with a variable mass flow over the condensers and a maximum computation time of 60 °C. ( $N_{McC}=3$ )



---

# Chapter 6

---

## Discussion

This chapter discusses the various results obtained from the modelling exercises of WANDA, and various control methods of PI(D) and MPC. First the validity of the WANDA model is discussed, followed by an in depth analysis of the PI(D) control methodology with an qualitative analysis of the system performance compared to the case study. Then the MPC control methodology is compared to the base case, concluded with an comparison between PI(D) and MPC control.

### 6-1 Model

In general the WANDA model behaves similarly to the real system, but with some sharper gradients. However, small differences in starting conditions or sensor inaccuracies can result in a different response. This also shows another challenge with the simulations, as the demand is based on the measurements and in reality sometimes the temperatures are overshooted, or not reached for a longer period, this can result in a different dynamic of the return temperature and thus influencing the complete operation. One starting condition that is particularly relevant and could not be changed, is that the initial temperature of the water in sections that are turned off is set to the ambient temperature. This should be remembered and considered when analysing the cases and control methods. Furthermore, the energy extracted by the heat pump in reality will not be completely constant and will also depend on the temperature setpoint and condenser inlet temperature. This is the result of different operating condensing pressures and temperatures as well as the temperature jump over the heat exchanger of the condenser.

### 6-2 Comparison control strategies

The goal of the controllers is to minimize the energy consumption of the conventional heater and thus maximising the heat pump capacities while maintaining building comfort (Chapter 2). As the building comfort itself is not directly defined and measured due to the many different rooms, it is based on the whether the temperature setpoint of the warm building

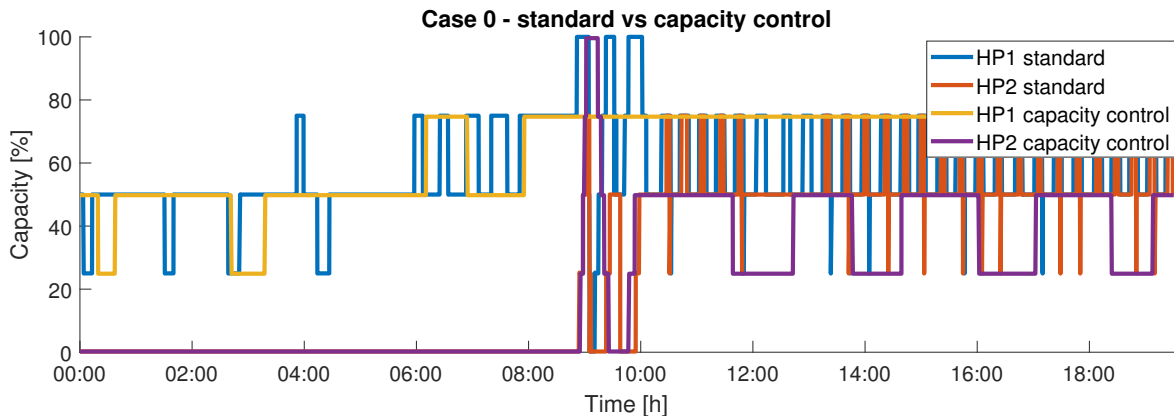


**Figure 6-1:** Case 0: Comparison of capacity changes for the current control methods and the capacity control method proposed

distribution network is being reached. It is defined that the goal is to maintain the building inlet temperature within a  $1.0^{\circ}\text{C}$  band of the setpoint, however the conventional heater would only be required to kick in if the difference between both is more than  $2.0^{\circ}\text{C}$  for more than 15 min.

### 6-2-1 Temperature & capacity control

For all cases, the temperature and capacity controller shows a reduction in capacity changes compared to the standard case. Besides a more stable operation this has the advantage of less component wear and strain, specifically at the compressors of the heat pumps.

Case 0 with a capacity and temperature control (Figure 5-20) compared to the standard (Figure 5-1) shows that the temperature setpoint is followed more closely and especially the heat pump capacity fluctuations are reduced significantly (Figure 6-1). Furthermore, the energy provided by the conventional heater is especially smaller for half an hour after it starts up, the total energy consumed during this case is reduced from 2.9 GJ by 8.7%.

The previously shown small peaks before capacity changes can be explained based on Figure 6-2. It can be observed that the temperature entering the building rises after the temperature entering the condensers rises. Which is again a result of a temperature rise at the bottom of the warm buffer. Also the opposite can be explained by this, which is a result of the temperature in the buffer decreasing due to flow in the opposite direction, eventually causing the buffer top temperature to decrease which finally causes the building inlet temperature to decrease. Possible ways to anticipate on these peaks are to change the setpoint of the capacity controller based on the temperatures of the buffer, the temperature entering the heat pumps or the net mass flow through the heat pump.

Case 1 with a temperature and capacity control (Figure 5-21) shows similar improvements compared to the currently applied control methods. In general it is able to track the setpoint with a maximum setpoint of  $46^{\circ}\text{C}$ . As the temperature difference between the setpoint and the building entering temperature remains small, the HT does not kick in during the fluctuations, reducing the energy produced by conventional heat sources.

Similarly to case 0, the capacity control for case 1 causes some spikes in the temperature. These do not exceed the limits where it becomes harmful for the heat pumps and as long as

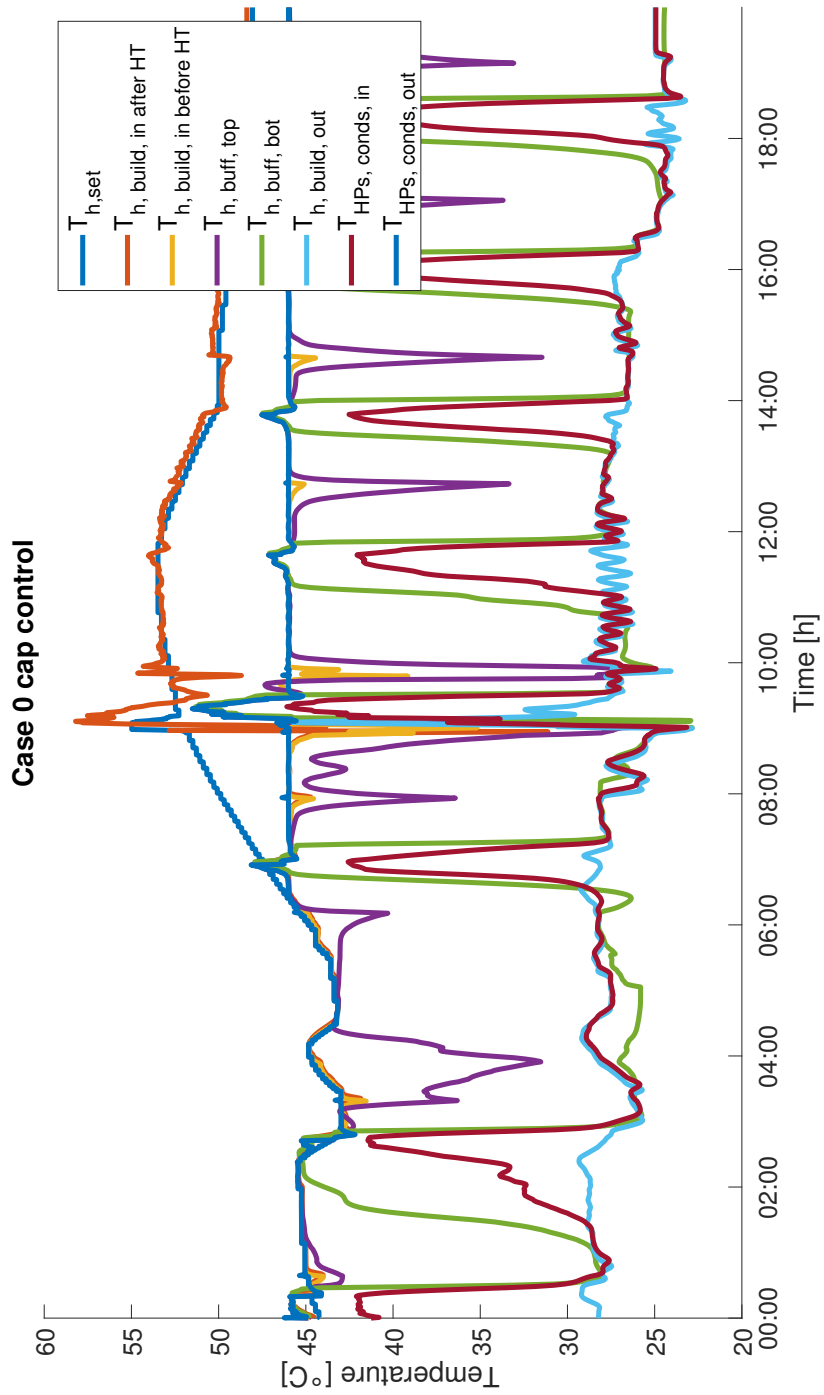


**Figure 6-2:** Case 0 using the capacity controller, the temperatures at all locations in the warm substation network.

the temperature setpoint is also in reach of the heat pump, these spikes remain within the 1.0 °C band of the setpoint. Just after 6:00h, the limit for the heat pump is exceeded and would normally have resulted in the second heat pump to be shut down immediately and only dissipating heat that is left. These safety guards could still be implemented, but have not been simulated, to properly identify what the response of the designed controller would be without interference of safety controllers to keep them within constraints.

Case 11 with a temperature and capacity control (Figure 5-27), where the security control is switched off, shows a problematic performance. As already discussed in Section 5-2-3 this is the result of simultaneously having a buffer that is fully filled upto 46 °C and simultaneously a decrease in the temperature setpoint. Even the immediate shut down of the heat pumps would still cause the temperature entering the building exceeding the setpoint. The increased condenser inlet temperatures would be a trigger for the security control to immediately shut down the second heat pump, which would also decrease the temperature entering the condenser of the other HP as less water is circulated over the buffer.

This particular case also shows the effect of the combined temperature setpoint and building mass flow adjustments on the substation. As the energy demand is increased or decreased, the flow over the building simultaneously increases/decreases with the temperature setpoint, causing a fill up of the buffers which is then also higher than the setpoint at a later moment. This causes high condenser inlet temperatures, due to the combined factor of a reduced building flow, thus larger buffer flow, and buffer temperatures above the setpoint, resulting in large temperature overshoots at the building.

From this it can be deduced that the safety controllers would still be required or at least some controller which cause a second heat pump to shut down in case of high condenser inlet temperatures.

### 6-2-2 MPC - constant flow

As MPC has to advantage that it can predict the systems behaviour it would therefore have better possibilities to anticipate on the changes in demand (energy/flow/temperature setpoint) or changes in buffer or building outlet temperatures. The objective function guides the performance of the MPC and thus adapting the objective function can provide us with different results, like a wider/smaller range around the temperature setpoint, fewer/more HP capacity changes or less/more energy supplied by the conventional heater. The result of the designed objective function is discussed here.

Case 0, as shown in Figure 5-32 provides with a nice tracking within the 1.0 °C bound of the temperature setpoint. Comparing it with the standard case (Figure 5-1), specifically after the temperature setpoint started rising a better tracking can be observed due to an earlier kick in of the conventional heater, while simultaneously the temperature entering before the conventional heater does not drop as low for the MPC controller. If this controller is compared to the temperature and capacity controller on the condensers, the MPC controller under performs which could be expected as no strict temperature control can be applied.

Case 1 (Figure 5-33) provides a better view on the advantage of the MPC controller. The standard case (Figure 5-2) shows problems with tracking the temperature at the start with fluctuating setpoint and temperature, while the MPC controller is better able to maintain within the 1.0 °C bound as it can anticipate for the increased demand and will therefore

not shut down a heat pump unnecessarily. This also results in a smaller operation of the conventional heater during this fluctuating part. When the temperature setpoint is high, the temperature leaving the condensers is maintained within the bounds around 46 °C, with smaller fluctuations compared to the standard case, resulting in a reduced energy consumption of the conventional heater.

It should be mentioned that the MPC controller does result in a short shut down of the conventional heater multiple times, but it does not result in problems with the energy delivery. These shut downs could also be mitigated by increasing the minimum time it should be on/off or decreasing the maximum ramp of the HT energy constraint, as it will then consider the dynamics and cannot be directly on the setpoint when turned on.

Case 11 is the most interesting one as it contains a highly fluctuating demand with temperature setpoint. As shown in Figure 5-34 the MPC performs well to these situations. The temperature remains within the 1.0 °C band almost all the time. At the start it is slightly off, but this is a result of the starting conditions chosen. The conventional heater is providing almost no energy and there are no significant temperature over- or undershoots. At some of the moments with a low demand, the temperature is shortly outside the 1.0 °C bound, but as the demand and temperature setpoint is low, there is also just a tiny adjustment necessary to reach outside these bands.

Comparing to the standard case, the MPC performs much better as it can accurately follow the temperature, it anticipates on the reduced demand and the already risen temperature in the buffer. Compared to temperature and capacity controller, this anticipation becomes particularly evident as it was causing large temperature over and undershoots. The standard case also has more capacity fluctuations.

For Model Predictive Control (MPC) to be implemented in reality the time it takes to compute the optimal control step should be smaller than the timestep. As the timestep is  $15 \text{ s} \cdot N_t = 1.0 \text{ min}$ , the computation time should be smaller than 60 s. In the modelling phase there was no time limit as to determine the MPC's best performance. In Figure 6-3 the computation time of every optimisation is also shown, where it can be observed that it is above 60 s for temperature setpoints above the maximum temperature of the HP. Setpoint temperatures above 50 °C the computation time is generally also within limits, but when the temperature setpoints are close the HP maximum the computation time becomes larger. This can also be confirmed in Figure 6-4 and Figure 6-5. Particularly in Figure 6-4 it is observed that the HT turns on/off more frequently in these ranges and around these moments when both HPs are on and the HT might be used, or is on the verge of being used, the computational power required is larger.

Currently, the branching priority on the binary variables  $\delta_{\text{HP1}}$  and  $\delta_{\text{HP2}}$  is used, however, it might be beneficial to also add the binary variables stating if the HT is on/off, but with a lower priority as the HPs are the most important. This will ensure that the binary variables  $\delta_{\text{HT}}$  are prioritised over some other binary variables that are a result of the imposed constraints and rewriting of constraints.

Another option to reduce the computational burden might be to increase the time the HT should be on/off from 5.0 min to 10 min, reducing the number of free binary variables. Besides improving the computation time, this might also result in a reduction of the HT use when the temperature setpoints are shortly not met, or a reduction in the fluctuations to shortly shut it down as can be observed in Figure 6-4 around 9:00h, 10:00h and 12:00h.

The fluctuation in the capacity can be reduced further by allowing a wider band around

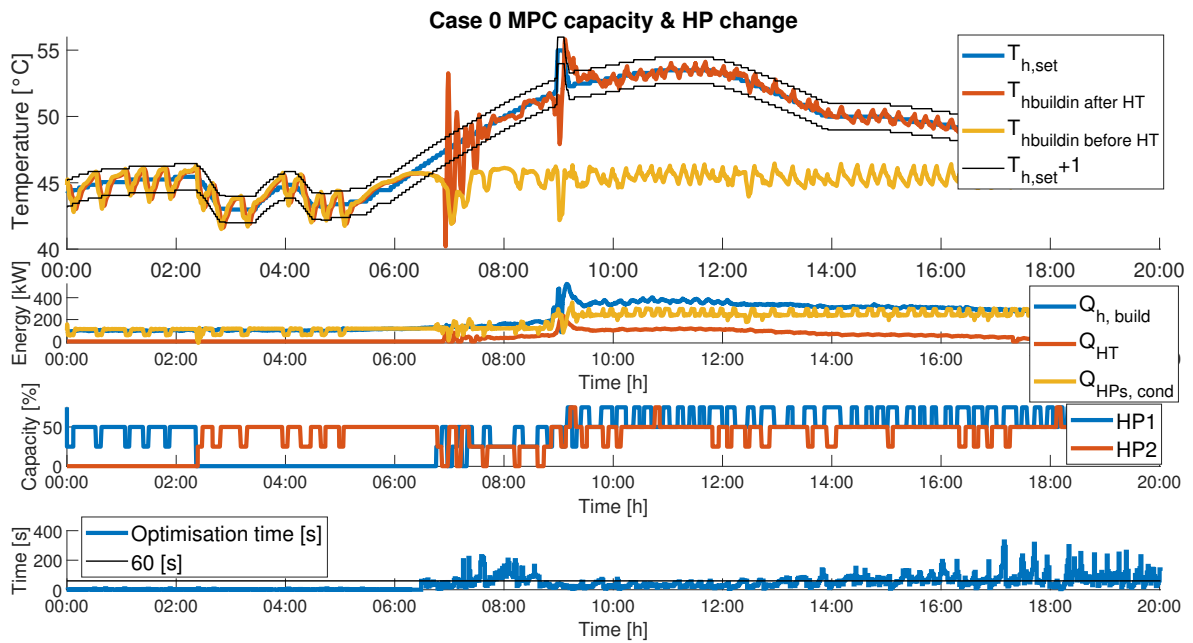


Figure 6-3: Case 0 using the MPC controller with the corresponding optimisation times.

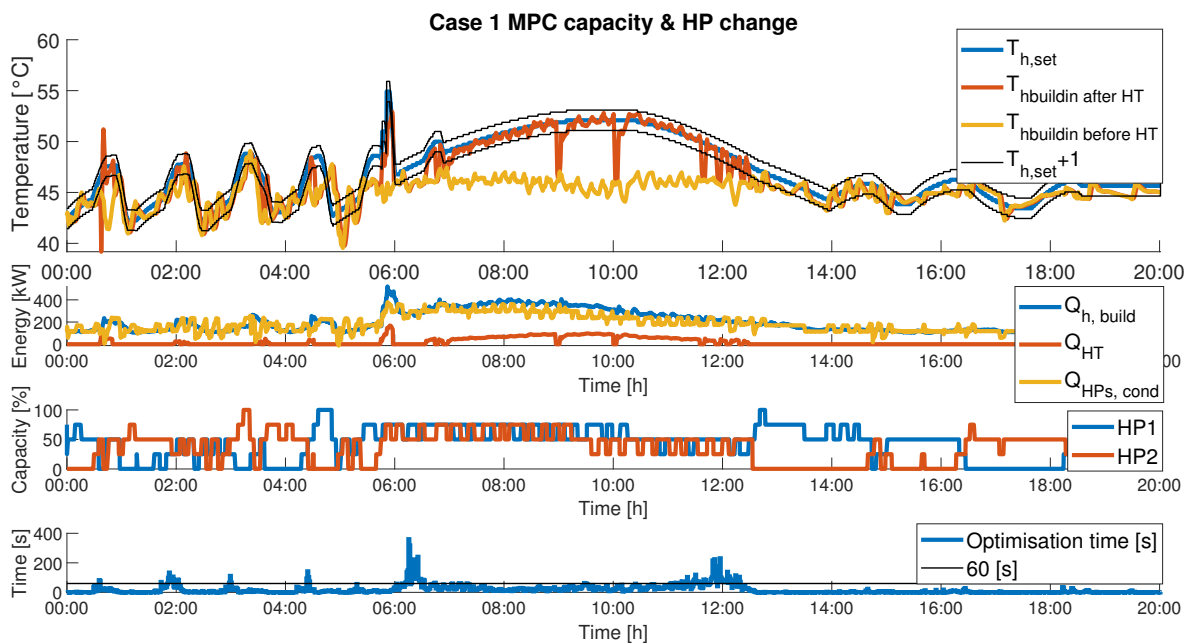
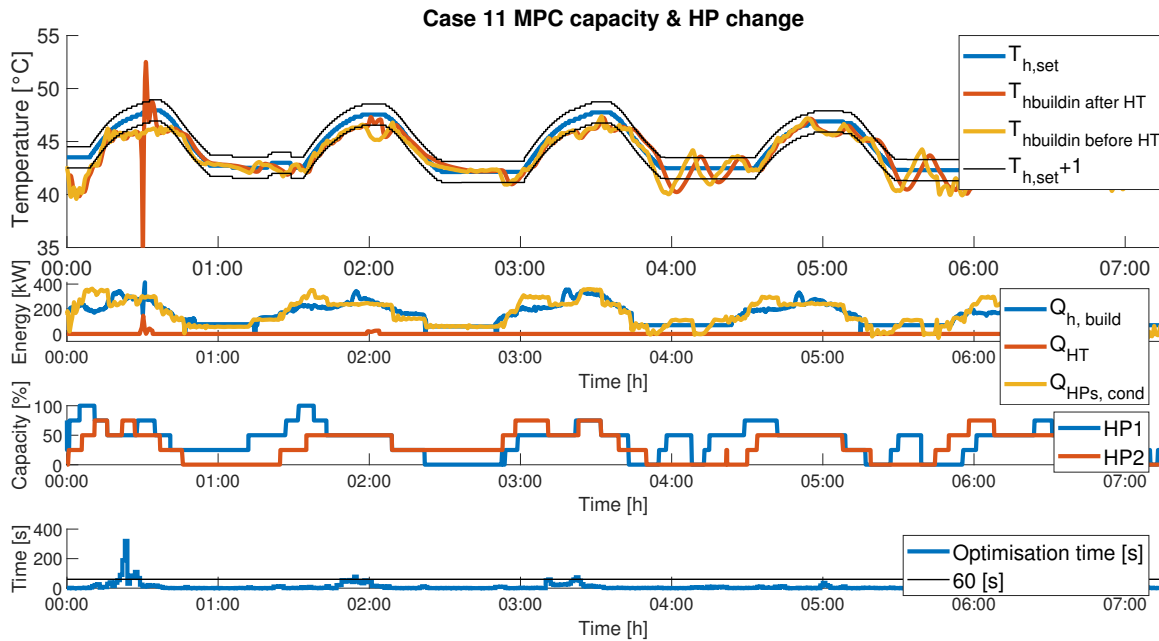


Figure 6-4: Case 1 using the MPC controller with the corresponding optimisation times.



**Figure 6-5:** Case 11 using the MPC controller with the corresponding optimisation times.

the temperature setpoint, penalising an exceeding of the band less or increasing the penalty on the capacity change. When the HT is in operation, the last option would work, but also a reduction in the penalty on the HT energy might be an efficient measure to reduce the capacity changes as it will allow a wider difference than  $2.0^{\circ}\text{C}$ . But as shown before, a significant improvement on the amount of capacity changes can be orchestrated by adding a three-way valve on the condenser side of the heat pump for temperature control.

### 6-2-3 MPC - variable flow

The MPC with a variable flow over the condenser allows to combine best of two worlds. Here an accurate temperature control can be provided by the condenser temperature PI controller, controlling the three-way control valve and the prediction and anticipation on the change of demand can be provided by the MPC controller.

Case 1, tracks the temperature setpoint properly within the  $1.0^{\circ}\text{C}$  band and till the maximum setpoint of  $46^{\circ}\text{C}$ . Compared to the PI temperature and capacity control, a capacity change is now earlier anticipated preventing the temperature overshoots. Especially after the setpoint temperature and energy demand rises quickly around 6:00h, the MPC with a variable mass flow over the condensers shows a significant improvement in terms of the temperature overshoot and undershoot.

Case 11, shows that at certain moments the temperature tracking contains a large error, for instance 4:15h to 4:30h where the temperature entering the building decreases significantly after which the heat pumps start up again. This is most likely a result of the relaxation of the bilinear term ( $mT$ ) as this can cause over and under estimations of the energy moved and

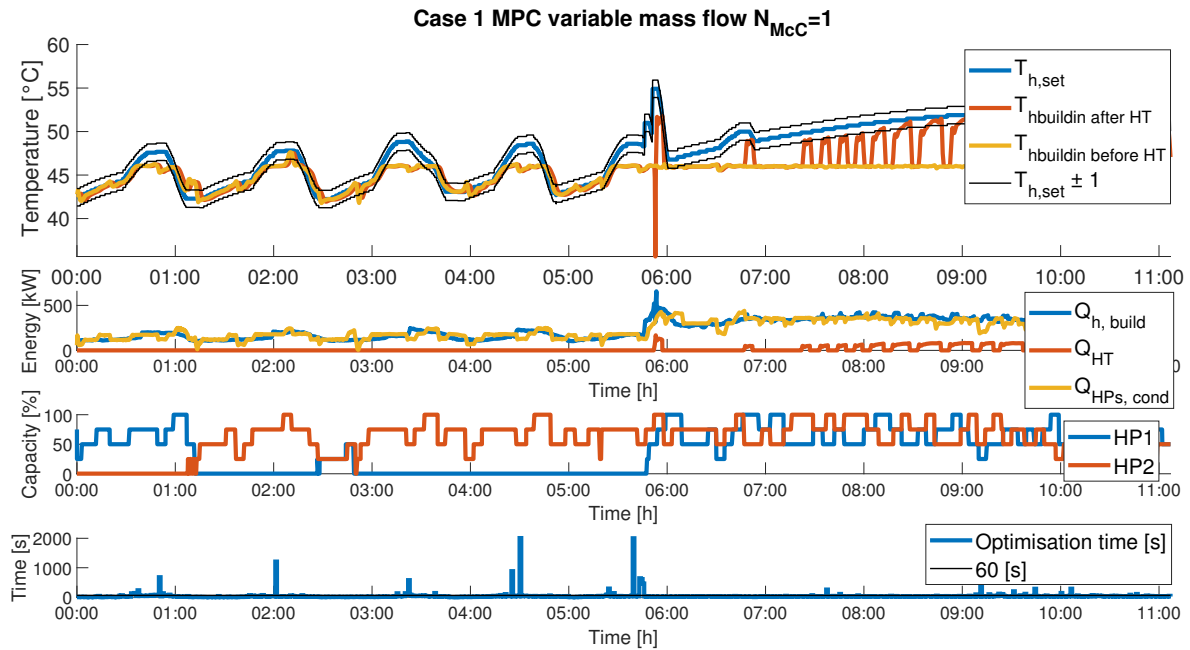


**Figure 6-6:** Case 1 using the MPC controller with a variable mass flow over the condensers with the optimisation times. ( $N_{McC}=1$ )

thus the temperature at separate cells.

Also numerical diffusion might contribute to the large undershoot as the current cell size is based on the maximum flow in 15 s. The moment this occurs, the flow is smaller than 5% of the maximum flow, thus this results in mixing of the temperature and the temperature front will therefore move less strongly towards the building entrance. The temperature only at the top and bottom of the buffer are updated every optimisation, while for the other locations in the buffer, the temperature previously calculated is used. The best way to counteract this is to make the cells as small as possible, thus related to maximum flow in 1.0 s, also the maximum used ( $23.8 \text{ L s}^{-1}$ ) has never been observed in the measurements, based on the heat pumps it could only be  $14 \text{ L s}^{-1}$ . The building flow could theoretically reach this, but in the measurements it does not reach above  $10 \text{ L s}^{-1}$ . Thus cell volumes could be reduced by almost a half.

It is particularly interesting that this sharp undershoot does not occur for the MPC with constant mass flow over the condensers. As the main difference between both methods is the variable mass flow and thus considering the bilinearity of the system, it is expected that the problem is in this region. Which would correlate to the under- or overestimation of the McCormick relaxation, when the start up of a heat pump is considered by the MPC.

The condenser outlet temperature properly tracks the temperature setpoint. For MPC with variable flow the temperature overshoots above  $46^\circ\text{C}$  are much smaller, they never reach close to  $48^\circ\text{C}$ . Thus possibly using MPC with variable flow, the maximum setpoint for the heat pumps could be increased to  $46.5^\circ\text{C}$  or  $47^\circ\text{C}$  which would reduce the energy consumption of the conventional heater further and still the temperature limits of the heat pump are not exceeded.

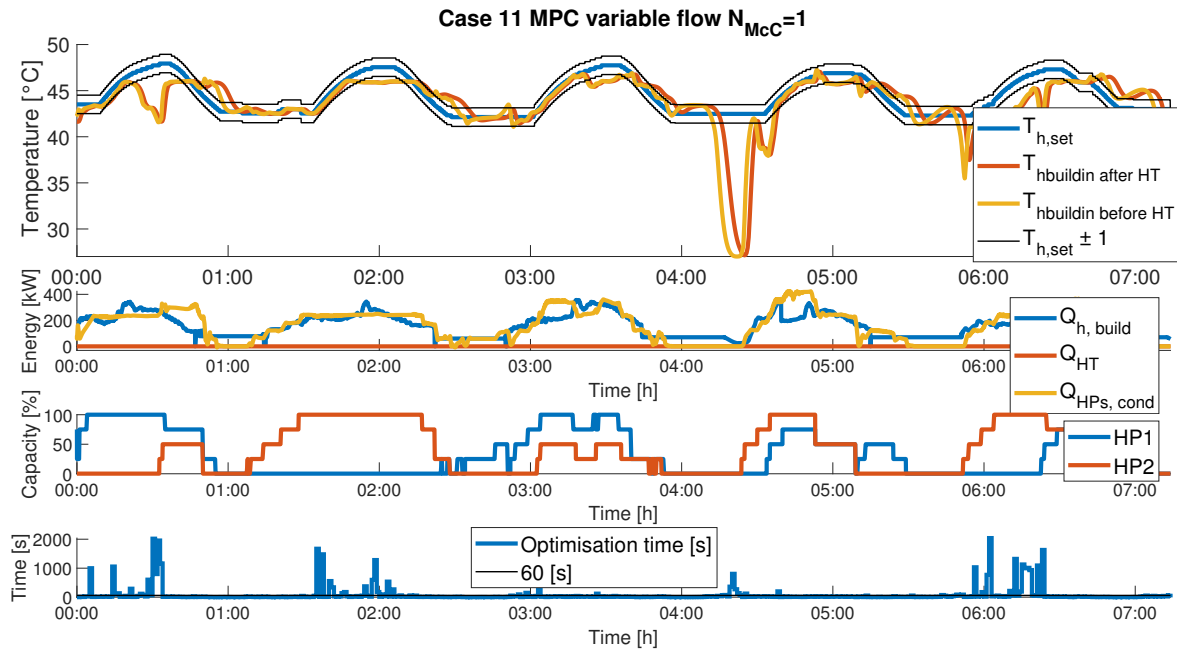


**Figure 6-7:** Case 11 using the MPC controller with a variable mass flow over the condensers with the optimisation times. ( $N_{McC}=1$ )

Unfortunately, the computer crashed multiple times during the simulations with more McCormick partitions and therefore, the optimisation times at each step are not saved. Yet the unfinished optimisations already required more than eight times the time which is simulated. Case 1, does not show a significant improvement when the number of McCormick partitions are increased from 1 to 3. Considering the simulation with a limit on the computation time, there are several differences to be observed. The temperature tracking, specifically in the fluctuating part, still works properly, however at the sudden rise of the temperature setpoint and the building mass flow, the temperature entering the building before the HT significantly undershoots the  $46^{\circ}\text{C}$  indicating it does not properly anticipate. Furthermore, the on/off switching of the HT is increased and there are slightly more frequent capacity changes of the HPs.

Case 11 with the partitioned McCormick relaxations in three, shows an improvement within the first hour as the temperature now nicely remains at  $46^{\circ}\text{C}$ . However, around 4:00h the same problems occur as for the standard McCormick relaxation.

Finally, the time limit on the computation time is used in several cases. For case 1, this reduce the performance a little, yet it was still functional. For case 11, there was a clear degradation in the performance as multiple over- and undershoots are observed. The only improvement would be that the start of the second HP after 4:00h is not pushed forward every timestep.



# Conclusion and recommendation

This chapter concludes the thesis with a summary of the results and discussion, and lists numerous recommendations for further research. The main research question of this thesis is: Can the substation be operated stably and the utilisation of the ATES system can be maximised, thus reducing the heat consumption from other sources, while maintaining the building comfort and meeting the network restrictions.

### 7-1 Summary of results and discussion

Several recommendations for the design of new substations and buildings or the adjustment in substations are recommended for stable, energy efficient operation of 5th Generation District Heating and Cooling (5GDHC) substations and have been substantiated in this thesis:

The 5GDHC network with thermal seasonal storage reduces the use of conventional heat sources resulting in lower CO<sub>2</sub> emissions.

The strict temperature limits of the ATES system can be better maintained by improving the physical and control system.

The stability and performance of the substation is key in maximising the use of the 5GDHC. The strict temperature requirements for seasonal storage have to be ensured to keep quality of the wells in condition and reduce the use of other heating or cooling sources. Several adaptations are proposed to improve the performance on the temperature limits, both from a hydro- and thermodynamic perspective and the control system.

First, the components should be matched properly with the minimum and maximum operational points. The pump at the secondary side of the warm Heat exchanger (HEX) should have its minimum operational point below or aligned with the minimum net flow over the evaporators of the Heat Pump (HP)s, to remove the effect of the short-cut buffer flow. The pump could also be equipped with a control valve after the heat exchanger to reduce the flow further, like operated on the primary side. If this is not possible, because of the minimum flow required over the heat exchanger, the switching scheme has to be adjusted. Such that

the warm HEX is also allowed to shut down based on the buffer temperature if there is no cold demand and only one HP is in operation at minimum capacity. This allows the cold buffer which might at occasions be at 12 °C to 14 °C to unload and prevent a short-cut buffer flow causing the temperatures limits in the grid to be exceeded.

Second, the on/off switching between the warm and cold HEX needs to be reduced, as the short operation causes the temperature limits to be exceeded. It can be reduced by increasing the hysteresis of the on/off switching between the warm and cold HEX.

Third, the outside temperature should be low enough as long as additional cold is loaded by the Dry Cooler (DC), to prevent too high  $T_{\text{HEX}_h, \text{sec}, \text{in}}$  and thus  $T_{\text{HEX}_h, \text{prim}, \text{out}}$ . This should be considered, both for the on and off condition for which some hysteresis is required.

Finally, the HP - HEX instability causes a frequent violation of the temperature requirements. It should first be ensured that the PI(D) controller of the evaporator three-way valve does not contain a derivative action. Furthermore the cascade controller on the flow of the primary side needs to be 'slowed down', to ensure that it does not cause a too sharp in/decrease in temperatures at the secondary side or too low temperatures. Both  $T_{\text{HEX}_h, \text{sec}, \text{out}}$  control and the adjusted  $T_{\text{HEX}_h, \text{prim}, \text{out}}$  setpoint are promising options as they stabilize the temperature to the heat pumps and thus the mass flow through the evaporators.

The tracking of the temperature setpoint and energy demand can be improved by adjusting the system design and changing the control system. The heat pumps are currently during heat leading operation capacity controlled based on the condenser outlet temperature and the second heat pump is turned on/off based on the condenser inlet temperature.

First of all, three-way control valves and short-cut flow at the condensers are required for accurate temperature control, allowing for a net flow adjustment. To reduce the electric energy required, it is advised to have a combined pump and three-way valve control. The best option for the pump speed control would be a constant temperature difference over the condenser or adjusting based on the three-way valve position. As a split range does require the lowest pumping power, but is less flexible and results in larger overshoots. Besides a reduced pumping power, the temperature jump over the condenser will increase, resulting in more heat transfer and thus a higher Coefficient Of Performance (COP).

Secondly, the capacity control has to be designed differently if the three-way valve temperature control is used. The capacity at which the heat pumps are operated could be determined using a PI controller. In the case of the HPs with only a few discrete steps, the building inlet temperature can be controlled and for continuous capacity controlled HPs the building demand can be used. The setpoint of the capacity controller could possibly be adjusted based on the buffer temperatures to anticipate on a changing demand, particularly important for the discrete heat pumps. However, the security controls, to shut down a heat pump if condenser inlet temperatures are too high are more reliable. Furthermore, the flexibility of decreasing/increasing demand can be increased if the capacity controller turns on the second heat pump after the first is in operation at 25% or 50% capacity. The heat pump that is started the first would than also be shut down the first, to ensure the minimum operation time.

The accurate temperature control and improved capacity control, can reduce the amount of unnecessary HT kick in as the response is faster and it can significantly stabilise the substation's operation as the frequency of capacity changes of the HPs reduce.

The control of the substation can be further improved to more closely meet the building demand and reduce the use of the conventional heater.

First of all, the switching conditions for the cold HEX have to be adjusted to reduce the amount of unnecessary switching. The temperature condition for which the cold HEX should not be shut down should be applied with a wider hysteresis if the heat pumps are not turned on and there remains a cold demand.

Secondly, to significantly reduce the use of the conventional heater, the components of the substation should be selected to match the building demand. Specifically this would require heat pumps that can reach the maximum temperature setpoints, resulting in the HT only to be used if the energy demand is larger than the total installed heating capacity of the heat pumps.

Thirdly, peakshaving could be applied to reduce peaks in the energy demand and thus increase the partition of energy provided by the heat pumps. This could be organised by Demand-Side Management (DSM) or by installing large buffers in the substation. If the higher temperature heat pumps cannot be installed, the demand profile should be changed. Such that each group would only increase the temperature setpoint till the maximum HP temperature after which the mass flow over the group is increased to its maximum before the temperature setpoint is increased further.

Fourthly, in the current system, the time constraint before the HT is kicked in should only start to count if the second heat pump is turned on, to prevent a simultaneous on switching of the HT and the second heat pump. Furthermore, the HT should be turned off if the second heat pump is shut down.

The last part of this thesis considers the design and effect of a Model Predictive Control (MPC) controller. The MPC controller is implemented on warm side of the substation with an objective to track the temperature setpoint while minimising the use of the conventional heater and reducing the capacity fluctuations of the HPs. The temperature setpoint, the mass flow of the warm building distribution network and the energy demand are considered to be provided information.

The system of the case study concerns fixed mass flows based on whether a subsystem is turned on or off, or is provided like the mass flow of the warm building distribution network. The optimisation problem is a Mixed Integer Linear Program (MILP) problem as there are many binary variables for the on/off and capacity states and is linear as the mass flows are fixed. The control horizon is 15 min as this is the minimum on/off time for a HP and thus the full action can be accounted for. The MPC controller shows significant improvements in terms of the temperature tracking and a reduced the energy consumption of the conventional heater as the heat pumps do now anticipate on a temperature setpoint or energy demand change. This is particularly visible for cases with a fluctuating behaviour where the temperature setpoint and energy demand reduction is also anticipated. It should be noted that the MPC controller can only operate as good as the prediction information it is fed with. If the energy demand or the temperature setpoint deviate largely, the performance is reduced. Furthermore, the accuracy of the sensors and the accuracy of the model have a large impact, therefore they need to be accurate and the model might be updated based on changed based on identification methods. The objective function of the MPC can be tuned such that it accomplishes the desired performance, with a larger focus on the capacity changes and an increased temperature setpoint bandwidth or a larger penalty for the HT. The final note to

implement the MPC controller, would be that the optimisation time might be longer than the timestep within which it has to operate, therefore it might cause problems does not provide the optimal control action.

The MPC controller has also been implemented for the system with a variable net mass flow over the condensers, i.e. the condenser three-way valve (and pump) control. As the net mass flow is variable, the system becomes bilinear, e.g. the mass flow multiplied with the temperature, and thus this would result in a non-convex optimisation problem. The bilinear terms have been linearised by the McCormick envelope. Additional constraints have been added and the McCormick envelope has been partitioned to reduce the under- and overestimation as the range for the mass flow is large ( $0.0 \text{ L s}^{-1}$  to  $14 \text{ L s}^{-1}$ ). The McCormick relaxations introduce many new binary variables thus increasing the computational time. Compared to the temperature and capacity control proposed earlier, the MPC with the McCormick envelope outperforms as the under- and overshoot of the heat pump is reduced yet underperforms considering the capacity changes most likely caused by the under- and overestimations. The penalty for the HT might also have to be retuned as it now switches off frequently. The fluctuating demand and temperature setpoint are better tracked in general compared to the PI capacity control, specifically the overshoot is reduced significantly, however, a large undershoot can occur. The partitioned McCormick envelope can improve this slightly, yet the computational time is increased significantly. The energy consumption of the HT can be reduced further as the maximum temperature setpoint of the HPs can be increased since the temperature is better tracked and the gap with the temperature limit in the HPs is now larger.

Overall the MPC controllers can improve the substation's operation however, the computational burden is still a problem as well as the accuracy of the variable mass flow MPC.

## 7-2 Further research

Recommendations for future research are formulated based on the findings of this research and insights gained during the development of the systems. The recommendation can be divided in two parts, first the hydro- and thermodynamics and the control system of the substation and secondly the Model Predictive Control (MPC) controller.

### Hydro- and thermodynamics and the control system:

- Effect of how to distribute the heat pump capacity (two equal sized or one small and one large heat pumps) and the effect on the control strategy. There might be a different preference depending on the building specific energy demand throughout the year.
- The effect of one heat exchanger for both heat and cold delivery or separate heat exchangers for heat and cold delivery when the capacity difference between both is large. (or from which capacity difference/fraction it would be better to have separate heat exchangers, depending on the performance variations with different flows)
- Stability and operational control effects of a continuous versus discrete heat pumps.
- Sensitivity analysis

- The size of the buffer tanks as it is used to stabilise and separate the building demand and the production.
- Heat pump capacity
- Heat transfer drops as a result of low operational capacities

### Model Predictive Control:

- Implementation on the cold side of the substation to determine the on/off of the heat exchanger.
- Increase the accuracy of the MPC by
  - increasing the number of McCormick partitions, but this will result in a higher number of binary variables thus increased computational cost. Logarithmic instead of linear relaxation partition scheme will have a smaller computational burden for larger number of partitions ( $N_{\text{McC}} \geq 4$ ) with the specific requirement that  $N_{\text{McC}}$  should be a power of two, as it will result in less binary variables. So far the effect on the MPC output has been minimal.
  - reducing the time step of the model from 15s to ideally 1.0s while maintaining optimisation steps of 1.0 min.
  - include a filter and identification step to improve the accuracy of the system parameters at  $t = 0.0$ s for every start of the MPC. E.g. now only the buffer top and bottom temperatures are updated based on the sensor measurements, but the temperature of the cells in between is only updated based on the MPC prediction.
- Implementation of continuous capacity controlled heat pumps instead of discrete capacity heat pumps, which reduces the number of binary variables.
- Reducing the computational optimisation time:
  - continuous instead of discrete heat pump capacities reducing the number of binary variables.
  - implementing a move blocking scheme for some variables at the end of the prediction horizon, reducing the number of free binary variables.
  - increasing the accuracy of the model might result in a better warm start.
  - reducing the prediction horizon till shorter than the minimum on/off time of the HPs
  - simplified model based on the energy in every cell and no longer considering the temperature, if the heat pumps can reach all the temperature setpoints. Would remove the bilinearity, however it should have to be considered carefully as the temperature in the buffer might be lower and thus you might not fully want to discharge it before turning the HP on.
  - formulate a reduced order model based on the accurate model.



---

# Bibliography

- [1] “Warmte koude opslag (wko).” <https://www.uu.nl/nieuws/universiteit-utrecht-zet-maximaal-in-op-wko-voor-warmte-en-koudevoorziening>. Accessed: 22-03-2021.
- [2] IEA, “Energy efficiency indicators,” tech. rep., International Energy Agency, Paris, 2020.
- [3] *ISSO-publicatie 39 Energiecentrale met warmte en koude opslag (WKO)*. Kennisinstituut voor installatietechniek, 2014. ISBN:978-90-5044-307-4.
- [4] M. Bloemendal, *The hidden side of cities: Methods for governance, planning and design for optimal use of subsurface space with ATEs*. PhD thesis, Delft University of Technology, 2018.
- [5] M. Behrendt, “Mpc scheme basic.” Wikimedia Commons, October 2009.
- [6] Kennisinstituut voor installatietechniek, *BRL 6000-21 Ontwerpen, installeren en beheren van energiecentrales van bodemenergiesystemen*, 2014.
- [7] M. Pellegrini and A. Bianchini, “The innovative concept of cold district heating networks: a literature review,” *Energies*, vol. 11, no. 1, p. 236, 2018.
- [8] H. Lund, S. Werner, R. Wiltshire, S. Svendsen, J. E. Thorsen, F. Hvelplund, and B. V. Mathiesen, “4th generation district heating (4gdh): Integrating smart thermal grids into future sustainable energy systems,” *Energy*, vol. 68, pp. 1–11, 2014.
- [9] H. Li and N. Nord, “Transition to the 4th generation district heating-possibilities, bottlenecks, and challenges,” *Energy Procedia*, vol. 149, pp. 483–498, 2018.
- [10] S. Buffa, M. Cozzini, M. D’Antoni, M. Baratieri, and R. Fedrizzi, “5th generation district heating and cooling systems: A review of existing cases in europe,” *Renewable and Sustainable Energy Reviews*, vol. 104, pp. 504–522, 2019.
- [11] S. Buffa, M. H. Fouladfar, G. Franchini, I. Lozano Gabarre, and M. Andrés Chicote, “Advanced control and fault detection strategies for district heating and cooling systems—a review,” *Applied Sciences*, vol. 11, no. 1, p. 455, 2021.

- [12] N. Nord, D. Schmidt, A. M. Kallert, and S. Svendsen, "Improved interfaces for enabling integration of low temperature and distributed heat sources—requirements and examples," *CLIMA 2016-proceedings of the 12th REHVA World*, 2016.
- [13] N. Nord, E. K. L. Nielsen, H. Kauko, and T. Tereshchenko, "Challenges and potentials for low-temperature district heating implementation in norway," *Energy*, vol. 151, pp. 889–902, 2018.
- [14] F. Ruesch, M. Rommel, and J. Scherer, "Pumping power prediction in low temperature district heating networks," in *Proceedings of International Conference CISBAT 2015 Future Buildings and Districts Sustainability from Nano to Urban Scale*, pp. 753–758, LESO-PB, EPFL, 2015.
- [15] A. Vandermeulen, B. van der Heijde, and L. Helsen, "Controlling district heating and cooling networks to unlock flexibility: A review," *Energy*, vol. 151, pp. 103–115, 2018.
- [16] S. Chyhryn, "Modelling and analysis of plate heat exchangers for flexible district heating systems," *Energies*, vol. 12, no. 21, p. 4141, 2019.
- [17] S. Moustakidis, I. Meintanis, G. Halikias, and N. Karcianas, "An innovative control framework for district heating systems: conceptualisation and preliminary results," *Resources*, vol. 8, no. 1, p. 27, 2019.
- [18] A. Afram and F. Janabi-Sharifi, "Theory and applications of hvac control systems—a review of model predictive control (mpc)," *Building and Environment*, vol. 72, pp. 343–355, 2014.
- [19] Y. Ma, F. Borrelli, B. Hancey, B. Coffey, S. Bengesa, and P. Haves, "Model predictive control for the operation of building cooling systems," *IEEE Transactions on control systems technology*, vol. 20, no. 3, pp. 796–803, 2011.
- [20] V. Rostampour, M. Jaxa-Rozen, M. Bloemendal, and T. Keviczky, "Building climate energy management in smart thermal grids via aquifer thermal energy storage systems," *Energy Procedia*, vol. 97, pp. 59–66, 2016.
- [21] M. Dongellini, M. Abbenante, and G. L. Morini, "A strategy for the optimal control logic of heat pump systems: impact on the energy consumptions of a residential building," in *Proceedings of the 12th IEA Heat Pump Conference*, vol. 2017, 2017.
- [22] H. Pieper, I. Krupenski, W. Brix Markussen, T. Ommen, A. Siirde, and A. Volkova, "Method of linear approximation of cop for heat pumps and chillers based on thermodynamic modelling and off-design operation," *Energy*, vol. 230, p. 120743, 2021.
- [23] H. Bastida, C. E. Ugalde-Loo, M. Abeysekera, X. Xu, and M. Qadrdan, "Dynamic modelling and control of counter-flow heat exchangers for heating and cooling systems," in *2019 54th International Universities Power Engineering Conference (UPEC)*, pp. 1–6, IEEE, 2019.
- [24] Deltares, Delft, Netherlands, *Wanda 4.6 User Manual*, 2019.
- [25] R. Sinnott and G. Towler, *Chemical engineering design: SI Edition*. Butterworth-Heinemann, 2019.

- 
- [26] M. Kind, H. Martin, P. Stephan, W. Roetzel, B. Spang, and H. Müller-Steinhagen, *VDI Heat Atlas*. Springer, 2010.
- [27] Y. Wang, S. You, H. Zhang, X. Zheng, S. Wei, Q. Miao, and W. Zheng, “Operation stability analysis of district heating substation from the control perspective,” *Energy and Buildings*, vol. 154, pp. 373–390, 2017.
- [28] V. Verdult and M. Verhaegen, “Bilinear state space systems for nonlinear dynamical modelling,” *Theory in Biosciences*, vol. 119, no. 1, pp. 1–9, 2000.
- [29] R. J. LeVeque *et al.*, *Finite volume methods for hyperbolic problems*, vol. 31. Cambridge university press, 2002.
- [30] R. Cagienard, P. Grieder, E. C. Kerrigan, and M. Morari, “Move blocking strategies in receding horizon control,” *Journal of Process Control*, vol. 17, no. 6, pp. 563–570, 2007.
- [31] R. Misener, J. P. Thompson, and C. A. Floudas, “Apogee: Global optimization of standard, generalized, and extended pooling problems via linear and logarithmic partitioning schemes,” *Computers & Chemical Engineering*, vol. 35, no. 5, pp. 876–892, 2011.



---

# Glossary

## List of Acronyms

<b>5GDHC</b>	5th Generation District Heating and Cooling
<b>ATES</b>	Aquifer Thermal Energy Storage
<b>HP</b>	Heat Pump
<b>HT</b>	Conventional Heater or High Temperature source
<b>DSM</b>	Demand-Side Management
<b>MPC</b>	Model Predictive Controller
<b>FVM</b>	Finite Volume Method
<b>MPC</b>	Model Predictive Control
<b>MILP</b>	Mixed Integer Linear Program
<b>DH</b>	District Heating
<b>COP</b>	Coefficient Of Performance
<b>MIP</b>	Mixed Integer Programming
<b>RBC</b>	Rule Based Control
<b>HEX</b>	Heat exchanger
<b>DC</b>	Dry Cooler



---

# List of Symbols

$\alpha$	Thermal diffusivity [ $\text{m}^2 \text{s}^{-1}$ ]
$\Delta$	Difference
$\nabla$	Differential operator
$\rho$	Density [ $\text{kg m}^{-3}$ ]
$\delta$	Binary variable
$\dot{m}$	Mass flow [ $\text{kg s}^{-1}$ ]
$\dot{Q}$	Energy flux [W]
$\dot{V}$	Volumetric flow rate [ $\text{m}^3 \text{s}^{-1}$ ]
$\bar{c}$	Maximum of $c$
$\underline{c}$	Minimum of $c$
$C$	Pressure loss coefficient [ $\text{s}^2 \text{m}^{-5}$ ]
$c_p$	Specific heat capacity [ $\text{J kg}^{-1} \text{K}^{-1}$ ]
$d_e$	Hydraulic diameter [m]
$e(t)$	Error signal
$f$	Weisbach friction factor
$H$	Head [m]
$h_{\text{conv}}$	Convective heat transfer coefficient [ $\text{W m}^{-2} \text{K}^{-1}$ ]
$i$	Cell number
$k$	Discrete time step
$k$	Thermal conductivity [ $\text{W m}^{-1} \text{K}^{-1}$ ]
$K_d$	Derivative gain
$K_i$	Integral gain
$K_p$	Proportional gain
$L$	Characteristic length [m]
$n$	Rotational speed
$N_p$	Prediction horizon

$N_{\text{McC}}$	Number of partitions for McCormick envelopes
$P$	Power [W]
$p$	Pressure [Pa]
$q$	Specific heat flux [ $\text{W m}^{-2}$ ]
$R_w$	Wall roughness
$T$	Temperature [ $^{\circ}\text{C}$ ]
$t$	Time [s]
$T_i$	Integration time
$u$	Velocity [ $\text{m s}^{-1}$ ]
$U_o$	Overall heat transfer coefficient [ $\text{W m}^{-3} \text{K}^{-1}$ ]
$V$	Volume [ $\text{m}^3$ ]
$v$	Auxiliary or slack variable
$w$	Weighting factor
$z$	McCormick relaxation variable
Re	Reynolds number
Nu	Nusselt Number
Pe	Peclet number
Pr	Prandtl number
Re	Reynolds number
RPM	Rotations Per Minute
buff	Buffer
build	Building
cond	Condenser
c	Cold
evap	Evaporator
h	Hot
in	Entering the section
out	Leaving the section
prim	Primary
sec	Secondary